Models for Managing the Deep Aquifer in Bangladesh

Mohammad Abdul Hoque
Hydrogeology Research Group, UCL Department of Earth Sciences

A thesis submitted in partial fulfilment of the requirements for the degree of Doctor of Philosophy in the Faculty of Mathematical and Physical Sciences at the University College London

University College London

March 2010

I, Mohammad Abdul Hoque, confirm that the work presented in this thesis '*Models for managing the deep aquifer in Bangladesh*' is my own. Where information has been derived from other sources, I confirm that this has been indicated in the thesis. The study was supported by a scholarship (BDCS-2006-37) from the Commonwealth Scholarship Commission (CSC) in the United Kingdom. The views expressed in this publication are those of the author and not necessarily of CSC nor University College London.

Mohammad Abdul Hoque

Date: 29 March 2010

Abstract

In southern Bangladesh excessive levels of As in shallow groundwater have led to deeper groundwater becoming the main alternative source of As-free potable water. Hydrogeological configuration indicates that tube-wells pumping from these depths may be vulnerable to As breakthrough from shallow levels. The thesis explores a range of methods of representing lithological heterogeneity of the Bengal Aquifer System (BAS) in models of groundwater flow and travel time. The aim is to support models of arsenic (As) flux to the deep groundwater flow-system of BAS, and hence to aid assessment of the vulnerability of deep groundwater to invasion by As. The research uses an array of geological information including geophysical logs (n=12), hydrocarbon exploration data (n=11), and drillers' logs (n=589) from a 5000 km^2 area to characterise the aquifer heterogeneity as a basis for alternative representations of hydrogeological structure in groundwater flow modelling. Groundwater samples from southern Bangladesh were analysed for ^{14}C in order to determine groundwater age (n=23) and for hydrochemical (n=75) and isotopic (n=50) characterisation. A new hypothesis 'SiHA (**S**ilt-clay layers **i**nfluence **H**ierarchical groundwater flow systems and **A**rsenic progression in aquifer)' is presented which integrates sedimentological heterogeneities, groundwater flow, and geochemical processes to explain the distribution and geological evolution of groundwater As in the aquifer. The hypothesis explains the spatio-vertical variability of groundwater As concentration by 'groundwater flow systems and differential flushing' in the aquifer. Groundwater flow models based on eight different yet plausible aquifer representations provide adequate simulations of hydraulic head, but contrasting implications for well catchments and travel times. The better representations are judged by comparing model outcomes of travel time with groundwater age determination using ^{14}C. Comparisons demonstrate the importance of incorporating hydrostratigraphy and spatial heterogeneity in order to optimise model representations, and implications for the security of As-free deep groundwater in the BAS.

Acknowledgement

With great pleasure, I would like to take the opportunity to express my indebted gratitude and appreciation to my teacher and advisor Dr. William G. Burgess, for his endless support towards completion of this research work and writing this dissertation. My stay in the UK as his student will remain as an unforgettable memory throughout my life. I believe it is not possible to acknowledge properly the efforts of Dr. Burgess in words.

I would also like to show my sincere gratitude to the supervisory committee members Professor John A Barker, and Professor Tim Atkinson for their advice on various occasions.

Discussion with many people has enriched my knowledge about the hydrogeology of the Bengal Basin and groundwater models. It is my pleaser to acknowledge Professor Monirul Hoque, Professor Kazi Matin Ahmed, Professor Ken Rushton, Dr. Clifford Voss, Mr. Jeffry Davis, Dr. Holly Michael, Dr. Alexander van Geen, Dr. Yan Zheng, Professor John McArthur, Professor Aftab Alam Khan, Professor Humayun Akhter, Professor Aziz Hasan, Professor Azizul Haque, Professor M Mozzammel Hoque, Professor David Polya, Mr. David Clark, Mr. Peter Revenscroft, Dr. Anawar Zahid, Mr. M. Shamsudduha, Dr. H. Dharmagunawardhena for their enlighten discussions.

I would like to express my gratefulness to my colleagues Qiong, Liang, Bethan, Gemma, Mike, Simon Q., Michael, Simon C., Joanne, Ciara, and Rakia for their help on various occasions and warm company during the research.

I am very grateful to Professor Kazi Matin Ahmed for his continuous support and guidance during the field work in Bangladesh. Help from my friends Masum, Moshiur, Polash, Bodrul and my younger brother Sumon are greatly acknowledged. I would like to thank Mr. N. Islam Babu, and Mr. Nikil Datta for their careful driving, and extended help with the field equipment. I am also grateful to Zahir and Tazul for their mechanical supports with the well head detachment. I am sincerely grateful to the inhabitants of Bangladesh for their tremendous hospitality and cooperation during the fieldwork. Particularly, I would like to appreciate Mr. Mazumder and Mr. Nazibul Hoque for their kind hospitably when all my field crew had fallen ill. I am very happy to express my appreciation to the DPHE, LGED, and BWDB for their support with the data.

I would like to take the opportunity to thank Dr. W. G. Darling at BGS for the stable isotope analysis. I am very pleased to express my thanks to Mr. Tony Osbon for his help with the field preparation and later laboratory analysis. I also acknowledge the help from the friendly staff at the UCL department of Earth Sciences (Ms Danuta Kaminski, Ms Celine Ahmed, Ms Leisa Clemente, Ms Barbara Harder, Ms Jen Willgress) who all made my work enjoyable.

Thanks must go to the Commonwealth Scholarship Commission (CSC) in the United Kingdom who funded this PhD through a scholarship (BDCS-2006-37). I am grateful to the award administrators

at the Association of Commonwealth Universities, and at the British Council for their kind support throughout the time. I also like to thank the Nansen Village – an international married student accommodation for their support during my stay in the UK. My friends and neighbours (Sumon, Shila, Sara, Sunny, Asad, Biplo, Moushomi, Palash, Shonima, Kochi, Monni, Liton, Sadia, Luciya, Shofiq) have been very helpful especially socialising thousands of miles away from home.

Most importantly, I wish to thank and express my devotion to my parents and in laws and my beloved brothers and sisters for their support and inspiration. I appreciate the sacrifice my daughter Siha made with her playtime. Lastly, but most lovingly, I would like to thank my beloved wife Sufia for her support, patience and inspirations. I also appreciate her for help with GIS and data processing.

Finally, I dedicate this thesis to my dearest wife and beloved daughter.

Table of Content

List of Figure

List of Tables

Part A: Introduction & Overview

Chapter 1
Introduction

1.1 Background and Rationale of the research

Groundwater in Bangladesh is widely available and in general, the groundwater resources of the country are plentiful. The country is blessed with prolific unconsolidated to semi-consolidated fluvio-deltaic sedimentary aquifers (*Ravenscroft 2003; Burgess et al. 2010*). Across the extensive floodplains of rural Bangladesh, hand-pumped tube-wells (HTWs) are used for domestic water supply and motorised pumps abstract groundwater for dry-season irrigation. Groundwater meets almost the entire national water-demand for domestic and industrial water supply and for irrigation, mostly from the shallow depth (20 to 70 m) below ground surface. The discovery of excessive dissolved arsenic in the shallow groundwater *(Dhar et al. 1997; Nickson et al. 1998; DPHE/BGS/MML 1999)* in the 1990s raised a serious concern against the exploitation of this resource. However, evidence of insignificant presence of arsenic below about 150 to 200 m (*Bhattacharya et al. 1997; BGS/DPHE 2001*) suggests deep groundwater as a potential source of 'arsenic-free' groundwater in the region. Therefore, attention is turning to the potential for deeper aquifers to provide an arsenic-free supply in the rural areas. The term 'Arsenic-free' here is defined as water containing <10 µg/l arsenic, the WHO drinking-water guideline, rather than the regulatory limit in Bangladesh and West Bengal of India, 50 µg/l arsenic. Socio-economic conditions and resource constraints lead this deep groundwater to be the principal and widely accepted alternative for arsenic-free water for millions of people in the area.

Simultaneously the provincial towns, also mostly developed on the floodplain areas, have started to develop the deeper aquifers to satisfy the growing demands of urban water supply. Thousands of deep tube-wells have been installed in rural Bangladesh over the past decade under the arsenic mitigation programme *(Ahmed et al. 2006)*. More than 75,000 deep hand-pumped wells had been installed *(Ravenscroft et al. 2009)* by 2007 in southern Bangladesh. Since 2000, deep wells

yielding 2500 m^3/d have been installed by local initiative in over 100 rural supply schemes *(DPHE/JICA 2008)*. Previously, the Bangladesh Department of Public Health Engineering (DPHE) had fitted deep wells with pumps, each capable of yielding 4,500 m^3/d, at more than 20 towns (DPHE, personal communication).

Recent 3D modelling studies at basin scale *(Michael and Voss 2008)*, at sub-regional scale (*Mukherjee et al. 2007b*) and as vertical 2D sub-regional sections *(Shibasaki et al. 2007)* have demonstrated how the deeper aquifer in the Bengal Basin may be developed using HTWs as a sustainable source of arsenic–free water. Possible hydrogeological configurations and preliminary numerical models of a deep tube-well catchment have however indicated that tube-wells pumping from these depths may be vulnerable to arsenic breakthrough from shallow level under some conditions and should not be assumed 'arsenic-free' everywhere, nor for ever *(Burgess et al. 2007)*. In places it is reported that high levels of arsenic exceeding the Bangladesh regulatory limit (50 µg/l) for groundwater arsenic are now present in some of the deep tube-wells *(DPHE/DFID/JICA 2006)* and a similar situation is reported from West Bengal, India *(Mukherjee 2006)*. A compilation of basin surveys by Burgess et al. *(2010)* indicates that arsenic exceeds 10 µg/l in 18% deep hand-pumped wells (n=1165), but whether as a result of breached well casings or hydrological response to pumping remains uncertain.

In fluvio-deltaic aquifers, such as exist in Bangladesh, depositional elements are often arranged in a linear fashion, and are spatially discontinuous and varied in nature. These characteristics have implications for groundwater flow. There is a requirement for additional studies, building on the emerging data, to investigate whether and to what extent arsenic may be transported to the levels of the 'deeper aquifer' from the shallower level, induced by pumping. This thesis addresses that need, exploring the most appropriate manners in which the hydrostratigraphy should be represented in order to judge strategies of pumping deep groundwater, in the face of its vulnerability to invasion by arsenic from shallower levels.

The logical basis for the current research is as follows:

- Emerging data from depths between about 150 m and 350 m present an opportunity to investigate the hydrogeological conditions, and the implications for sustainability of arsenic-safe groundwater extraction from these greater depths.

- The heterogeneities of the lithostratigraphy in the floodplain areas make any hydrogeological assessment uncertain. However, this uncertainty may be able to be constrained and may be quantifiable. At issue is the conceptualisation of lithological heterogeneity and its representation in models.

- The assessment of the deeper aquifer conditions requires a quantitative approach, based on modelling, yet virtually no monitoring data exist against which to calibrate models of the

responses (hydraulic and hydrochemical) to pumping. It may be possible to constrain plausible representations of the deeper aquifer conditions by independent observations of the groundwater age or age indicators.

1.2 Objectives of the research

As models are all simplified descriptions of complex reality and the manner of representation of aquifers can have a profound effect on model outcomes, the research explores a range of possible representations of the deeper hydrogeology of Bangladesh, and tests their applicability for investigating the implications for sustainable development of deeper groundwater.

The project aims to provide an improved understanding of the hydrogeology of the deeper aquifer of Bangladesh, through answering the following questions:

- How can the deeper aquifers best be represented, in order to investigate their vulnerability to vertical leakage?
- There are several sources of uncertainty - how can uncertainty be incorporated?
- How is arsenic distribution linked to groundwater flow at local to regional scale, from shallow to deeper region of the aquifer?
- Can hydrochemical and isotopic profiles be used to constrain the hydrostratigraphy as reproduced in groundwater models?
- What further research is needed in order to develop useful guidelines for sustainable development of the deeper aquifers?

To achieve these objectives this research will:

a) Assemble data relating to the deeper aquifer environment

b) Describe the aquifer heterogeneities and the uncertainties associated with these descriptions

c) Develop a range of plausible representations of the deeper aquifer environments

d) Constrain the alternative hydrogeological models derived from these representations against independently acquired data on groundwater age and isotope character

e) Seek to develop a coherent conceptual model linking groundwater flow to As distribution at local to regional scale, from shallow to deeper aquifer region.

f) Work at a sub-basinal (regional) scale to make most use of available data and the existing basin-scale models which provide a wider context.

These objectives will be achieved by an approach combining conceptual and numerical models consistent with the hydrogeological uncertainties and constrained by observations on the hydrostratigraphy, hydrochemistry and isotopic character of the groundwater system at a regional (sub-basinal) scale. The research will be presented with the further aim of providing preliminary guidance concerning the sustainable development of deeper groundwater for water supply in the floodplain regions of Bangladesh.

1.3 Study area

To maximise the use of available data (see section 2.1) the objectives of the research were addressed through hydrogeological analysis and groundwater modelling studies in the southern part of the Bengal Basin in Bangladesh (Figure 1-1), an area facing serious environmental health risk associated with excessive presence of dissolved arsenic (As) in groundwater *(Smith et al. 2000; Das et al. 2009)*.

The model area lies east of the confluence of the River Meghna with the River Ganges (locally known as Padma River) in southeast Bangladesh, extending to the coast and bounded by the rugged hilly terrain in the east. The study area was demarcated in consideration of the 'hydrogeological unit basin' as described by Anning and Konieczki (*2005*). The hydrogeological unit basin is defined to have coincident groundwater and surface-water basins. The model region is elevated in the eastern part, and slopes westward toward bounding rivers and the coast. It covers more than 5000 km^2 in eastern Bangladesh.

Figure 1-1: Map shows Bangladesh and neighbouring regions. Bangladesh and West Bengal, India share most part of the Bengal Basin. Southern part of the Bengal Basin is indicated by a rectangle and model area by a curvilinear polygon. (Map adopted from: Google Earth)

Chapter 2
Data and Methodology

To comply with the aims and objectives of the project an integrated approach was followed in data collection, analysis and interpretation of the components required for developing alternative models of the hydrogeological variability and boundary conditions. In this chapter an outline of the data used and the methodologies applied in the analysis is made.

2.1 Data

The hydrogeological characteristics of deep regional alluvial aquifers are not easy to determine due to the large areas involved. A large amount of data was collected and collated. The focus for data coverage varies from basin scale to regional (sub-basin) scale in the study area.

2.1.1 Basin scale data:

Basin-scale data and information were mostly used for understanding the basin-scale geology and for conceptualisation of geological evolution, and development of the aquifer system in the basin. These are done through combining a variety of data.

1. A database of 1584 deep boreholes was built from several sources (e. g., BWDB 2005; LGED/BRGM 2005; DPHE/DFID/JICA 2006) and organizations (e. g., BWDB, DU, BUET, IWM).

2. Around 80 lithologs with sediment colour information distributed throughout southern Bangladesh were collated from different sources (e. g., BWDB 2005; LGED/BRGM 2005; DPHE/DFID/JICA 2006)

3. One deep seismic section from southwestern Bangladesh *(Lindsay et al. 1991)*.

4. Basin-wide sediment radiocarbon ages were compiled from various sources (e. g., Umitsu 1993; Goodbred and Kuehl 2000; BGS/DPHE 2001)

5. Basin-wide groundwater radiocarbon data (*e. g., Aggarwal et al. 2000; Zheng et al. 2005*) and isotope (stable and tritium) data were compiled from various sources *(e. g., Aggarwal et al. 2000; BGS/DPHE 2001; Darling et al. 2002; Zheng et al. 2005; Mukherjee et al. 2007; Shamsudduha 2007; Stute et al. 2007).*

6. Country-wide hydraulic parameter values (pumping-test derived) at 280 locations were compiled from the BWDB. The depth of the wells used for these hydraulic tests was <100 m in depth.

7. Country-wide piezometry and water-level data were collated (weekly measurement of water-table monitored by the BWDB at >1200 locations).

8. National scale soil type (*BARC 1988*) and thickness of surface silt-clay layers (*MPO 1987*) were also collated.

2.1.2 Study area specific:

Large amounts of data distributed over the study area were used for geological understanding and hydrogeological conceptualizations, and also for estimating some model inputs. These are listed below.

1. Drillers' logs of 589 boreholes with depth range 80-375 m. Most of these (75%) are over 250 m depth *(DPHE/DFID/JICA 2006 and other organisations)*.

2. Lithological information from 11 petroleum exploration boreholes, to 2000 m depth (*MPO 1987; Reimann 1993; HU/NPD 2001*)

3. Geological structural data from published sources (e. g., *Reimann 1993; HU/NPD 2001*)

4. Piezometry at 20 locations (all from measurement levels exceeding 100 m depth), including one deep profile from Kachua Upazila – the innermost sub-district in the study area (D. Clark, USGS, Personal Communication).

5. Hydrochemistry for Kachua (D. Clark, USGS, Personal Communication) and for Lakhimpur *(BGS/DPHE 2001)*.

6. Upazila-wise irrigation abstraction data for the year 2003 *(BADC 2003)*

7. Gridded population on a 1 km^2 or finer (30" X 30" latitude/longitude) grid for the area were collected from the Oak Ridge National Laboratory (ORNL) global population data set LandScanTM 2006 *(ORNL 2008)*.

8. Population census data were collected from the Bangladesh Bureau of Statistics *(BBS 2004)*

9. Groundwater abstraction and sanitation data were collated from the Bangladesh Bureau of Statistics *(BBS 2004)*

10. Groundwater development history in the area *(e. g., Bhuiyan 1984; Rahman and Ravenscroft 2003)*.

11. Average water-well screen depth data from a variety of sources *(*e. g., *BGS/DPHE 2001)*

12. Digital elevation data (90 m resolution) from SRTM-90 *(EROS 2002)*

13. Surface geology collated from Bangladesh and Indian geological and soil maps (*Gupta 1981; Alam et al. 1990;* e. g., *Dasgupta et al. 1993; Bhattacharyya et al. 1996*).

14. River courses and bathymetry including coastal area *(Al-Salek 1998; Rahman et al. 2004)*

15. Upazila-wise 25 year average rainfall data from BDWB.

2.1.3 Field work and primary data:

Field work was carried-out between 25 December 2007 and 12 February 2008, aimed to generate primary data on isotopic and hydrochemical character of groundwater mainly from the deeper part (>200 m depth) of the aquifer. At every location a shallow well was also sampled. Relevant secondary data and reports available locally were assembled.

1. Groundwater samples were collected for general hydrochemical analysis, and isotopic characterisations: 80 paired samples (shallow, deep) for O, H isotopes and hydrochemistry, 23 water samples (with 3 deep 'profiles') for C-14, $\delta^{13}C/^{12}C$. Most samples were collected from the study area, with some from western and north-eastern part of the country for comparative purposes.

2. During the field work 12 borehole geophysical logs were collected from the University of Dhaka, which were originally logged by the author with Mostafa *(2005)*. The geophysical log data are distributed over 25 km^2 area in Kachua.

2.2 Methodology

The current research engaged several interactive components of research each with a definitive method, contributing towards groundwater modelling (Figure 2-1). Research components range from basin-scale geological conceptualisation to understanding groundwater flow through data-derived subsurface visualisations and the hydrochemical-piezometric constraining of geohydrological interpretations.

Hydrogeological interpretations were mainly made in a framework of hydrostratigraphical analysis based on the drillers' log, petroleum exploration logs, and geophysical logs. Moreover, a basin-scale geological understanding for the Plio-Quaternary deposits in the basin was revisited to facilitate better understanding of hydrogeological framework. Lithological and hydrofacies modelling in 3-D were carried out to interpret aquifer heterogeneities. These heterogeneities were described in terms of hydraulic conductivity values so that groundwater models could be constructed to simulate the effects of heterogeneities on flow. Several possible hydraulic-equivalents of the hydrogeological variability were considered.

Groundwater samples were collected from several locations within the study area and the wider area of interest. These samples were analysed for hydrochemical composition, and for isotopic characterisations. Groundwater ages based on radiocarbon analysis, and water-table data (from a wider area in the model domain) for the depth of irrigation abstraction (~90 mbgl), including a time-series of head at multiple depths measured at a central-location of the study area, were used to constrain the groundwater models.

Individual silt-clay layers are variable in thicknesses and depth of occurrence, and lateral correlation is frequently unjustified. Effects of these discontinuous silt-clay layers on groundwater flow in the basin have been investigated using 2-D vertical groundwater flow modelling. A range of simple models were used to understand the effect of the architecture, pattern, thickness etc. of silt-clay layers on groundwater flow in the fluvial-deltaic aquifers. In these 2-D models the hydrogeological system was considered to be composed of two permeability classes (i. e., composed of silt-clay, and sands), and recharge is represented as fixed head at the ground surface.

The objectives of the research work were addressed using a groundwater flow modelling framework incorporating multiple modelling approaches. The modelling has assimilated a range of representations of the hydrogeological architecture into groundwater models of the region. The goodness of the model representations was tested by comparisons of independently-derived (radiocarbon-based) groundwater age interpretation against the model-derived residence time.

2.3 Thesis Structure

Thesis is organised into three parts – A. Introduction and Overview, B. Descriptions and Characteristics, and C. Representations and Modelling. In part A, basin-scale hydrogeological overview is made following two chapters outlining the thesis objectives, the study area, and a description of the methodologies. The hydrogeological overview in turn acted as a basin-scale knowledge-base for alternative conceptualisations of the hydrogeological framework described in part B along with interpretation of hydrochemistry, isotopic nature and groundwater age. Part C presents the development of the groundwater models based on alternative hydrogeological representations, considers the models results, and draws conclusions addressing the thesis objectives.

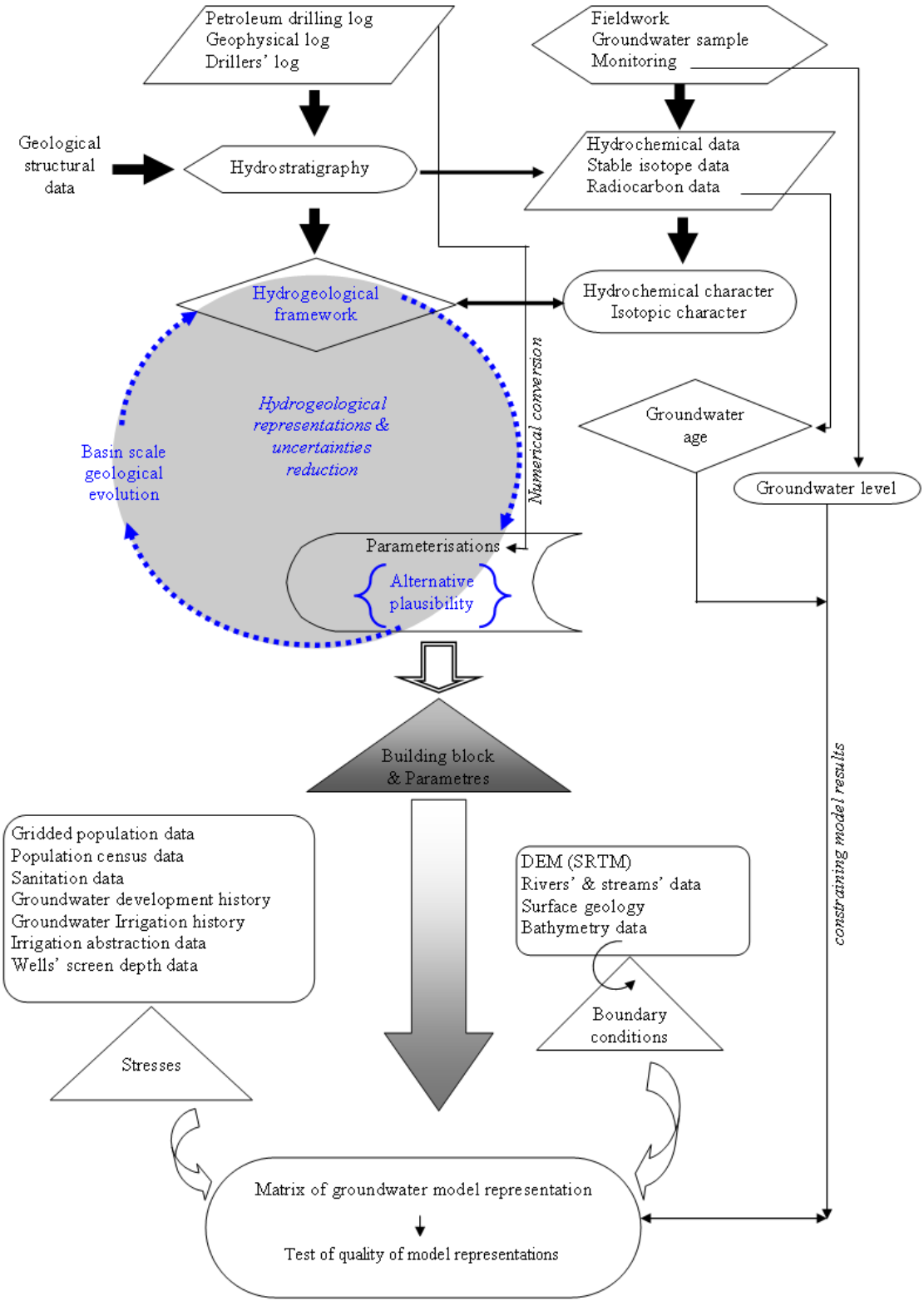

Figure 2-1 Outline of steps applied in the project.

Chapter 3
Quaternary Geological Evolution and Hydrogeology

3.1 Introduction

The Bengal Basin is one of the most prolific sedimentary basins holding the world's largest delta, Ganges-Brahmaputra [G-B] delta, fertile enough to support one-thirtieth (220 million) of the world population. The basin is characterised by widespread Quaternary alluvial-deltaic plains nourishing the agricultural base and livelihood. It has a few hundred metres to several kilometres thick sedimentary sequence overlying the basement, deposited in a remnant ocean basin setting. The thickness of sediments is lower in the western part (up to 8 km) whereas post-Cretaceous sediments in the eastern part of the basin are 16 to 22 km thick. The uppermost few hundred metres of the geological sequence form a very productive unconsolidated to semi-consolidated sedimentary aquifer system, which provides almost the entire water demands (>80%) for irrigation, drinking and other industrial activities.

The geology of the basin is widely described elsewhere as part of the geology of Bangladesh *(e. g., Khan 1991; Lindsay et al. 1991; Reimann 1993; Alam et al. 2003)*. However, those descriptions have largely concentrated on the petroleum and mineral resources studies of the basin. Groundwater irrigation development *(e. g., UNDP 1982; Bhuiyan 1984; MPO 1987; Ravenscroft 2003)* and the discovery of the groundwater arsenic problem *(e. g., Dhar et al. 1997; Nickson et al. 1998; BGS/DPHE 2001; Ahmed et al. 2004; Ravenscroft et al. 2005)* has led to a number of studies of the basin in the context of hydrogeology and groundwater resource potential. Much literature dealing with Quaternary evolution of the basin *(e. g., Morgan and McIntire 1959; Umitsu 1993; Goodbred and Kuehl 2000; Allison et al. 2003)* contains information and data relevant to hydrogeological conditions. Considerations of sedimentation, stratigraphy and geological evolution of the basin give insight into the likely structure of the aquifer fabric at small scale and the hydrogeological framework at basin-scale.

Hydrogeology of alluvial terrain is heterogeneous and complicated because of inherent geological complexities of the terrain. Hydrogeological architecture of the Bengal Basin is greatly influenced by the geological nature of the basin, and complicated by the morphotectonic modifications and sea-level fluctuation during the Plio-Quaternary times. The nature of the aquifers and their hydraulic character are strongly associated with the geological evolution which took place in the basin during Plio-Quaternary time. In this chapter an attempt is made to give an overview of the basin scale hydrogeology in relation to Plio-Quaternary geological evolution of the basin, the genesis and geological modification of the aquifer system, and opportunities and challenges for groundwater development. Hydrogeological descriptions are based on the existing ideas, and an updated understanding is developed from a new analysis of the variety of data and interpretations.

3.2 Basin geography and geology

3.2.1 Location and hydrogeological basin boundaries

The Bengal Basin contains some parts of India and the entire country of Bangladesh (Figure 3-1). The basin is bounded by hilly areas and mountainous geological shield terrain except in the south where the basin is open to the Bay of Bengal. There is no sharp well-defined boundary for the basin. It is considered that the Himalayas in the distant north and Indo-Burma range in the east have acted as effectively inexhaustible sources of sediment, as do the Indian Shield and Shillong plateau bounding the basin in the immediate west and north respectively. The basin in general is very flat. In the south where it is open to the Bay of Bengal, ground elevation is <1 m above MSL and gradually increases towards the north, and to the basin edges where it meets the mountain and shield area (Figure 3-1). There are isolated intra-basinal Pleistocene tracts of land *(Morgan and McIntire 1959)* with elevation between 30 to 50 m above MSL.

However, if consideration is given to hydrology, the basin would extend far beyond these aforementioned mountainous boarders i. e., the catchment of the G-B river extends over millions km^2. Hydrogeologically, *(definition by Anning and Konieczki 2005)* the basin can be considered to a terminally-open, multiple-area hydrogeological flow unit, where terminals are open to the surrounding hydrological and hydrogeological units. Hydrogeological flow systems are delineated on the basis of the hydrogeological boundaries and the presence or absence of interbasin flows between hydrogeological areas. Groundwater divides - along the basin terminal formed by the relief, topography and rock type of the complex mountainous region, may make the hydrogeological basin slightly bigger than the topographic Bengal Basin.

3.2.2 Climate

A tropical monsoon climate, with a hot and rainy summer and a dry winter dominates the basin (e. g., Sanderson and Ahmed 1979). January is the coolest month with temperatures averaging near 20^0C and April is the warmest with temperatures ranging from 33 to 36^0C. It is one of the wettest

basins in the world. Most places receive more than 1500 mm of rain per year, and areas near the hills in the east and northeast receive a precipitation greater than 4000 mm (Figure 3-1). Most of the rainfall occurs during the monsoon period (June-September) and only a small amount in winter (November-February).

3.2.3 Landform and hydromorphology

High rainfall, the position of the mountains and the adjacent Bay of Bengal have made the Bengal Basin possibly the richest hydromorphological region in the world. The mountainous ground of the basin margin and the large plain nurture thousands of surface water courses and the world's largest river system. In addition to the Tertiary mountains in the east, and Precambrian shield in the north and west, localised morphotectonic blocks viz., the Madhupur and Barind Tracts *(Khandoker 1987)* subdivide the basin into several hydrodynamic zones (Figure 3-1). Across this vast deltaic plain, a corridor along the intra-basin morphotectonic depressions allows the flow of the mighty rivers - the Ganges (known as Padma in Bangladesh), the Brahmaputra (known as Jamuna in Bangladesh), and the Meghna to the Bay of Bengal.

The Ganges-Brahmaputra-Meghna (GBM) river system drains a wide spectrum of metamorphic, magmatic and sedimentary rocks aged from Precambrian to Quaternary, and carries an estimated 1 billion tons of suspended sediments per year *(Coleman 1969; Milliman and Meade 1983)*. The geology of the basin has been dominated by the influence of these major rivers since the Tertiary period. Under the changing climatic conditions, shifting of monsoon winds and fluctuation of sea level, the hydrology of the humid low-latitude GBM river system has suffered dramatic variability during the Late Quaternary *(Goodbred and Kuehl 2000)*. The present landforms of the basin have been formed by fluvio-deltaic processes over the late-Quaternary period.

High rainfall, mighty rivers with hundreds of tributaries and distributaries, unconsolidated surface sediments, and a shallow groundwater table facilitates the dynamic hydrological system of the basin. The basin is characterised by seasonal flooding from the overtopping of the river bank and rainfall, and in the dry season part of the basin experiences drought due to lack of rain and lowering of the groundwater table. In the recent decades the natural groundwater dynamics of the region has been greatly affected by the intensive abstraction related to irrigation, industrial, urban and drinking purposes *(e. g., Bhuiyan 1984; Harvey et al. 2006; Hoque et al. 2007)*. Offshore the basin is characterised by a prograding subaqueous deltaic clinoform on the 100 - 250 km wide shelf, deepening from a few metres at the shore-line to 100 m at the shelf-slope break *(Curray et al. 1982; Goodbred and Kuehl 1999)*. At the edge of the west-central part of the shelf within 30 km of the shoreline, ground depth increases to 1200 m in a canyon-like feature known as Swatch of no Ground (SnG). The SnG has a seaward continuation for almost 2000 km across the Bay of Bengal in the form of fan valleys with levees *(*e. g., *Curray 1991)*. In addition to the surface water

drainage of the mighty rivers, large amounts of groundwater are also discharged into the Bay of Bengal along the whole face of the shelf *(Moore 1997)*.

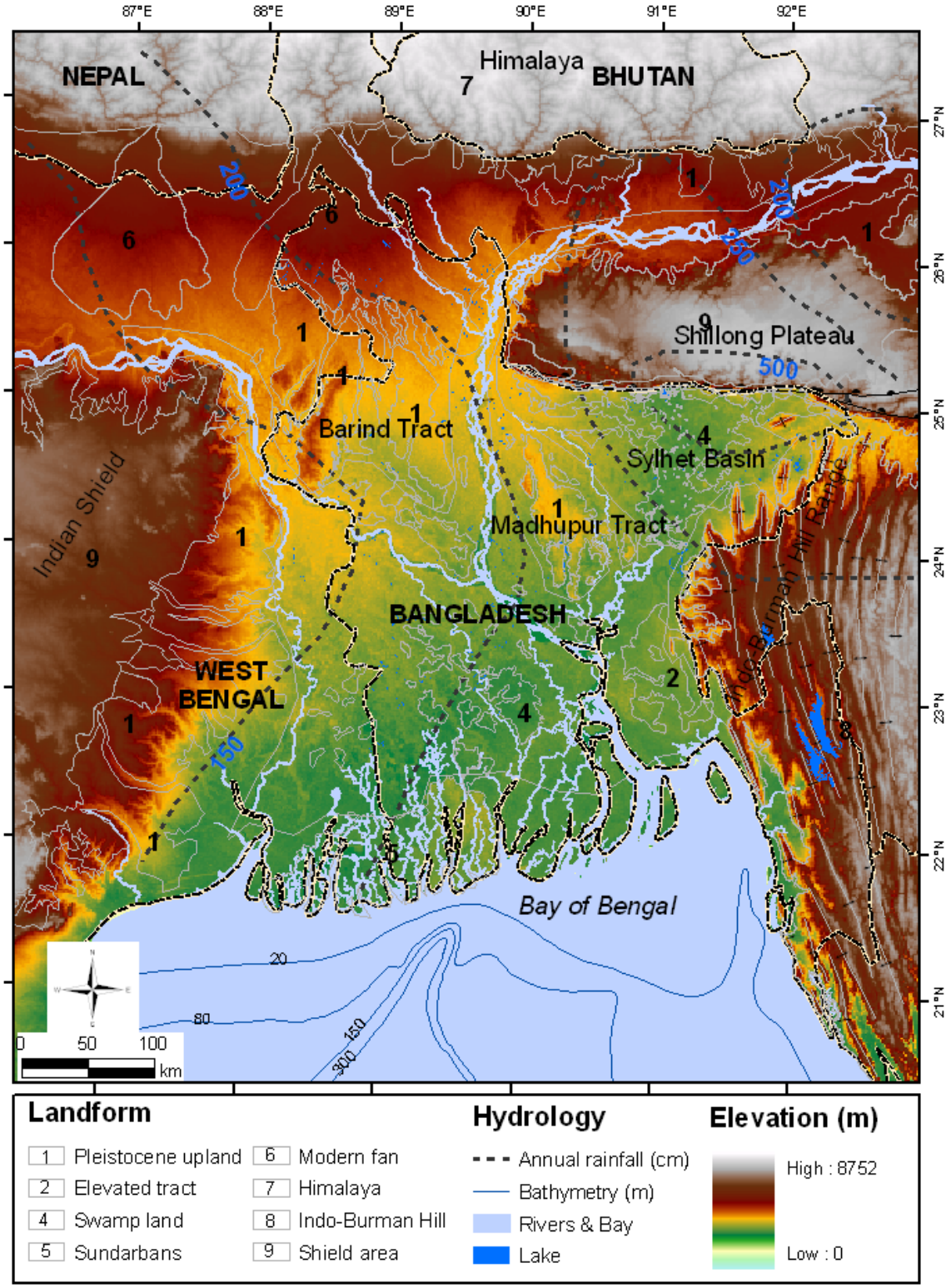

Figure 3-1: Bengal Basin: geography, major landforms, surface elevation, and rainfall pattern. Data were collated from: Landform *(Alam et al. 1990; Khan 1991; Dasgupta et al. 1993; Reimann 1993; Brammer 1996)*, Rainfall *(Reimann 1993, www.imd.gov.in accessed on 08 May 2009)*, and surface elevation *(EROS 2002)*.

3.2.4 Sedimentation and stratigraphy

Sedimentation in the basin started during the late Cretaceous *(Curray 1991)*. A detailed description of the basin-scale stratigraphy and sedimentation history can be found in earlier literature *(Khan 1991; Reimann 1993; Alam et al. 2003; Goodbred et al. 2003; Uddin and Lundberg 2004 and references there in)*. A generalised and brief description of the stratigraphy is presented in table 3-1. The thick sequence of alluvial cover and a relative paucity of fossils have hindered a better characterisation of the stratigraphy. There are exposures of rock of up to Palaeocene age in the NE region; Tertiary sequences are exposed in the eastern hilly area. Geological exploration has identified similar sedimentary successions in the subsurface elsewhere in the basin *(Reimann 1993)*. The thickness of the sedimentary sequence increases to more than 20 km in the SE shore-face part of the basin, from a few hundred metres on the basin margin, a palaeo-continental shelf, in the northwest (Figure 3-2). The present-day aquifer-system occupies the uppermost few hundred metres of the stratigraphical sequence deposited since Mio-Pliocene time.

Rapid uplift of the Himalayas to the north and the Indo-Burman range to the east associated with Oligocene collision of the Indian and Eurasian plate intensified the sedimentation rate far beyond the space created by basin subsidence, leading to the inception of the fluvial regime during the Mio-Pliocene time (*Worm et al. 1998; Alam et al. 2003; Uddin and Lundberg 2004*). The dominant facies evolved from a near-shore shallow marine to deep marine mud to a sandier facies regime during this time *(Alam et al. 2003)* (Figure 3-2). In the western part of the basin Gondwana sediments, with coal layers and volcanics, are followed by a thick sequence of shallow-marine clastic-carbonate sediments known as the Sylhet Limestone (Figure 3-2). Equivalent rock types in the eastern part of the basin are not known but are expected to be dominated by deep water mud. The Miocene sequence, the Surma Group, consists of alternating sandstone, siltstone, and shale *(Khan 1991)*, and is characterised by a 50-150 m thick laterally extensive marine clay at the top *(MPO 1987; Sohel et al. 2009)*, at least in the eastern part of the basin *(Imam and Hussain 2002; Mannan 2002)*. This appears as the Upper Marine Shale (UMS) in the stratigraphical column and is a major seismic reflector in the region *(Imam and Hussain 2002; Sohel et al. 2009)*. The UMS may separate fluvio-deltaic deposits above from marine mud–dominated deposits below. The UMS has very low vertical permeability as indicated by its role as a hydrocarbon cap rock in the region *(Reimann 1993)*. In the same way, the UMS likely marks the deepest extent of groundwater flow systems currently recharged at the surface of the basin *(Michael and Voss 2008)*.

The sedimentation history was different in different parts of the basin, with a passive margin, prograding-delta in the west *(Lindsay et al. 1991)* and active-margin, trench-slope depositional regimes in the east *(Gani and Alam 1999; Khan et al. 2002)*. In the eastern part, Mio-Pliocene sediments were deposited by a palaeo-Brahmaputra river, together with inputs from other easterly

derived rivers *(Uddin and Lundberg 1999)*, onto a shallow tidal shelf. Ganges fluvio-deltaic processes were active in the western part of the basin *(Lindsay et al. 1991)*. At the beginning of the Quaternary period, the Brahmaputra shifted its course and converged with the Ganges at the centre of the basin as a result of regional tectonic modification *(*e. g., *Steckler et al. 2008)*. Together, the Rivers Ganges and Brahmaputra have played a vital role in the formation of the extensive aquifer system in the region (section 3.3.1).

The Plio-Pleistocene Dupi Tila sands form the main aquifer of the elevated Barind and Madhupur Tracts. The Dupi Tila is also the main aquifer in the hilly region of Sylhet and parts of Chittagong. The Mio-Pliocene Tipam sandstone serves as an aquifer in the eastern folded hills of the Chittagong Hill Tracts. Holocene sediments form an aquifer at shallower depth (<100m bgl) in rest of the country.

The age of the rock units is difficult to determine as they do not contain fossils, and ages, in practice, are estimations based on the geological correlation with equivalent lithology in the nearby basin (Assam basin). A magnotostratigraphical approach was used by Worm et al. *(1998)* to determine the age of the exposed rocks in the north-eastern corner of the basin. Their study indicates that UMS is ~3.5 Ma old, while the Miocene rock unit, Upper Bhuban (Upper part of Lower Surma Group), is found to be ~4.5 Ma old i.e. Pliocene age (Figure 3-2).

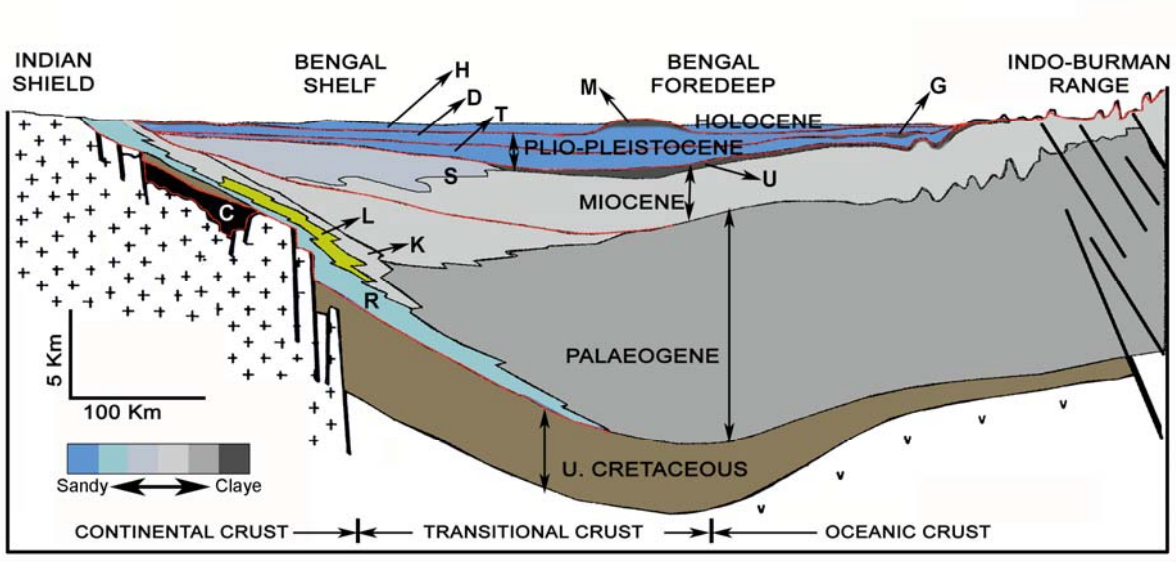

Figure 3-2: Generalised west to east geological section. Red colour indicates major period of non-deposition. In the diagram C= coal, R= Tura sandstone, K= Kopili shale, L= Limestone, S= Surma group, U= Upper marine shale – top surface of Surma Group, a major seismic marker, G= Girujan clay, M, Madhuphur clay, T= Tipam sandstone, D= Dupi Tila, H= Holocene alluvial deposits. Generalised distributions of the geological units were adopted from Imam and Shaw *(1985)*, Alam et al. *(2003)*, Reimann *(1993)* Alam et al. *(1990)*.

Table 3-1: Generalised stratigraphy of the Bengal Basin (adopted from *Alam et al. 1990; Dasgupta et al. 1993; Reimann 1993; Alam et al. 2003; Ravenscroft et al. 2005*).

Age		Stratigraphical unit		Lithology	Notes
Holocene		Alluvium	*Throughout, but mostly eastern part of the basin*	Fining upward, unconsolidated grey micaceous, fine to medium sand with organic silty-mud and peat	Forms the shallow aquifer throughout the floodplains
Pleistocene		Madhupur/Barind clay Dihing Dupi Tila/(Debagram & Ranaghat)*		Yellowish –brown to light grey, medium and coarse sand to clay; Very weekly consolidated; depleted in mica and organic matters	Forms major aquifers in the terraces, and deeper aquifer beneath the floodplains
Pliocene		Girujan clay Tipam/(Pandua)*		Yellowish-brown, weakly consolidated sandstone and mudstone	Minor aquifers in the eastern hills; Includes the UMS, a regional aquitard
Miocene		Surma/Jamalganj/ (Pandua)*		Alternating semi-consolidated sandstone and shale	
Oligocene	*Palaeogene*	Barail/Bogra/(Memari & Burdwan)*	*Well documented in the NW part of the basin*	Consolidated sandstone and shale	Minor aquifers in the northeast / Sylhet area
Eocene		Kopili shale Sylhet limetsone		Fragile shale and limestone	No significant aquifer
Palaeocene		Tura/(Jalangi)*		Sandstone with coal fragments	
Cretaceous		Rajmahal		Basalt, shale and sandstone	
Permian		Gondwana		Sandstone and thick/thin coal seams	
Precambrian		Basement Complex		Gneiss and schist	

() Denote equivalent unit of West Bengal, India*

3.2.5 Geological structure

The regional landform along with the basin margin features are the direct results of active tectonics in the region. Tectonically, the basin is sandwiched between the late Mesozoic NE-SW trending passive rifted margin of the Indian plate to the west, and the active Indo-Burman subduction related deformational complex to the east. Interaction of these mega-tectonic elements has resulted in diverse and active geological structural features in the basin, subduction-related features in the east, and intra-plate crustal readjustment features in the west (*Hoque and Khan 2005 and references therein*). Over the Quaternary time, these tectonic activities resulted in faults and lineaments in the basin which control the river courses. They were also responsible for block uplift and subsidence, and as a result, the generation of intra-basin elevated blocks and linear subsiding sub-basins (*Khandoker 1987; Goodbred and Kuehl 2000*). The Brahmaputra course follows the graben-like zone between the elevated Barind and Madhupur Tracts. :The Ganges kept its predominant course since inception of the delta along the Padma lineament, as has the

river Tista in the north along Tista lineament *(Khandoker 1987)*. In addition, the subsiding sub-basins enhanced the extent of marine transgression in the late Quaternary period *(Khan et al. 2003)*. There are a number of sub-regional basins (e. g., Sylhet basin, Hatia trough, Faridpur trough etc) *(Alam 1989; Reimann 1993)* with a range of subsidence rates. In the south-west coastal area the subsidence rate is 10 mm/yr, and in the Sylhet sub-basin subsidence is 15 mm/yr *(Steckler et al. 2007)*.

The aforementioned Shillong plateau in the immediate north of the basin is demarcated by an east-west trending inter-crustal fault, the Dauki fault *(*for detail see *Steckler et al. 2008 and references there in)*, on the northern periphery of the Sylhet sub-basin (Figure 3-1). Southward thrusting of the Shillong plateau has led to a smaller fold-thrust deformational front in the northern edge of the Sylhet sub-basin *(Hoque 2001)*. This hill range, and its equivalent in the eastern margin of the basin associated with the Indo-Burman subduction, exposes sandy sediments that may have been acting as a recharge zone for the aquifer-system in the basin. It is indicated by *Steckler et al. (2008)* that during the beginning of the Quaternary the deformation front associated with Indo-Burman subduction took its position along the along the present course of Brahmaputra River.

3.3 Geological evolution and aquifer system

Deposition of sediments in the Bengal Basin varied considerably with age and location. Despite the fact that present-day groundwater development is confined to the uppermost 100-400 m. For consideration of aquifer-system definition (*Maxey 1964; Laney and Davidson 1986; Seaber 1986*) it is necessary to understand the geology down to the Mio-Pliocene sequence (section 3.2.4). Geological evolution of the Bengal Basin, particularly during the Plio-Quaternary period, has had a strong control on the hydrogeology and the aquifer system. A number of studies have focused on aspects of Quaternary geology of different parts of the basin (e. g., *Morgan and McIntire 1959; MPO 1987; Davies 1989; Davies and Exley 1992; Umitsu 1993; Ahmed 1994; Roy and Chattopadhyay 1997; Worm et al. 1998; Goodbred and Kuehl 1999; BGS/DPHE 2001; Monsur et al. 2001; Allison et al. 2003; Goodbred et al. 2003; Ravenscroft et al. 2005; Acharyya and Shah 2007; Shamsudduha and Uddin 2007*). Almost all of these works are confined to the upper 100-150 metres of the sequence; as a result, hydrogeological understanding of the area remains incomplete, at least at depth. In this section, an attempt has been made to conceptualise the Plio-Quaternary geological evolution of the basin and its hydrogeological implications.

3.3.1 Plio-Quaternary evolution

The Bengal Basin entered a continental to deltaic depositional setting around the last episode of the Himalayan orogeny at the end of the Miocene / beginning of the Pliocene. Before this, a marine depositional environment prevailed *(*e. g., *Curray 1991)*. Globally, the time corresponded to a period of climatic instability *(Peizhen et al. 2001)*. At the same time a strong monsoonal

climate developed, leading to stronger denudation of the hilly ground and greater sedimentation in the basin areas. Sea-level low stands are marked as a gap in sedimentation in continental deposits, in contrast to continuous sedimentation in the equivalent marine sequences. Due to the basin setting, and active tectonism, the Bengal Basin experienced tremendous modification in a cyclic pattern over the whole Quaternary period *(*cf., *Niyogi 1972)* and attained its present form after the last glacial maximum.

3.3.1.1 Sea-level changes

Sea level has been a transient surface over geological time (*Haq et al. 1987; Pirazzoli 1993; Williams et al. 1993; Caputo 2007; Müller et al. 2008*). However, the global sea level trend is uncertain as tectonic influences on sea-level prior to Quaternary time are unknown (*Pirazzoli 1993; Williams et al. 1993; Müller et al. 2008*). Lisiecki and Raymo *(2005)* constructed the Plio-Quaternary climate record by combining isotopic measurements from 57 globally-distributed deep sea sediment cores. Their reconstruction since ~2.5 Ma, shows high amplitude global climatic cyclicity and variability in glacio-eustatic sea-level. The cyclicity was variable, changing to 100 ka cyclicity around ~1 Ma BP from the 41 ka cyclicity which was initiated around the end of the Pliocene. Approximately 10 such cycles occurred since the beginning of the late Quaternary i. e., since about 1 million years BP (*Williams et al. 1993; Caputo 2007*), but the sea-level record is best known from the upper Quaternary (*Williams et al. 1993; Caputo 2007*), particularly from 500-600 ka BP (Figure 3-3).

The magnitude of the sea-level low-stand has been found to be -120 to -130 m with respect to present day sea-level over the last several eustatic cycles (Figure 3-3). This magnitude may have been similar over the last 1 Ma, and half or even less during ~2.5 to 1 Ma BP judging from the magnitude of periodicities in the oxygen isotope record *(Lisiecki and Raymo 2005)*.

Sea-level in the recent eustatic cycle, at the time of the glacial maximum around 19 ka BP, declined by up to 130 m below the present-day level (Figure 3-3). Sedimentation and Quaternary delta evolution of the Bengal Basin reconstructed with respect to the sea-level variation over the last eustatic cycle (*Goodbred et al. 2003*) is limited to the sedimentation history of the upper 100-150 m. What happened in earlier glacial cycles? How did the basin evolve over these earlier eustatic cycles? How did continental sedimentation start after the Pliocene retreat of the sea? Answers to these questions would contribute to understanding of the hydrogeology of the basin.

3.3.1.2 Sedimentation, morphotectonics and landform evolution

Extensive marine clay deposition occurred, at least in the eastern part of the basin, around 3.5 Ma BP possibly associated with pre-Pleistocene high sea-level *(Worm et al. 1998)*, while the inherited basin margin topography determined the upstream limit of terrestrial sediments aggradations. The extensive marine clay is known as the Upper Marine Shale (UMS) (section 3.2.4), and is overlain

by a thick deposit of fluvial to deltaic origin. The switch from basin infilling to fluvial dissection coincided with a phase of Early-Pleistocene tectonic adjustment (the last episode of major orogeny in the Himalaya). This episode may have coincided with the sea-level fall. During much of the Quaternary time the Bengal Basin experienced cyclic erosion (during sea-level low stands) and subsequent infilling (during sea-level high stand). Remnants of the middle to late Quaternary deposits between Plio-Pleistocene equivalent deposits and Holocene deposits are to be expected. Sediments above the UMS, particularly the Holocene alluvium and the Pleistocene Dupi Tila sediments are widely exploited as aquifers.

Fluvial incision along the present-day major rivers during the Late Pleistocene time is widely accepted to have been initiated by sea-level decline (*Goodbred et al. 2003*). How was the Dupi Tila or equivalent deposit affected by cycles of fluctuating sea-level?

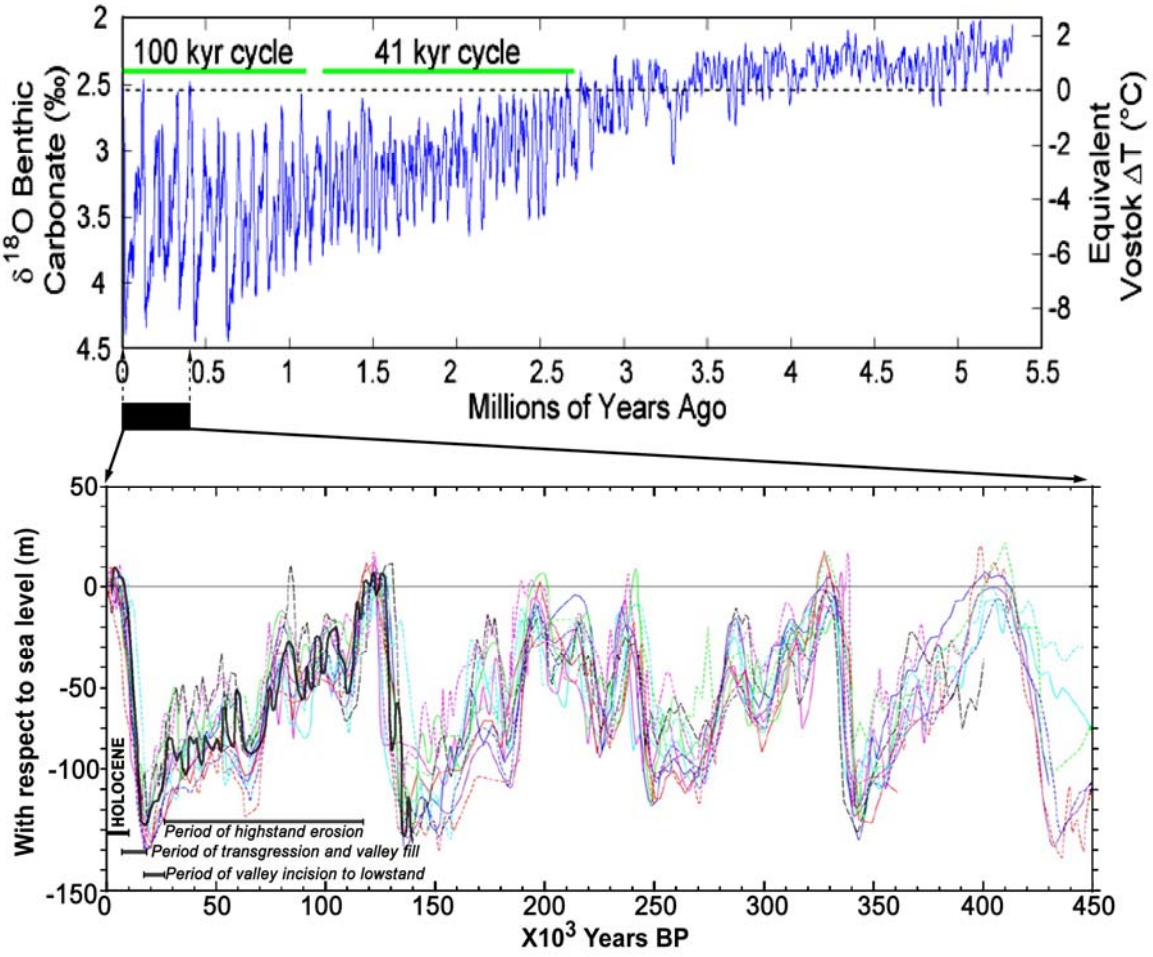

Figure 3-3: [Upper panel] Periodicities in the oxygen isotope record which may be a proxy of sea-level periodicities over the last 5 million years *(Lisiecki and Raymo 2005)*. [Lower panel] Global sea-level over the last 450 ka *(Caputo 2007)*; different colours represent 12 different studies complied by Caputo *(2007)*. Last glacial cycle is annotated with respect to sedimentation and the sea-level curve after BGS/DPHE *(2001)*.

Reconstruction of the depositional front is difficult for the Late Pliocene (~3.5 Ma BP). However, palaeogeographical reconstructions for the Miocene (*Alam 1989; Uddin and Lundberg 1999; Khan et al. 2002; Alam et al. 2003*) can be used to infer the Late Pliocene depositional front (Figure 3-4). It is assumed that depositional setting did not change significantly over the Mio-Pliocene due to a lack of tectonic movements until the beginning of the Pliocene, and the steady high stand of sea-level (Figure 3-3). The Bengal Basin became a remnant ocean basin *(Ingersoll et al. 1995)* at the beginning of the Miocene in response to the continued oblique subduction of India beneath and southeast extrusion of Burma. This remnant ocean basin setting may have continued up to the deposition of UMS (Figure 3-4). During this time a continental regime may have prevailed around the basin margin. The equivalent of the river Tista in the northwest, the Ganges in the west, and the Meghna and palaeo Brahmaputra in the east would have acted as the continental depositional frontier. At the same time much of the basin may have remained under the influence of the sea, as indicated by the extensive occurrence of UMS.

The Mio-Pliocene episode of the Himalayan orogeny *(Reimann 1993)* may be coupled with the beginning of the global high-amplitude oscillation in sea–level. As a result, the sea may have retreated southward (Figure 3-4). Dramatic changes in the depositional environment from deltaic to a chiefly fluviatile system would have taken place during this time *(Reimann 1993)*. Erosion in the newly created elevated terrain at the basin margin would be enhanced, and the river system would redistribute a large amount of coarse detritus across the vast, flat floodplain. Most of the sediment transport occurred from the northeast to southwest, while erosion of western hinterlands was providing sediments for the newly created sub-Himalayan basin. The Tipam Sandstone or equivalent deposits were deposited during this time, and alluvial to fluvial fan deposition took place in the northwest region of the basin. Gravelliferous beds in the Tipam-Dupi Tila sequence (*Mukhopadhyay 1982; Hossain and Zaman 2003; Haque 2006; Meetei et al. 2007*) may represent this alluvial to fluvial fan setting. Sedimentation caused channels to aggrade and then migrate or avulse to lower elevations. Repetition of these events developed the large-scale fan morphology in the shape of a fan in the region. Progradation of the alluvial fan may have been arrested by the position of the strait between subsiding Sylhet basin in the north-east and sea in the south (Figure 3-4). Alternating grey and oxidised brown sediments in the Dupi Tila *(Davies and Exley 1992)* may indicate early Plio-Pleistocene sea-level (40 ka cycle) fluctuation.

The paleo-Brahmaputra may have migrated to its current course during the Plio-Pleistocene episode of the Himalayan orogeny, following activation of the Oldham faults *(Bilham and England 2001)* in the northern side of Shillong Plateau which control the course of the river. Establishment of the Brahmaputra course would have reshaped the landscape and depositional setting. Deltaic depositional may had been underway during this time in the southern part of the basin.

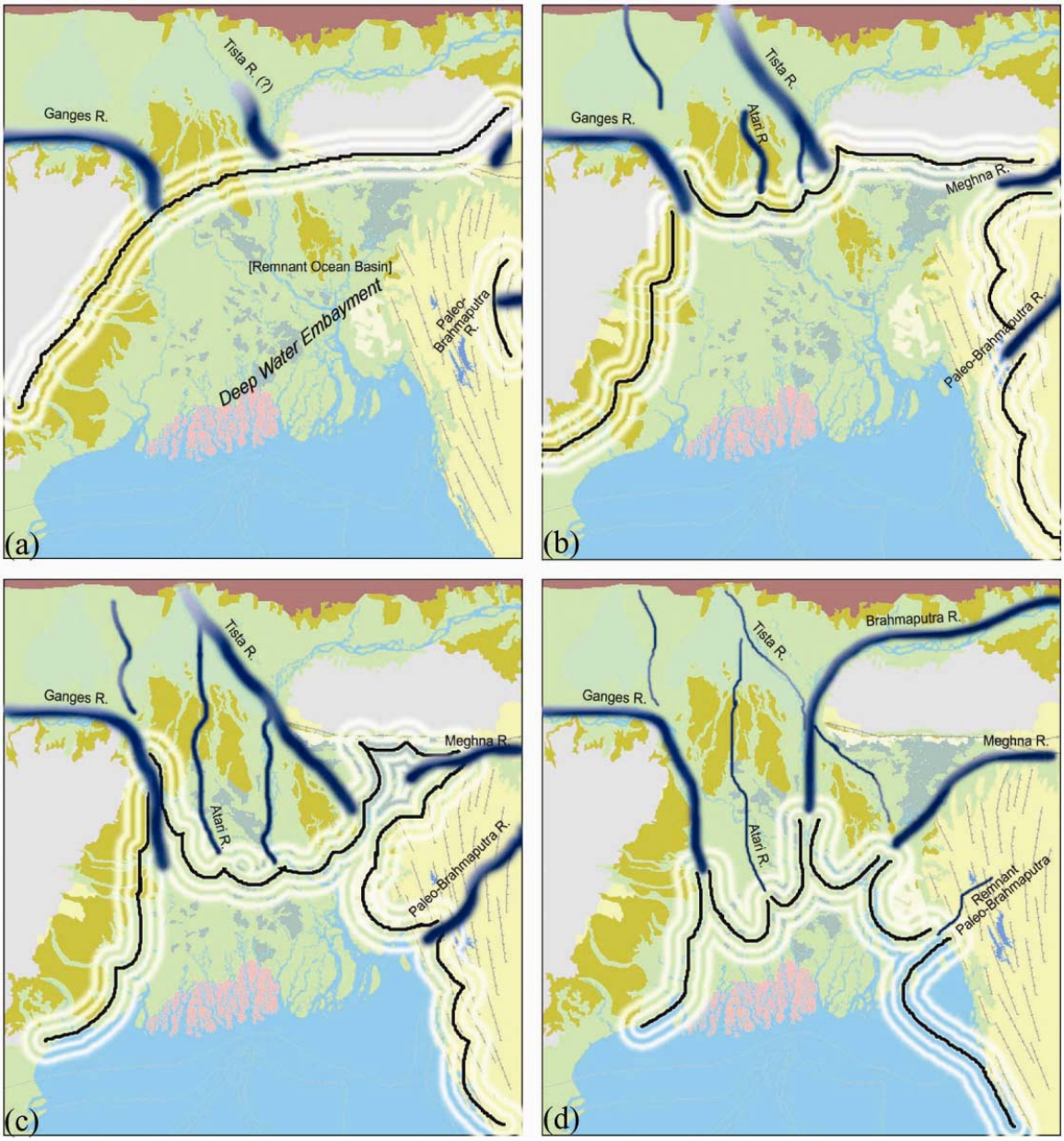

Figure 3-4: Conceptual cartoons of depositional fronts. (a) Late Miocene *(Alam 1989)* and (b) Pliocene depositional front; (c) Initiation of marine regression during Pliocene, and (d) possible establishment of Brahmaputra river course to its present position during Pleistocene from the paleo-Brahmaputra.

A continental to near-shore depositional environment appeared in the Bengal Basin following the Pliocene sea retreat. During most of the early Quaternary (3 to 1.5 Ma) a fluvial depositional regime appears to have been active, with the resulting widespread occurrence of the thick Dupi Tila Formation. Increased accommodation space in the basin may also be linked to global disequilibrium of the base-level associated with the fluctuating sea level *(Peizhen et al. 2001)*. Influx of sediment to the basin would have also increased during the time due to infilling of the sub-Himalayan basins and Indo-Gangetic plain. Curray *(1991; 1994)* and Peizhen et al. *(2001)* indicate that the sedimentation rate in the Bay of Bengal was not high during that period, however, Worm et al. *(1998)* report one of the highest rates of sedimentation in the world, 1.2 m/ka. Sediments carried by the rivers may have been trapped inland during the time. Moreover,

due to infilling of the foothill basins, the sediment source areas may have become closer. The proximity of the source areas is denoted by the poor sorting of the Dupi Tila sediments. The characteristic of Dupi Tila or equivalent sediments varies across the basin. For example, Dupi Tila in the north-west and north-east comprises gravelliferous beds while in the southeast, and probably also in the south, there is no significant amount of gravel. The Dupi Tila in the south is less coarse grained than in the north.

The basin geometry and sources of the sediments indicate that the Dupi Tila sediments possibly have been deposited in alluvial fan to fluvial settings in some parts *(Gani and Alam 2004)*. In the northwest, it is apparent *(*by definition of *North and Warwick 2007)* that the Dupi Tila was deposited in an alluvial to fluvial fan settings. The shift of the paleo-Brahmaputra from the east to the current course might have lead to the birth of several small rivers (equivalent to current Gumti River) in the eastern region. The Dupi Tila or equivalent sediments in the eastern region may have been deposited in a fluvial fan setting. Channel-fill sand bodies distributed in a regionally radiating orientation support this conceptualisation (see section 4.2.6 and 4.3.4).

Koss et al. *(1994)* conducted a laboratory study of the effect of sea-level induced base-level change on fluvial, coastal plain and shelf systems. The study revealed that the major period of sediment deposition occurs during marine transgression (induced by sea-level rise) following the glacial maximum of each cycle. This suggests that during Quaternary time, the Bengal Basin would have experienced several cycles of deposition and erosion from around 1 Ma BP when the 100 ka cyclicity appeared (Figure 3-3). This regime leads to deposition during sea-level high stands and the trangessive phase of each cycle, and erosion of almost all the previous deposits during the sub-sequent sea-level low stand and the steady fall in base level. Similar magnitude of base-level drop during the sea-level low stands (Figure 3-3), and insignificant subsidence rate, have led to a limited preservation of the sediments deposited during the earlier eustatic cycles. In the stratigraphical column *(Alam et al. 1990; Reimann 1993)* these mark an unconformity i. e., a long time of virtually non-deposition.

Some of the deposits of the previous eustatic cycles may have preserved in the southern part of the basin, and in the Sylhet sub-basin region, due to subsidence. In contrast, in areas of steady tectonic uplift associated with subduction tectonics (e. g., elevated land in the east, the Khashia hills in the north, the Pleistocene Tracts) there is an insignificant potential for preservation of the earlier deposits. Deposits from the earlier high stands and transgressive phases may have been completely eroded due to base level fall in the following low stand. Steady erosion during low stand conditions was further facilitated by the long duration of steadily falling sea-level after each high stand (Figure 3-3). If the subsidence rate is assumed to be 2 mm/year for 10,000 years of effective sedimentation in each cycle, over 10 such cycles (during the later part of the Quaternary period) a 200 m thick sequence of deposits would be expected in between the Holocene and earlier Pleistocene deposits (~1 Ma to 18 ka BP), at least in the southern part of the basin. The

thickness of the pre-Holocene sediments is dependent on the rate of subsidence and uplift. This is evident in the higher thickness of silty-clay to clay deposits below the Holocene deposits in the southern part of the basin, particularly in the SW, (associated with penecontemporaneous pedogenessis in stacked floodplains over several eustatic cycle - section 3.3.2.2). Sub-surface modelling based on 1573 lithological logs from the southern part of Bangladesh indicates juxtaposed stacked channel-fill sand bodies and thick interfluves in some parts (Figure 3-5). The most recent episode of transgressive and high-stand deposits (starting ~18 ka BP) characterise the topmost ~100 m of the sedimentary sequence. These deposits are widely known as Holocene deposits, and host the shallow aquifer system with excessive dissolved arsenic. Many descriptions of the origin and variability of these deposits are found in literature (e. g., *Goodbred and Kuehl 2000; Allison et al. 2003; Goodbred et al. 2003 and references therein*).

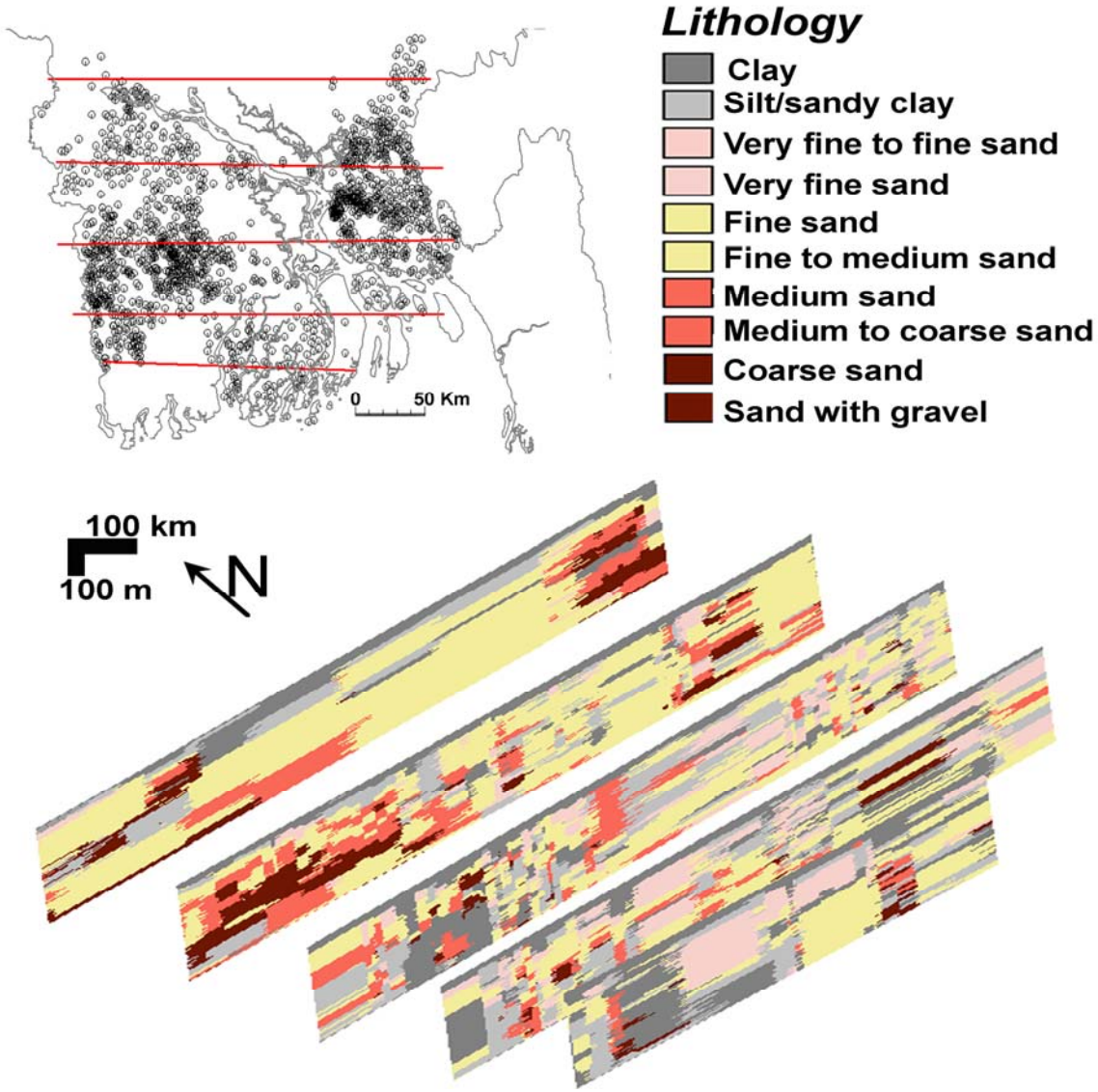

Figure 3-5: Distribution of sediment lithologies in southern Bangladesh. Lithological cross-sections in southern Bangladesh based on 1573 lithological logs, in a 2000x2000x3 m grid, were interpolated using the Rockwork mapping package (RockWare Inc. Golden, CO, USA) applying the inverse distance algorithm.

The Late Quaternary history of the basin (~18 ka to present) was influenced by immense sediment loads, eustasy, and tectonics *(Goodbred and Kuehl 2000)*. The last episode of rapid sediment trapping and delta growth started around ~10 ka BP with the inception of sea-level rise. This transgression led to back flooding of low-stand alluvial valleys. Channel sands continued to be deposited, and fine-grained sediments were deposited on adjacent newly developed floodplains. By ~7 ka sedimentation slowed as the rate of sea level rise began to ease. At the same time the stability in the shoreline led to instability of the channels and widespread dispersal of sand. The current shape of the delta appears to have developed between ~5 ka and by ~3 ka. By the mid-Holocene a ~50 m thick transgressive sequence had been deposited, which was overlain by a ~30-40 m thick high-stand deposit. Goodbred and Kuehl *(2000)* estimate Late Quaternary sequences (from ~20 ka) to be 50-90 m thick, locally thinner around uplifted Pleistocene terraces. However, BGS and DPHE *(2001)* reported ~140 m thickness of the equivalent deposits in eastern and south-central Bangladesh, possibly from an incised channel-fill location.

Sediment colour is an attribute of these Plio-Qauternary deposits, and is greatly varied spatially and vertically throughout the basin. Sediment colour has two influences: syn-depositional pedogenesis, and post-depositional weathering. Intra-strata oxidation of thinner layers may be largely associated with syn-depositional processes. In contrast, at the basin margin, across elevated Pleistocene upland areas, and possibly preserved within the basin, thick oxidised sequences would be associated with post-depositional aerobic weathering (section 3.3.3). In general however, throughout the basin, sediments are gray in colour reflecting the predominant reduced conditions.

3.3.2 Geological evolution of the aquifers

3.3.2.1 Aquifer genesis and age of the aquifer sediments

With the exception of the NW where depth to the basement is within 200 m of ground surface in places, the upper 2000 metres of the sedimentary sequence has the potential to be used as an aquifer in most parts of the Bengal Basin. In terms of economic feasibility and development practices, the uppermost 400 m comprises the aquifer under exploitation. Sediments overlying the UMS form an interconnected aquifer system locally manifested as multi-aquifers due to the ubiquitous distribution of low permeability strata within the predominantly sandy sequence (section 3.3.1.2). The entire aquifer system is composed of horizontal to sub-horizontal discontinuous layers of sand, silt, clay, and their mixtures, with the occasional presence of gravel. In addition, channel sand bodies associated with channel migration or avulsion make the aquifer fabric complex and heterogeneous.

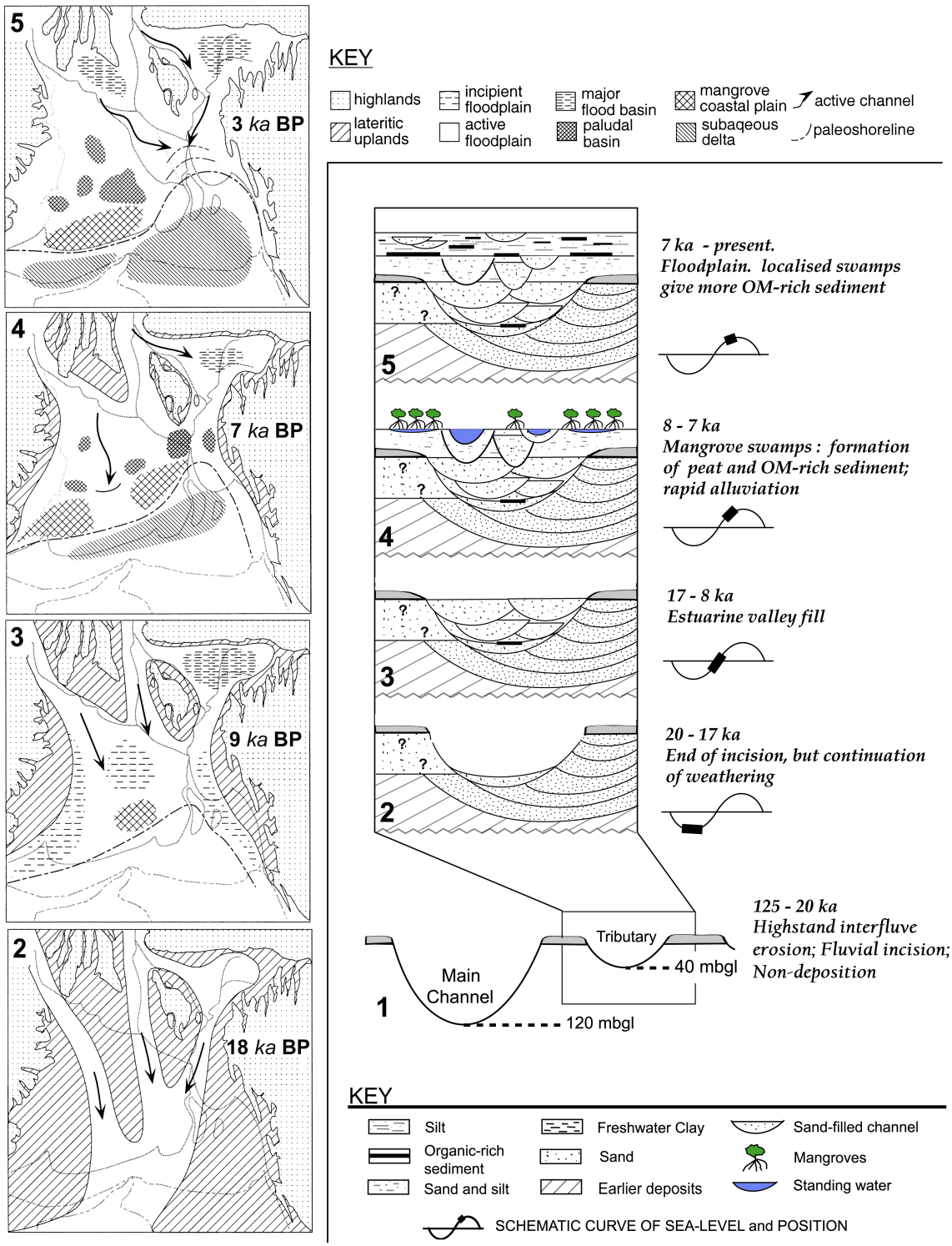

Figure 3-6: Sedimentation during the last glacial highstand. Left in a map view taken from *(Goodbred and Kuehl 2000)*, and right shows sedimentation in a tributary adopted from *(McArthur et al. 2008)*.

The aquifer system comprises sediments of Upper Miocene to Recent age *(Reimann 1993)*. During these times there were several phases of deposition and non-deposition. Taken with the lack of dating data, this makes it difficult to construct a chrono-stratigraphy of aquifer sediments. Compilation of radiocarbon dates *(Brammer 1967; Davies and Exley 1992; Umitsu 1993; Hait et al. 1996; Goodbred and Kuehl 2000; BGS/DPHE 2001; Zheng et al. 2005; von Brömssen et al.*

2008) indicates that sediments in the uppermost 90 m (and to 137 m in places) were deposited after the last sea-level low stand around ~20 ka (Figure 3-7). There is no available ^{14}C age deeper than 137 m. In the northern part of the basin, Pleistocene sediments outcrop and in the surrounding region sediments of age <20 ka are very thin. Two ^{14}C dates, from 45 m depth between the Madhuphur and Barind Tracts *(Davies and Exley 1992)* and from 21 m depth, 40 km east of Dhaka at the edge of Madhupur Tract *(Zheng et al. 2005)*, are reported at >45 ka, close to the practical limit for radiocarbon dating *(Zheng et al. 2002)*. Using the cumulative inventory of 10Be atoms Whitney et al. *(1999)* determined the age of the pedogenic alteration and isolation of the Madhuphur and Barind Tracts to be 110 ka and 25 ka BP respectively. This indicates that these tracts were exposed throughout the last glacial cycle, at least at the last sea level low stand. In terms of magnetostratigraphy, Worm et al.*(1998)* estimate <2 Ma for the age of the Dupi Tila sediments whose topmost few metres (at places tens of metres) on the Madhuphur and Barind Tracts weathered to a clay residuum under prolonged sub-areal exposure and low groundwater table conditions (see section 3.3.2.2).

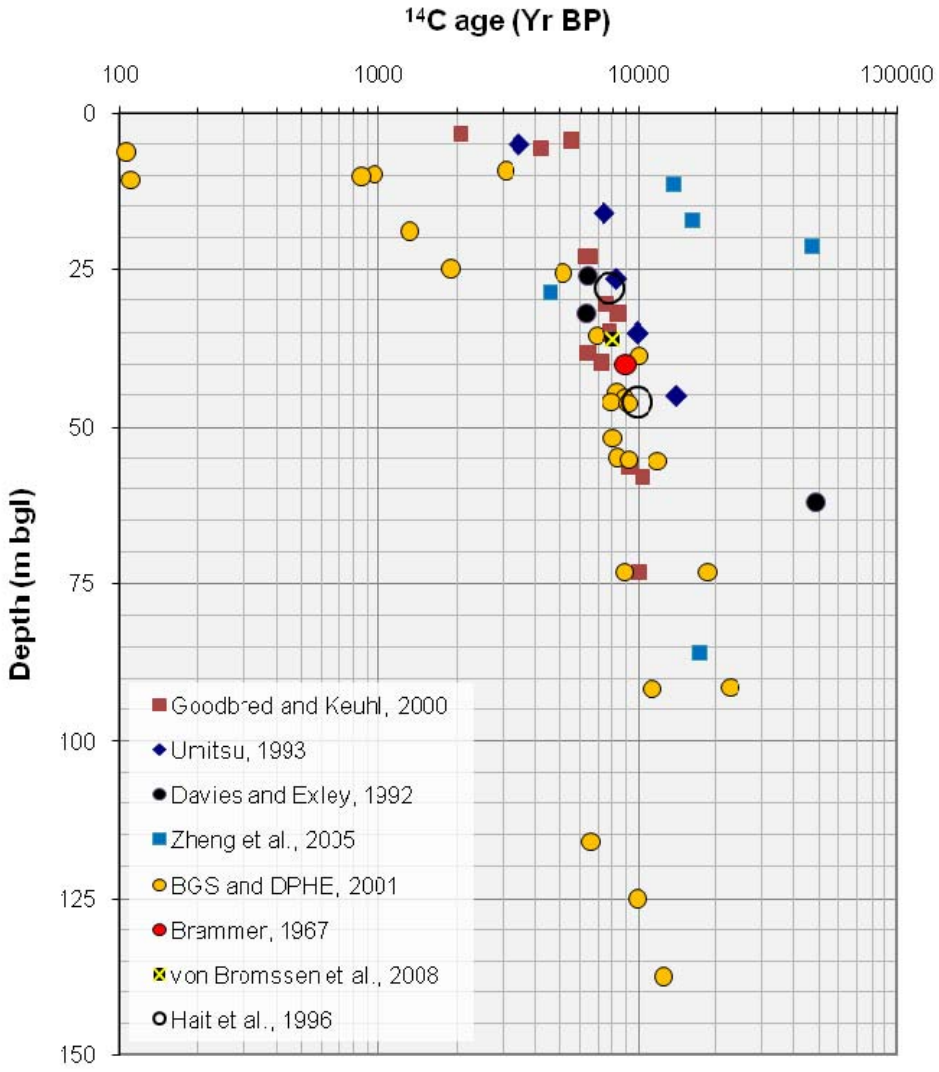

Figure 3-7: Complied ^{14}C ages of sediment from different parts of the basin (sources of data are shown in the legend).

Sediments around the Barind Tract and between the Barind and Madhupur Tracts are mostly of Holocene age (<20 ka BP). In some areas around the Barind Tract Holocene sediments may rest directly on Precambrian basement, which occurs at <200 m depth. Due to the shallow depth of the basement and the steep topographic gradient along the river Brahmaputra including its tributaries, this area may have experienced complete erosion during the sea-level low stands. If so this area receives fresh sediments in each eustatic cycle during the transgressive period. Conversely, in the southern part of the basin subsidence leads to preservation of sediments from earlier eustatic cycles (100 ka cycle) (Figure 3-8). Therefore, ages of sediment between the Holocene and Dupi Tila sediments might be expected to be > 20 ka but <1 Ma. The thickness of these sediments is estimated to be around 200 m (section 3.3.1.2). Equivalent sediments would not be expected to exist where tectonic uplift occurred in the current piedmont areas of the eastern Indo-Burman (Chitagong-Tripura) hill range.

Ages of the stratigraphic units in Bangladesh have been estimated on the basis of lithostratigraphical analysis and geological correlation with the upper Assam basin in the NE (e. g., *Reimann 1993; Alam et al. 2003*). The age of the UMS, which corresponds to the last pre-Pleistocene high sea-level stand (Figure 3-3), is found to be 3.5 Ma based on magnetostratigraphical dating. The Tipam Sandstone, overlying the UMC, is dated at between 2.6 and 3.5 Ma BP.

In summary, sediments up to 90-140 m thick of Holocene age (<20ka), overlie about 200 m thickness of sediments aged 20 ka to 1 Ma. Both these sediments overly and/or overstep Plio-Pleistocene sediments of 1-3.5 Ma age. The entire sequence lies on the UMS aged >3.5 Ma (Figure 3-8).

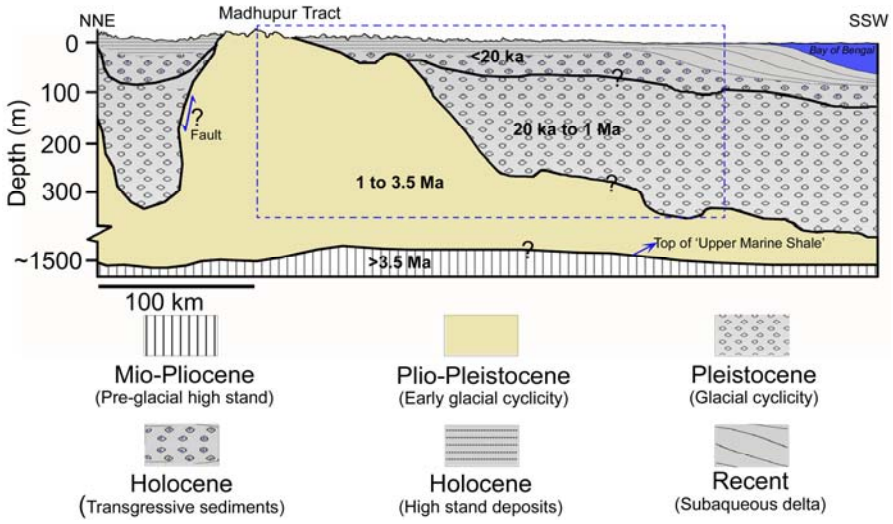

Figure 3-8: Conceptual diagram on the age of aquifer sediments in a NNE to SSW section across the basin. Thicknesses of the sediments are estimated; note the breaks in the depth scale. Thickness for the Holocene is taken from Goodbred and Kuehl *(2000)*, while other are estimated based on the logs and subsidence (see text). Area marked with dashed-blue-line is detailed in figure 7-2.

3.3.2.2 Aquifer modification and development of hydraulic anisotropy

As described in the preceding section the aquifer system in the basin was developed over the past 3.5 million years. Over this time, the Bengal Basin experienced tectonic disturbance and eustatic cyclicity. All the sediments within this aquifer system are unconsolidated to semiconsolidated in nature, and deposited under fluviatile-deltaic settings. Penecontemporaneous pedogenesis and post-depositional weathering induced by a low groundwater-table, have played a significant role in addition to post-depositional diagenetic changes. Eustatic cyclicity over the entire Quaternary period has caused erosion during the onset of every low stand, and almost equivalent re-deposition during the subsequent sea-level rise and high-stand phase. However, subsidence has facilitated preservation of the deposits of earlier eustatic cycles in the southern part of the basin. These phases of erosion-redeposition and preservation of the remnant sediments have influenced evolution of the aquifer and its characteristics across the region.

The age of the aquifer sediments varies spatially as Pleistocene sediments are exposed as blocks of elevated ground, around which Holocene sediments are thin, becoming thicker across the neighbouring floodplain and the southern deltaic areas. Sediments in the Madhupur and Barind Tracts may have been deposited in an alluvial to fluvial fan setting over several episodes of intense sedimentation, forming an interconnected landmass (Figure 3-4). This landmass may have been dissected with the establishment of the present course of the Brahmaputra during late Pleistocene orogenic episode, which in pre-Pleistocene time flowed through the Indo-Burman Hill range as the paleo-Brahmaputra *(Uddin and Lundberg 1999)*. The same orogenic episode may have triggered the genesis of compressive faults in the east and west of Lalmai Tract *(Hossain et al. 2001)*. Uplift-induced aerobic weathering led to the formation of the tracts landscape, similar to that of the present-day Barind and Madhupur Tracts. Present-day landform in the central and NW part of the basin is the result of geological modifications by the Brahmaputra and other rivers, over the entire Quaternary period. Pleistocene Tracts suffered non-deposition during most part of the Late Quaternary, although BGS and DPHE *(2001)* report thin layers of 2 - 3 m thickness of earlier eustatic cycles on the western edge of the Madhupur tract. In general, the area along the Brahmaputra and the extreme NW are the most active areas, and these suffered several cycles of almost entire erosion and re-deposistion during the eustatic cycle of sea-level rise and fall. It can be suggested that a maximum of about 100 m thickness of Holocene sediments rest on the Pleistocene deposits across the region. These most recent sediments are hydraulically more transmissive than that of their neighbouring and underlying Pleistocene sediments *(Ravenscroft 2003)*.

Sediments deposited in different phases of the eustatic sea-level cycle have specific characteristics. Sandier deposits of the TST (transgressive system tract) grade towards an organic-rich mud with the HST (high stand tract) condition attained in a fluvio-deltaic setting (Figure 3-6). Location in the basin (i. e., proximity to the source area) determines the size fraction of the

deposits. In vertical column they form a sequence of alternating, laterally-discontinuous sands and silt-clays.

Pedogenesis (Figure 3-9) remains active as a process intimately related to floodplain-deltaplain sedimentation *(Kraus 1999)*, and is the main cause of colouration of the sediments and genesis of paleosols. Channel-floodplain-deltaplain and marine deposits are gray in colour as they are deposited by water, and / or the groundwater-table remains close to the surface *(Van Houten 1973)* and reducing conditions predominate. The penecontemporaneous pedogenesis and weathering associated with a low groundwater-table alter the sediment colour to dark-gray, bluish gray, and brown to red depending on the redox environment. Relatively well drained, light brown paleosols with a yellowish to orange subsurface horizon form on sandy natural levees and crevasse splays. In contrast, dark-coloured silty clays interpreted as gleyed alluvial soils form in the backswamps *(Kraus 1999)*. Kraus *(1999)* also explained the formation and maturity of plaeosols in a sequence stratigraphical framework: abundant overbank deposits with weakly developed paleosols should characterize the TST, whereas lower amounts of overbank deposits with well-developed paleosols are typical of the HST (Figure 3-9). Whatever the case, paleosol formation leads to a reduction of permeability, and in many cases to the formation of clays.

In contrast to penecontemporaneous pedogenesis, lowering of the groundwater-table associated with sea level decline may induce aerobic weathering throughout a thick unsaturated zone over several metres above the groundwater level *(Van Houten 1973)*. Across the Barind and Madhupur Tracts aerobic weathering during past eustatic sea-level cycles has resulted in the formation of a thick sequence of oxidised sediments. A similar mechanism may have acted in the eastern hilly areas, as indicated by the yellowish colour of the Tipam and Dupi Tila formations. In addition, these fluvio-deltaic deposits have also undergone penecontemporaneous pedogenesis and the weathering of mica within the sediments which have reduced the bulk permeability of the sediments. In many places throughout the basin, red coloured sediments occur at depth which may be associated with the pedogensis or aerobic weathering. For example, a reddish to yellowish brown sand layer in Matlab at 36 m depth *(von Brömssen et al. 2008)*, and the occurrence of a oxidised sand layer in Khulna below 46 m *(Umitsu 1993)* indicate aerobic weathering during the last LST. In both cases the overlying sediments were dated to be around 10 ka BP, the beginning of the latest TST.

Reddish to yellowish brown Holocene sediment in the Lakshmipur area *(BGS/DPHE 2001)* may also be associated with pedogenesis. However, reddish to yellowish brown sediments are also to be found at greater depth in the southeast Bangladesh, at around 100-200 mbgl (Figure 3-10). These oxidised sediments may be the product of earlier eustatic TST and LST phases. Confirmation of this requires dating of the sediments. Repeated aerobic weathering would lead to a pervasive reddish colouration as seen on the Barind, Madhupur, and Lalmai Tracts. The reddish-

coloured sediments of earlier cycles may be better preserved in the SW than in SE and NW Bangladesh due to nature of sedimentation-subsidence-erosion prevailed in those regions.

Channel migration and avulsion are frequent in fluvio-deltaic environment, leading to spatial and vertical variation between channel and interfluve deposits. If however channels and interfluves remain static over a long period of geological time, greater thicknesses of channel and interfluve deposits may be expected in the sedimentary sequence. Interfluves may have been static in some regions in the southern part of the basin, leading to the preservation of stacked interfluve sediments 100 to 200 m in thickness (Figure 3-5), of bluish to dark gray coloured clays to silty-clays.

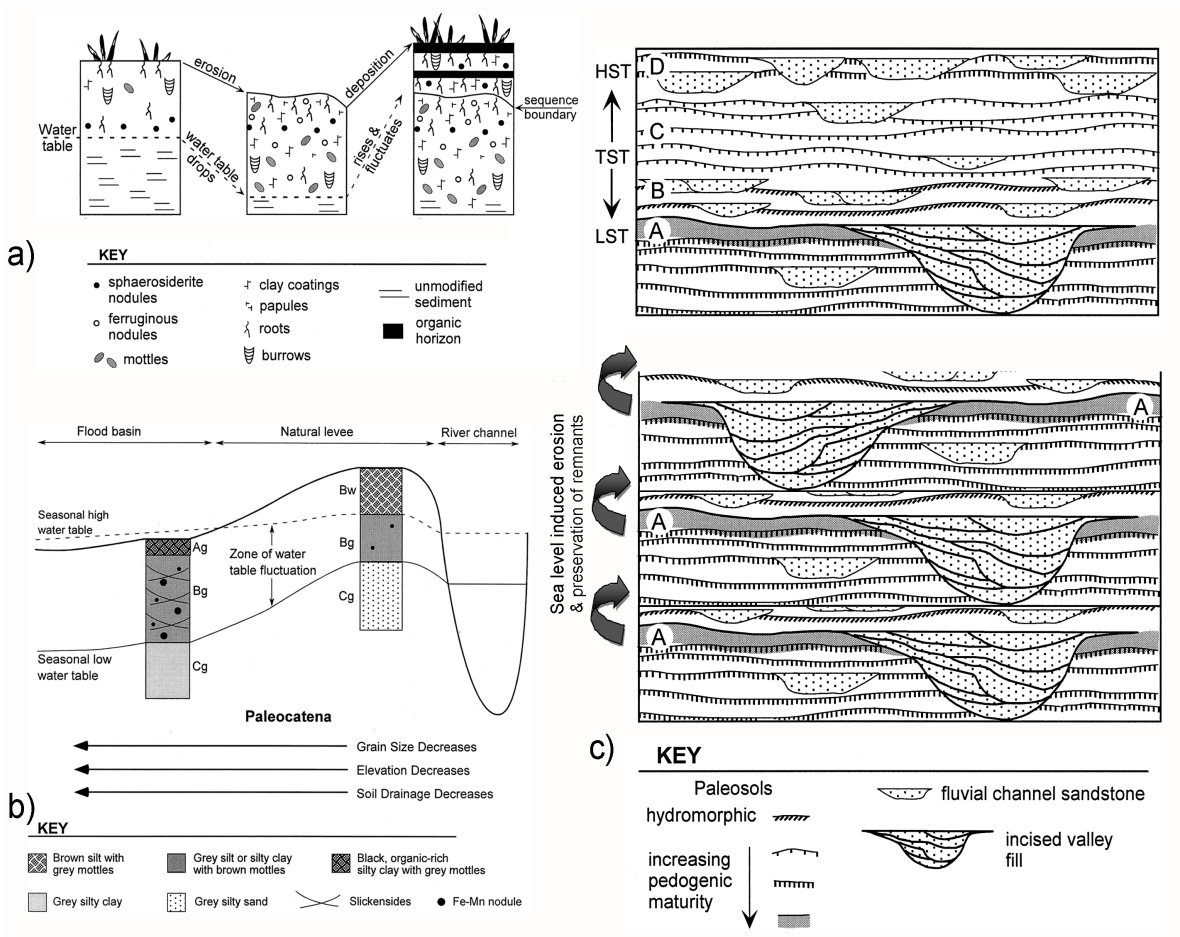

Figure 3-9: Two main processes of penecontemporaneous pedogenesis in the fluvio-deltaic terrain, and pedogenic development related to the sea-level cycle *(*after, *Kraus 1999)*. (a) sequential development of an interfluve paleosol, (b) Pedogenesis processes in channel-floodplain setting. A moderately or well-drained soil generally forms on theeleve although subsurface horizons can be gleyed_Bg horizon, because of proximity to the groundwater-table. Poorly to very poorly drained soils are more typical of the floodbasin; (c) pedogenic development related to the sea-level cycle (upper part), while lower part shows how repetitive eustatic cyclycity, and subsidence would lead to erosion of the upper part of the TST and the entire HST deposits, and preserve the entire LST and the lower part of TST in the sediment sequence.

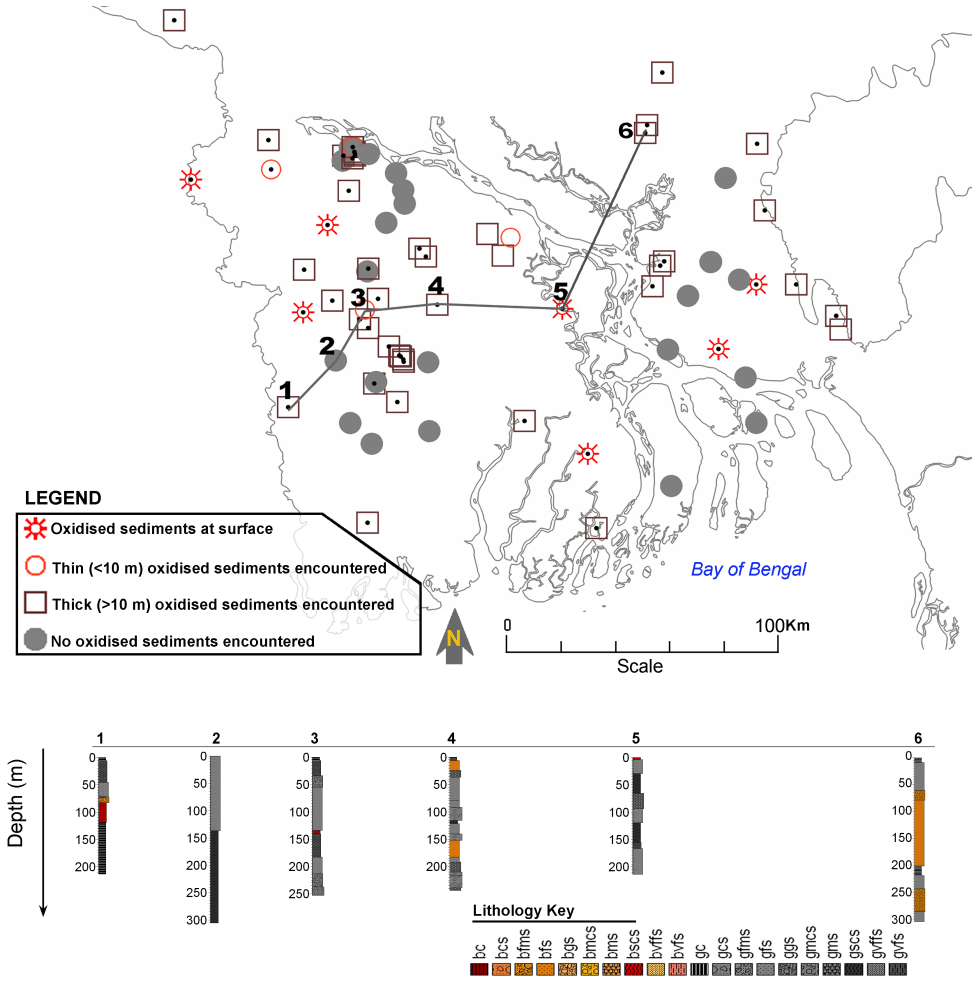

Figure 3-10: Sediment colour distribution in southern Bangladesh. Lithological code prescript 'b' indicates yellowish-brown i.e. oxidized sediments; prescript 'g' indicates grey i.e. reduced sediments. 'c' = clay, 'scs' = silt-sandy clay, 'vfs' = very fine sand, 'vffs' = very fine to fine sand, 'fms' = fine to medium sand, 'ms' = medium sand, 'mcs' = medium to coarse sand, 'cs' = coarse sand, 'gs' = sand with gravel. Where symbols contain a centrally placed black dot, oxidised sediments are encountered at <100 m depth. Note that oxidized horizons occur at depth within predominantly reduced sequences in places (1, 4) and reduced horizons occur at depth within predominantly oxidized sequences of the Pleistocene inliers (6).

In recapitulation, a dispersed pedogenic colouration of sediments should be expected throughout the aquifer system, and more regularly in the Pleistocene deposits which also underwent areal several episodes of weathering under conditions of a low groundwater-table. Deposits of HST, and part of TST of past sea-level eustatic cycles would have been eroded during the following low-stand. The Holocene HST sediments would be expected to contain large amount of discontinuous silt-clay layers distributed throughout the sands. Relatively low permeability sediments affected by pedogenesis and/or aerobic weathering during the earlier eustatic cycles could be anticipated between Holocene and Early Pleistocene sediments in the southern part of the basin. These would be expected to be laterally discontinuous and vertically thin because of the migratory channel-interfluve deposition and erosional settings.

3.3.3 Aquifer nomenclature and classification

The classification of the aquifer of the Bengal Basin is a matter of long standing debate; whether it is a single or multiple aquifer (*Mukherjee et al. 2007b; Michael and Voss 2008*). By nature, it is not a laterally continuous layered aquifer system. Rather silt-clays layers are distributed ubiquitously, varying spatially and vertically, and forming a multi-aquifer locally. The putative lateral continuity of low permeability materials in between shallower and deeper sediment gave the impression of two aquifers: a shallow and a deep aquifer. The debate gives rise to two key issues: the level of physical separation between the aquifers, and the interconnectedness of the flow system – is it a single interconnected system or two separate flow systems (Figure 3-11)?

3.3.3.1 Existing aquifer nomenclature

Not until 1980s was attention paid to aquifer classification in the Bengal Basin (*MMP/HTS 1982; UNDP 1982; MPO 1987*). However, interest was limited to the upper 100-150 m until the discovery of excessive dissolved groundwater arsenic (As) in the 1990s. The discovery of As has led to the development of deeper groundwater below 150 m, which is essentially As-free. Nonetheless, deep groundwater (>150 m) was exploited in the coastal areas before the advent of As due to high-salinity of the shallower aquifer.

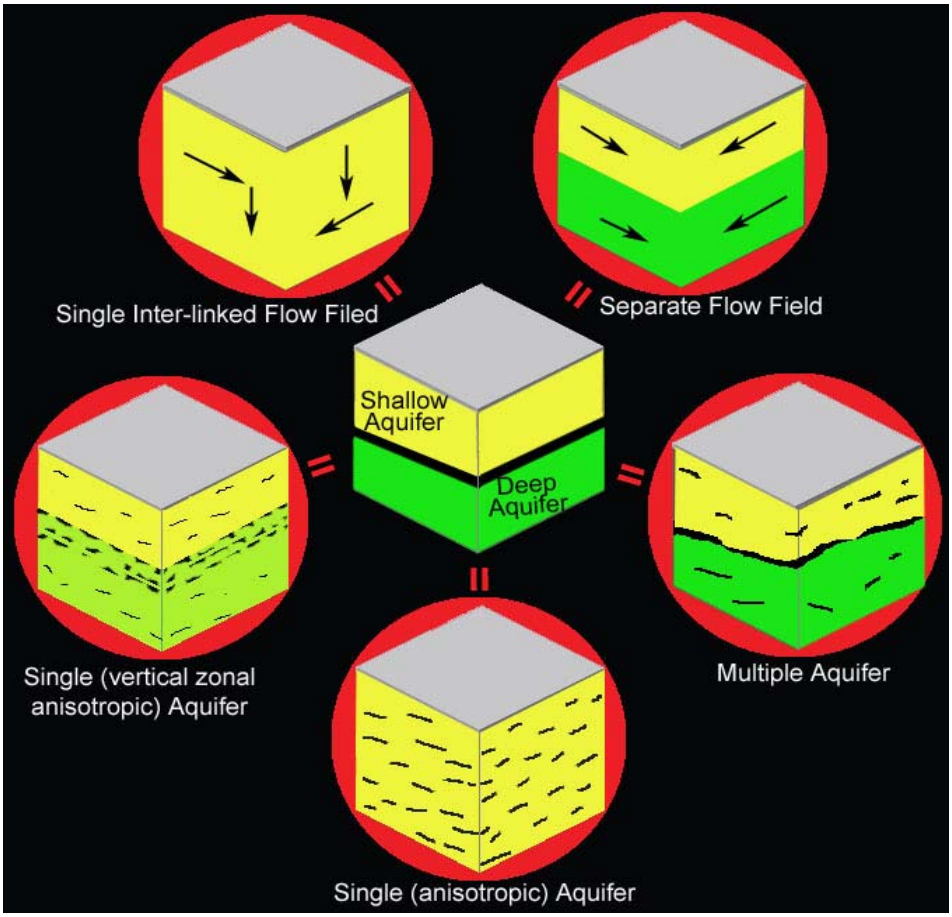

Figure 3-11: Conceptual possibilities of flow and nature of distribution of low permiability materails in the Bengal Aquifer System

Jones *(1985)* proposed six separate aquifers to a depth of ~1500 m bgl by analysing petroleum drilling log data from the eastern part of the country. UNDP *(1982)* described the aquifer as having three layers in the upper ~100 m when previously 2-layer descriptions had been accepted *(*see in *Ravenscroft 2003)*. A 3-layered model was later adopted by MPO *(1987)*. EPC/MMP *(1991)* uses a four-layered system in modelling studies of central Bangladesh. These early views of the hydrogeology of Bangladesh were summarised by Ravenscroft *(2003)* (Figure 3-12a) who proposes a stratigraphically-based hydrostratigraphical classification. Due to lack of data on the extent of the stratigraphical units and their hydraulic continuity, and subtle differences in the hydraulic characteristics, this recommendation is however difficult to follow.

Several classification have recently been put forward which include the deeper part of the aquifer (*Aggarwal et al. 2000; BGS/DPHE 2001; DPHE/DANIDA 2001; GWTF 2002; DPHE/DFID/JICA 2006; Mukherjee et al. 2007b*). The conception of a discrete deeper aquifer has its basis in the experience of utilisation of a deeper aquifer in the coastal regions. In the coastal regions, a silt-clay aquitard is present at about 100-150 m. On the basis of isotopic composition of groundwater IAEA described the aquifer as having four water types in a 3-layered system *(Aggarwal et al. 2000)* (Figure 3-12b). BGS/DPHE *(2001)* adopted the UNDP *(1982)* classification for the upper ~150 m with the 'upper shallow aquifer' and 'lower shallow aquifer' nomenclature, and added a 'deep aquifer' to the classification for depths greater than 150 m bgl (Figure 3-12c). The Groundwater Task Force *(GWTF 2002)* has proposed a chronostratigraphical classification of the aquifer system: Upper Holocene aquifer, Middle Holocene aquifer, Late Pleistocene-Early Holocene aquifer, and Pleistocene aquifer (Figure 3-12d). A similar chronostratigraphical classification has been proposed by Ahmed *(2003)* incorporating the north to south variation in the distribution of the chronological units. In contrast to all these classification DPHE/DFID/JICA *(2006)* proposed a 'deep aquifer' as 'As-free' and with a clay layer (at least 10 m thick) separating it from the shallower aquifer, which may occur at shallower depth (<150 m) depending on the local geology. None of these studies adequately consider the lithological framework of the aquifer in their classification. In a recent study in the western part of the basin in West Bengal, India (*Mukherjee et al. 2007b*) classified the aquifer as an interconnected single aquifer system with a multi-aquifer in the coastal areas based on lithological analysis (Figure 3-12f).

With all these classifications, the question remains whether there is a discrete deeper aquifer which is hydraulically separated from the shallow aquifer. If the confining unit(s) are discontinuous how does the flow system operate, and if they are different, how stable are they?

3.3.3.2 Single or multi aquifer

Aforesaid analysis by *Mukherjee et al.*(*2007b*) indicates there is no physical separation by continuous low-permeability material between a shallower and a deeper part of the aquifer. An

equivalent conclusion was reached by reanalysis of 1573 driller's log from DPHE/DFID/JICA *(2006)* for the southern Bangladesh to an average depth >250 m in the present research (Figure 3-5). Regional 3D hydrostratigraphical analysis for eastern Bangladesh (see chapter 4) reveals a similar scenario, however with a zone of higher frequency of occurrence of finer materials between the shallower and deeper part of the aquifer (see chapter 4). Moreover, in all these studies it is found that the low permeability materials have a limited areal continuity. Although, this situation may facilitate discrete flow systems locally, they may not be sustained under large scale development of groundwater.

Monitoring of hydraulic head data is carried out by BWDB through a network of about 1200 monitoring wells, but is limited to the shallower part of the system. However, some previous studies in Bangladesh have observed different heads in the shallower and deeper part of the system locally (e. g., *BWDB 2005; Zheng et al. 2005; Harvey et al. 2006*). The age of groundwater in the shallower and deeper part of the system is different: shallow groundwater is young (in the order of a hundred years) and deeper groundwater is old (up to several thousand years) (e. g., *Aggarwal et al. 2000; Harvey et al. 2002b; Zheng et al. 2005; Stute et al. 2007; also Chapter 5*). Distinct geochemical differences between groundwater of the shallower and deeper part of the aquifer have also been reported from different parts of the basin (*BWDB 2005; Zheng et al. 2005; DPHE/DFID/JICA 2006; Mukherjee 2006; Mukherjee et al. 2007a; Mukherjee and Fryar 2008*).

In summary, although physical separation between the shallower and deeper part is not continuous, hydraulic head, groundwater age and groundwater chemistry may be indicative of separate flow systems. The separation may not be sustainable when stresses by pumping, where physical separation is not present, and this requires further study. A previous study by *Mukherjee et al.* (*2007b*) describes the aquifer as a single aquifer regionally, and a model study by *Michael and Voss (2008)* represented the aquifer as a single anisotropic aquifer at the whole basin scale. This study also supports the view of a single aquifer system (chapter 4), but proposes that discrete flow-systems operate at the shallower and deeper levels of the aquifer (chapter 6). In this thesis the term 'Deep Aquifer' will be used throughout to mean the aquifer or part of the aquifer below 100 m. This is the paradigm currently in use in Bangladesh.

3.3.3.3 Possibility of preferential flow paths

In reference to section 3.3.2.2 it is understood that aquifer is composed of linearly extensive channel-fill sand bodies, and interfluves of finer materials (clay, silty-clay, very fine sand). It has been assumed that the channelized bodies of sand may be acting as preferential flow paths *(*e. g., *Ravenscroft 2003)*. In general, sand is the dominant component of this aquifer system (see section 4.2.6.1), but analysis presented below suggests that if consideration is given to the sand-clay ratio these linear sands would not produce significant preferential flow paths (see section 4.3.4).

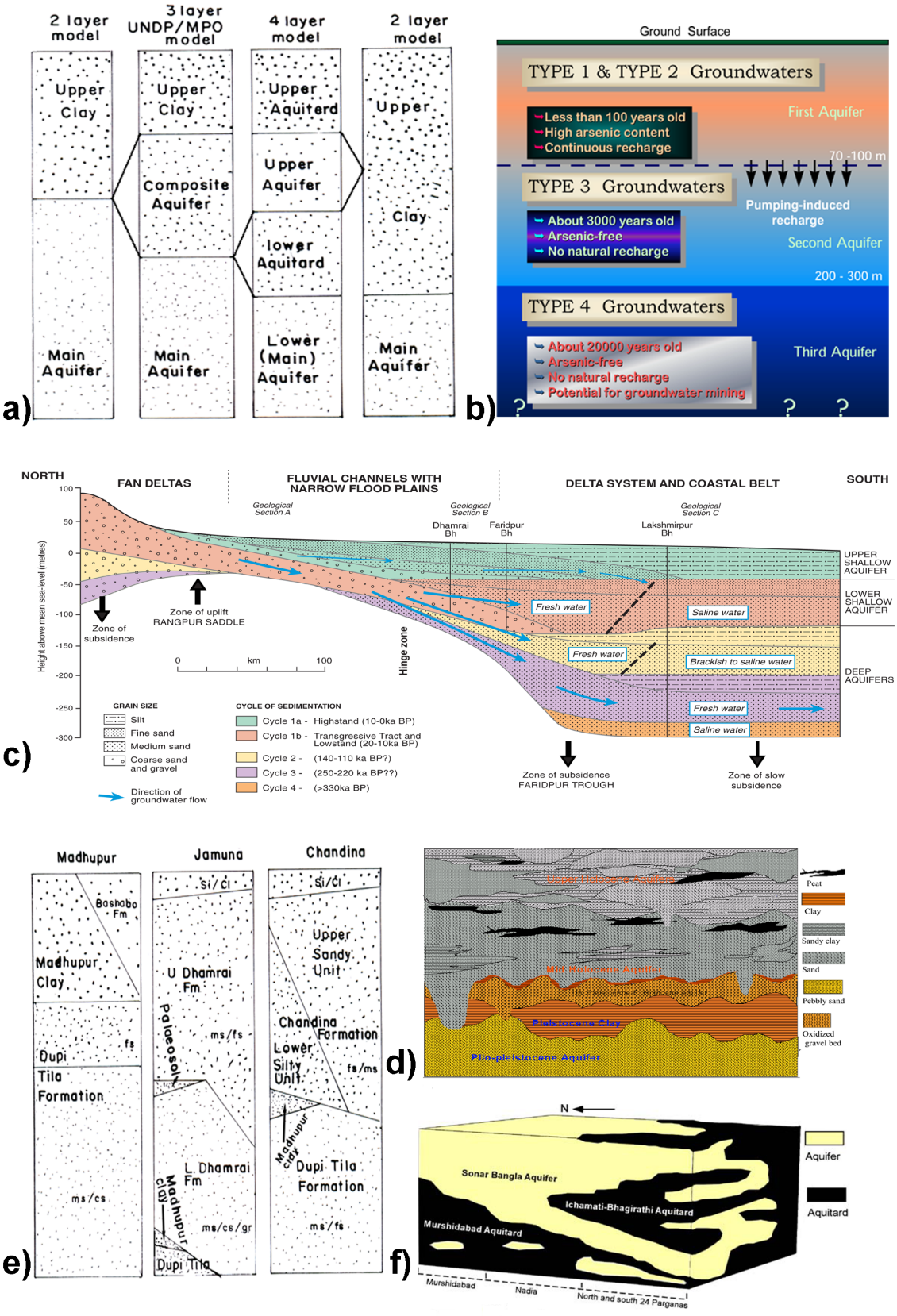

Figure 3-12: Different aquifer classification to date. (a) several aquifer classifications up to 2000, as summarised by Ravenscroft *(2003)*, mostly for upper 150 m; (b) aquifer classification based on isotopic nature of groundwater *(Aggarwal et al. 2000)*; (c) Aquifer classification as of BGS/DPHE *(2001)*; (d) Chronostratigraphy based aquifer classification proposed by GWTF *(2002)*; (e) Stratigraphy based aquifer classification as of Ravenscroft *(2003)*; (f) Single interconnected aquifer system proposed by Mukherjee et al. (*2007b*).

3.4 Surface water-groundwater interaction

A conceptual model of surface water and groundwater interaction in the Bengal Basin is illustrated (Figure 3-13). An example has been reported from the central Bangladesh *(Zheng et al. 2005)* using water-level monitoring at multi-level wells, a nearby river, and precipitation data (Figure 3-14). Note that the site is in a rural area with groundwater abstraction by hand pumped tube-wells, but with no abstraction for irrigation. The seasonal amplitude of variations in water levels is about 4 m for all monitored wells. The lowest water-levels in the shallow well match the lowest river stages of the local stream closely, while the deeper well matches the low stands of the larger regional rivers (Figure 3-14). During the November-December water-levels coincide and they approach the ground surface (in response to rainfall) during the July-August time of the year. This indicates that the groundwater and surface water in the region are an interlinked resource.

3.4.1 Groundwater levels and piezometry

Bangladesh Water Development Board (BWDB) has since the early 1960s developed a national monitoring network of ~1200 wells. Depth to the screen of the monitoring wells varies from region to region depending mostly on the local thickness of surface clay or silty-clay, from <10 m to rarely >100 m, with a median depth of 22 m, indicating that the wells are monitoring water-level or piezometric head (depending on the aquifer structure) of the shallower part of the aquifer. Piezometry of the deeper part of the aquifer is not monitored regularly by any organisation in Bangladesh. However, BADC monitors water level at an intermediate depth (~90 mbgl, depth of irrigation wells) *(BADC 2004)*. Some data are available for greater depths at specific research sites (e. g., *BGS/DPHE 2001; BWDB 2005; Zheng et al. 2005; Harvey et al. 2006*).

Spatial analyses of water level data monitored by BWDB, assuming they represent the water-table, indicate water level follows the regional topographical gradient (Figure 3-15). Water-levels throughout the country are found to follow a similar seasonal fluctuation as observed by Zheng et al. *(2005)* in figure 3-14, being deepest in April and shallowest in September. Falling groundwater levels (Figure 3-16) have been observed in the recent years in many parts of the country, and ascribed to intense abstraction for irrigation and urban-water demand exceeding the amount of recharge *(e. g., Hoque et al. 2007; Shamsudduha et al. 2008)*. Data for the deeper levels (>100 m) indicate a similar seasonal fluctuation but with some lag and different magnitude (section 8.1.2). The water-table configuration at intermediate depth (irrigation abstraction level between 30-110 m, vary from place to place) at the national scale shows a similarity with the shallower spatial head structure (Figure 3-17), but with areas of low water-table being more closely coincident with the areas of groundwater irrigation. Note groundwater abstraction for irrigation is seasonal and the most intensive abstraction for irrigation occurs during November, December, January, and February each year.

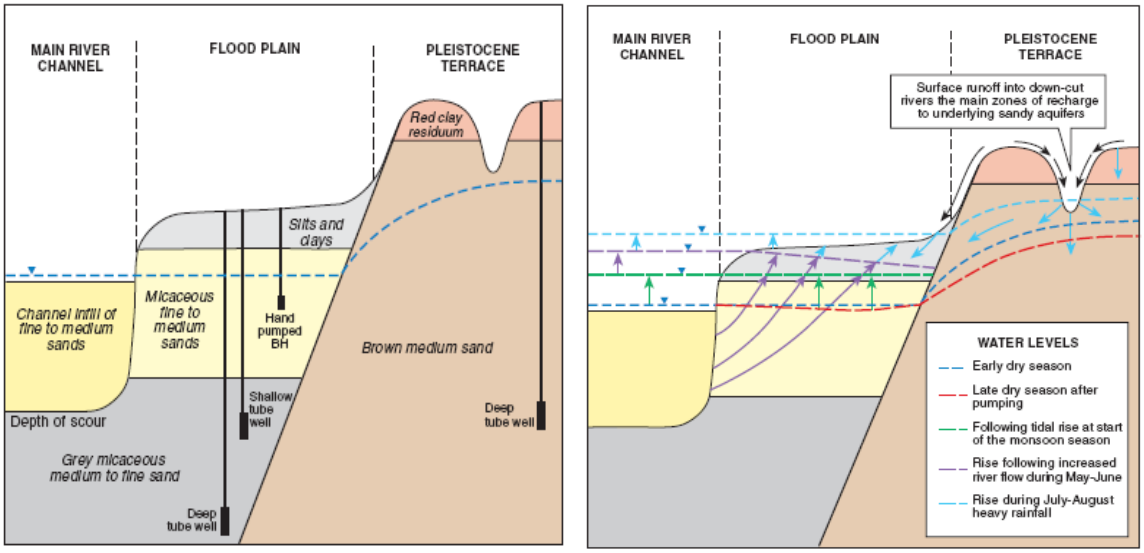

Figure 3-13: Conceptual model; a) Basic hydrogeological units and interventions, b) Surface and groundwater interaction *(BGS/DPHE 2001)*.

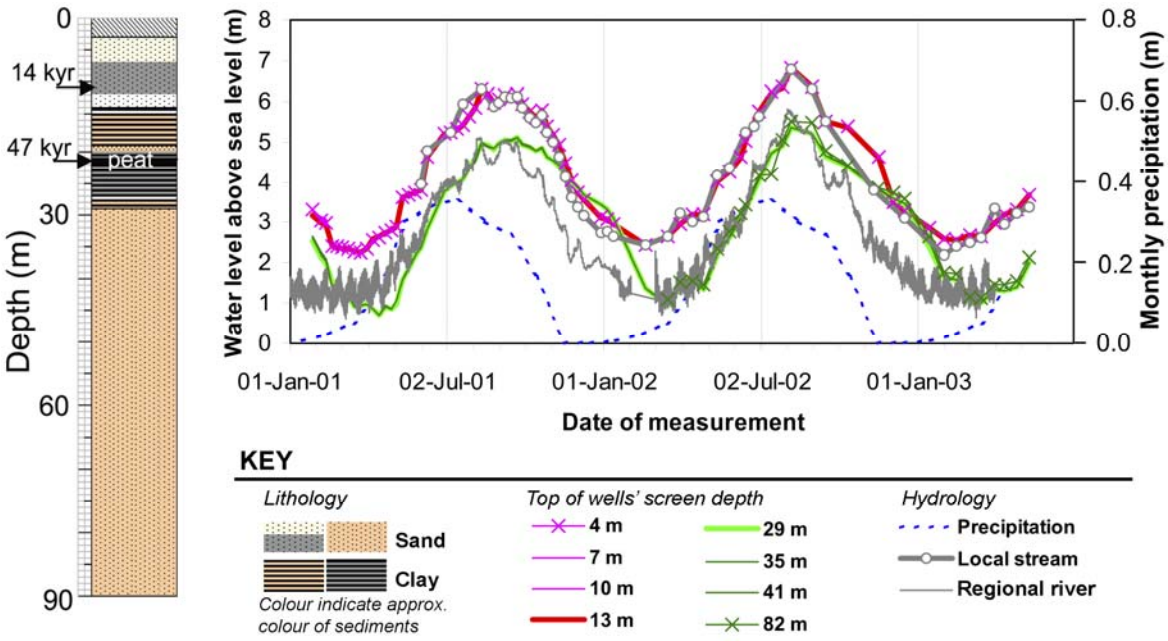

Figure 3-14: Variations of water-level relative to sea level in a nest of monitoring wells at location – 40 km SE of Dhaka, from January 2001 to March 2003. Lithology of the site is also shown with two ^{14}C derived ages of sediments. Average precipitation, nearby stream and regional river level data for the same duration are also plotted *(*adopted from, *Zheng et al. 2005)*.

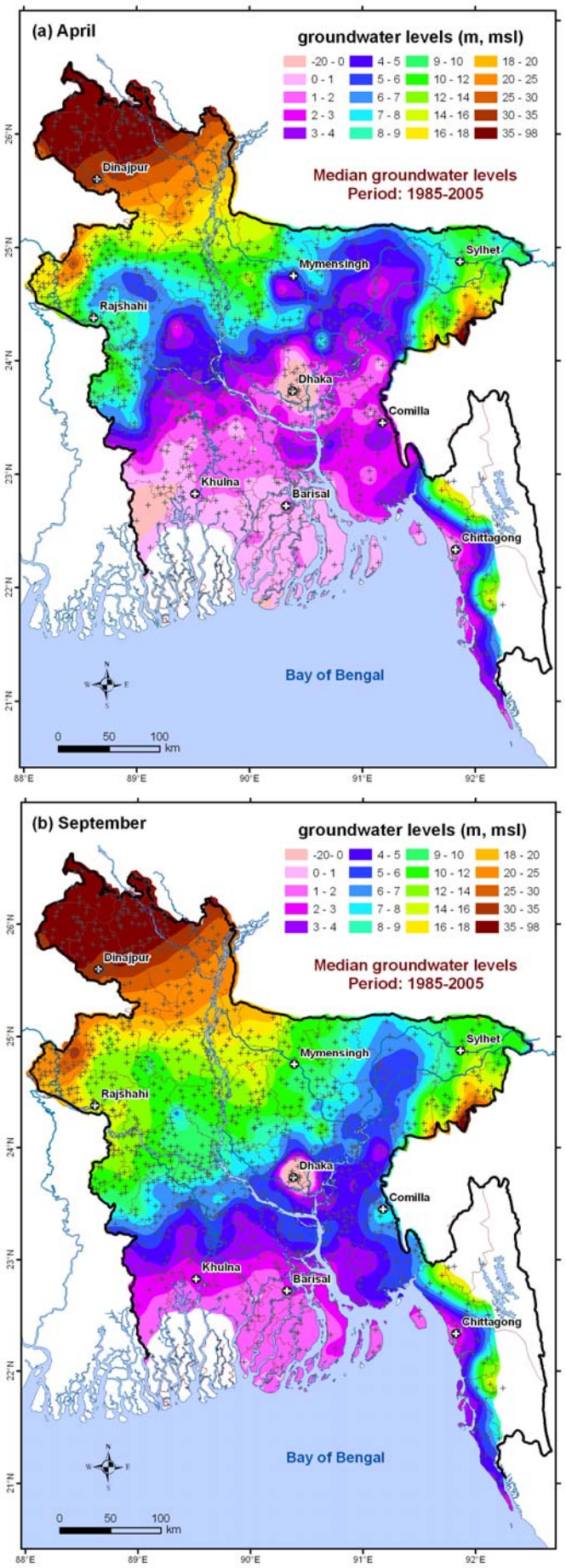

Figure 3-15: Hydraulic head distributions in April (a) and September (b) over a median period of 22 years showing groundwater levels during dry and wet seasons in Bangladesh *(*from *Shamsudduha et al. 2008)*.

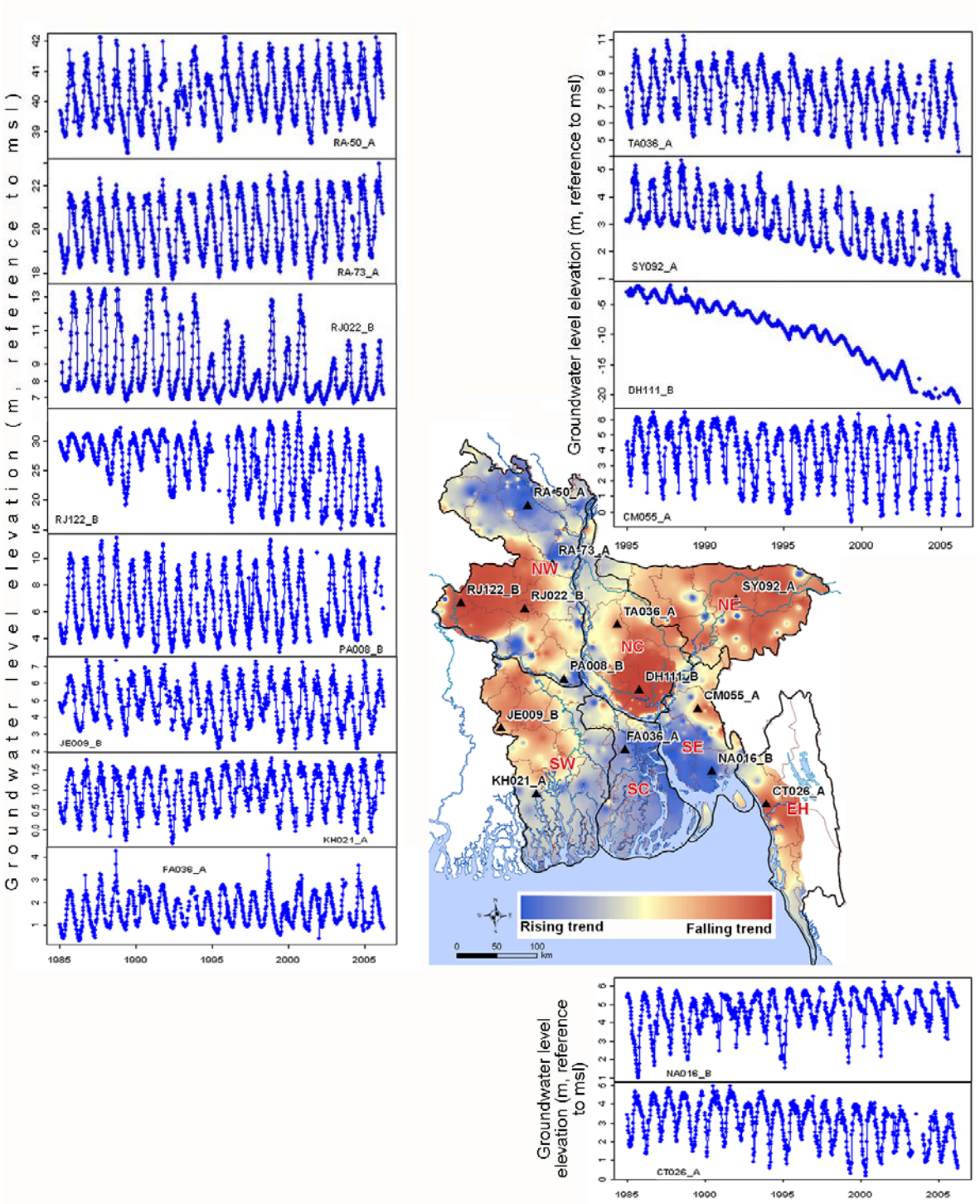

Figure 3-16: Mean water level trend over the last two decades along with well hydrographs from different parts/hydrogeological units of the country (M. Shamsudduha, UCL, personal communication 2009).

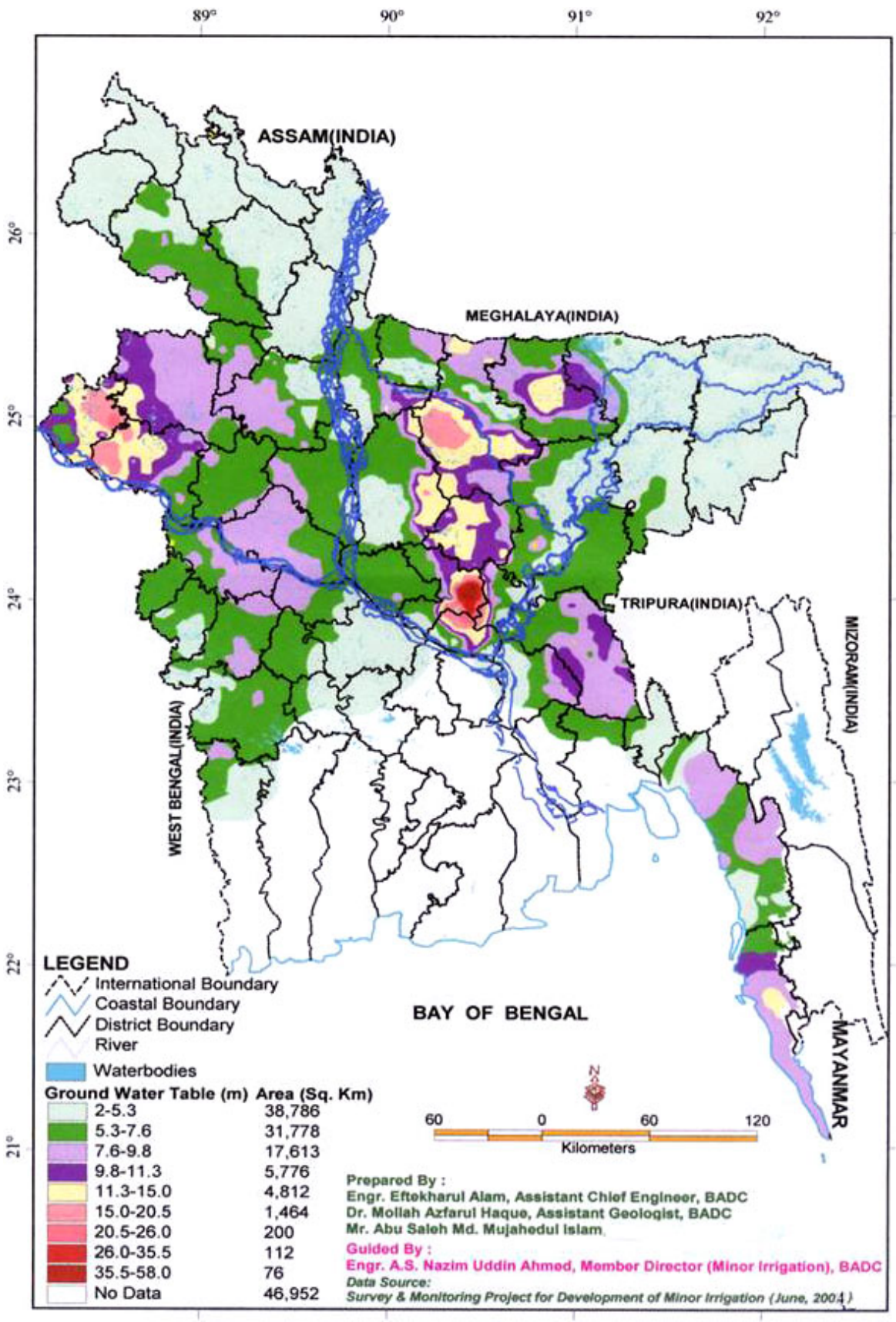

Figure 3-17: Water table configuration at the depth of irrigation abstraction (*from BADC 2004*).

3.4.2 Surface geology, hydrostructural features and recharge

Surface water and groundwater interaction is a function of potential recharge, availability of aquifer storage, and the hydraulic characteristics of the sediments. In Bangladesh the surface geology is predominantly sandy except in the Madhuphur and Barind Tracts where surficial low permeability clay does not facilitate recharge.

The shallow water-table aquifer in Bangladesh is replenished every year during monsoon time through vertical percolation of rainwater, and also possibly by surface water bodies (river, lakes, swamps etc) *(Ahmed and Burgess 2003; Ravenscroft 2003)*. In general, the eastern part of the country has large potential recharge but availability of groundwater storage is less. In contrast, the western parts including in West Bengal part have large available aquifer storage due to irrigation and urban abstraction, which in recent times have exceeded the available recharge. The recharge mechanism to the deeper part of the aquifer is not clear, but it is believed to be occurring by the vertical movement of water from the shallower level, and as well as directly to the exposed Dupi Tila sands at the basin margins *(Ravenscroft 2003)*.

It is reported that many river courses in Bangladesh are controlled by structural features *(*e. g., *Khandoker 1987)* and hence may have influence on groundwater flow *(*e. g., *Hoque et al. 2007)*. The structural zones and elements which may have an influence on aquifer replenishment and groundwater flow are termed 'hydrostructural features' (e. g., *Potter et al. 2002; Kopera 2006; Hoque et al. 2007*). In Bengal Basin structural features have a two-fold influence on groundwater: (1) they give rise to the high topography along the basin margin which may have facilitated a 'Tothian' regional flow system *(Tóth 1963)*, and (2) along the basin margin, sands of the deeper part of the aquifer are exposed and may be recharged directly.

The NNE margin of the basin is bounded by the Dauki fault *(Steckler et al. 2008)* against a Precambrian basement mass where rainfall reaches to >4000 mm/year, which may act as a zone of recharge for the deeper part of the aquifer. Within the basin the tracts of elevated ground (Barind and Madhupur Tracts) have lower permeability compared to adjacent sediments, and so may affect the regional flow system *(Hoque et al. 2007)*. Structural control on the course of river Brahmaputra may cause it to have been stable over the several eustatic sea-level cycles, and therefore to have led to a zone of more highly conductive sediments. This area has been interpreted as an active region of surface and groundwater interaction in the basin *(Shamsudduha et al. 2008)*. In addition, the Indian shield in the west and northwest occurs at shallow depth, sloping toward the deeper part of the basin, and hence may generate flow towards the major rivers (Ganges, Brahmaputra, Hogley) in that part of the basin. Understanding the importance of these hydrostructural features for the groundwater dynamics of the Bengal Basin (Figure 3-18) has so far failed to attract attention in the literature.

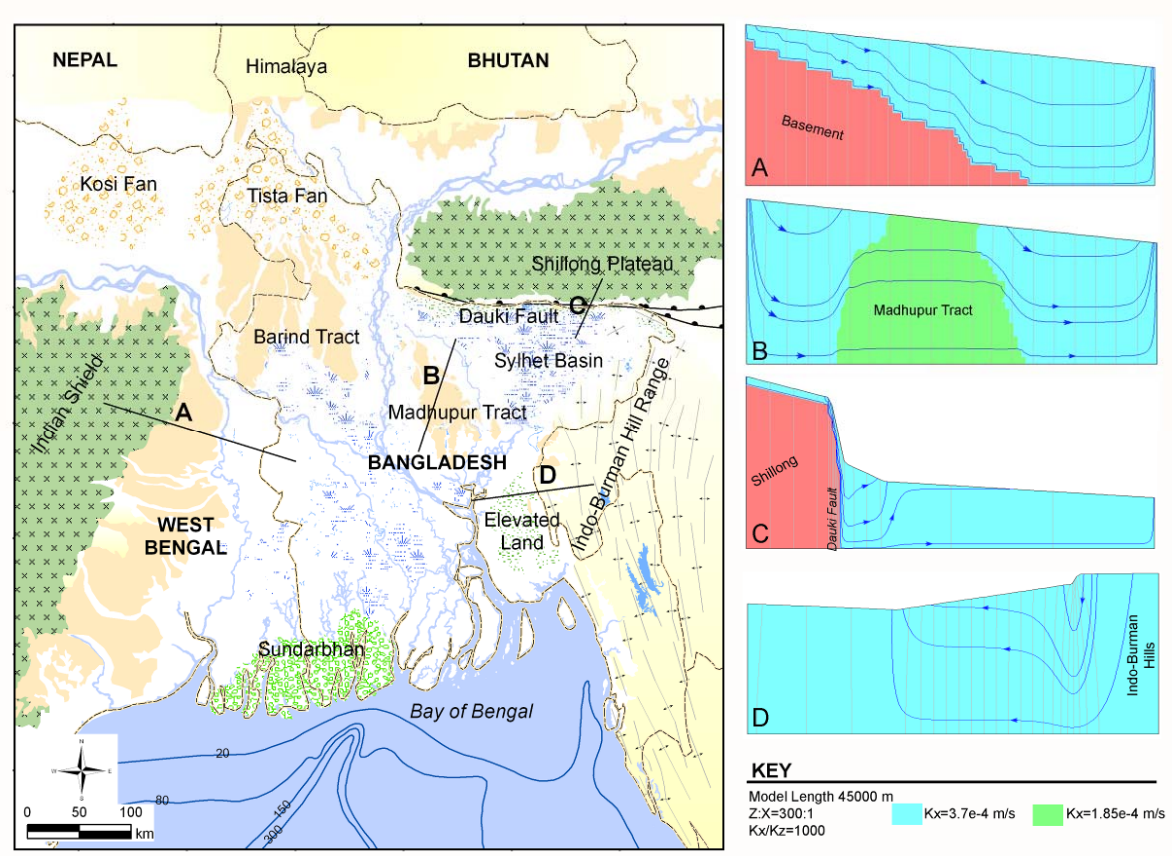

Figure 3-18: Hydrostructural features in Bengal Basin along with simplified modelled flow field in steady state using TopoDrive *(Hsieh 2001)* code.

3.4.3 Groundwater flow

Topography plays the leading role in determining elevation of the water-table and hence in generating local, intermediate to large scale groundwater flow systems *(Tóth 1963)*. However, basin geometry, distribution of impermeable strata in the subsurface, the state of groundwater abstraction, and recharge associated with the climatic conditions also affect the groundwater flow system in a basin *(e. g., Freeze and Witherspoon 1967; Ophori and Tóth 1990)*. Based on the theoretical basis of groundwater flow it can be opined that groundwater flow in Bengal Basin is controlled by the coupling of topography and the distribution of low permeability anisotropic materials (section 6.2).

The Bengal Basin is surrounded by hilly topography in the east and north, and by gradually increasing topography in the west and northwest. The topography within the basin is minimal on regional scale, with an elevation <1 m along the coast increasing to ~30 m along the eastern piedmont area, and in the northwest direction to ~100 m giving a regional slope of about 1:3000. The distribution of major rivers and their tributaries divulges sufficient topographical differences to support groundwater flow system at regional, intermediate and local scales *(Ravenscroft 2003)*. The depth of penetration of groundwater flow systems in the case of a homogeneous subsurface is approximately equal to the distance between the respective streams, local rivers, or major rivers

(Tóth 1963; Zijl 1999). As the sub-surface is in reality heterogeneous the depth of penetration is approximated by the product of the topographical wave length and square root of the ratio of vertical to horizontal hydraulic conductivities of the underlying sediments *(Zijl 1999)*.

Recent basin-scale modelling of groundwater flow (*Michael and Voss 2009a*) considers the basin as comprising of a single anisotropic aquifer (Kh>>Kz) and shows that deep groundwater flow is towards the major rivers from the basin margin, and also to the sea in the south (Figure 3-19).

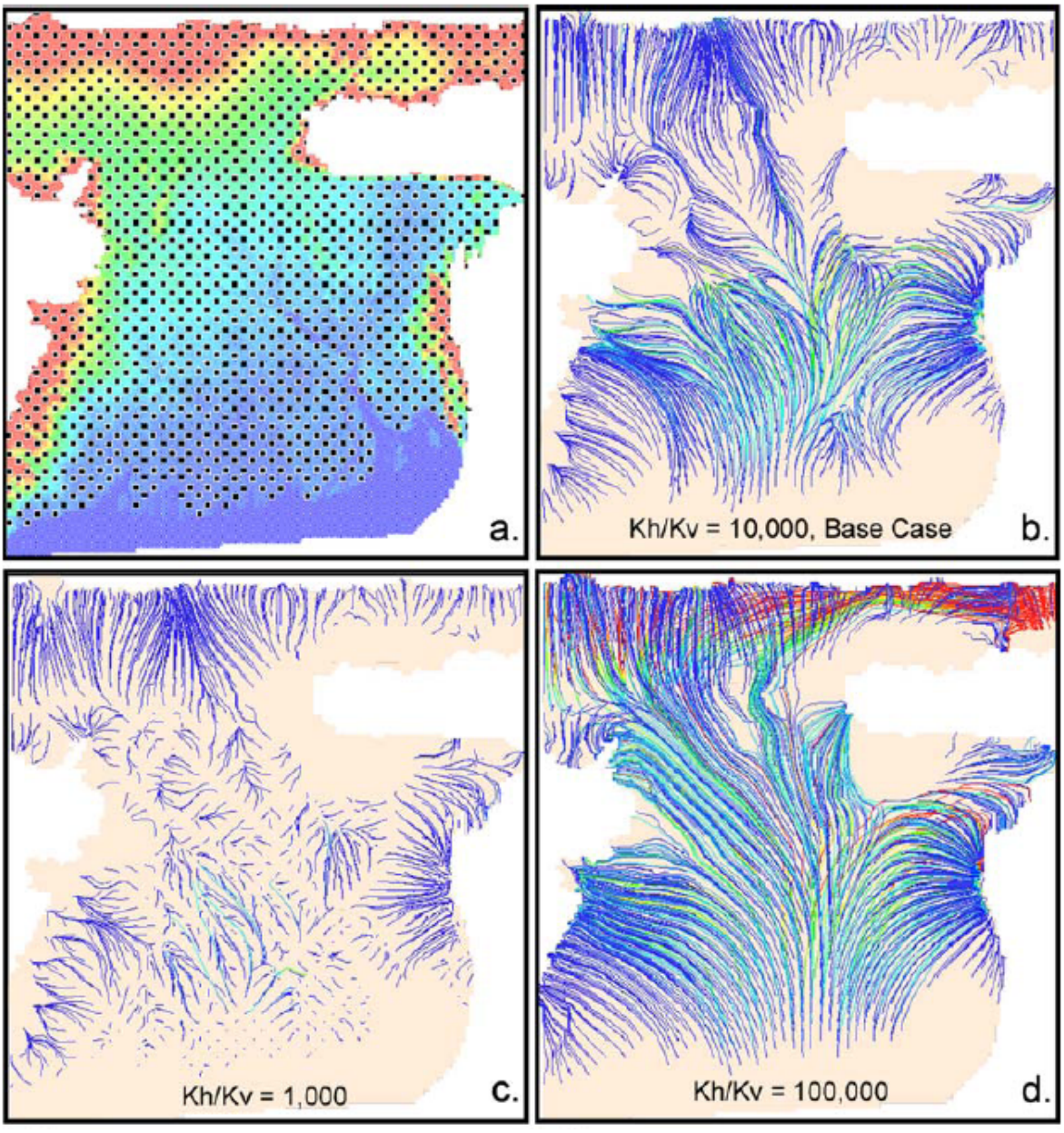

Figure 3-19: Basin-scale groundwater flow as modelled by Michael and Voss (*2009a*). Predevelopment flowpaths ending at depths of 200 m for different values of vertical hydraulic anisotropy: a) Locations of flowpath endpoints selected for visualization; colours represent land surface topography (red>60 m above sea level (asl), blue<1 m asl). Flowpaths in b–d are from recharge locations to these endpoints. Colours change with travel time along each pathline, beginning with blue and changing to red at the endpoint if travel time 160,000 years.

3.5 Geology and groundwater chemical character

Groundwater in the Bengal Basin is generally fresh (EC <2000 μS/cm) except in the coastal region *(Ravenscroft 2003)*. Spatial trends in solute concentrations and geochemical modelling have indicated that silicate weathering, carbonate dissolution, mixing with seawater and cation exchange control the major-ion chemistry of groundwater and river water *(e. g., Hasan et al. 2007; Mukherjee et al. 2008)*. Bicarbonate is the dominant anion in fresh groundwater, with some exception where chloride is dominant, while sulphate is generally absent. The cation composition is dominated by either calcium or sodium, and rarely magnesium. A detailed description of site-specific hydrochemical composition can be found elsewhere (*BGS/DPHE 2001; McArthur et al. 2004; Zheng et al. 2005; Hasan et al. 2007; Mukherjee et al. 2008*). Distinct hydrochemical differences between shallow and deep parts of the aquifer have been indicated (*Zheng et al. 2005; Mukherjee and Fryar 2008*). Elevated arsenic concentrations occur throughout the southern part of the basin shallow aquifer (section 3.7).

Geochemical processes, hence hydrochemical character, are strongly influenced by the spatial and vertical lithological differences within the basin. In the absence of aerobic weathering aquifer sediments are mostly grey coloured and chemically reduced. Sediments which have undergone pedogenesis or aerobic weathering are yellow to red coloured and chemically oxidised (see section 3.3.2.2). During oxidation, organic carbon and ferromagnesian minerals are transformed. Oxidation results in precipitation of red-brown iron oxides and authigenic kaolinite further reduces the porosity and permeability of the sediments *(Davies and Exley 1992)*. The oxidised aquifer sediments are relatively inert chemically, due to higher order of crystallisation of the iron oxides and the lack of organic matter. Reducing conditions prevail in the sediments containing organic carbon in the form of wood fragments and peat deposits. *Davies and Exley (1992)* conceptualised the hydrochemical differences within the basin in relation to aquifer lithology (Figure 3-20). They showed that where the aquifer has oxidised sediments at shallow depth the groundwater is recently recharged and of $Ca(HCO_3)$ type. Deep, older groundwater, in the adjacent aquifer is of $NaHCO_3$ type. Similar water characteristics are found to occur in the southern part of the basin and elsewhere *(von Brömssen et al. 2007; von Brömssen et al. 2008)*. The oxidised horizons in the southern parts are found to be bounded by reduced sediments above and below. The oxidised sediments at depth in the south of the basin are younger than those of Madhuphur or Barind Tracts (see section 3.3.2.2).

3.6 Geology and groundwater development constraints

Although groundwater is plentiful and sediment characteristics are conducive there are limitations to groundwater development in some regions *(MPO 1987; Ravenscroft 2003)*, with the main constraints (Figure 3-21) being:

- occurrences of salinity in the coastal region,

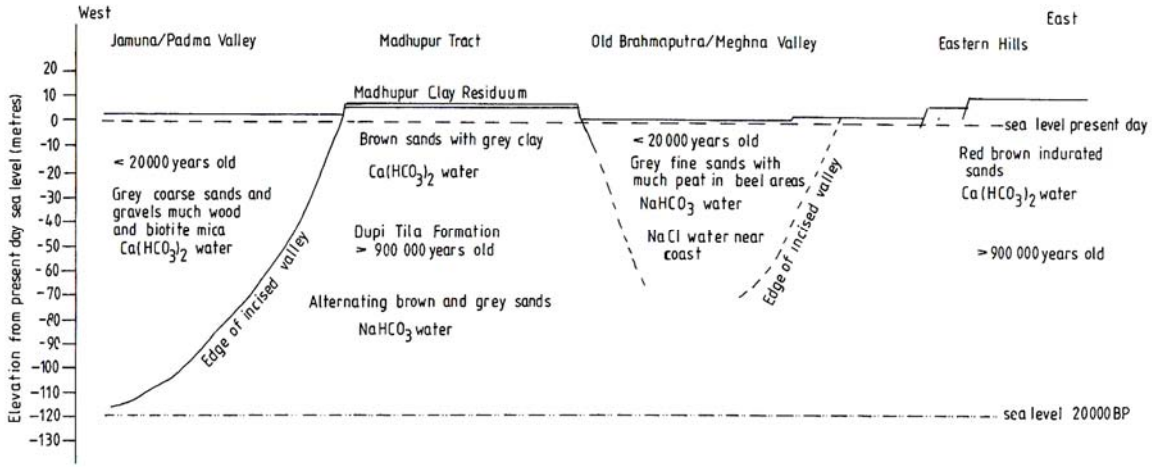

Figure 3-20: Generalised groundwater chemistry in relation of lithology and hydrostratigraphy *(Davies and Exley 1992)*.

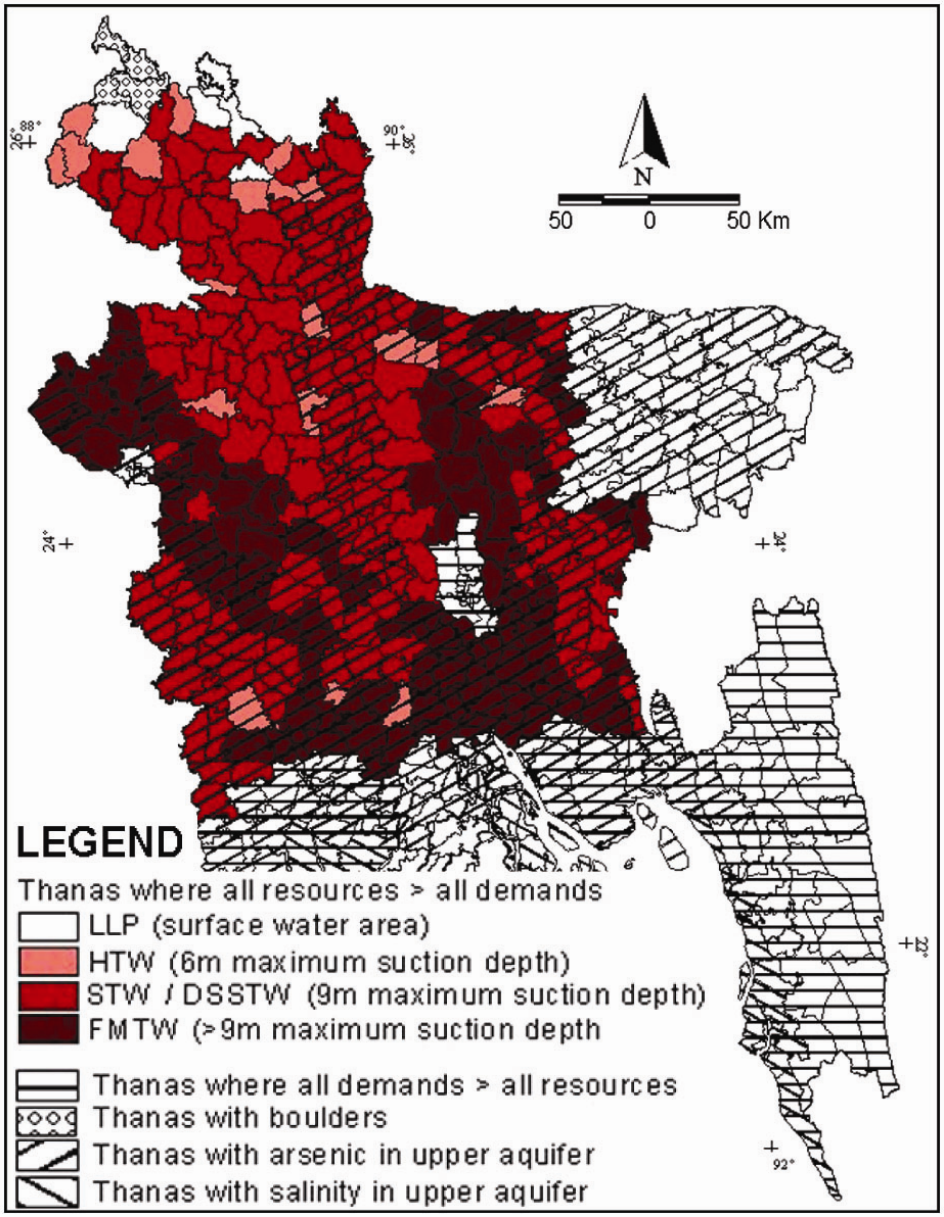

Figure 3-21: Groundwater development constraints in Bangladesh *(WARPO 2000)*

- excessive level of dissolved arsenic in the shallow groundwater throughout southern Bangladesh and West Bengal, India,
- thick surface clay or silty-clay in Sylhet basin in the northeast,
- occurrence of biogenic gas along the Meghna-Titas floodplain region in the east,
- dry-season low water-table in the northwest, and
- complex geology in hilly terrain in the east.

The basin geology has a strong influence on these constraints. Complex geology in the east is a direct result of Tertiary geological evolution. A relatively higher subsidence rate in the Sylhet basin in the NE favoured the deposition of thick silt-clay in the uppermost 100 m. Sedimentation in the water-logged boggy environment of the Meghna-Titas floodplain over the later part of the Quaternary period favoured the concentration of organic matter. The decomposition of these organics leads to the overpressured-biogenic gas zone at depth in the region. Occurrences of dissolved arsenic in the shallow aquifer are geogenic (see section 3.7). Saline water in the coastal aquifer is a freshwater-salinewater density equilibrium process. However, there are pockets of saline water in the inland aquifers and along the course of the lower Meghna river, which are believed to result from invasion of saline water during the last marine transgression in the Late-Quaternary period *(BGS/DPHE 2001; Ravenscroft and McArthur 2004)*

3.7 Excessive arsenic in shallow groundwater

Similar to other Southeast Asian deltas the presence of elevated arsenic (As) in shallow groundwater is a serious threat in the Bengal Basin (Figure 3-22) putting at risk >50 million people. There have been extensive studies on the sources of As, the factors controlling its spatial and vertical variability, and the mechanisms leading to mobilization of As to groundwater. However, lack of consensus limits the predictability of spatial variation, and future concentrations of As, and the impacts of human activities on As concentration. In this section an attempt is made to synthesize the existing knowledge and understanding in broad terms. Details can be found in the cited references.

3.7.1 Extent and occurrences

Until the early 1990s, before the discovery of excessive dissolved As in groundwater, bacteriologically safe drinking water was extracted by shallow hand pump tube-wells, under a program started by the United Nations Children's Fund (UNICEF) in collaboration with the Department of Public Health Engineering (DPHE) in the early 1970s. This was thought to be the most significant accomplishment in reducing human mortality associated with surface water pathogens in the region (*Saha 1984; Smith et al. 2000; Das et al. 2009*).

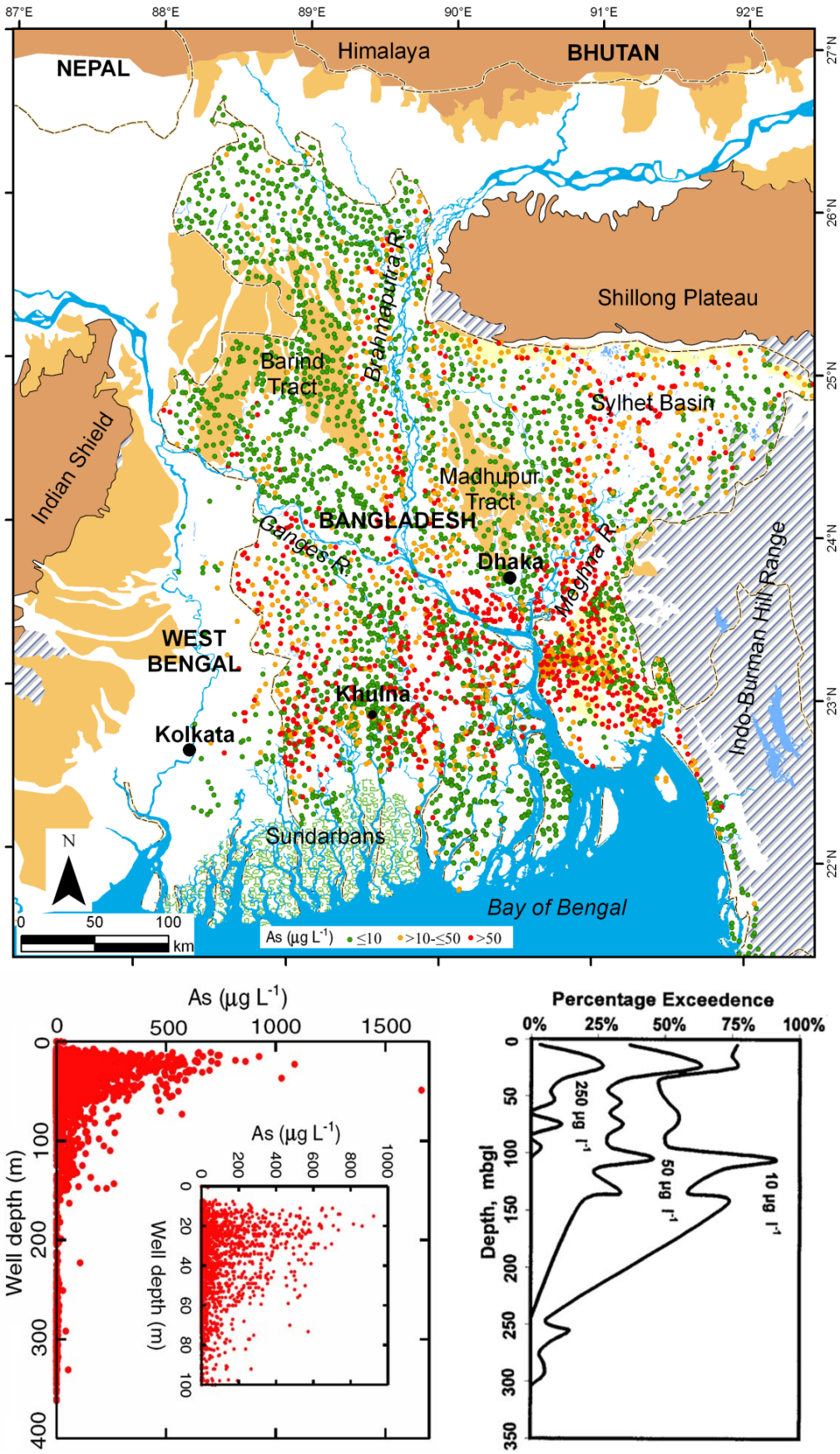

Figure 3-22: Spatial extent of groundwater arsenic (As) in tube well water (dots represent sampled wells location). Data used for Bangladesh is from BGS/DPHE *(2001)*, and West Bengal, India is from Mukherjee *(2006)*. Vertical distribution of well with As are shown *(BGS/DPHE 2001; McArthur et al. 2001, respectively)*.

Excessive As in groundwater of the Bengal Basin is geogenic. Initially it was suspected that the As-contaminated wells were associated with groundwater irrigation *(Mallick and Rajagopal 1996)* and agricultural activities *(Acharyya et al. 1999)*, and restricted to the areas of heavy groundwater irrigation. Progressive research and field surveys indicated that the problem is not area specific, but rather a feature of the entire basin (*PHED 1993; Bhattacharya et al. 1997; Dhar et al. 1997; Nickson et al. 1998; DPHE/BGS/MML 1999; Nickson et al. 2000; BGS/DPHE 2001; McArthur et al. 2001*). A landmark national survey of >3500 wells samples from across Bangladesh *(BGS/DPHE 2001)* explores the problem on regional scale. A recent study by Winkel et al. *(2008)* indicates the problem is not unique to the Bengal Basin but also occurs in geologically similar deltaic environments in South and Southeast Asia.

The distribution of groundwater As concentration varies both spatially and vertically throughout the Basin (Figure 3-22). In Bangladesh 61 out of 64 districts, and in West Bengal, India, 14 out of 19 districts are affected *(Das et al. 2009)*. However, the severity of As occurrences is found to be more in the southern part of the basin (Figure 3-22). In addition, there are reports of excessive As in the hilly states of India in the east *(Chakraborti et al. 2008)*. Excessive dissolved As is limited to tube-wells at shallow depth in the aquifer, in most cases <100 m or even less (Figure 3-22). In contrast, almost 100 % of the deep wells screened at >100 m depth are As-free. 50% of the shallow wells, as a national average in Bangladesh, are As-free. However, most of the wells in northern Bangladesh, particularly in the northwest, are As-free irrespective of depth (Figure 3-22).

3.7.2 Arsenic source and mobility

It is almost two decades since the discovery of excessive dissolved As in groundwater in the region. There is a consensus that As occurs naturally in Bengal Basin sediments due to weathering of Himalayan sediments and subsequent deposition by the Ganges–Brahmaputra–Meghna River system. In contrast, the mechanism(s) of mobilisation of As to groundwater remain controversial. No unified hypothesis has been proposed which links the geology, groundwater flow system and the geochemical processes.

3.7.2.1 Sources

All workers recognise that As-rich pore-water is limited to the Holocene sediments. Arsenic is believed to be released from the aquifer sediments. The majority of the scientific community contends that the aquifer sediments contain arsenic (*Nickson et al. 1998; Acharyya et al. 2000; BGS/DPHE 2001; McArthur et al. 2001; Harvey et al. 2002b; Anawar et al. 2003; Khan et al. 2003; Ahmed et al. 2004; Zheng et al. 2004; Meharg et al. 2006; Seddique et al. 2008*). Others advocate that near-surface wetland sediments are the source (*Swartz et al. 2004; Polizzotto et al. 2005; 2006; Kocar et al. 2008; Polizzotto et al. 2008; Datta et al. 2009*). Most agree that As is adsorbed to FeOOH, (and also to MnOOH) and is released under reducing conditions. An

exception is Seddique et al. *(2008)*, who argue that As is associated with biotite and released due to chemical weathering along with Fe. As is found co-precipitated in or co-adsorbed on a number of minerals in both the Holocene and Pleistocene aquifers at concentrations consistently <10 μg/g *(Swartz et al. 2004)*. In contrast, dissolved As has a distinct distribution with depth, but no clear pattern of spatial distribution (see section 3.7.3). There are contrasting explanations for the deposition and formation of FeOOH in the sediments. It is commonly believed that the high rate of fluvio-deltaic sedimentation during the Holocene has facilitated As to be adsorbed to authigenic FeOOH minerals *(Ahmed et al. 2004; McArthur et al. 2004; Ravenscroft et al. 2005)*, while others argue that Holocene marine transgression led to elevated alkalinity, facilitating geochemical trapping of As in the sediments *(Acharyya et al. 2000; Dowling et al. 2003; Khan et al. 2003)*. Meharg et al. *(2006)* propose that co-deposition of organic matter and As, plausibly in a wetland setting, promotes As adsorption into the root zone where oxygen induces formation of iron minerals.

Sequential chemical leaching demonstrates that arsenic is mainly present in three solid phases: (1) oxide phases of Fe and Mn, (2) organic matter and (3) sulfide and silicate phases *(Anawar et al. 2003)*. Solid phase arsenic concentrations are relatively uniform with depth and are typically below 3 μg/g in the aquifer sands *(Swartz et al. 2004)*, but average ~20 μg/g *(Meharg and Rahman 2003)* and can be as high as 800 μg/g *(Breit et al. 2004; Datta et al. 2009)* at the near-surface redox boundary, a few metre below ground surface. Detailed studies on the solid phase sediment chemistry by Polizzotto et al. *(2005; 2006)* indicate two dominant pools of arsenic in the Holocene aquifer sediments of Bangladesh: As in sulfide minerals (>60% of the total solid phase As) and weakly adsorbed As (15% of the solid-phase As as retrieved in the batch experiments).

3.7.2.2 Mobilisation mechanism

Since the distribution of As in the subsurface sediments is not solely controlled by a single solid phase, dissolution–desorption from different phases may contribute to the total As concentration in groundwater. A number of hypotheses have been proposed regarding the modes of As release, ranging from the oxidative or reductive degradation or weathering of As-bearing solids to competitive displacement of sorbed As by phosphate or bicarbonate. During the 1990s, As in groundwater was explained to occur due to the oxidation of arsenical pyrite in the alluvial sediments as irrigation pumping induced water level decline *(Mallick and Rajagopal 1996)*. This hypothesis is not supported by the field evidence *(McArthur et al. 2001)*. Correlation between As occurrence and reducing conditions have led to the broadly-accepted hypothesis that dissimilatory Fe oxyhydroxide reduction leads to the release of adsorbed and coprecipitated As *(Bhattacharya et al. 1997; Nickson et al. 1998; 2000)*. Acharyya *(1999)* criticised the reductive dissolution hypothesis, and proposed the competitive exchange of phosphate anions derived from application of fertilizer to surface soils, which displaces sorbed As from the sediment into groundwater. However, this competitive exchange hypothesis also suffers lack of field evidence *(McArthur et*

al. 2001). Another hypothesis of competitive exchange has been proposed by Anawar et al. *(2004)*, that As is released to solution by competitive exchange with HCO_3, but this has also failed to gain wide acceptance *(McArthur et al. 2004)*.

The majority of the scientific community asserts that microbial oxidation of organic matter (including a localized peat layer) leading to reductive dissolution of Fe and Mn oxyhydroxide are the important processes of As mobilisation (*BGS/DPHE 2001; McArthur et al. 2001; Ahmed et al. 2004; Zheng et al. 2004; Ravenscroft et al. 2005; Mukherjee et al. 2008*). Respiration of organic carbon present in the aquifer *(McArthur et al. 2004)*, or infiltrating from the surface (*Harvey et al. 2002b; Neumann et al. 2010*) leads to anoxic conditions, under which other electron acceptors, such as Fe and As, are employed. Incubation experiments by Islam et al. *(2004)* support the view that infiltration of fresh organic matter facilitates reduction in the aquifer. Later studies *(Polizzotto et al. 2005)* advocate against a necessity for fresh organic matter, for As release from the Holocene sediments, and McArthur et al. *(2004)* indicate the sedimentary organic matter and peat to be the reduction drivers within the aquifer. Klump et al. *(2006)* argued that irrigation-induced infiltration/recharge of young water mixing with older water at depth ~30 m generates an environment conducive to As release, but does not proposed a mechanism. Meharg et al. *(2006)* explain the codeposition of organic and As within the aquifer sediments, with the organics as the drivers of reducing conditions and As being released from the FeOOH formed in the root zone in wetland settings. However, co-deposition of organics with As may not be applicable in the northwest, where the terrain is thoroughly sandy (*van Geen et al. 2008b*). The overall pattern As occurrence in the aquifer supports the notion that reduction of Fe hydroxides is a necessary but not a sufficient condition for elevated As concentrations in groundwater in Holocene aquifers *(Horneman et al. 2004; Zheng et al. 2004)*. The amount of As released to the groundwater is neither related to the bulk sediment As contents, nor to the fraction associated with crystalline phases. Rather it is the predominance of reducing conditions, combined with a moderate Fe/As ratio that drives As mobilization from the sediments (*van Geen et al. 2008b*).

The lack of correlation between As and Fe concentrations in groundwater may indicate that both elements are initially associated in the solid phase, but that a new Fe(II)-containing phase acts as a sink for Fe and not for As (*Harvey et al. 2002b; Horneman et al. 2004; Swartz et al. 2004; van Geen et al. 2008b*). Detailed analysis of solid phase sediment geochemistry *(Polizzotto et al. 2005; 2006; 2008)* indicates that Holocene As-bearing aquifer sediments do not contain FeOOH. They found As is associated with the near surface sediments, is released under (seasonal) reductive dissolution to the aquifer, where it remains in solution. They argue that As is not released from the aquifer sediments but rather from the near-surface sediments, from where it enters to the aquifer as a contaminating phase.

Mineralogical analysis of sediment core led Ahmed et al. *(2004)*, Breit at la. *(2004)*, Shamsudduha *(2007)*, and Seddique et al. *(2008)* to argue that chemical weathering of biotite is

the primary mechanism of As release, and that prevailing reducing conditions contribute to the widespread occurrence of As-enriched groundwater. This was indicated by the positive correlation of As concentration with Al and Fe concentration but not with total organic C. However, this biotite weathering mechanism is criticised by Anawar and Mihaljevic *(2009)* as relying solely on correlation of aqueous species.

In summary, reductive dissolution of Fe(III) (hydr)oxides and concomitant arsenic release (Figure 3-23) is the most widely accepted explanation of high arsenic groundwater concentrations.

3.7.3 4D variation of arsenic

The extent of As-bearing groundwater in the Bengal Basin is regional, yet As concentrations are spatially and vertically heterogeneous (Figure 3-22) (*DPHE/BGS/MML 1999; BGS/DPHE 2001*). High resolution data have been used to explain local scale variability (e. g., *van Geen et al. 2003b*). There has been no long-term monitoring to observe the potential temporal variability of As in tube-well water. However, a 3-year monitoring study indicates no significant change over this short time *(Dhar et al. 2008)*. In this section the explanations of the spatial, vertical and temporal changes of dissolved As in groundwater are summarised.

3.7.3.1 Spatial variability

Regional spatial variability in As concentrations is found to be controlled by the distribution of sediments of different redox condition. As concentrations are below the WHO guide line (<10 µg/l) in the oxidised sediment, 'while' the Holocene reduced sediment contains As > 50 µg/l (the Bangladesh drinking water standard) but with significant spatial variations and exceptions with about 50% wells <50 m bgl (*Ravenscroft et al. 2001; van Geen et al. 2003b; Ahmed et al. 2004*).

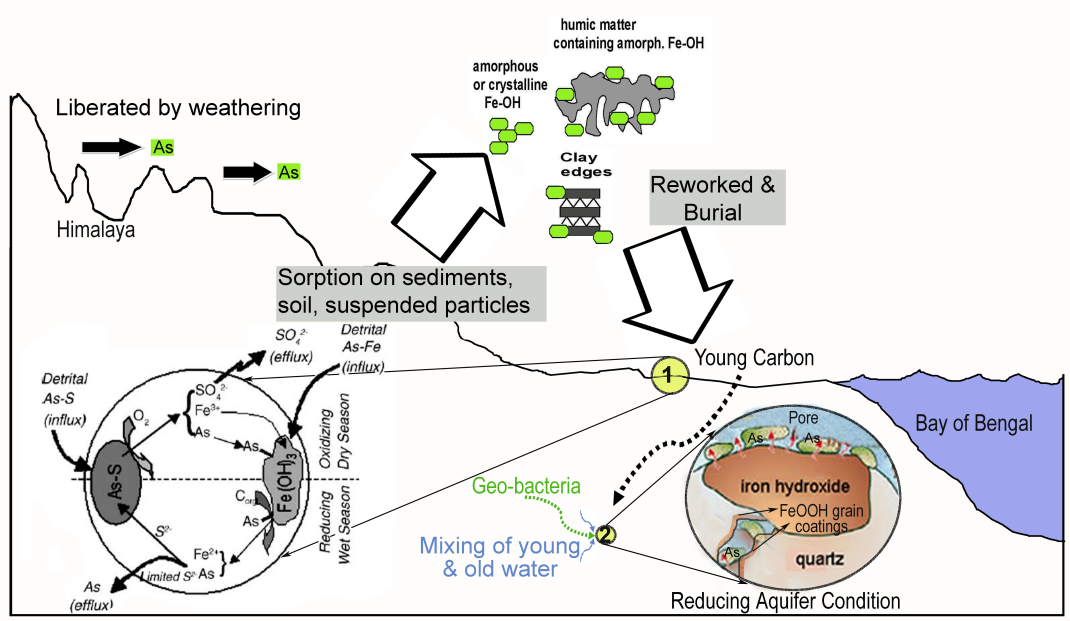

Figure 3-23: Schematic summary of sources and mechanism of As release in groundwater. In the figure (1) indicates near-surface liberation of As into solution *(Polizzotto et al. 2006)*, while (2) indicates within aquifer release of As (see text).

The concentration of dissolved As can vary significantly between two neighbouring wells, by one to two orders of magnitude within a distance of 100s m *(McArthur et al. 2004)*. Several studies link this variability to the floodplain processes which determined the sand-clay distribution in the shallow subsurface. These studies show that where surface sediments are sandy, As is less concentrated than where surface sediments are clayey (*Ravenscroft et al. 2005; van Geen et al. 2006a; Weinman et al. 2008; Zahid et al. 2008; Hoque et al. 2009*) (Figure 3-24). Groundwater recharge indicated by groundwater age suggests that sandy areas contain low As because of active recharge and downward flushing of As *(Stute et al. 2007)*. Some studies have tried to link the spatial variability with the spatial variability in the slope of the land surface, and the water-table (*Ravenscroft et al. 2005; Shamsudduha et al. 2009b*). These studies show that As concentration is elevated where the slope is low and the water-table is close to the surface. The spatial variability of As concentration may also be related to the occurrence of oxidised sediments at depth, where As is negligible or absent compared to the neighbouring gray sediment zone of the aquifer *(McArthur et al. 2004; von Brömssen et al. 2007; von Brömssen et al. 2008)*. Despite all these explanations the spatial variability of As remains complex and incompletely understood.

3.7.3.2 Vertical variability

Throughout the basin, groundwater As concentrations decrease with depth. At some study sites the concentration profile has been found to peak between the depths of 28 and 45 m in the Holocene aquifer (*BGS/DPHE 2001; Burgess et al. 2002; Harvey et al. 2002b; van Geen et al. 2003b*) (Figure 3-22). The concentrations are below the regulatory limit (<50 µg/l) in tube-wells with intake depths greater than 150 m bgl. Almost all of the earlier works described the arsenic as associated with Holocene sediments, and explained the greatest depth of As occurrences as the depth of the Holocene sediments. However, oxidised sediments contain less As even if they are Holocene *(von Brömssen et al. 2007; von Brömssen et al. 2008)*. Some studies linked the occurrence of As to the presence of grey sediment *(*e. g., *McArthur et al. 2004)*. However, pre-Holocene grey sediments below the floodplains do not contain high dissolved As, but do have elevated Fe. McArthur et al. *(2004)* suggest that partial reduction of deeper sediments, as a consequence of the deposition of overlying, organic-rich, Holocene sediments, has been sufficient to mobilise some Fe into groundwater, but insufficient to reduce the FeOOH, the remains of which act as a sorptive buffer to prevent As from accumulating in solution. Moreover, Lowers et al. *(2007)* have argued that the presence of adequate sulfur allows As in the deeper part (>150 m) of the aquifer to be scavenged by pyrite during diagenesis. In addition, red coloured, oxidised (red-bed) sediments (section 3.3.2.2) at depths in the southwest part of the basin may also host low As groundwater.

In summary the vertical control of As is associated with the occurrence of Holocene sediments, and it appears likely that groundwater flushing at times of earlier sea-level low stands has removed As from the deeper part of the aquifer.

3.7.3.3 Temporal variability

The lack of long-term monitoring makes it difficult to understand the temporal dimension of the dissolved As in well discharge. However, Burgess et al. *(2007)* use tube well age as a proxy to understand the temporal dimension of As concentrations, suggesting that with time As concentration increases in tube-well water (Figure 3-25). Modelling studies of a representative hand-pumped tube well catchment indicate an increase of As concentration in tube-well discharge (with a discharge 10 m^3/day and a flat topography) over 10–15 years *(Cuthbert 1999; Cuthbert et al. 2002)*.

A 3-year monitoring programme of 20 wells in Bangladesh documented a noticeable increase of dissolved arsenic in only one shallow well *(Cheng et al. 2005)*. A recent paper *(Dhar et al. 2008)* reported another set of 3-year monitoring data with no significant temporal variation in dissolved As, when other chemical parameters including redox-dependant parameters exhibit seasonal variability. The inert nature of As in the aquifer may be related to chemical buffering and rapid equilibrium between solute and solid As (*van Geen et al. 2008b*).

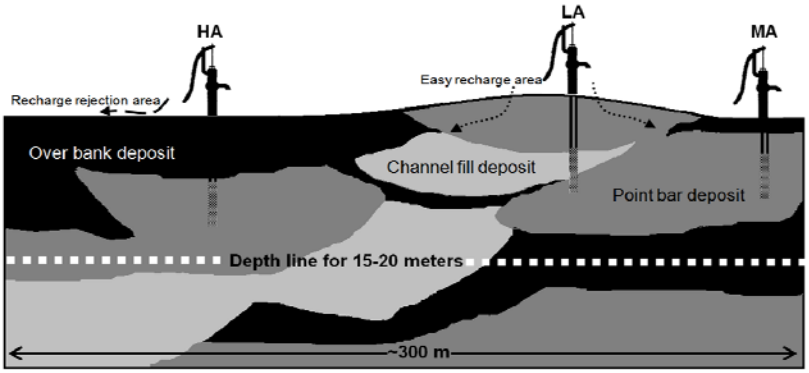

Figure 3-24: A conceptual cross-section shows how the surface lithology deposited by the meandering streams influence the aquifer redox condition *(Hoque et al. 2009)*. In the figure 'HA' 'LA' and 'MA' are the locations of three hypothetical wells. Water from 'HA' and 'LA' would contain the highest and lowest concentration of As respectively, while 'MA' would have an intermediate concentration.

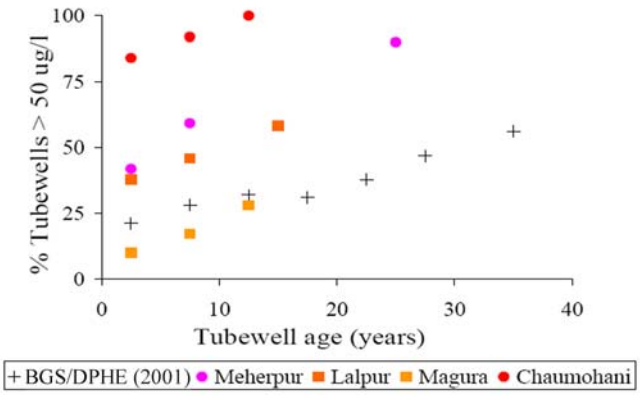

Figure 3-25: Trend of increasing As content with tube-well age in Bangladesh, illustrated based on BGS/DPHE *(2001)* data consolidated into 5-year groups, and other area-specific studies from different parts of the basin *(*after, *Burgess et al. 2007)*

A hypothesis is presented in chapter 6 which explains all the aforesaid 4D observations of As occurrence and variability within a consistent geological framework where groundwater flow plays the primary role controlling As distribution (see section 6.4).

3.7.4 Arsenic transport

From the previous section it is apparent that As is not present in all groundwater of the Bengal Basin. This knowledge is put to use to supply As-free water to millions of people in the county. However, a big concern is whether the As-free wells will remain free of As or whether those wells in turn will become affected. Modelling studies of tube well catchments (*Cuthbert 1999; Burgess et al. 2002; Cuthbert et al. 2002; Burgess et al. 2007*), of the aquifer at regional-scale (*Mukherjee et al. 2007b; Shibasaki et al. 2007*), and at basin-scale *(Michael and Voss 2008)* and also geochemical experiments *(Stollenwerk et al. 2007)* indicate that these wells may not remain 'As-free' forever, due to the potential transport of dissolved As within the well catchment. The detail of aquifer representation in groundwater models is a crucial issue for predictive modelling for this sort of terrain, because it is topography coupled with the distribution of subsurface clays that control the pathways of groundwater flow in the region (see sections 6.2). The stability of the flow system in the basin has yet to be investigated. However, modelling may help guide the sensible and planned use of the As-free regions of the aquifer and help to sustain it As-free for longer.

Bacteriological study indicates that the shallow and deep regions of the aquifer support different communities of bacteria, but both have the potential to support bacteria which reduce FeOOH and release As into solution *(Sutton et al. 2009)*. There has been no specific observation of the 'invasion' of the deep aquifer in the Bengal Basin by As, however, there are some deep wells with elevated As *(DPHE/DFID/JICA 2006; Mukherjee 2006)*. However, there are reports that an analogous deep aquifer in Vietnam has been invaded by As from the overlying Holocene aquifer on a result of heavy groundwater abstraction at depth *(Norrman et al. 2008)*. This possibility needs further study, where the groundwater carries excessive As concentration (*van Geen et al. 2002; Ahmed et al. 2006*).

3.8 Alternative sources of arsenic-free groundwater

Paucity of alternative water sources (As-free and /or pathogen free) forces a significant number of people still use the wells with unsafe level of dissolved As (*Smith et al. 2000; Ahmed et al. 2006*). Many of the proposed solutions are not cost-effective and/or are ineffective in decreasing As in drinking water to an acceptable level *(Ahmed et al. 2006)*. Moreover, surveys show a preference for tube-well water as it is readily available and maintenance is easy (*Ahmad et al. 2006; Ahmed et al. 2006; Johnston and Sarker 2007; Opar et al. 2007; Hoque et al. under review*). From the earlier discussions in sections 3.7.2, and 3.7.3 it is possible to outline three alternatives for As-free groundwater sources (Figure 3-26), and these are explained in the subsequent sections.

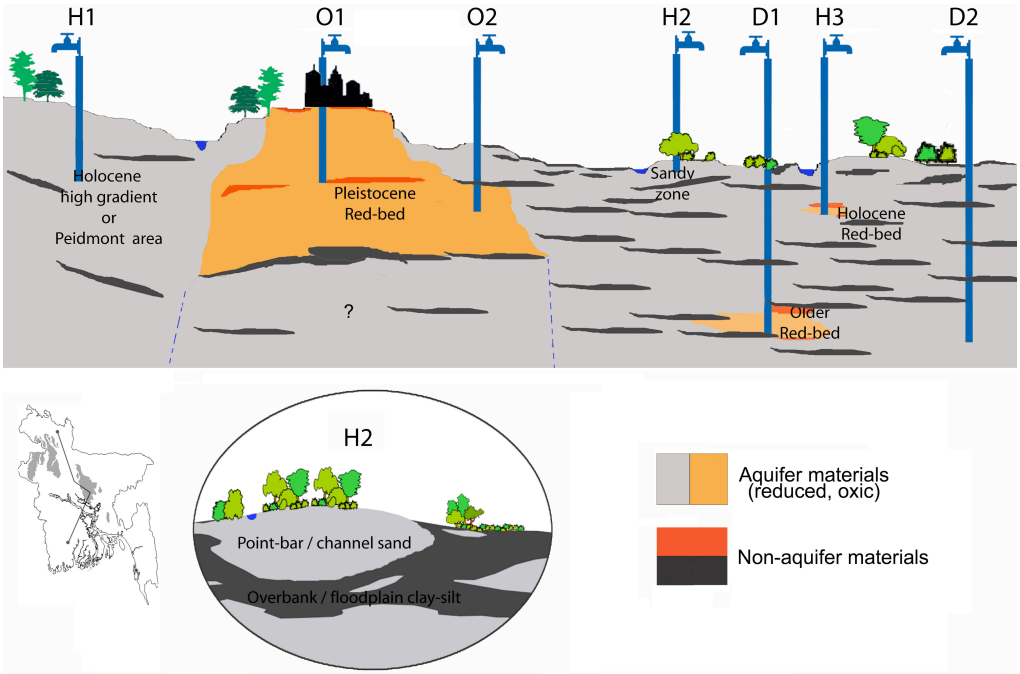

Figure 3-26: Alternative As-free groundwater sources. In the diagram, H1 to H3 indicate different situations within the Holocene sediments where tube well would tap As-free water, and D1 & D2 denote deep As-free water context. D1 & H3 would have higher sustainability with red-bed As adsorption providing geochemical protection, as at O1 & O2 in the Pleistocene elevated tracts.

3.8.1 Very shallow As-free contexts

Statistical analysis of the national survey data shows that >70% of the surveyed shallow wells (<50 m bgl) have As within the Bangladesh drinking water standard (<50 µg/l). These wells in many instances are found to be situated on sandy ground, slightly elevated, and to remain above the seasonal flood-level (*Ravenscroft et al. 2005; van Geen et al. 2006a; Weinman et al. 2008; Zahid et al. 2008; Hoque et al. 2009; Shamsudduha et al. 2009b*). Identifying these areas conducive to low As would be an alternative for deeper aquifer development, at least as a temporary solution *(Hoque et al. 2009)*. Multi-parameter regression modelling with existing data on As, ground elevation and slope, surface soil, geomorphology and satellite data could be used to map the areas for potential low As wells. The spatial limits of the shallow (<30 m) low-As groundwater environments were delineated (Figure 3-27) by spatial modelling of areas for which (a) surface soil contains ≥50% loamy silt, (b) the water table is ≥ 1 m and ≤ 7 m depth below ground surface, and (c) surface silt-clay is <15 m thick. The regions delineated in this manner should encompass the shallow low-As groundwater environments of the Holocene floodplains in Bangladesh, situated beneath land of slight elevation which remains above the seasonal surface flood-level. Monitoring of these wells is needed as pumping has the potential to draw As water from adjacent high As zones to jeopardise the As-free shallow wells (*Cuthbert 1999; Cuthbert et al. 2002; Burgess et al. 2007; Hoque et al. 2009*). Moreover, a recent study shows that these shallow low-As wells have the potential for microbial (*E. coli*) contamination (*Jessica et al. 2010*).

3.8.2 Red-bed aquifer As-free contexts

Pleistocene sediments are found to host As-free groundwater, and it has been explained that these sediments have Fe(III) minerals of higher crystallinity with the capacity to adsorb and immobilize As, and which prevents dissolution *(McArthur et al. 2004)*. Similar, comparatively less crystalline, yet oxidised sediments are found with low As in some parts of the country close to the base of the Holocene *(von Brömssen et al. 2007; von Brömssen et al. 2008)*. These sediments are associated with the low stand to transgressive phase of sedimentation and pedogenesis (see section 3.3.2.2). Oxidised sediments of similar genesis associated with earlier sea-level cycles are found to occur at depth in the SW Bangladesh (Figure 3-10) and within and around the Pleistocene inliers (Figure 3-27). Colour descriptions on the drilling logs can be used to identify the occurrences of these red-bed aquifer zones. Moreover, geological modelling can also be used to correlate those zones within the subsurface.

The widespread, though dis-continuous, existence of oxidized sediments at depth could be exploited for the development of these red-bed aquifer zones as a source of As-free water *(Jakariya and Bhattacharya 2007)*. Geochemical modelling *(Stollenwerk et al. 2007)* adapted for porosity of 0.2, a downward flow velocity of 0.1 m/yr, and for an As source at 900 µg/l indicates that a 10 m thickness of oxidized sediment could delay the arrival of arsenic concentrations at >10 µg/l for 4,200 years. This indicates that the setting of tube-well screen a few metres below the gray-orange sediment interface could be used as a long-term As-free strategy.

3.8.3 Deep aquifer As-free context

As mentioned in section 3.3.3 the deep aquifer is defined as the deeper part (> 150 m bgl) of the basin-wide aquifer system, and is essentially As-free. This aquifer environment is under exploitation as an As-free water source across the whole of southern Bangladesh *(Ahmed et al. 2006; DPHE/DFID/JICA 2006)*. Currently >200,000 deep HTWs are in operation (K. M. Ahmed, Personal communication). Spatial variation in depth of the existing (deep) wells indicates a southerly increase (Figure 3-27). Guidance on the depth for tube-well installation needs to be developed, and an effort has been made to map the ‘deeper aquifer’ by DPHE *(DPHE/DFID/JICA 2006)*.

Deep groundwater for the most part originates from outside the As affected area. Although the physical separation of the ‘deep aquifer’ from the shallow aquifer by an impermeable layer is not continuous, age data indicate that the deeper groundwater is very old *(Aggarwal et al. 2000; Zheng et al. 2005)* and is derived from the basin margin. Before further development of the aquifer, research must focus on the stability of this deep flow system, and the occurrence of the ‘deeper aquifer’ at least in the southern part of the country. In addition, monitoring of the As concentration of the deep wells is recommended because of the potential of As breakthrough from shallow levels.

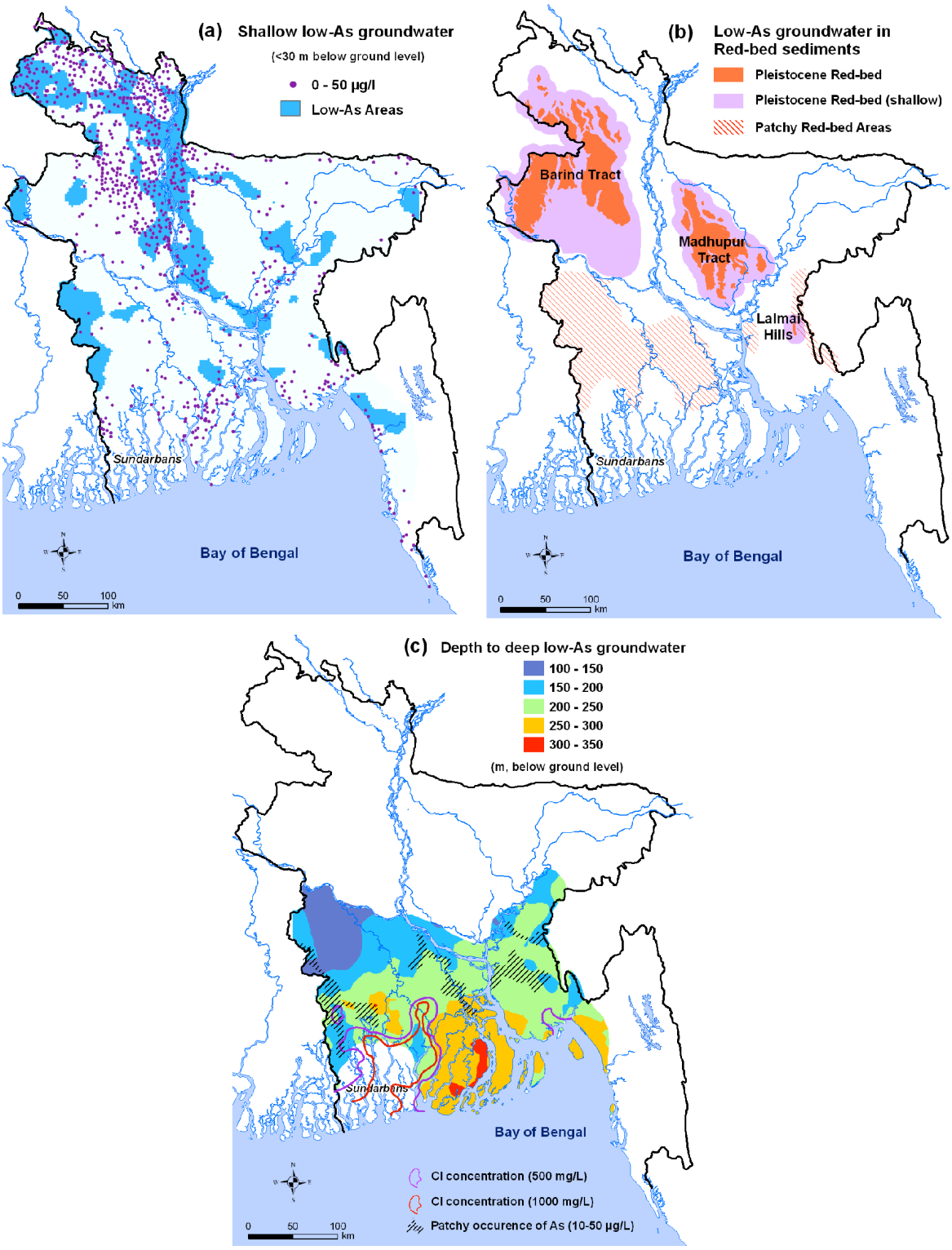

Figure 3-27: A preliminary delineation of the low-As groundwater environments of Bangladesh; a) Shallow (<30 mbgl) low-As groundwater of the Holocene floodplains, for details see text; b) Low-As groundwater in oxidised 'red-bed' sediments; c) depth to deep low-As groundwater, which may contain some red-bed aquifer zones as well. Compilation of 80 lithological logs with information on sediment colour from southern Bangladesh and surface geological information are used to map the red-bed aquifer context. A total of 1380 deep (>100 m) wells of southern Bangladesh (*DPHE/DFID/JICA 2006*) for which quality-controlled As data were available are used to map the depth to 'deep aquifer' in southern Bangladesh.

Part B: Descriptions & Characterisations

Chapter 4
Hydrostratigraphical analysis

4.1 Introduction

Maxey *(1964)* defined hydrostratigraphical units as bodies of rock with considerable lateral extent that act as a reasonably distinct hydrological system. A hydrological system may include a formation, part of a formation, or a group of formations, and this is why hydrostratigraphy does not equate directly to a traditional stratigraphical code. Hydrostratigraphical units are considered informal economic units in the North American Stratigraphic Code *(NACSN 1983; 2005)*. At present, there is no widely accepted code for hydrostratigraphy *(Seaber 1986)*. However, subdividing the geology according to permeability in order to define and map aquifers and aquitards has become the norm for hydrostratigraphy. Hydrostratigraphy coupled with hydrofacies has evolved as a tool to understand, characterise and predict the heterogeneity of sedimentary deposits in their hydrogeological context (*Anderson 1989; Fogg et al. 1998; Eaton 2006*). Hydrostratigraphy is the 3-D geometric representation of aquifer-aquitards and hydraulic conductivity of a hydrological system *(Anderson 1989)*. Hydrofacies indicates lithofacies having similar hydraulic properties (*Anderson 1989; Ritzi et al. 1995; Fogg et al. 1998; Klingbeil et al. 1999; Eaton 2006*).

Geological heterogeneities in the Bengal Basin aquifers are linked to the intrinsic nature of unconsolidated alluvial aquifers. Geological complexities of the hydrogeological-framework evolved through incisions, erosion, and deposition of the rivers during the Plio-Quaternary cyclicity in sea-level (section 3.3). In a fluvio-deltaic terrain under eustatic cyclicity deposition occurs in channel-interfluve settings. These depositional elements, often arranged linearly, are spatially discontinuous and varied in nature but may be vertically stacked. Their deposition in turn affects the groundwater flow-field. A hydrogeological framework is attributed through the arrangement of clay, silty-clay, different grades of sands, and the occasional presence of gravels.

A variety of hydrostratigraphical models have been proposed by earlier workers in the Bengal Basin (see section 3.3.3). Before the discovery of excessive dissolved arsenic in groundwater, hydrogeological investigations were mostly limited to depths of 100 to 150 mbgl i. e., to the base of a 'shallow' aquifer of which the deeper part was termed the 'deep aquifer' by irrigation engineers *(BADC/MMI/HTS 1992)*. Under the current scenario of groundwater exploitation, the term 'deep aquifer' refers to depths >150 mbgl which is essentially arsenic–free, but which is not necessarily separated by an aquitard from the shallow aquifer. Some studies have represented the whole system as a single aquifer (*Mukherjee et al. 2007b; Michael and Voss 2009a*), some as a discrete aquifer system (*UNDP 1982; Aggarwal et al. 2000; BGS/DPHE 2001; DPHE/DFID/JICA 2006*), but in each case the lack of data has made the interpretation uncertain and locally restricted.

A general approach of using facies models to predict spatial variability in aquifer properties was presented by Anderson *(1989)*, who used facies models of glacial-meltwater-stream sediments and till to predict large-scale spatial changes in hydraulic properties. Idealized descriptions of depositional environments and facies models help in estimating spatial trends in geological attributes, to infer paleo-environemnt and interpret depositional histories (*Miall 1996; Catuneanu 2002*). In contrast, hydrogeologists use observations together with facies models to estimate spatial patterns in hydraulic properties *(Anderson 1989; Johnson and Dreiss 1989; Ritzi et al. 1995)*. Recent attention has focused on extracting more information from interpretative depositional models, to estimate spatial variability in aquifer properties (*Anderson 1989; Desbarats and Bachu 1994; Johnson 1995; Ritzi et al. 1995; Fogg et al. 1998; Klingbeil et al. 1999; Weissmann and Fogg 1999; Novakovic et al. 2002; de Marsily et al. 2005; Ezzy et al. 2006; Mikes and Geel 2006; Zhang et al. 2006*). Facies models are most useful to a hydrogeologist in identifying grain-size relationships and connectedness of coarse-grained deposits, that can be related to spatial changes in hydraulic properties and to infer preferential flow paths *(Koltermann and Gorelick 1996)*.

In the current study, 589 drillers' log were collated for a 5000 km^2 area. These drillers' logs coupled with 11 petroleum exploration and 12 geophysical logs were used to interpret the underlying hydrogeological framework and hydrostratigraphy, using the concept of hydrofacies *(Anderson 1989)* rather than the indicator geostatistics method *(Johnson and Dreiss 1989; Ritzi et al. 1995)*. Indicator geostatistics require the stratigraphy to be divided into aquifers and aquitards, which is not appropriate given the variability within the aquifer materials. In the current project an attempt has also been made to describe the spatio-vertical variability within the aquifer materials. Special attention has given to the layering of finer materials that could separate the shallow and deeper part of the aquifer system.

4.2 Approach and analysis

4.2.1 Study area

Hydrostratigraphical analysis has been undertaken for the eastern part of the Bengal Basin complying with the groundwater model domain (section 7.1). Even with a research interest in the eastern part of Bangladesh, the study area had to be extended beyond the territorial boundary of Bangladesh into the hilly regions of India, the Indo-Burman ranges (Figure 3-1). The study area was demarcated in consideration of the hydrogeological flow units as described by Anning and Konieczki (*2005*).

4.2.2 Data acquisition

The information on the drillers' logs is very scanty, although there are millions of wells in Bangladesh. Recently, a project has been completed on the development of a 'deep aquifer database' *(DPHE/DFID/JICA 2006)*. The national database contains information on ~2000 drillers' logs compiled mostly from Department of Public Health Engineering (DPHE), Groundwater Hydrology Centre (GHC) of Bangladesh Water Development Board (BWDB), and Bangladesh Agricultural Development Corporation (BADC) for the entire Bangladesh. In the current research 589 logs from eastern Bangladesh have been used (see Figure 4-1). These logs vary in depth from 87 to 375 m with a median value of 227 m; 75% of the logs contain lithological data to a depth of ≥258 m.

Exploitable aquifers occur in the upper few hundred metres of a sedimentary sequence several km thick. In such a thick basin it is impractical to equate the geological basement to the hydraulic basement, where extensive, basin-wide marine clays are present at shallower depth. Moreover, several silt-clay layers are encountered at every point in the basin and this in turn generates a distinct hydraulic anisotropy leading to insignificant amounts of recharging water penetrating to depth in the basin. A marine clay of Pliocene age, UMS, occurs widely in the basin (Section 3.2.4). The UMS varies in depth from 400 to 2500 m below the ground surface, and for the current research has been taken as the hydraulic basement. To map this hydraulic boundary, 11 petroleum-exploration drilling logs *(MPO 1987; Uddin and Lundberg 1999; Uddin and Lundberg 2004)* (Figure 4-1) were interpreted, in the context of geological structural information (*Reimann 1993; HU/NPD 2001*) and surface geology (*Gupta 1981; Alam et al. 1990; Dasgupta et al. 1993; Reimann 1993; Bhattacharyya et al. 1996*).

Apart from the drillers' and petroleum logs, 12 geophysical logs were conducted with Mostafa *(2005)* in the Kachua area (Figure 4-1), in the middle of the study area. These logs contain responses of electromagnetic (EM) conductivity and natural gamma counts, performed digitally in the existing DPHE deep tube-wells according to the procedure mentioned in RGlogging *(2000)*.

These logs were used to constrain the regional hydrostratigraphical observations (essentially inferred from poor quality drillers' log information) at local scale.

4.2.3 Data treatment: Lithofacies and hydrofacies

Drillers' logs contain information on sediment classes according to grain-size, such as – clay, fine sand, medium sand, etc. These descriptions vary from driller to driller, and also with methods of drilling. In most cases these logs were developed based on bore-hole washed samples. It is assumed that the description is consistent irrespective of drillers and drilling-methods. These logs were re-coded into 10 different lithofacies based on grain-size (e. g., clay, silty clay to gravel with sand) (Figure 4-2). Similar lithofacies attributes were interpreted from the petroleum drilling logs which were re-coded up to the base of UMS in individual logs. Core samples from the region document very thin (~cm) clay or silty-clay intercalations within the sandy aquifer materials *(BGS/DPHE 2001)*, not present in the drillers' log records, which impose additional vertical hydraulic anisotropy on the system.

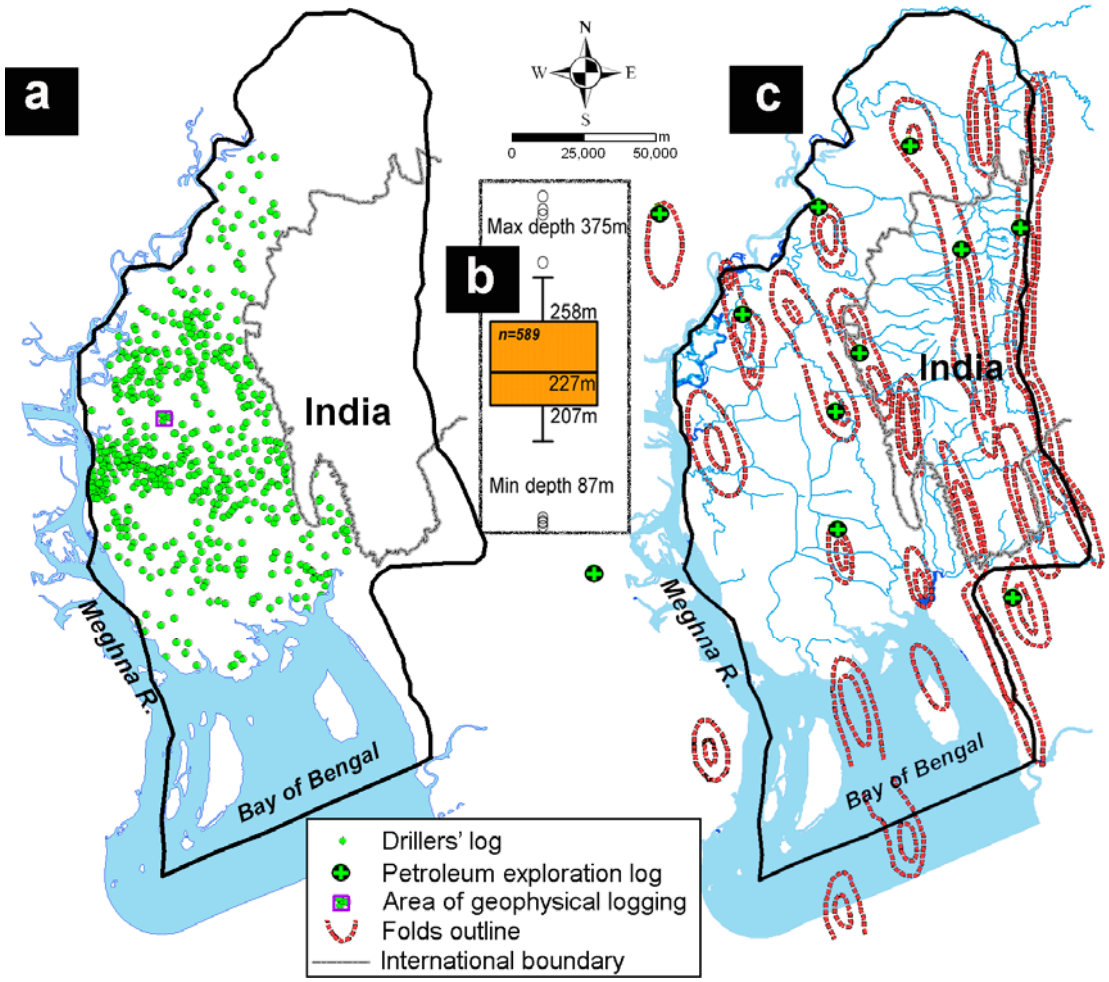

Figure 4-1: Spatial dimension of data used in hydrostratigraphical analysis. a. Indicates the locations of drillers' log, and area of geophysical logging, b. summary statistics of the drillers' log, and c. Shows location of petroleum exploration drilling data point along with traces of the folds (surface and sub-surface) in the region.

Finer lithofacies are associated with floodplain processes and coarser facies are linked to channel processes as these are generic to the fluvio-deltaic and alluvial settings *(Miall 1996)*. Grouping of lithofacies according to the finer and coarser elements would give better picture of the hydrofacies, i. e., paleo-channel and floodplain deposits. With a view to depict subsurface distribution of coarser, finer and mixed lithofacies, lithofacies were grouped into two hydrofacies: finer (non-aquifer materials) and coarser (aquifer or screenable materials). The term 'hydrofacies' was introduced for relatively homogeneous but anisotropic units that are hydrogeologically meaningful *(Poeter and Gaylord 1990)*. But 'hydrofacies' here are designed to indicate the internal heterogeneity arising from different lithofacies. Different weightings were given to individual lithofacies within the hydrofacies to discern the internal variation (Figure 4-2). A large gap in the weighting value between finer and coarser lithofacies ensured a distinction between the two, i. e., in areas made of migrating channels and unstable floodplain. A special attention has given to find layering of finer facies materials through combining 'very fine sand (vfs)' into the finer hydrofacies group as they are often associated with floodplain facies. Floodplain silty-clay facies often contain 'very fine sand' and occasionally 'very fine to fine sand (vffs)' *(*e. g., *Miall 1985)*. During drilling, due to the drilling technique, most of the silt and clay fragments may be washed away while sand remains in the container and is recorded as 'very fine' or 'very fine to fine sand' instead of 'silty clay' or ' sandy clay'. To address this uncertainty in data recording, 'vfs' and 'vffs' were included into the finer hydrofacies group, it is acknowledged that these lithofacies could be associated with channel processes in the low energy rivers. The current study area has always been under the depositional regime of high energy rivers due to its proximity to the Tertiary hills in the east (section 3.2.3).

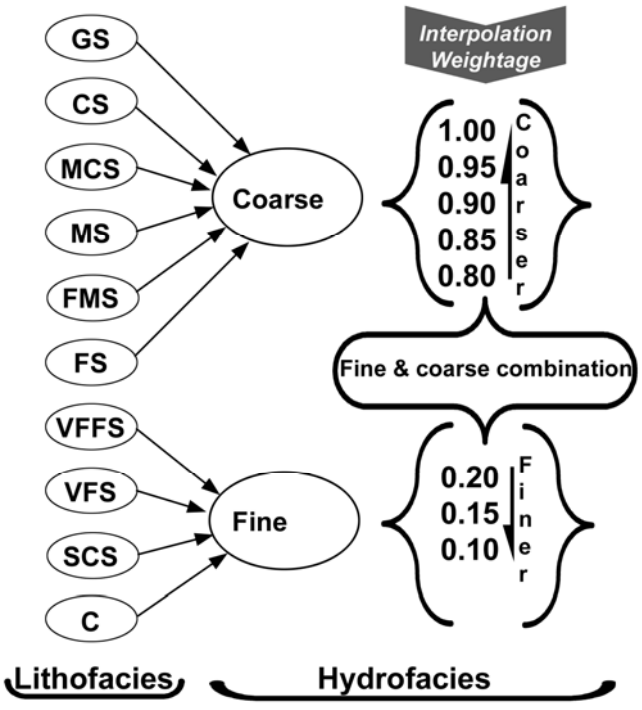

Figure 4-2: Lithological classes into 10 lithofacies, and hydrofacies categorisation with their interpolation weightage used in the lithological modelling.

Geophysical logs were arranged according to depth and the corresponding response of the natural gamma (CPS) and EM conductivity (mS/cm) log using a spreadsheet programme. A moving average was applied for smoothing the spiky signal of natural gamma logs and conductivity logs (Figure 4-3). The logs provide 50 to 60 measurements count per metre. This led to adoption of a 48-point moving average for conductivity and gamma logs. As gamma responses are spikier, smoothing was applied in two stages. The data were used to prepare graphs of natural gamma and EM conductivity vs. depth. These graphs were then printed on vertically exaggerated paper (Figure 4-3) to visualise the log response more clearly. In every case log responses were amplified by several times to make the responses more visible and distinct. These paper logs were then visually interpreted for apparent sedimentary lithofacies (clay, fine sand / with silt, and medium to coarse sand). The log signature can suggest the type of lithofacies *(Miall 1996)* in consideration to the general geological setting. Here, visual interpretations of the log are based on the general method of log interpretation described in Rider *(1996)*. The interpretations are subjective, and a summary of steps and consideration is shown in figure 4-3.

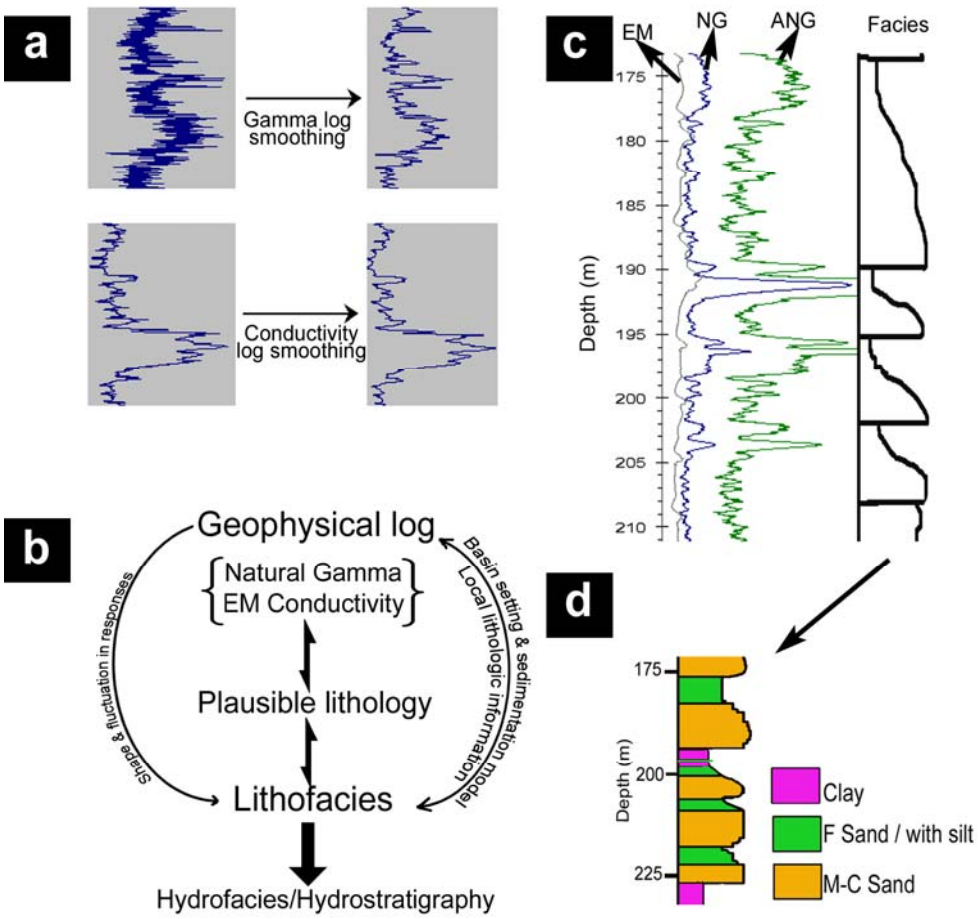

Figure 4-3: Steps followed in geophysical log processing and interpretation. (a) Smoothing of raw log response for interpretation; (b) Steps in extracting lithological information from log response; (c) Part of a log response with amplified natural gamma (ANG) log, EM and NG indicate Electromagnetic and Natural Gamma log signals respectively; (d) Facies signature extracted from the geophysical log responses.

4.2.4 Hydrostratigraphical basement delineation

Petroleum exploration drillings have been performed in the anticline crest area of subsurface folds in the region (MPO, 1987), providing a structurally biased data set for depth to the UMS across the region. Data on fold geometry and structural contours are available in literature. Consideration has been given to the dipping angle of strata in the subsurface folds before interpolating between points to derive a map of depth to the top of UMS. First collated data on depth to the top of marine clay were plotted over structural map (Figure 4-1) of the area and then interpolated values were plotted around the known points. Dip angles were determined from the structural contours (as of *Reimann 1993; HU/NPD 2001*) for individual folds. These folds are exposed at the surface in the eastern part of the area. Surface exposures of marine clay were extended to the subsurface according to dip angle for mapping of the unit in eastern part of study area.

4.2.5 Lithology and hydrofacies modelling

Lithological and hydrofacies modelling used RockWorks (RockWare Inc. Golden, CO, USA) 2000 and 14® versions respectively. It is a multipurpose, multi-dimensional bore-hole utility package, which works in block-centric finite-difference grid. The package has several algorithms (closest point, distance-to-point, inverse-distance weighting, directional weighting, and horizontal biasing) for interpolation. Having tested the ability of the empirical model to estimate the lithological variations at each of two control areas, the 3-D inverse distance weighted average (IDWA) interpolator *(Shepard 1968; Weber and Englund 1994)* was selected. The weighting power *p* controls how the influence tapers off with respect to distance *d*

$$Z_o = \sum_{i=1}^{n} w_i Z(x_i) \quad \text{..... Eq. 4-1}$$

$$w_i^p = \frac{\left(1/d_i\right)^p}{\sum_{i=1}^{n}\left(1/d_i\right)^p} \quad \text{..... Eq. 4-2}$$

Where Z_0 represents the estimated value, w_i is the weights, $Z(x_i)$ are sample values at location x_i, and the summation is over the n samples included in the estimates. It was found by trial and error testing that a value of $p = 2$ produced a sensible lithology at the control boreholes.

The grid discretisation for the lithological and hydrofacies models was carried out by projecting the data locations into Universal Transverse Mercator (UTM 1983) metre for zone 46 N to minimise spatial distortion. Models were developed to a depth of 250 m below MSL and the topographic elevation was defined by the Shuttle Radar Topography Mission (SRTM) 90 m X 90 m horizontal to 1 m vertical resolution digital elevation data model *(EROS 2002)*. Sensitivity of

the models was tested to varying the grid dimension. A grid dimension 1000 m (x) × 1000 m (y) × 2 m (z) was found to be a better basis for 3-D representation of the density of data available. In the current dataset the average spatial density of the logs is 1 in ~8 km^2; in some areas logs are very closely spaced at less than 500 m distance. Moreover, there are few big spaces of no-data in the spatial distribution of data (Figure 4-1a). It should be noted that the results contain uncertainties associated with the poor data density as spatial variability and heterogeneities commonly occur at <100 m scale in a fluvial-deltaic/alluvial setting. However, the analysis will certainly give a plausible picture of the regional to sub-regional lithological variability, the assemblage of hydrofacies, and hence the hydrostratigraphical configuration of the area. A fence diagram containing 3 N-S, and 6 E-W lines was developed from the solid models of lithofacies and hydrofacies (see section 4.3.3).

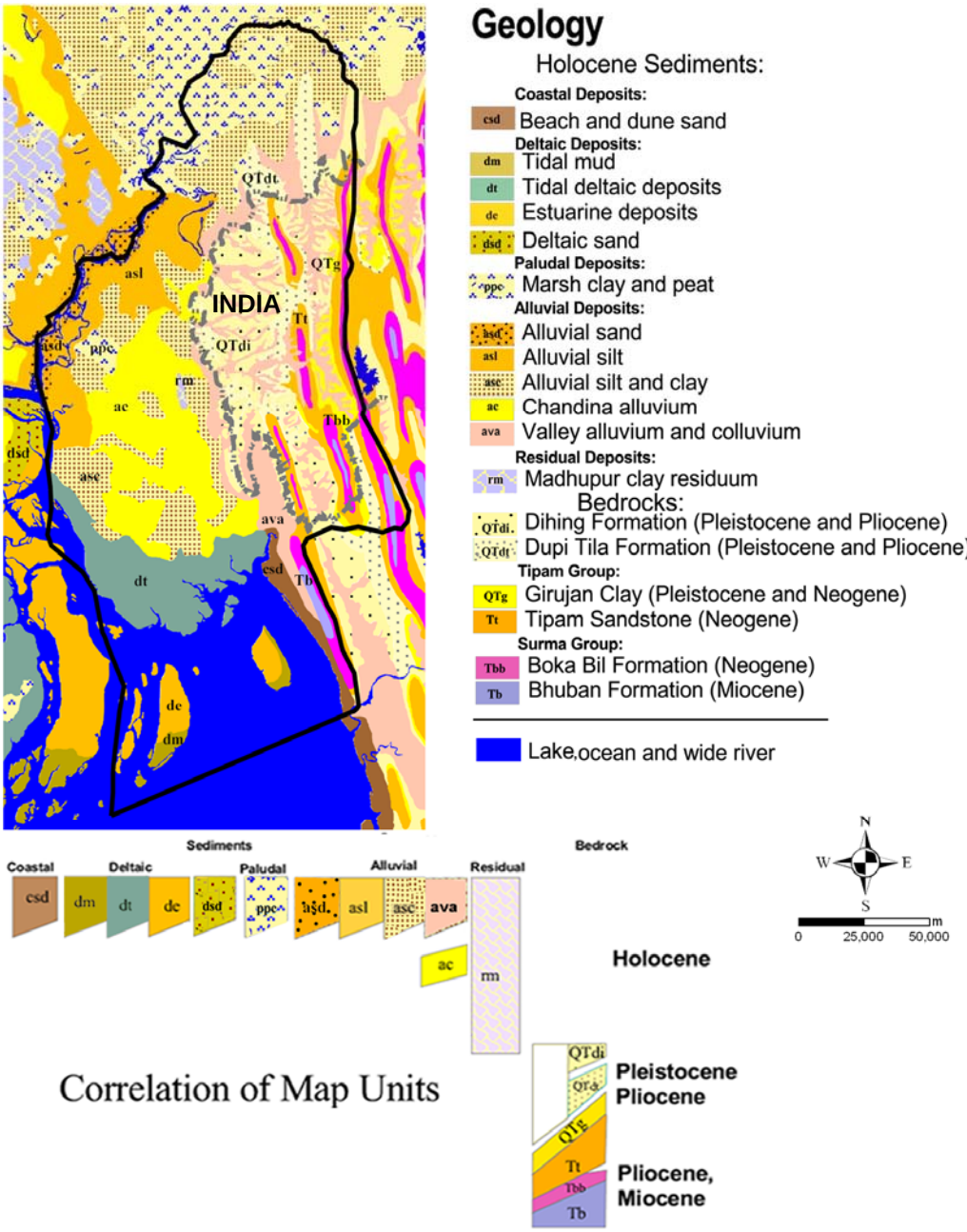

Figure 4-4: Surface geology of the model area, compiled from various sources (see text).

4.2.6 Sedimentological analysis

Analysis of lithofacies and hydrofacies (sections 4.3.2, and 4.3.3) indicate discontinuities in layering of finer hydrofacies and the discontinuities are filled with coarser sand-bodies, which may indicate paleo-channels. These characteristics have implications for groundwater flow. To substantiate the aforementioned observation and position of the paleo-channels, drillers' log datasets were analysed for sand to silt-clay ratio, identification of channel sands and regions of stacked channels.

4.2.6.1 Sand to silt-clay ratio

Individual drillers' log was analysed to calculate the cumulative thickness of the clay and silty-clay. Thicknesses were calculated for the entire depth, and also slab wise (0-100, 100-200, and 200-300 m). This gives four sets of data at each location of the drillers' log if the maximum depth of the log record is ≥280 m (preferably ≥300 m). Interpolation between the data points was performed using the IDWA interpolator for all depth slices.

4.2.6.2 Stacked channels

The hydrogeological framework of the area is determined by the channel-interchannel-interfluve fluvio-deltaic deposits. Whatever the uncertainty due to poor records of the drillers' log, it is likely that fine-medium or coarser grade sands should be recorded as drillers target these lithologies, and so should silty-clay and finer be included, as these are difficult to drill through. Several N-S and E-W log to log lithological sections were prepared. Subsequently, channel-sand bodies were identified in each individual log, and the identifications were collated to derive the 3-D configurations of paleo-channels sand bodies.

4.2.7 Hydraulic conductivity: estimation of effective hydraulic conductivity

Estimation of hydraulic conductivity is the major concern for uncertainty reduction in hydrogeological applications (*Renard and de Marsily 1997; Sarris and Paleologos 2004; de Marsily et al. 2005*). Uncertainties depend on various aspects (e. g., scale of measurement, nature of medium) and upscaling of the hydraulic conductivity measurement is a big concern (*Schulze-Makuch et al. 1999; van den Berg and de Vries 2003; Michael and Voss 2009b*). Hydraulic conductivity is still the dominant parameter by which geological variability in groundwater flow and transport models can be represented. Hydraulic conductivity can be estimated in the field by pump-test, in the laboratory from core tests, and from lithological data (e. g., *Freeze and Cherry 1979*) and may also from consolidation test data (*Tellam and Lloyd 1981*) using empirical relationships. Each has limitations and advantages depending on the objectives. Estimation of hydraulic conductivity using empirical relationship is, however found to reduce uncertainty many folds than others in case of regional-scale studies *(Nilsson et al. 2007)*.

In the current study, lithological attributes derived from drillers' log were used to estimate the effective hydraulic conductivity as a means of representing hydrogeological observations in groundwater models. Two different approaches were taken to estimate the effective hydraulic conductivity as described below.

4.2.7.1 Limited extent of lithofacies: applying the method of Ababou (1996)

In a layered system of strata with constant thickness and infinite extent, the direction of highest equivalent hydraulic conductivity (μ_α) will be parallel to layering, and the direction of lowest conductivity (μ_h) will be perpendicular to layering, given by the arithmetic mean (Eq. 4-3) and harmonic mean (Eq. 4-4) of the conductivity of the layers respectively *(Freeze and Cherry 1979)*. These are known as Wiener bounds, the maximum and minimum possible values of effective hydraulic conductivity *(Renard and de Marsily 1997)*.

$$\mu_h \leq K_{eff} \leq \mu_\alpha$$

$$\mu_\alpha = \frac{\sum K.b}{\sum b} \quad \text{..... Eq. 4-3}$$

$$\mu_h = \frac{\sum b}{\sum b/K} \quad \text{..... Eq. 4-4}$$

K = hydraulic conductivity of a particular lithological unit, and

b = thickness of lithological unit

However, in fluvio-deltaic alluvial settings lithological layers have limited extent and the above empirical equations are not valid. Ababou *(1996)* derived an equation for layers with limited extent assuming an anisotropic and statistically homogeneous medium:

The effective hydraulic conductivity in any direction (K_{eff}) is

$$K_{eff} = \mu_a^{\alpha} \mu_h^{1-\alpha} \quad \text{..... Eq. 4-5}$$

μ_α= as defined in eq. 4-3

μ_h = as defined in eq. 4-4

α = as defined in eq. 4-6

$$\alpha = \frac{D - l_h/l_i}{D} \quad \text{..... Eq. 4-6}$$

D = space dimension (value 3 for 3D problems)

ℓ_i = correlation length, and

ℓ_h = harmonic mean of ℓi in the principal directions of anisotropy

Hydraulic conductivity (K) values for all lithofacies were selected from earlier literature (*BGS/DPHE 2001; GWTF 2002; Rahman and Ravenscroft 2003; Michael and Voss 2009b*) and are summarised in table 4-1. Correlation length, a length representing the statistical homogeneity, was considered as a parameter to use to integrate uncertainty associated with spatial extent of homogeneities in the fluvial-deltaic sediments – as discussed in the following paragraph.

In a layered system of finite extent, the effective hydraulic conductivity largely depends on the spatial extent of lithological layers. The vertical hydraulic anisotropy which controls vertical flow relies on the extent of the confining layer(s) *(Ababou 1996)*. Poor data coverage (section 4.2.2) leads to uncertainty in the lateral extent of the lithological units, which could range from a few 10s of metres to a few kilometres and is intrinsic to the nature of the deposits. River channels in Bangladesh are separated by a few 10s of metres to a few 1000s of metres. Therefore, to encompass the range of expected lateral extents of sediment layers, values for ℓ_i were considered to range from 50, 100, 500, 1000, 5000, 10000, and 50000 m. For simplicity ℓ_i was taken as isotropic on x and y plane, when in reality, they may vary. Effective hydraulic conductivity values were calculated for the entire depth of each individual log record assuming a single thick slab, and also depth-wise slabs (0-100 m, 100-200 m, and 200-300 m). In this manner four values of effective hydraulic conductivity were calculated at each log location where the maximum depth of the log record is ≥280 m. Subsequently, these point values were interpolated using the IDWA interpolator in order to derive a map of hydraulic conductivity by all depth-wise slabs.

4.2.7.2 A method based on sand and clay fraction

The permeability of sand and clay differs by five to seven orders of magnitude. In fluvio-deltaic terrain the finer lithologies (clays and silts) are often found to occur ubiquitously within the sand matrix, hence contributing to the net permeability of the sand-clay system. The effective hydraulic conductivity can be estimated from the sand-clay fractions *(Fogg 1986)*, but generalisation into two conductivity facies is a critical step toward characterising fluvial aquifer systems which are inherently complex.

Geological materials are naturally heterogeneous and anisotropic. During modelling the intrinsic complexities of the media are upscaled by calculating the properties of media effective at the grid scale of the models. In a layered system of fluvio-deltaic alluvial settings, lithological layers have limited extent and empirical estimation established for infinite extent should not be valid. On the contrary, these terrains can be considered to be composed of channel fill and inter-channel sediments, where channel fill sediments are linearly extensive.

Table 4-1: Hydraulic conductivity values for different lithofacies are used to estimate the effective hydraulic conductivity (see text).

Lithofacies	Hydraulic conductivity (m/d)
Gravel with sand (gs)	120
Coarse sand (cs)	95
Medium to coarse sand (mcs)	72
Medium sand (ms)	50
Fine to medium sand (fms)	38
Fine sand (fs)	25
Very fine to fine sand (vffs)	20
Very fine sand (vfs)	12
Silt/ clayee sand / sandy clay (scs)	0.397
Clay (c)	6.05e-5

The arithmetic mean (Eq. 4-3), as opposed to the geometric mean or harmonic mean (Eq. 4-4), is considered appropriate for linearly extensive channel-fill sand bodies. The inter-channel sediments, on the other hand, are much less extensive, consisting of a heterogeneous mosaic of relatively thin sands, silts, and clays. Geometric mean of individual K_h measurements was recommended to be best the estimate of equivalent horizontal hydraulic conductivity for this deposit *(Warren and Price 1961)*.

It can be assumed that in a fluvio-deltaic aquifer system composed of channel fill sand and/or inter-channel interfluve sediments, their respective proportions can be approximated by the ratio of silt-clay to sand of the aquifer materials. In this way an estimation of the effective horizontal hydraulic conductivity (K_{eH}) of the sand-silt-clay aquifer system can be approximated as of equation 4-7 below, modified after Fogg *(1986)* to account for the effect of clay interfluves. K_{eH} is the arithmetic mean of individual K_h values where the aquifer matrix is sandy and approaches the geometric mean when silt-clay becomes dominant. The sand fraction in some (inter-channel) areas approaches to zero i. e., dominated by silt-clay and spatially less extensive. Davis *(1969)*) shows a difference of at least 3 orders of magnitude for the K values of fine sands and silts. To address this issue in the estimation of K_{eH} a dividing factor of 100^c is used. When the sand content is >25%, the exponent c is given a value of zero to account for the generalised sandiness of the area, and possibility of sand intercalation.

$$K_{eH} = \frac{1}{100^c}\mu_g\left(\frac{\mu_a}{\mu_g}\right)^{S_0} \quad \text{.....Eq. 4-7}$$

μ_g = Geometric mean of hydraulic conductivity data from the area

μ_a = Arithmetic mean of hydraulic conductivity data from the area

S_0 = Sandiness [ranges from 0 to 1, represents 0 to 100% sand]

c = 0 when S_0 >0.25, and 1 when S_0 <0.25

In general, geological porous materials at a small scale behave as homogeneous isotropic media, which become heterogeneous and anisotropic with an increase in unit size. However, a heterogeneous system can be described mathematically as anisotropic in order to encompass the heterogeneity. The primary cause of anisotropy on a small scale is the orientation of clay minerals in sedimentary rocks and unconsolidated sediments *(Freeze and Witherspoon 1967)*. On a larger scale, layered heterogeneity with intrinsic anisotropy such as clay and silt layers contribute to the regional and basin-scale anisotropy. Ababou *(1996)* shows how the lateral dimension of clay and other finer materials contributes to the system anisotropy. Often in groundwater modelling vertical hydraulic conductivity is estimated as a fraction of the effective horizontal hydraulic conductivity in order to describe the anisotropy. Equation 4-8 is proposed here as an approach to estimate the effective vertical hydraulic conductivity (K_{eV}) with respect to K_{eH} considering the sources of anisotropy in the system. This approach is consistent with the general observation that anisotropy of geological media is in the range 10^2 to 10^7.

$$K_{eV} = \frac{K_{eH}}{100 \times 10^{z}} \times \left(\frac{10^{n}}{100^{m}} \right) \quad \text{.....Eq. 4-8}$$

K_{eH} = Effective horizontal hydraulic conductivity

z= 1 if silt+clay >75% and clay >20%

z= 0.5 if either silt+clay >75% or clay >20%

z= 0 if silt+clay <75% and clay <20%

n=1 when S_0 >0.75

n= 0 when S_0 <0.75

m=0 when S_0 >0.95

m=0.75 when 0.95>S_0 >0.75

m=0.50 when 0.75> S_0 >0.50

m=1.0 when S_0 <0.50

These parameter value ranges for c, m, n, and z were chosen to reproduce observed heads and travel times (see Chapter 8) over a coarse model grid at least as well as the representations based on the ‘Ababou method’.

The Bangladesh Water Development Board (BWDB) conducted 31 pump-tests in the study area between 1987 and 1993. The (horizontal) hydraulic conductivity values acquired from analysis of these pump tests are summarized in figure 4-5. The K values form a log normal distribution. These characteristics are due primarily to the fact that the aquifers under development are mostly in regions of major channel sand, whereas the inter-channel areas are not developed. The broad distribution of (pump tests derived) K values, from 3 to 30 m/d, may be representative of complex fluvial depositional systems. These K data were used to calculate geometric and arithmetic mean for use in equation 4-7.

4.2.7.3 Hydraulic conductivity for areas with limited data

Drillers' log data were available only for Bangladesh territory but the area of interest extended beyond the territory into the Indo-Burman hills. The available geological information has been collated (Figure 4-4). Effective hydraulic conductivity values for the area were estimated on the basis of the geological information.

There is a thick sequence between the maximum depth of the drillers' log and top the UMS, which lacks lithological information. Only 11 petroleum drilling lithological descriptions are available for this part of the sequence. Basin-scale model analysis shows that 6 % of the total recharge penetrates deeper than 350 m and only 0.4% of the total recharge penetrates >1000 m for reasonable parameter values (*Michael and Voss 2009a*). Due to lack of data and insignificant involvement of the sequence at depth a simplistic representation is estimated. Note that the entire sequence above the UMS is fluvial-deltaic origin. A single representative anisotropy value is estimated from the median of hydraulic conductivity value of the upper 300 m thickness, and an anisotropy (K_h/K_z) is taken as 10^4 for the lower sequence.

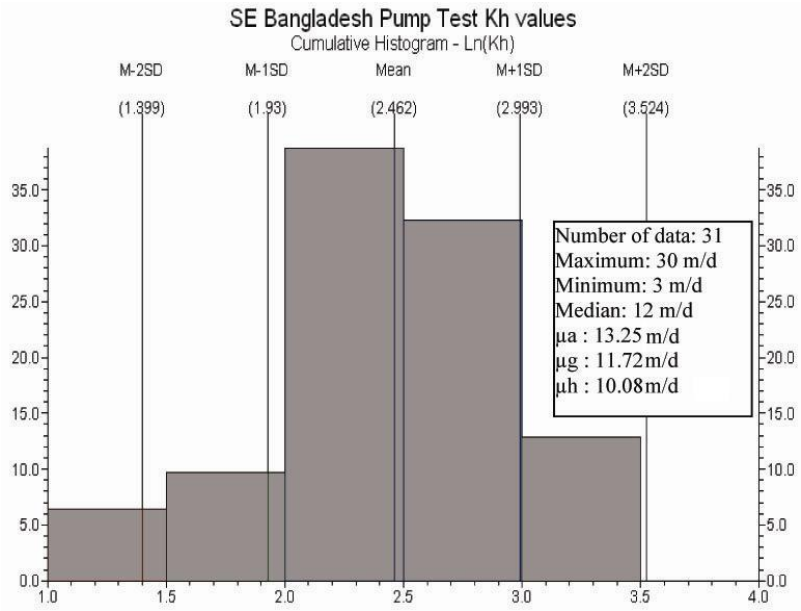

Figure 4-5 Histogram of ln(K_h) values, pumping test analyses from SE Bangladesh; a summary of pump-test data is given in the rectangle.

4.3 Results and Discussion

4.3.1 Hydrostratigraphical basement

Hydrostratigraphical basement, the UMS, is exposed at the surface in the eastern hills and lies ~2500 m below ground surface in the western part of the area (Figure 4-6). A shallow marine environment prevailed in the area during the Mio-Pliocene time *(Gani and Alam 1999)*. At the onset of the Himalayan orogeny the marine clay was subject to uplift, and the depositional regime changed to a fluvio-deltaic setting. *En-echelon* folding *(Hoque 2001)* led to localised doming. The UMS is present throughout the area with variable thickness (ranges from ~50 to 150 m) and westward increasing depth. Its impervious nature is indicated by its role as hydrocarbon seal in the gas-fields of the region *(Reimann 1993)*.

4.3.2 Lithofacies and lithostratigraphy

The entire lithological sequence above the marine clay is composed of clay, silt, sand, and their mixture, assembled by the fluvio-deltaic depositional engine. The sequence is spatially and vertically heterogeneous. Correlation of low permeability units is found not to be credible (Figure 4-7). In some areas low permeability materials are more widely extensive and may confine discrete aquifers locally. In the other contexts, sand bodies may be embedded within the low-permeability materials, and form bounded, leaky aquifers.

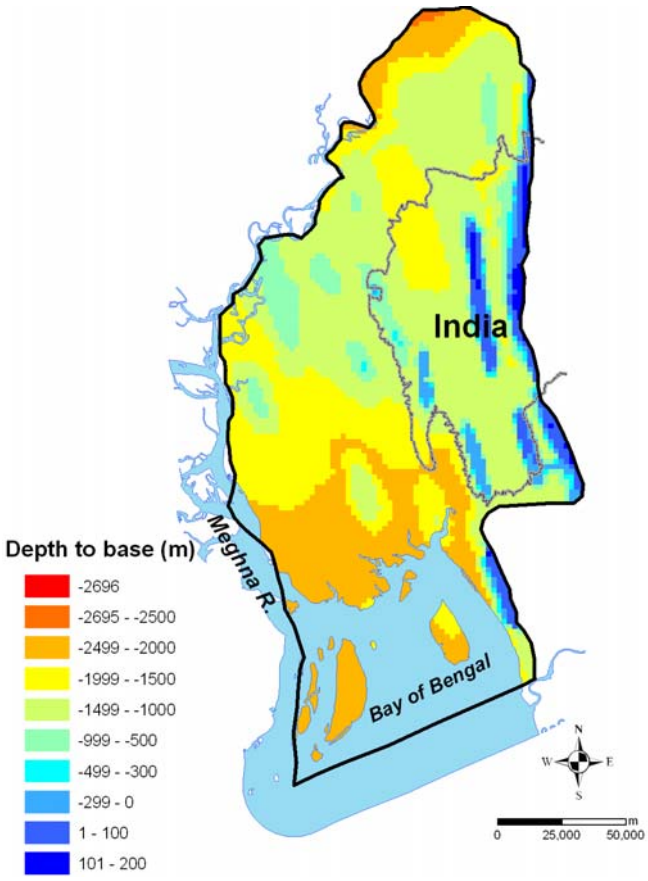

Figure 4-6: Depth to the top (reference, relative to sea-level) of UMS, hydraulic basement of the aquifer system in the area

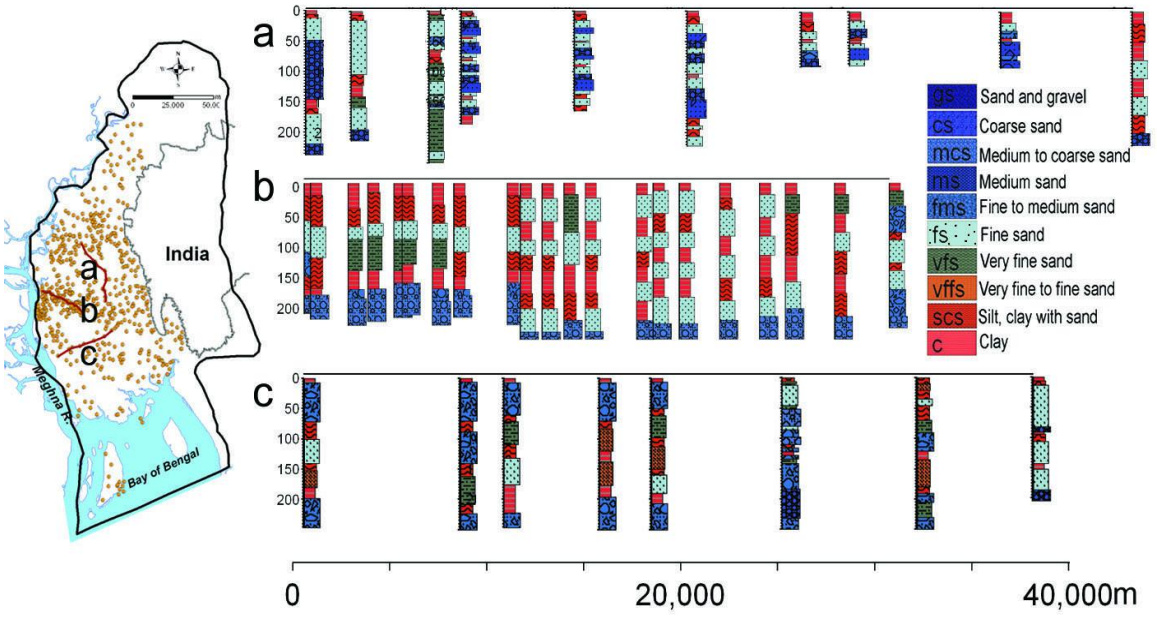

Figure 4-7: Log to log section indicating spatial variability in lithofacies

Lithofacies modelling illustrates the distribution of lithologies in 3-D (Figure 4-8). The sedimentary sequence up to 250 m depth is dominated by sand, ~60%, and the reminder silt-clay. In general the distribution of lithologies is patchy and none form regional or sub-regional layers. The fence diagrams show that the finer materials (clay and silty clay) are the dominant surficial sediments. The eastern, north-western, and south-western parts of the area are dominantly clay and silty-clay and in some cases they appear as an intermediate low permeability layer. The central and deeper regions are dominantly sandy, and in some places clay is absent. Moreover, there is a general trend of increasingly coarse grain size with depth. At the Holocene high stand finer deposits overlie incised channel-fill sand deposits of the previous low stand. Indications of sandier embodiments within relatively finer lithologies may indicate channel-fill sand bodies.

Interpretation of high resolution geophysical logs from a sandier area (as identified by lithofacies modelling) comply with inferences of drillers' log, which are poor in quality, and often lack detail. Geophysical logs illustrate that the shallower sequence is finer grained than the deeper part (Figure 4-9). Individual logs were divided subjectively into four layers, by reference to patterns of the log responses. These layers may indicate alternating variation in heterogeneities. Similar layering elsewhere, from the drillers' log was found to be not credible due to lack of recorded detail. To discern the vertical variation upper 300 m was considered 3 equal layers. This approach was used as a basis for vertical analysis of hydrostratigraphy and the estimation of effective hydraulic properties.

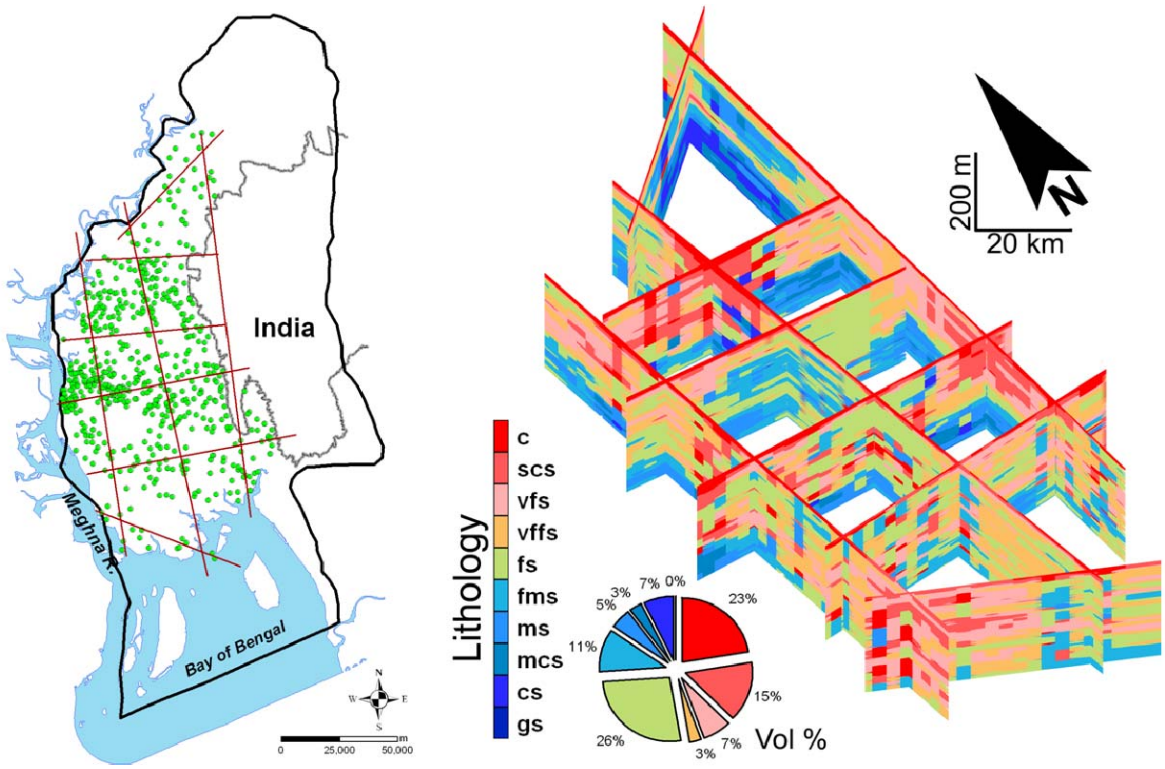

Figure 4-8: Fence diagram based on hydro-facies modelling - used RockWorks 2002 with IDWA algorithm with a grid size 1000 m × 1000 m × 2 m. The pie chart indicates the modelled volume (%) of different lithologies.

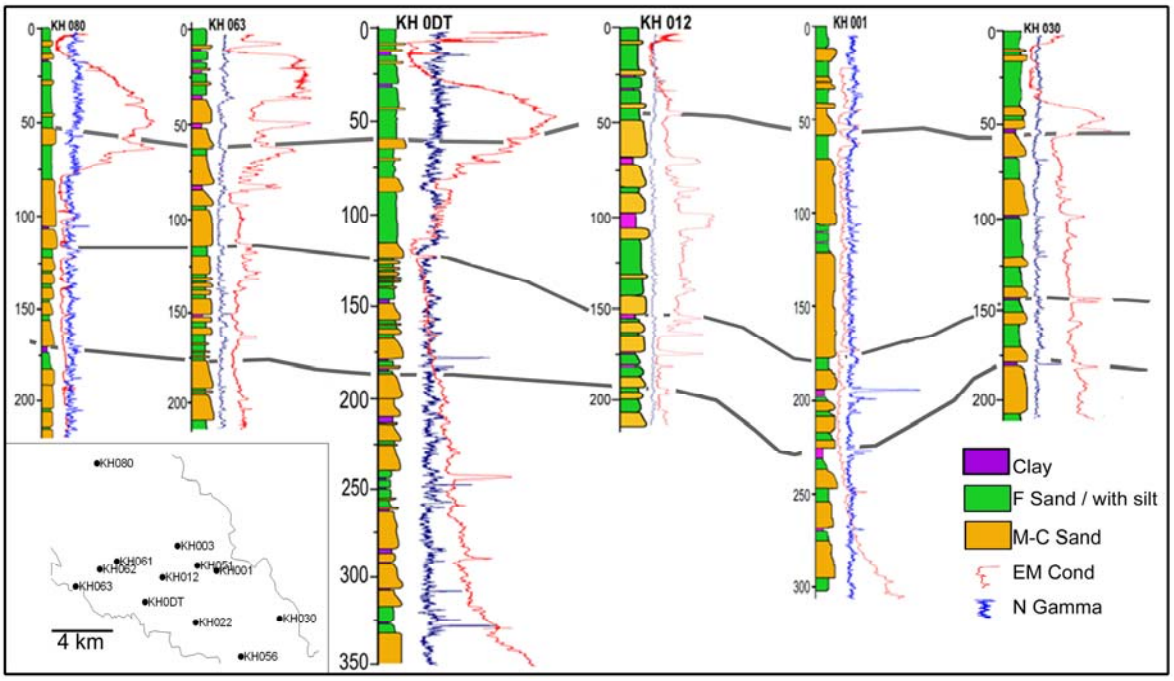

Figure 4-9: Bore-hole geophysical logs with interpreted sedimentary facies, and log response (γ log) indicating alternating apparently heterogeneous deposits. The area is shown in the inset (see figure 4-1, for location). Note that EM conductivity log responses were influenced by the salinity of the pore-water at some depths and locations.

4.3.3 Hydrofacies and aquifer configuration

Hydrofacies modelling demonstrates zones of coarser- or finer grained lithofacies, and areas of mixed-lithofacies, in 3-D (Figure 4-10). Finer hydrofacies are dominant in the northwest and southwest of the area, where they separate the shallower and deeper parts of the aquifer. Coarser hydrofacies dominate the whole sequence in the middle-north part and the deeper level throughout the whole area. In general the mixed hydrofacies at shallower levels indicates greater spatial variability. This spatial variability may be related to the nature of sedimentation during the Holocene, when channel migration, avulsion and crevasse splay continuously modified the interchannel floodplain deposits *(Goodbred et al. 2003)*.

The hydrofacies modelling depicts a single aquifer which is hydraulically connected throughout. In most of the area fine sand is the dominant constituent of the aquifer, with coarser materials in some parts. Particularly, the shallower level of the aquifer is composed of finer lithologies while the deeper levels contain coarser sands.

The hydrofacies indicates the hydrogeological implications of the spatial variability of grain-size within the aquifer materials, notably the spatial continuity of the finer layers and stacking of the coarser sand bodies (Figure 4-11). These coarser sand bodies are the sedimentary products of larger paleo-channels, discussed in the following section.

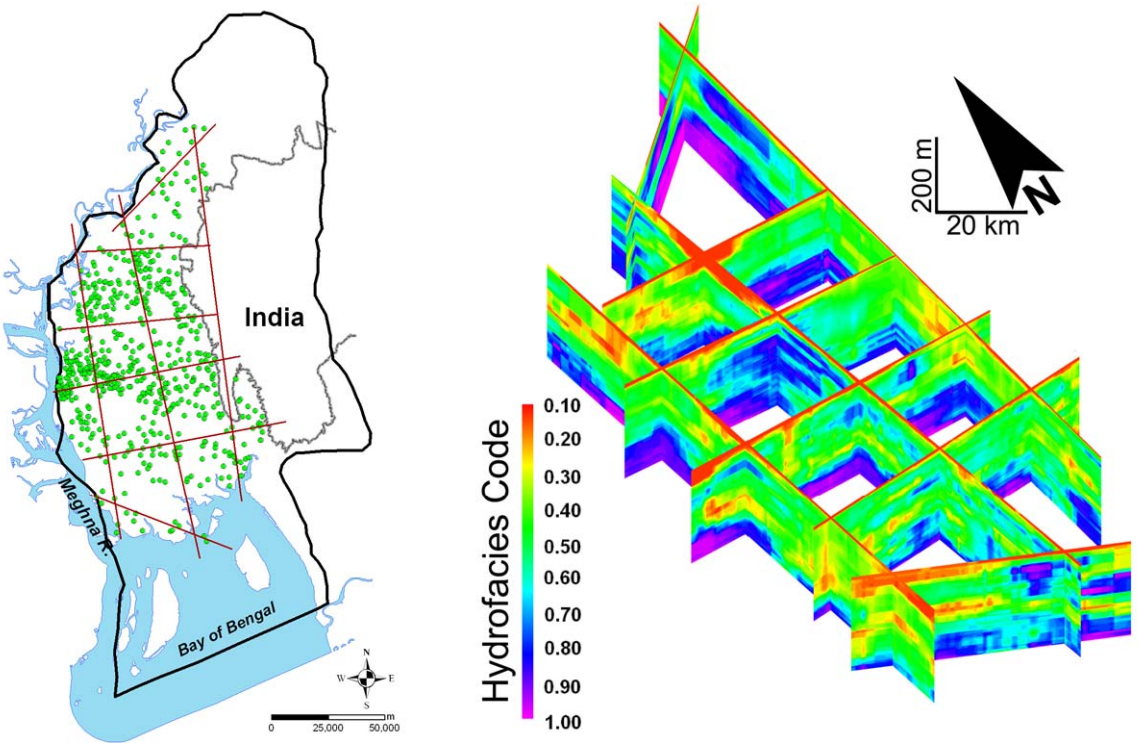

Figure 4-10: Fence diagram based on hydro-facies modelling - used RockWorks 14® with IDWA algorithm for a grid size 1000 m × 1000 m × 2 m. Fence faces are shown in the left panel, and '1' in hydrofacies code indicate coarser sand while '0.1' stands for clay.

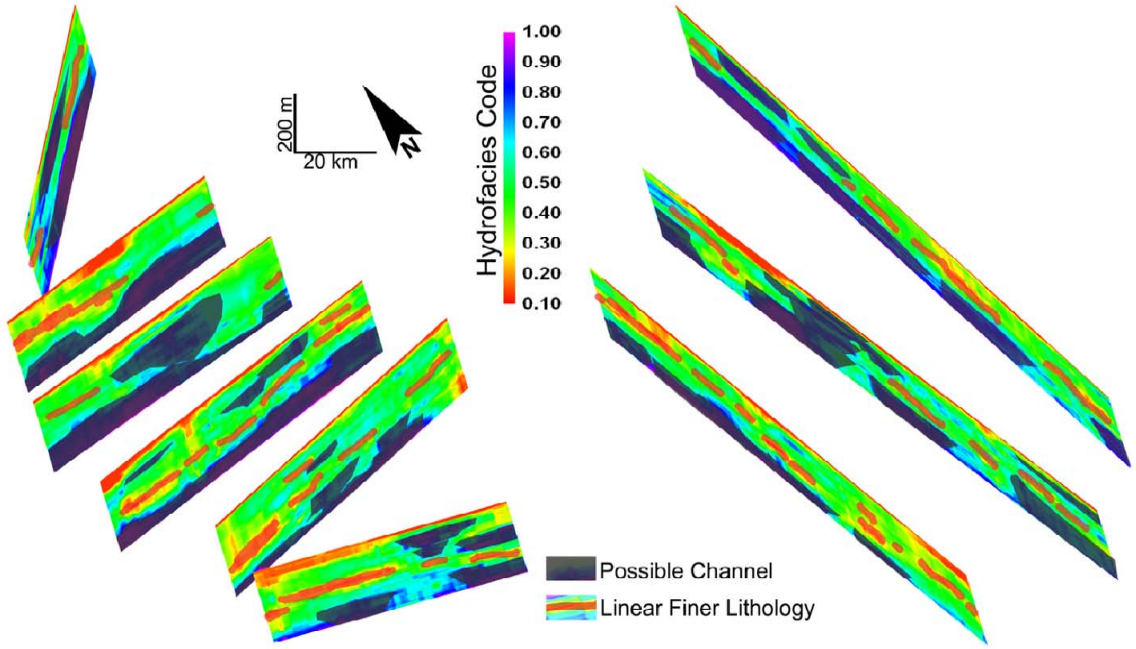

Figure 4-11: Exfoliated version of figure 4-10 with annotated channel-fill sand and layering of finer materials. The coarser sandy embodiments in the aquifer may result from aligned paleo-channels. Channel stacking may provide vertical connectivity, and affect horizontal and vertical anisotropy.

4.3.4 Paleo-channels and preferential flow paths

The entire sequence overlying the UMS is made of fluvial-deltaic sediments, deposited in channel-interfluve settings. In such setting deposits are characterised by channel-fill sands and floodplain deposits. Hydrofacies analysis illustrates the characteristics of these deposits (Figure 4-11). In some parts stacked sand bodies extend all the way to the surface. Equivalent channel-fill sands were previously documented on the seismic sections at a greater depth (*Lindsay et al. 1991; BGS/DPHE 2001; Alam et al. 2003*). Note that the seismic sections were interpreted for petroleum exploration and data for the shallower (<500 m) levels are not processed.

Sand to silt-clay ratio analysis depicts a low cumulative thickness of finer (clay and silty-clay) materials in a curvilinear pattern, which may indicate the orientation of paleo-channels at depth (Figure 4-12). Depth-wise analysis demonstrates that the channels were not fixed in time, and the number and direction of the channels also changed. In figure 4-12c the 200-300 m depth-slab shows a N-S channel which may represent a paleo-course of the Meghna River (~300 ka BP or earlier) during a sea-level low stand. Later (i. e., ~200 ka BP or earlier), under high-stand condition the Meghna River shifted westward to its current course, and rivers drained from the eastern hills to the Meghna in the west and to the coast in the south. This distribution may have persisted over the last two glacial maxima. The present day river courses are very close to those depicted in the depth slab 100-200 m of figure 4-12c.

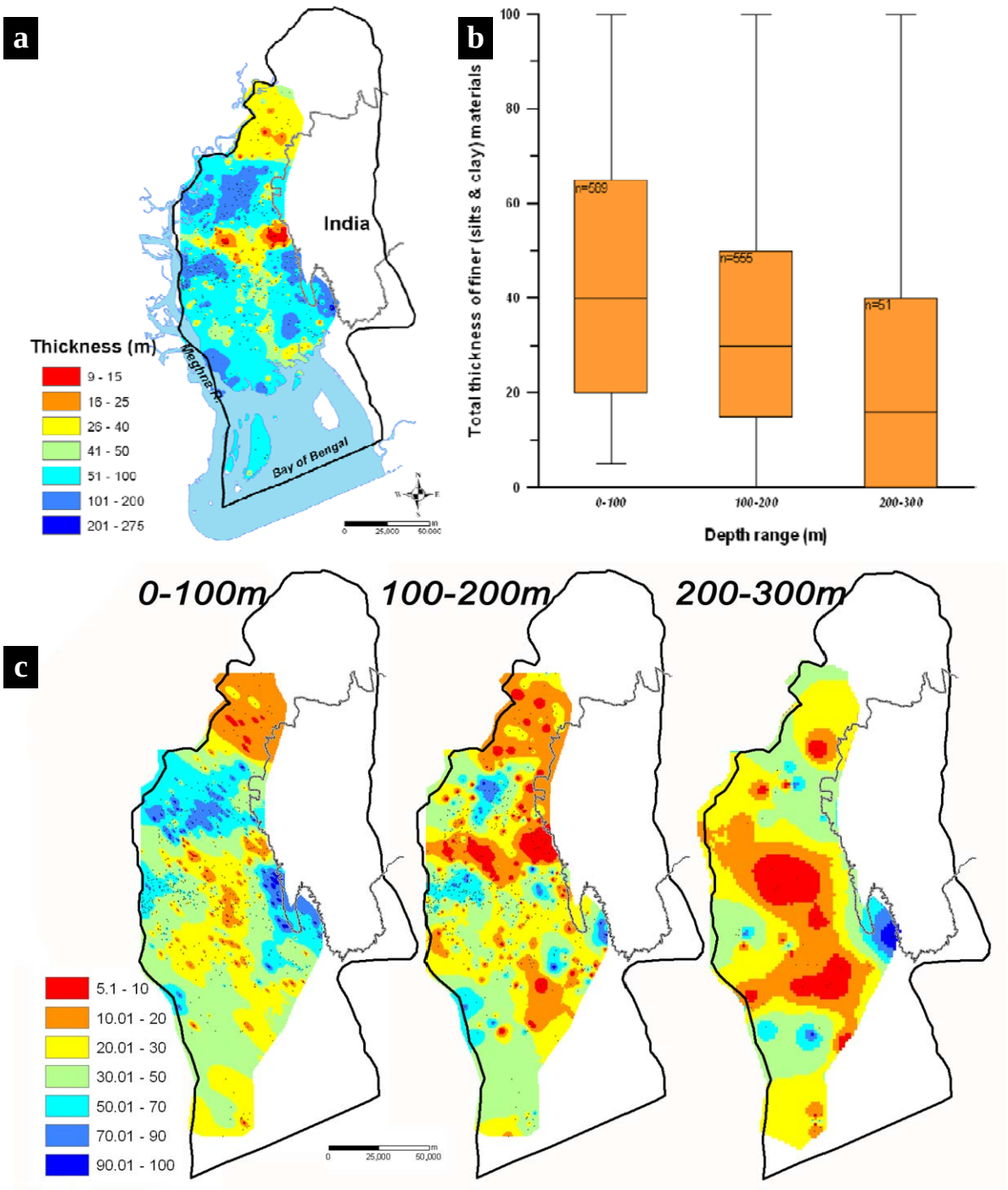

Figure 4-12: (a) Cumulative thickness (m) of finer materials (silts and clay) over full depth of log; (b) Box plot of percentage of finer materials in different depth slabs, indicating a coarsening with depth; (c) Cumulative thickness of finer (clay and silts) materials for sequential depth slabs.

Analysis of channel-fill sands reveals several episodes of stacking of channel-fill sands, particularly in the upper 200 m. In some areas (Figure 4-13) stacking of channel sands produces direct connection between shallow and deeper levels of the aquifer. Channel-fill sands in the area are mostly medium to fine grained with occasional coarse sands which may be reworked sediment from the Indo-Burman Hill Ranges in the east. N-S log to log sections were created as the depositional axis is from east to west, towards the Meghna River.

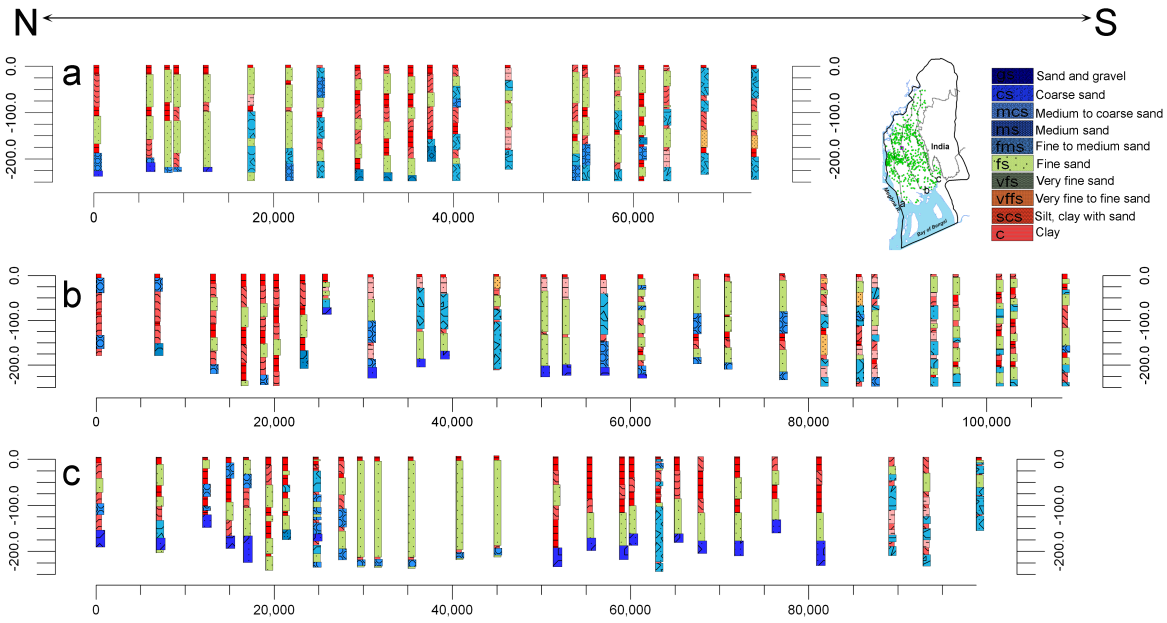

Figure 4-13: N-S log to log sections. Map (upper right corner) indicates the location of the lines; colour code shows lithologies. The sections illustrate the intercalation of finer and coarser materials, which indicate that neither channel nor interfluve remained static for long duration. In panel (c) the thick fine sand may indicate stacked channels extending up to shallow depth.

A 3-D distribution of paleochannel sand bodies is inferred from the hydrofacies modelling and sedimentological analysis. These channels may act as preferential flow paths for groundwater in the region *(Ravenscroft 2003)*. However, the paleochannels are filled with relatively coarser and the surrounding is also sandy though relatively finer, maybe due to frequent channel migration across the floodplains. This general sandiness and hence low hydraulic contrast would not favour preferential flow *(Glezen and Lerche 1985)* along the paleo-channels. If consideration is given to the general sandiness of the region (which is here ~60%) preferential flow along the channel may not be significant. The potential for vertical leakage is however substantial.

4.3.5 Hydrostratigraphical nomenclature

An essential part of any hydrogeological investigation is to define and map hydrostratigraphical units (aquifer and confining units) in the subsurface. Previous studies (*Aggarwal et al. 2000; BGS/DPHE 2001; DPHE/DANIDA 2001; GWTF 2002; DPHE/DFID/JICA 2006; Mukherjee et al. 2007b*) have discussed the general nature of aquifers in the basin (section 3.3.3). Most have described the aquifer system as a discrete multi-aquifer. The current analysis suggests a single aquifer system on regional scale with aquifer zones locally distinguished between finer sediments.

There are several different descriptions of the aquifer system nomenclature (section 3.3.3). These variations in classification of the aquifer system reflect a range of perception about the system. At present there is no widely accepted national or international code for hydrostratigraphy to practice. Laney and Davidson *(1986)* prepared guidelines for hydrostratigraphical nomenclature,

applied by the United States Geological Survey (USGS). In the guidelines, from smallest to largest, the terms used to classify hydrostratigraphy are *zone*, *aquifer*, and *aquifer system*. A *zone* is used to identify a segment of an aquifer with a particular hydrological characteristic that is not typical of the entire aquifer. An *aquifer* is a formation, group of formations, or a part of a formation that contains sufficient saturated permeable material to yield significant quantities of water to wells and springs. An *aquifer system* was originally defined by Poland et al *(1972)* as a 'heterogeneous body of intercalated permeable and poorly permeable materials that function as water-yielding hydraulic units; it comprises two or more permeable beds separated at least locally by aquitards that impede groundwater-movement but do not greatly affect the hydraulic continuity of the system. The guideline indicates that aquifer names should be derived from lithological terms, rock-stratigraphical units, or geographical name, and recommends against the use of time-stratigraphical names, relative position, alphanumeric designations, depositional environment, depth of occurrence, acronyms, and hydrological conditions. Confining units should not be named unless doing so clearly promotes understanding of a particular aquifer system.

In terms of hydraulic continuity at basin and regional scale it seems that above the UMS the sedimentary sequence fulfil the criteria for and are hydraulically behaving as *an aquifer system*. This *aquifer system* may locally host discrete *aquifers* and a number of *zones*, separated by confining layers. One question is how extensive the confining units need to be to define a discrete aquifer. This is largely depends on the scale of development i. e., level of exploitation. If a single well is considered the required extent may be the well catchment or radius of influence. However, in case of regional groundwater flow, the extent of a clay layer controls the maximum depth of gravitational flow penetration, and thickness of the clay plays a lesser role (see section 6.2.1.4). The Ababou *(1996)* equation (section 4.2.7.1) shows at a certain lateral extent clay layers have no additional effect on the vertical anisotropy i. e., on the vertical flow. For the silt-clay layers in the study area this limiting areal extent is 5x5 km^2. This lateral extent of clay layering may therefore support a hydraulically discrete aquifer. In that consideration at basin scale, the Girujan Clay (a stratigraphical unit) would be able to support a discrete aquifer in the north-east part of the basin, and the Lower Dupi Tila aquifer *(Haque 2006)* in Dhaka by a locally extensive silt-clay layer. By this analysis several local aquifers may be identified in the northwest and southwest corner of the study area (Figure 4-8).

Considering the Laney and Davidson *(1986)* guidelines and the nature of the hydrogeology of the Bengal Basin, aquifers above the UMS should be named based on a geographical name. The basin is shared by West Bengal, an Indian state, and Bangladesh; together known as Bengal before 1905 (http://en.wikipedia.org/wiki/Bengal, accessed on 08 August 2009). As several lithostratigraphical units are incorporated, it is appropriate to name the aquifer system 'the *Bengal Aquifer System'* as suggested by Burgess et al. *(2010)*. This aquifer system hosts several local aquifers which can be named according to geographical or rock units or lithological name (Table 4-2).

Table 4-2: Proposed nomenclature for the aquifer system and potential aquifers

Proposed aquifer system	Time	Stratigraphical unit	Proposed name of Aquifers / Zone	Comments / Area of development
Bengal Aquifer System	Holocene	Alluvial	Alluvial	As *shallow aquifer* throughout the country except in the Barind and Madhupur Tracts area, and in the eastern hilly areas
	Plio-Pleistocene	Dupi Tila	Dupi Tila	As *Dupi Tila* in Dhaka, and in the Barind Tract area; In the floodplain as *Deep Aquifer;* Aquitard is not present as a continuous layer so the aquifers are locally discrete
	Mio-Pliocene	Tipam	Tipam	Partly is use in the hilly areas. In Sylhet area the Girujan Clay may be acting as wider aquitard confining the Tipam aquifer
Pre-Pliocene marine mud rich sequences				

4.3.6 Effective hydraulic conductivity

Geological heterogeneity must be described by numerical values of appropriate hydraulic properties in order to be represented in groundwater models. To be useful for flow and transport modelling, the hydraulic conductivity is used as a means of quantification of the hydrogeological variability and aquifer heterogeneity including flow paths analysis *(de Marsily et al. 2005)*. Fluvial reservoirs are known to be heterogeneous on a wide range scales *(Mikes and Geel 2006)*. Here, channel-floodplain heterogeneities are considered over a 100 - 300 m measurement thickness, and calculations were made at the individual location of each drillers' log. These values were then interpolated and extrapolated to determine gridded values at unknown locations.

4.3.6.1 Limited extent of lithofacies: applying the method of Ababou (1996)

Analyses of drillers' log data leads to 3-D views of subsurface which are plausible. Uncertainties are mostly due to the unknown spatial extent of lithological continuity. Effective hydraulic conductivity values were calculated using Ababou *(1996)* equation for 4 measurement-volumes at each location for each of seven correlation lengths (50, 100, 500, 1000, 5000, 10000, 50000 m) making 28 sets of data at each point. The data sets could be assembled in more than 3,000 representations of the sub-surface geology. The following limited number of representations (W1-5) have been selected for the basis of groundwater flow models (Figure 4-14). Note that codes within brackets are the model codes used in the modelling section:

Representation **W1 (M5):** Single homogeneous anisotropic aquifer. A recent study (*Michael and Voss 2009a*) shows that on the regional scale of groundwater-flow analysis, the aquifer can be represented with a single value of hydraulic conductivity, with anisotropy ($K_h/K_z=10^4$).

Representation **W2 (M8):** Single layer vertically homogeneous, spatially heterogeneous varied anisotropic aquifer; homogeneity (correlation) length, l=500 m.

Representation **W3 (M11):** Multi-layer heterogeneous aquifer with spatio-vertically varied anisotropy. Correlation length considered to be 100 m for the upper, 500 m for middle and 1000 m for the third layer respectively.

Representation **W4** (**M13):** Multi-layer heterogeneous aquifer with spatio-vertically varied anisotropy. Correlation lengh considered to be 500 m for each layer.

Representation **W5 (B6):** Multi-layer heterogeneous aquifer with spatio-vertically varied anisotropy. Correlation length considered to be 100 m for each layer.

4.3.6.2 A method based on sand and clay fraction

Effective hydraulic conductivity values linking to pump-test hydraulic conductivity were calculated using equation 4.7 and 4.8, at each drillers' log location. Two different representations were considered: a single layer aquifer, and a multi-layer aquifer.

Representation **W6 (SC2):** Single layer vertically homogeneous but spatially heterogeneous varied anisotropic aquifer (Figure 4-14).

Representation **W7 (SC3):** Multi-layer heterogeneous aquifer with spatio-vertically varied anisotropy (Figure 4-14).

4.3.7 Heterogeneity and effective hydraulic conductivity

Effective hydraulic conductivity varies greatly with measurement-volume *(Schulze-Makuch et al. 1999)* as well as with correlation length i. e., dimension of the homogeneity *(Ababou 1996)*. Increasing the volume of measurement increases the horizontal effective hydraulic conductivity, as also happens if the correlation length is increased (Figure 4-15). This increase is irrespective of the K_h measurement method (pump-test, core or laboratory measurement) *(Schulze-Makuch et al. 1999)*.

Spatial lithological variation results in spatial variation in effective hydraulic conductivity values (Figure 4-16). Effective hydraulic conductivity values are greatly influenced by the presence of low permeability materials. It is seen that the continuity of the low permeability materials is more significant than the thickness. In general, it is seen that for a reasonable correlation length, patterns of hydraulic conductivity replicate patterns of lithological heterogeneity including for example the implications of channel sands (Figure 4-12 and Figure 4-16).

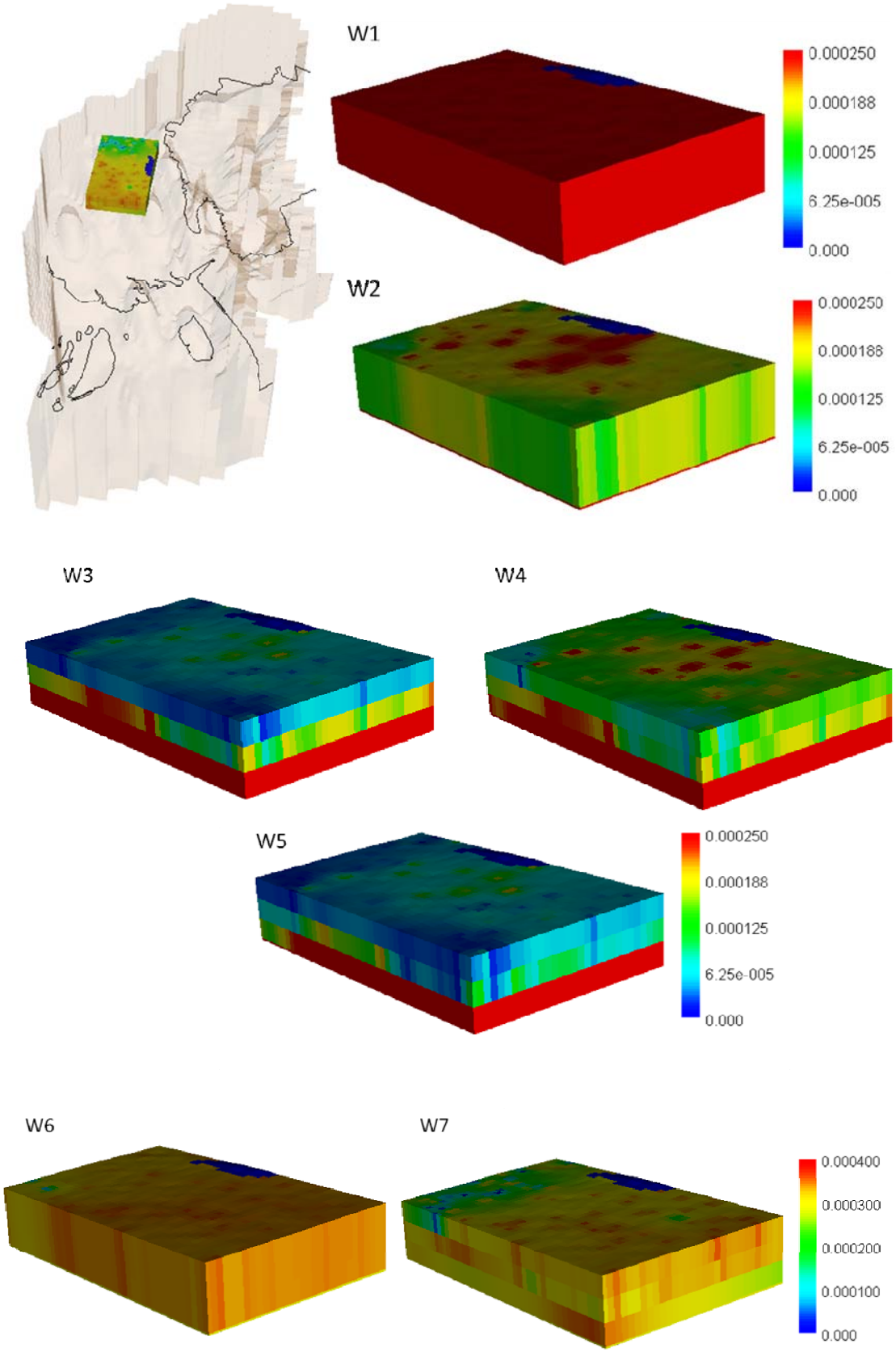

Figure 4-14: Alternating hydrogeological representations of the aquifer (Up to 300 m bgl) in terms of hydraulic conductivity (right colour bar, m/s). Left panel represents study area in 3-D and shows sample area which is used for depiction of different representations. W 1 to W7 indicates models of aquifer representation as of text.

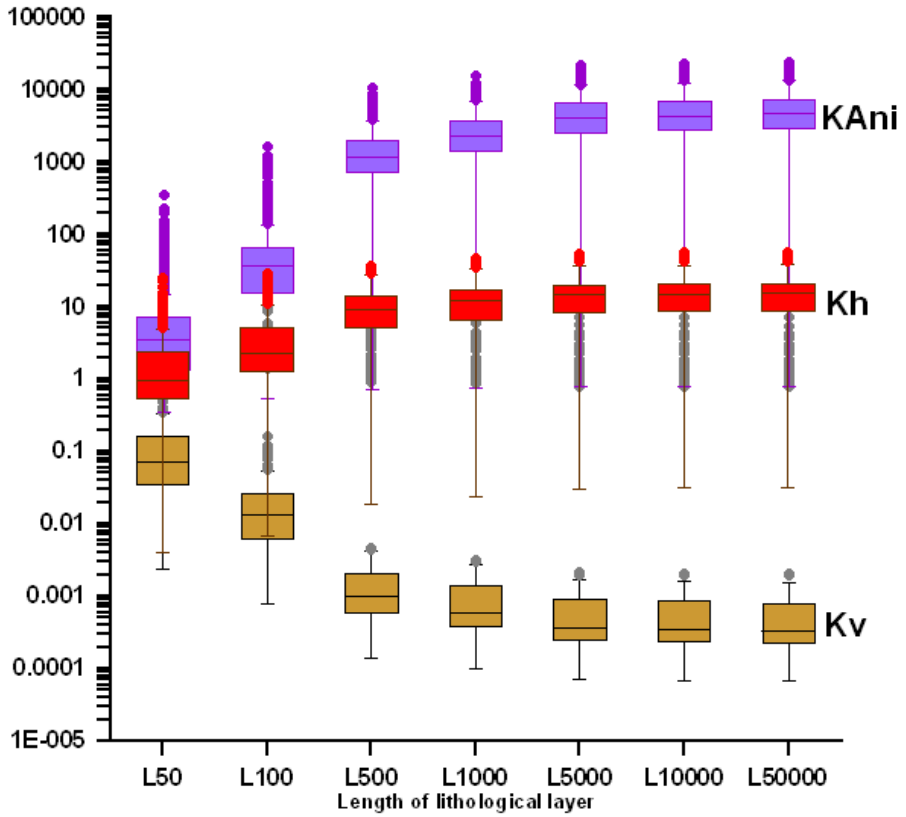

Figure 4-15: Graphs (with box-plot) indicating how increase of the correlation length increases effective hydraulic conductivity K_h and decreases effective K_v. Beyond a limiting extent the correlation length has negligible influence on the effective K values.

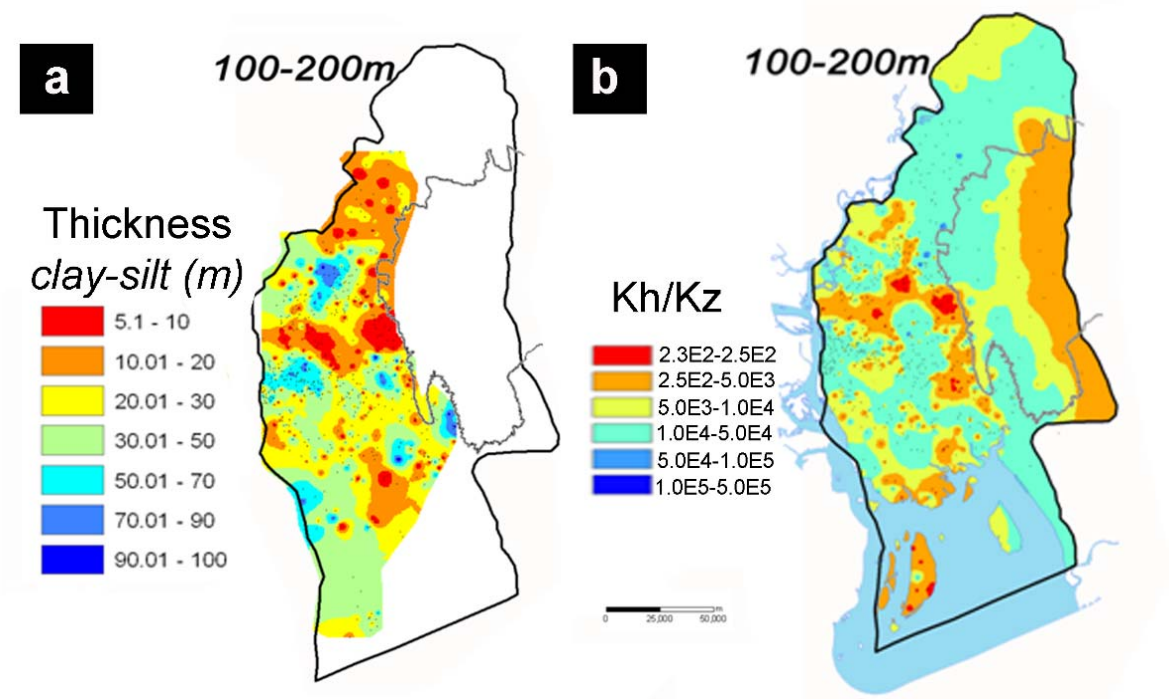

Figure 4-16: Conversion of lithological heterogeneity into hydraulic heterogeneity. (a) Spatial variation of cumulative silt-clay thickness; (b) spatial variation of the hydraulic anisotropy (Kh/Kz) retains sedimentological patterns.

4.3.8 Recognising the ubiquity of silt-clay layers

Hydrostratigraphical analysis indicates accumulations of finer and coarser materials including layered heterogeneities arising from discontinuous silt-clay layers within the aquifer system. The analysis also shows that the aquifer is dominantly sandy, though inspection of the logs reveals one or multiple silt-clay layer(s) at every log record (Figure 4-13 and Figure 4-17).

Individual silt-clay layers are variable in terms of thicknesses and depth of occurrence making lateral correlation inappropriate, but extrapolating silt-clay layers half-way to the adjacent logs indicates a structure in the occurrence of silt-clay bodies (Figure 4-17). It is found that in some areas silt-clay layers are at shallower depth compared to other areas. In addition, in some areas silt-clay layers are surrounded by sandy-bodies. Interestingly, mosaics of the stacked silt-clays layers in blocks of up to 100-300 m show continuity of silt-clay layering. This distribution pattern of silt-clay layer is defined as '*stacked-mosaic-continuous*' (see section 6.2.1.4). The discontinuous silt-clay layers coupled with topography are found to control groundwater flow in the basin (see section 6.2).

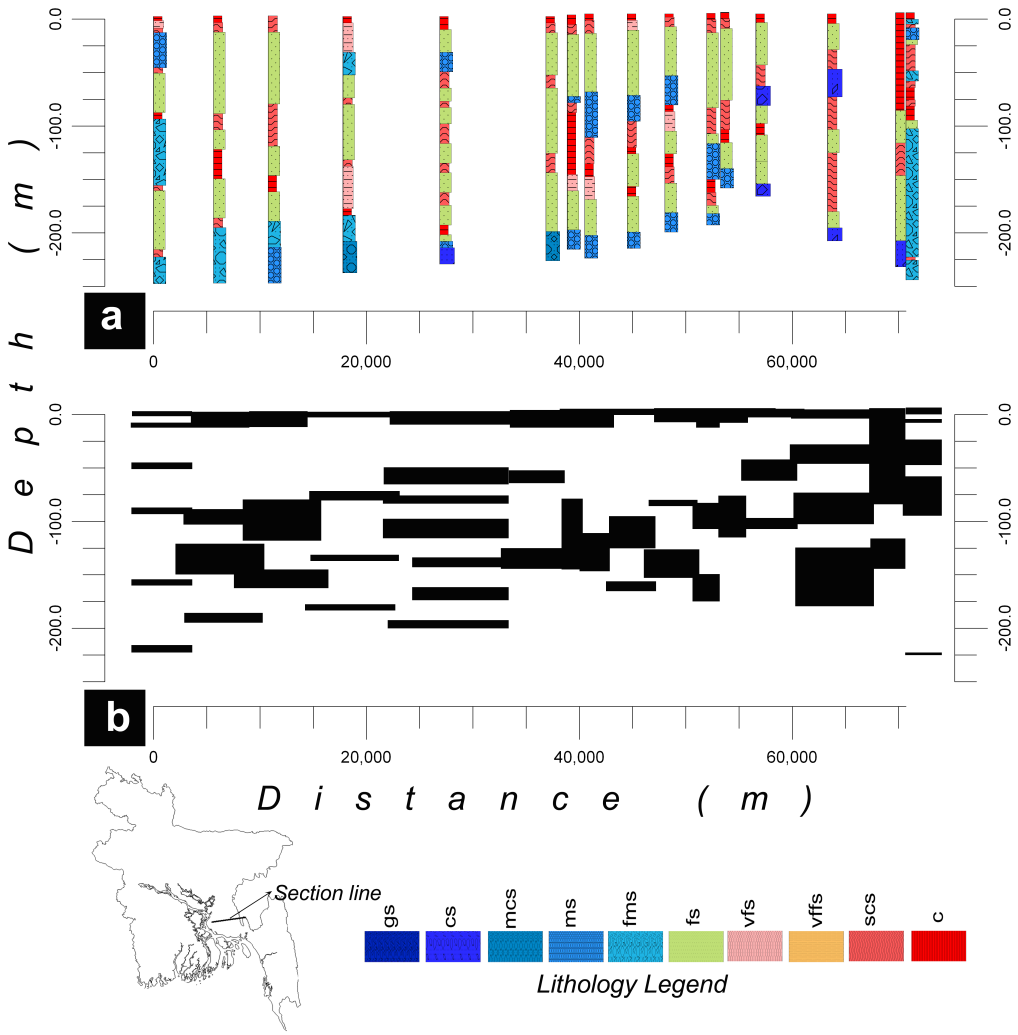

Figure 4-17: Lithological log section showing arrangement of the silt-clay layers, (a) Lithologs with depth-wise lithological records, (b) clay and silts extrapolated half-way to adjacent logs to indicate that mosaic of the stacked silt-clay layers could form an effective continuous layer.

4.3.9 Implications

Neither the mapping of individual silt-clay layers nor consideration of their individual hydraulic effect is possible in a fluvio-deltaic aquifer system. The limitation is rooted in our incomplete knowledge and lack of computational power. Methodologies to upscale the effect of these heterogeneities may lead to understanding the system at a larger scale. Hydrostratigraphical analysis was carried out in the current project on the basis of the generalised heterogeneities in terms of channel-floodplain processes i. e., channel-fill sand and interfluves silt-clay areas. The volumetric content of sand was found to be ~60% and paleo-channel sand bodies were identified.

Hydrogeological variabilities in the region are linked with the hydraulic conductivity, and leading to several ways by which hydrogeology could be incorporated into groundwater models. The representations presented here, are plausible, but the reality is more complex. The data quality, density of data, lack of detail, and inconsistency between drillers are the main sources of uncertainties in the current analysis. It is however plausible that the complex reality is encompassed within the range of representations presented. If model outcome for all representations indicates a management objective viable, there can be more confidence in its reliability.

4.4 Synthesis of the key points

a) In this chapter the hydrostratigraphy of the study region has been considered by -

- deriving hydrofacies from lithofacies
- interpolating between nearly 600 data points (drillers' logs)
- consideration of the geological history of the basin
- determining anisotropy in hydraulic conductivity using the method of Ababou (*1996*)
- Applying an additional method, for comparision with the above, based on sand/clay ratios

b) The Mio-Pliocene Upper Marine Shale (UMS) is identified as the hydraulic basement.

c) Seven alternative representations of the post-UMS hydrostratigraphy have been prepared (W1-W7).

Chapter 5
Hydrochemistry, Isotopic Nature and Groundwater Age

Deep groundwater is the main source of arsenic-free groundwater in southern Bangladesh. There are other alternatives for arsenic-safe water *(Ahmed et al. 2006)* but all have their own limitations and uncertainties. Use of deep groundwater through installation of deep tube-wells has been increasing over the past two decades; however hydrochemistry and isotopic nature remain poorly characterised. Those studies that have been carried out have mostly been at local scale or in general terms (*BGS/DPHE 2001; JICA 2002; McArthur et al. 2004; Ravenscroft et al. 2005; Zheng et al. 2005; DPHE/DFID/JICA 2006; Mukherjee 2006*). Earlier studies rarely looked at the characteristics of the groundwater at both shallow and deeper levels in consideration of groundwater flow and the hydrogeological framework. In this chapter a regional description of the hydrochemical variations between shallow and deep groundwater including their isotopic nature will be made in terms of groundwater flow-system and hydrostratigraphy. Moreover, these observations, particularly concerning groundwater age, will later be used for constraining groundwater flow models.

5.1 Water sampling, and site characterisation

5.1.1 Sampling location

A total of 75 groundwater samples were collected from domestic and monitoring wells emplaced at shallow to deeper depths (10 to 350 m) from two regions of Bangladesh. The Eastern region comprises the whole eastern part of the country. Sampling in the western region was restricted to within the boundary of Khulna City Corporation. In the eastern region relatively high resolution sampling was carried out within one local area Kachua Upazila (Figure 5-1).

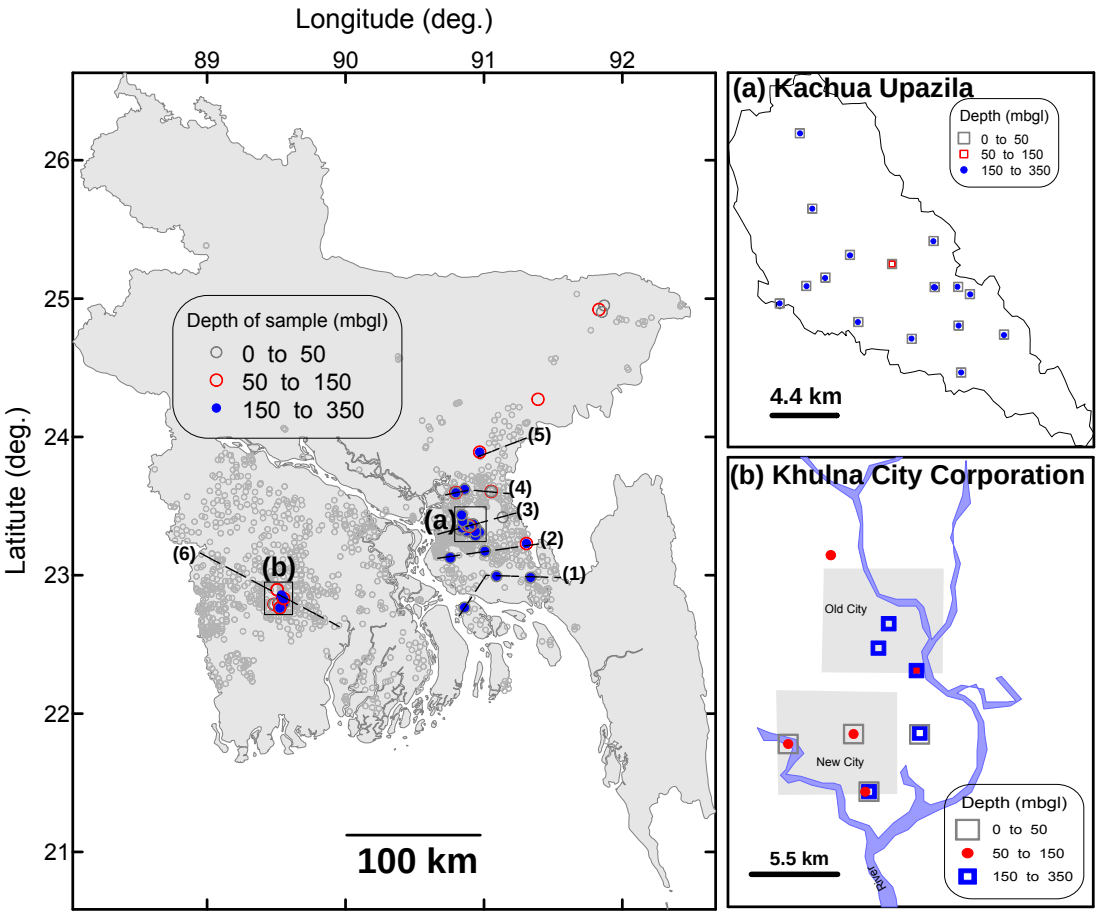

Figure 5-1: Location of the samples on a map of Bangladesh. High resolution sample locations are shown on 'a' and 'b' in the right side. Gray smaller open circles are the location of lithologs and lines 1 to 6 indicate the lines of lithological log sections given in the figure 5-2.

Almost in every case paired shallow (<100 mbgl) and deep (>100 mbgl) groundwater samples were collected except in areas of Pleistocene red-bed out-crop where deep tube-wells are very rare. This is because red-bed areas are arsenic-free at all depths. One sample (SU0116-17) was collected from a well taping water from greater depth in Sylhet (NE Bangladesh) - a red-bed out-crop area. In three locations a depth profile (with 3 samples in two cases, and 4 samples in one case) was established.

5.1.2 Site characterisation

Lithological data from the available drillers' log are used to characterise the sampling sites along E-W sections (Figure 5-2). This alignment follows the topographic gradient which coupled with the sub-surface anisotropy is expected to facilitate generally E-W groundwater flow. In the case of samples in the western region in Khulna the hydrostratigraphical framework was considered from NNW-SSE, as the topographic gradient is in that direction. Moreover, the Mehgna River is expected to act as a groundwater discharge zone for water from both sides, due to the regional topographic depression along the river. It can be inferred from the sections that deep groundwater is separated from the shallow groundwater by silty-clay layers which alternate with sandy

horizons. Due to the density of the lithologs it is not credible to infer the lateral continuity of these silty-clay layers, and they must have finite extent as they were deposited in a fluvio-deltaic depositional setting.

Drillers' logs do not include sediment colour information. Sediments of red to brown colour indicate oxidizing conditions and have been found to host arsenic-free, low electrical conductivity and HCO_3^- type water *(*e. g., *von Brömssen et al. 2008)*. From field observation and available information it can be confirmed that samples (Appendix A5.1) SM0116-18, CU0104-7, SP0116-16, HG0115-12, CG0103-5S, CG0103-5D, and SU0116-17 are from the Dupi Tila sand aquifer which has a generally oxic-redox condition.

The areas of high resolution sampling (Khulna city and Kachua) are geologically contrasting. In Khulna, a deep aquifer is found to be separated by clay and silty clay layers from the shallower level. In Kachua there is no extensive silt-clay layer. To increase the confidence in the site characterisations geophysical logging was carried out in Kachua (Figure 5-3 and section 4.3.2). Interpretation of the geophysical logs confirms the relative absence of silt-clay layers in the Kachua area.

Drillers' logs in Khulna indicate that samples taken from the deeper (>100 m) wells are certainly separated by several alternating silt-clay layers from the shallower counterpart (<100 m). These silt-clay layers may not laterally be continuous; however, their *stacked-mosaic-continuous* demonstrates an effectively continuous separation between these two horizons. This style of lithological heterogeneity can generate distinct flow systems in the shallow and deeper regions (see section 6.2).

5.2 Methods

More than a month long fieldwork and sampling expedition was completed in Bangladesh between 25 December 2007 and 12 February 2008. All the samples were brought back to London for hydrochemical and stable isotope analysis. Samples collected for radiocarbon activity analysis were submitted to University of Waterloo in Canada from Bangladesh. Analyses were completed by June 2008. Certain procedures were followed in the field to reduce uncertainties. These are discussed in the section below. Standard procedures were followed during laboratory analysis.

5.2.1 Groundwater sampling

A standard, systematically applied sampling procedure was followed throughout (Figure 5-4). This involved purging of the well for 30 to 70 minutes (at a rate 20-25 l/minute) depending on the depth of the well prior to collection of samples. In every case a flow-cell was installed half-way through the well-purging. In almost all cases stability in the flow-cell readings was achieved before the required volume of purging. Here, the required purging volume was aimed to be a withdrawal of three borehole volumes of water.

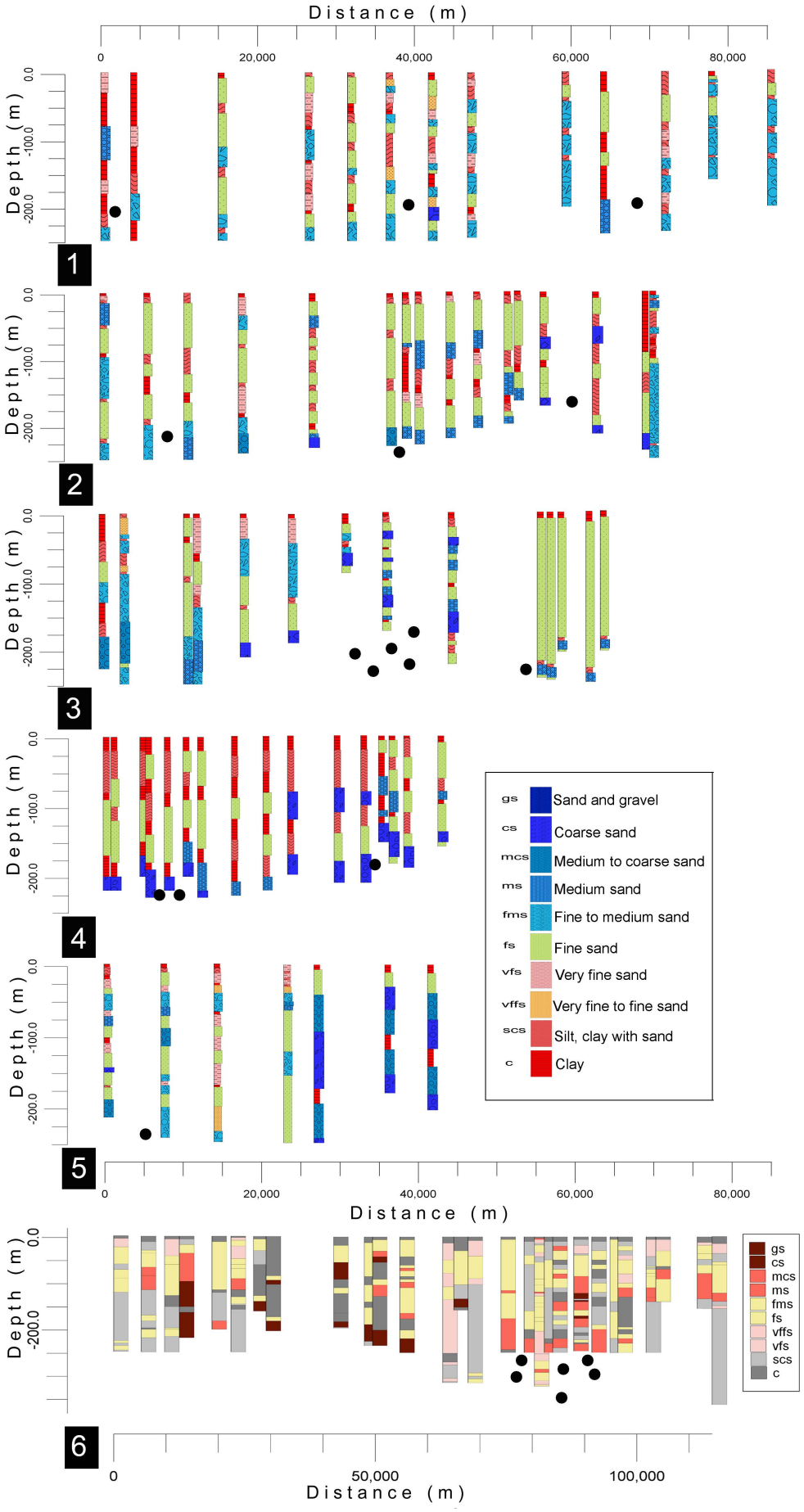

Figure 5-2: Drillers' log sections along the line of sampling (dots denote sample position). These show the presence of multiple silt-clay layers at every location in the vertical direction. Note the difference in colour scheme. For location of the lines see figure 5-1.

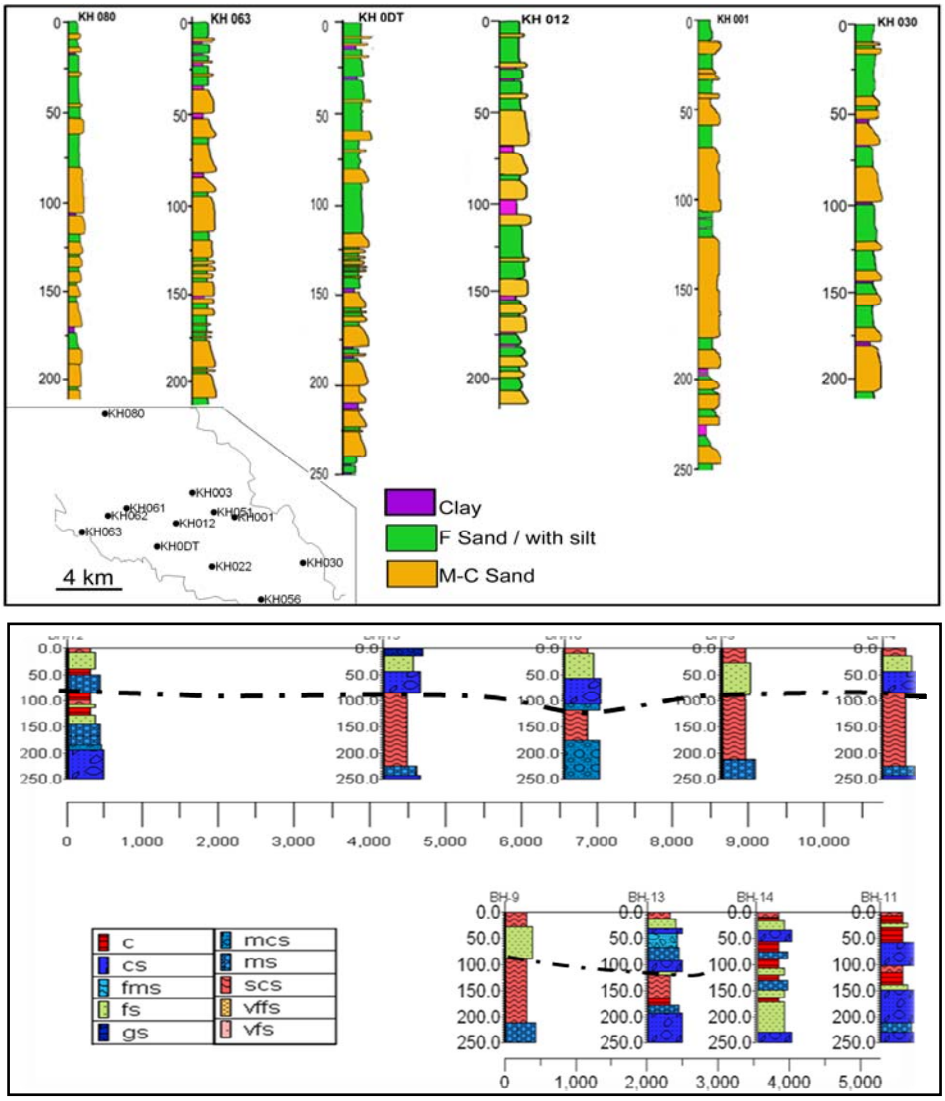

Figure 5-3: Geophysical log derived lithologies (see figure 4-9) indicating the absence of thick silt-clay leyers in Kachua (upper panel), while Khulna (lower panel) has thick silt-clay layers between the shallow and deep aquifers. Note the lithological codes for the lower panel are same as figure 4-13 and location of the logs are within the map area of figure 5-1b.

After the reading stabilised in the flow-cell, two 30 ml water samples along with water samples for stable isotope analysis and ^{14}C activity analysis were collected. Groundwater samples for major element (cations and anions) and trace metal analyses were collected through 0.25 µm polycarbonate filters at the field collection sites. For the trace metal (including arsenic) and cation samples, the filtered water was acidified to ~pH 2 with ultrapure nitric acid on site. The un-acidified samples were collected in a way so that no air remains in the bottle. Unfiltered water samples were collected and stored in glass bottles with rubber-lined metal caps, usually of 20 ml capacity to provide adequate volume for the separate analysis of $^{18}O/^{16}O$ and $^{2}H/^{1}H$. After collection of the sample an air-tight cap was attached. Carbon isotope samples $^{13}C/^{12}C$ and ^{14}C activity were collected from each well in 250 ml or 500 ml (thick) plastic bottles, determining on HCO_3 content. To each water sample 0.1 ml to 0.2 ml of 1% Sodium Azide solution was added to prevent biological activity. Groundwater samples remained exposed for very short duration (~1

minute) during sampling, and in every case samples were stored in an ice box at the site and subsequently in a freezer. Twenty five samples including 3 duplicates were analysed for radiocarbon activity.

Most of the sampled wells were fitted with a 1.5 inches diameter pipe, extending from <50 m to >200 m depth. From the general design of the well the well screen length is 1-3 m is known, and samples collected using these wells can be treated representing a point sample. In most cases two wells were sampled at each site: a shallow and a deep sample from close proximity (Figure 5-4). It is important to mention that paired sampling was done from the same compound within a radius of 10 m, and never exceeding 100 m. These paired samples can therefore be treated as defining a vertical profile.

Purging was done in most cases by using a (generator run) motorised pump, and inserting a ¾ inches diameter pipe into the tube (of the well) 3-4 m below of the water-table. The pump of the HTWs (Hand Tube Well), and in the case of Tara Technology the pump-piston-pipes including the check-bulb were first removed. In all cases the depth to the water-table was measured using a dip-meter. In the first week of field-sampling wells were manually purged, but subsequently a motorised purging technique was adopted. The discharge rate of the well in both cases, motorised and manual, was almost similar (20 to 25 litre/minute), but the motorised discharge was more steady. It can be calculated that a well with 200 m depth with a pipe diameter of 1.5 inches needs to be purged for ~27 minutes (at 25 l/min) for 3 volumes of water withdrawal. In most of the cases purging was done for a little longer, up to 5 volumes. In the case of sampling from monitoring wells the purging volume was set to be 5 to 7 volumes, because these are not in regular use like domestic wells.

Well intake depth is necessary information for hydrochemical interpretation. Well-depth is however often uncertain as the owner of the well often fails to acknowledge the actual depth. Depths of sampled wells (with some exception) were measured using a manual depth-measuring tool (Figure 5-4). A hand-held Garmin GPS receiver was used to geo-reference the sampled wells.

All field parameters (pH, ORP, EC, Temperature, TDS, DO, and Salinity) were measured onsite using a composite portable instrument, HI 9828 Multiparameter by Hana Instruments Ltd. (Bedfordshire, UK). The instrument was calibrated every day at the first time of sampling according to the manufacturer instruction. In every case the well head was detached except the motorised-pump to measure the depth of water-table and total depth of well. Depth to water-table, depth of well, and GPS location were measured on-site after a few minutes of the well head detachment. Information of the well owner, location and installation year were collected through interviewing the owner of the well. Alkalinity (i.e., HCO_3) was determined on site by colourometry with 1.4N H_2SO_4 solution. Calculation of alkalinity was made in mg/l.

Figure 5-4: Photographs showing field-camp activities during the groundwater sample collection in December 2007 to February 2008 in Bangladesh. 1. Total activities at a sampling site: 1a well purging, 1b flow-cell, 1c onsite titration for HCO_3 measurement, 1d onsite measurement of field parametres; 2. Onsite calibration of the Multiparametre instrument; 3. Well-depth measurement using self-designed (3a) 400 m string in a spool with number marking (every 5 metres) and a weight at the end; 4. Flow-cell and multiparametre instrument are in use; 5. Sampling: 5a radiocarbon sample bottles, 5b stable isotope sample bottles, 5c sample bottles for major ions and trace-element analysis, 5d flow-cell (inside the bucket) kept submerged; 6. Wells were sampled: 6a shallow well, 6b deep well, are within 2 m distance; 7. Well-purging before setting up flow-cell.

5.2.2 Laboratory

5.2.2.1 Major ions

Analyses were carried out at the Wolfson Laboratory for Environmental Geochemistry at University College London, UK. The major anions (F, Cl^-, NO_3 and SO_4^{2-}) were analysed with a Dionex DX-120 ion-chromatograph with an IonPac As14 column. The precision and accuracy of analyses were tested by running duplicate analyses on selected samples. For samples with higher

EC values (>3000 µS/cm) F, NO_3 and SO_4 may be semi-quantitative as inappropriate dilution is used otherwise Cl^- values run beyond the capacity of the IC column.

The cations (Ca^{2+}, Mg^{2+}, Na^+ and K^+) and trace elements (Fe, Mn, As, P, Si, Al, B, Mo, Sr, V, and Zn) were analysed by ICP-AES. Following a run of every nine samples, certified standards, SLRS-4 (National Research Council, Canada) and GRUMO 3A (VKI, Denmak) and synthetic multi-element chemical standards were run and background correction was made. Relative percent difference among the duplicate runs was within ±10%.

5.2.2.2 Stable isotope

Analysis was carried out in the British Geological Survey (BGS) isotope lab by Dr. W. G. Darling using standard preparation techniques followed by isotope ratio measurement on VG-Micromass 602E or Optima mass spectrometers. All data are expressed in ‰ with respect to Vienna Standard Mean Ocean Water (VSMOW) on the delta scale:

$$\delta = [(R_{sample}/R_{standard})-1] \times 10^3 \quad \text{.....Eq. 5-1}$$

Where R_{sample} is $^{18}O/^{16}O$ or $^{2}H/^{1}H$ ratio of the sample, and $R_{standard}$ is corresponding ratio in VSMOW. Analytical precisions are ± 0.2‰ for $\delta^{18}O$ and ± 2‰ for $\delta^{2}H$ (W. G. Darling, personal communication).

5.2.2.3 Radioisotope

Radiocarbon analyses were determined by the IsoTrace lab at University of Toronto, Canada. The lab analysed the ^{14}C activity in collaboration with University of Waterloo, Canada. Accelerator Mass Spectrometry (AMS) technique was used to analyse the ^{14}C. Mass spectrometry is the technique of separating and counting the constituent atoms of a sample according to their mass (http://www.physics.utoronto.ca/~isotrace/ accessed on 10th July 2009).

5.2.3 Database and data grouping

The hydrochemical data were grouped in two different ways: according to depth (<100 m as shallow and >100 m as deep); and by region (Appendix A5.1). Computation and analysis have been performed on individual groups of data to investigate the hydrochemical and isotopic characteristics.

5.3 Results

5.3.1 Hydrochemical characters

5.3.1.1 Field parameters

There are notable differences in field parameters between the shallow and deep groundwater. Variations can also be seen in the deeper groundwater of different regions (Table 5-1). The pH is

generally higher in the shallow groundwater (median 7.14, n=27) compared to the deeper groundwater (median 6.76 n=27), with the exception of Khulna area where the reverse is the case. The field measured redox potential (ORP) varies between -158 to +29 mV (median -119, n=27) in shallow groundwater while -95 to +22 mV (median -34, n=27) in the groundwater at deeper level. The ORP in Khulna deep groundwater (median -142, n=9) is lower than that of the eastern area (median -36, n=28), which itself is lower than in the Dupi Tila groundwater (median +26, n=6). Groundwater EC and TDS vary considerably in the shallow and deep groundwater, and between the regions. High EC values (Table 5-1) indicate presence of saline groundwater. It is seen that EC of deep groundwater is relatively low (698–3324 µS/cm) at Khulna while relatively high (725–4939 µS/cm) at Kachua. Temperature ranges from 24°C to 30°C, with lower values associated with shallow groundwater. However, the Khulna deep groundwater temperature is higher compared to the eastern deep groundwater.

5.3.1.2 Major ions and hydrochemical facies

A summary of basic statistics for major ions are given in the table 5-1; very wide ranges and high standard deviations are apparent for most of the ions. Such wide ranges suggest multiple sources and/or that hydrochemical processes act heterogeneously to generate the variety of chemical composition observed. Major ion concentrations in shallow and deep groundwater samples are presented in figure 5-5. HCO_3, Na, and Cl are the dominant ions in all the groundwater samples followed by Ca, Mg, and K, though, wide regional variability in major ions obscure the differences between shallow and deep groundwater (Table 5-1). Dominance of HCO_3, Na, and Cl ions may be associated with freshwater and seawater mixing, water-rock interaction and ion exchange.

For a qualitative evaluation of the seawater mixing TDS vs. inter-ionic ratios (Ca/Na and HCO_3/Cl) diagrams (Figure 5-6) are examined. A weak negative correlation between the variables is visible. These trends suggest high TDS groundwater is typically enriched in Na and Cl, implying a saline end member. Other geochemical processes such as ion exchange and silicate weathering cannot be ruled out. Chloride (Cl) concentration data (n=75) (Figure 5-7) shows a negatively skewed log-normal distribution. The samples with high Cl concentrations can be considered as an anomalous population whose chemistry might locally be affected by seawater mixing.

Seawater has a very high Cl/HCO_3 molar ratio (>200) while meteoric freshwater usually has Cl/HCO_3 <1 *(Raghunath 1996)*. Most of the shallow groundwater samples and some deep counter parts fall below the unity line, indicating freshwater (Figure 5-8). However, most of the deep groundwater sampled from Kachua and shallow groundwater sampled from Khulna fall above the unity line implying mixing with a seawater component.

Table 5-1: Hydrochemical summary statistics (Minimum [Min], Maximum [Max], Median [Med], Standard Deviation [Std]) for different group of samples.

Attributes		Depth (m)	ORP (mV)	pH	EC (µS/cm)	Temp (^{0}C)	TDS (mg/L)	Na (mg/L)	Ca (mg/L)	Mg (mg/L)	K (mg/L)	Cl (mg/L)	SO4 (mg/L)	HCO3 (mg/L)
Shallow n=27	Min	7.2	-158.9	6.39	234	25.2	117	9.6	11.0	7.5	2.2	4.5	0.0	149
	Max	87.8	29.0	7.73	5229	26.6	2614	625	174	136	22.2	1406	18.1	693
	Med	21	-119.7	7.15	760	26.0	380	74.8	26.1	29.1	8.4	21.4	1.5	404
	Std	17	38.7	0.30	1046	0.3	522	160	31.9	24.5	6.0	305	3.6	141
Deep n=27	Min	125	-95.1	5.99	235	26.3	117	20.2	3.1	3.8	2.0	1.3	0.0	90
	Max	336	22.2	7.08	4939	29.2	2470	805	211	93.1	47.8	1509	145	363
	Med	216	-34.7	6.58	1232	27.2	616	234	33.0	20.9	6.0	336	7.3	176
	Std	43.1	32.8	0.34	1348	0.7	656	215	57.9	28.7	8.6	450	31.8	68
Dupi Tila n=7	Min	34	-119.5	5.04	33	24.5	17	0.6	0.1	0.6	0.7	0.7	0.2	17
	Max	185	235.9	7.04	274	27.9	137	26.9	22.3	11.1	2.3	2.9	1.4	155
	Med	55	-8.4	6.28	138	25.3	69	14.3	8.5	3.2	1.4	1.0	0.8	73
	Std	60.1	141.3	0.68	83	1.2	41	9.4	8.5	3.5	0.5	0.8	0.4	46
Kachua (Shallow) n=16	Min	17.4	-150.1	6.59	277	25.6	139	9.6	13.8	16.3	4.7	4.5	0.0	193
	Max	45	-91.7	7.48	5229	26.6	2614	625	174	136	21.9	1406	18.1	634
	Med	22.1	-122.4	7.13	869	26.1	435	95.9	25.0	31.3	9.3	19.2	1.9	432
	Std	7.2	16.3	0.22	1210	0.3	605	174	38.5	29.3	5.5	350	4.3	128
Kachua (Deep) n=18	Min	125	-87.0	5.99	725	26.3	363	57.0	3.1	3.8	3.8	145	0.0	90
	Max	336	22.2	7.01	4939	29.0	2470	805	211	93.1	47.8	1509	145	361
	Med	216.5	-28.8	6.39	1948	27.1	905	301	54.9	36.5	8.1	470	10.2	173
	Std	41.6	32.4	0.33	1244	0.7	612	196	65.2	31.2	9.8	431	37.2	64
Khulna (Shallow) n=6	Min	24	-123.3	6.13	2577	26.1	1298	418	33.3	14.8	2.5	335	0.0	378
	Max	58.2	18.3	6.94	9091	27.1	4544	781	267	106	15.8	2692	32.7	888
	Med	32	-53.8	6.67	3890	26.4	1946	591	150	77.4	6.5	841	0.4	747
	Std	14.7	54.1	0.33	2339	0.4	1167	127	78.5	31.4	5.6	837	13.0	185
Khulna (Deep) n=9	Min	119	-205.6	6.87	698	25.9	349	94.0	14.1	8.8	3.9	36.5	0.0	289
	Max	311	-37.1	7.93	3324	30.4	1662	547	247	95.3	10.6	870	12.1	546
	Med	245	-142.5	7.60	1351	28.5	676	179	36.5	19.8	5.9	285	0.8	366
	Std	81.6	52.7	0.34	975	1.8	487	141	75.3	29.5	2.3	302	4.5	86

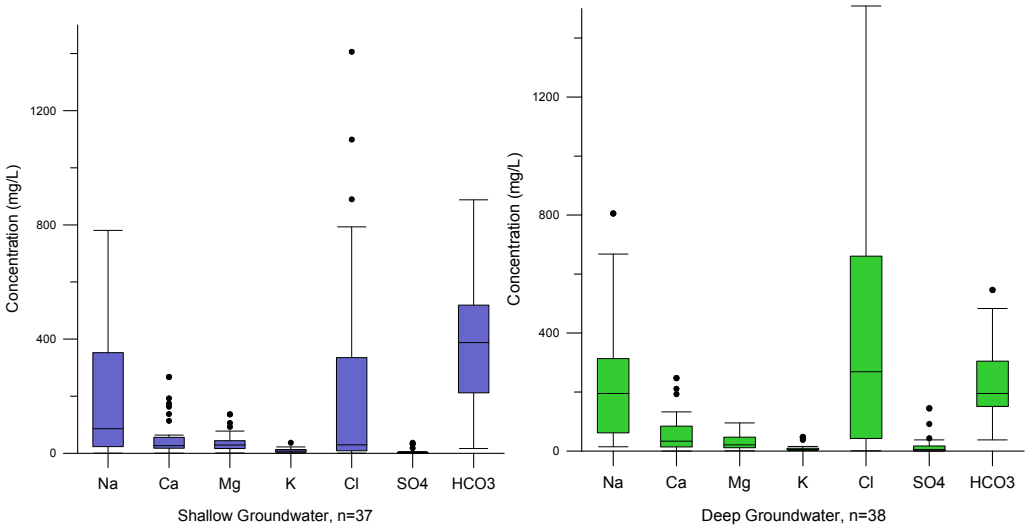

Figure 5-5: The range of major ions in shallow and deep groundwater

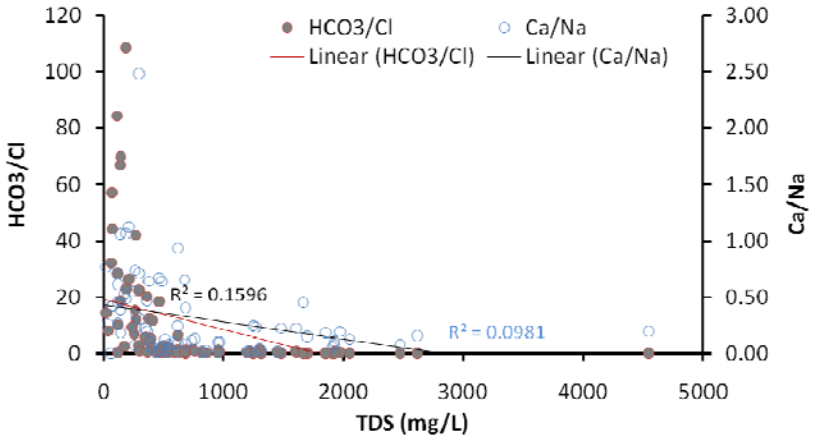

Figure 5-6: Graph showing the relationship between TDS and inter-ionic (molar) ratio

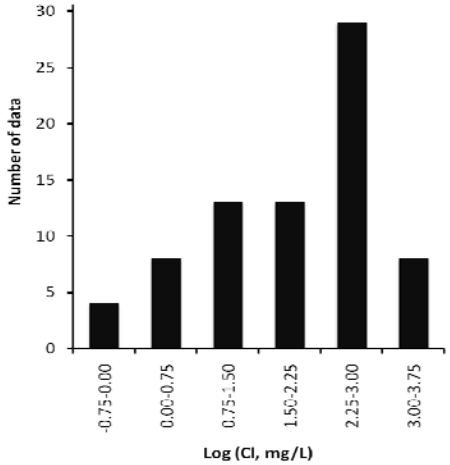

Figure 5-7: Frequency distribution of Cl data.

A good correlation of EC with Na and Cl implies mixing of freshwater and seawater. Strong correlation between Na and Cl (r=0.89) as well as variations in their Na/Cl ratios between 0.4 and 36 (Figure 5-9) indicates seawater and freshwater mixing. Mixing of seawater (Na/Cl = ~0.86) with freshwater (Na/Cl>1) may give rise to Na/Cl molar ratio close to unity *(Vengosh and Rosenthal 1994)*. Most of the samples cluster around a molar ratio of 1.0, in both shallow and deep groundwater. Molar ratio >1 indicates contribution of Na from silicate weathering through dissolution of Albite (Na-feldspar) present in the alluvial sediments. A molar ratio close to unity may indicate the widespread effect of mixing of freshwater with seawater intruded or entrapped throughout southern Bangladesh.

The relative concentration of silica (SiO_2) and HCO_3 are reversed in the shallow and deep aquifers, with HCO_3 higher in the shallow aquifer and SiO_2 higher in the deeper (Figure 5-10). Weathering of silicate and carbonate are indicated by the molar ratio of HCO_3/SiO_2 <5, and >10 (Figure 5-10) respectively *(Hounslow 1995)*. Hasan (*2008*) suggests carbonate (calcite and dolomite) weathering is not dominant in this aquifer system because plot of Ca+Mg /HCO_3 (Figure 5-11) shows HCO_3 exceeds Ca+Mg. Previous studies (*Nickson et al. 1998; McArthur et al. 2004; Hasan 2008; Mukherjee and Fryar 2008*) have shown that excessive HCO_3 comes from the oxidative degradation of organic matters.

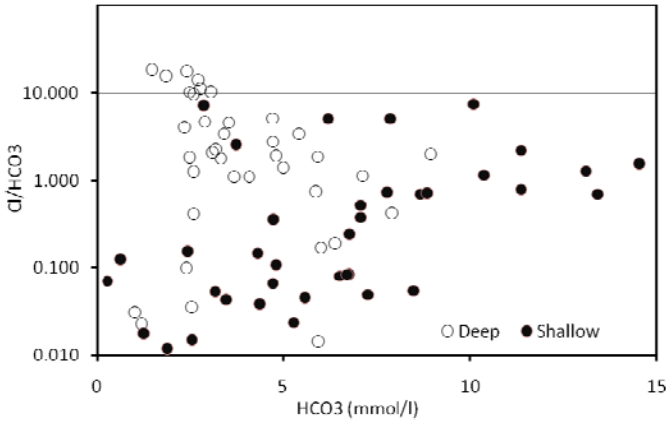

Figure 5-8: Graph showing molar ratio of Cl/HCO3 vs HCO_3 (mmol/L)

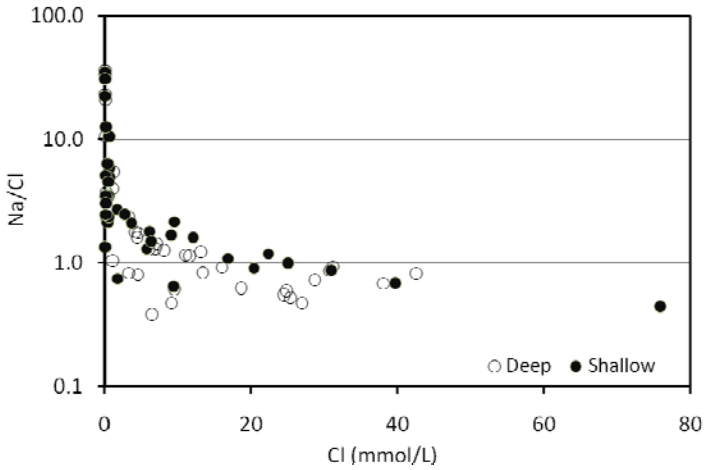

Figure 5-9: Graph showing molar ratio of Na/Cl vs Cl (mmol/L)

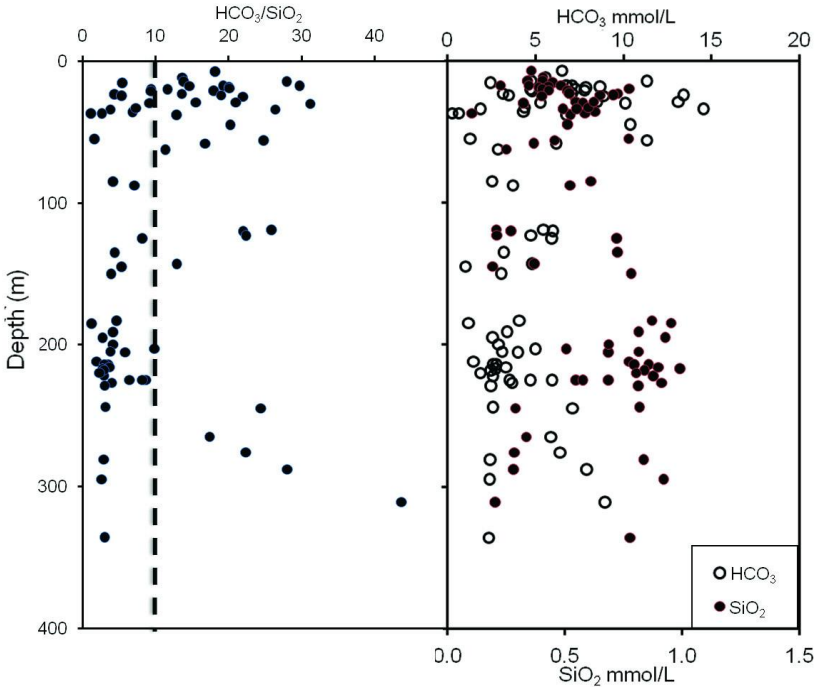

Figure 5-10: Depth-wise variation in HCO_3/SiO_2 molar ratio (left); and molar concentration of SiO_2 and HCO_3 (right).

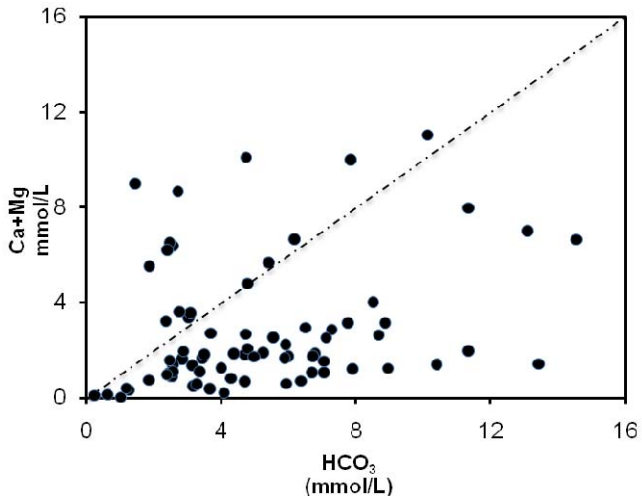

Figure 5-11: Plot of Ca+Mg /HCO3 shows HCO3 exceeds Ca+Mg (with some exception).

A variety of hydrochemical facies both in shallow and deep groundwater are evident from a Piper plot (Figure 5-12). Six hydrochemical facies were identified based on the classification by Hounslow *(1995)* and Freeze and Cherry *(1979)*. Most of the groundwater samples fall in water type fields of Ca-Mg-HCO_3, Na-HCO_3-Cl and Na-Cl facies. Samples in the Ca-Mg-HCO_3-Cl and Na-HCO_3-Cl facies respectively are of mixed type, indicating mixing of fresh water (Ca-Mg-HCO_3) with saline water (Na-Cl). The Na-HCO_3 facies suggests ion-exchange processes. Close observation reveals that most deep groundwater is in Na-Cl facies field, while shallow groundwater falls in the Ca-Mg-HCO_3 and Na-HCO_3-Cl facies fields. It is indicated that seawater intrusion complicates the facies distribution of both shallow and deep aquifer. On the other hand, samples from the eastern oxidized sediments of the Pleistocene outcrop are dominantly of Ca-Mg-HCO_3 type. Some groundwater samples show a mixing trend as well as a trend towards Na–HCO_3 type of water, probably indicating cation exchange processes *(Hounslow 1995; Ravenscroft and McArthur 2004)*).

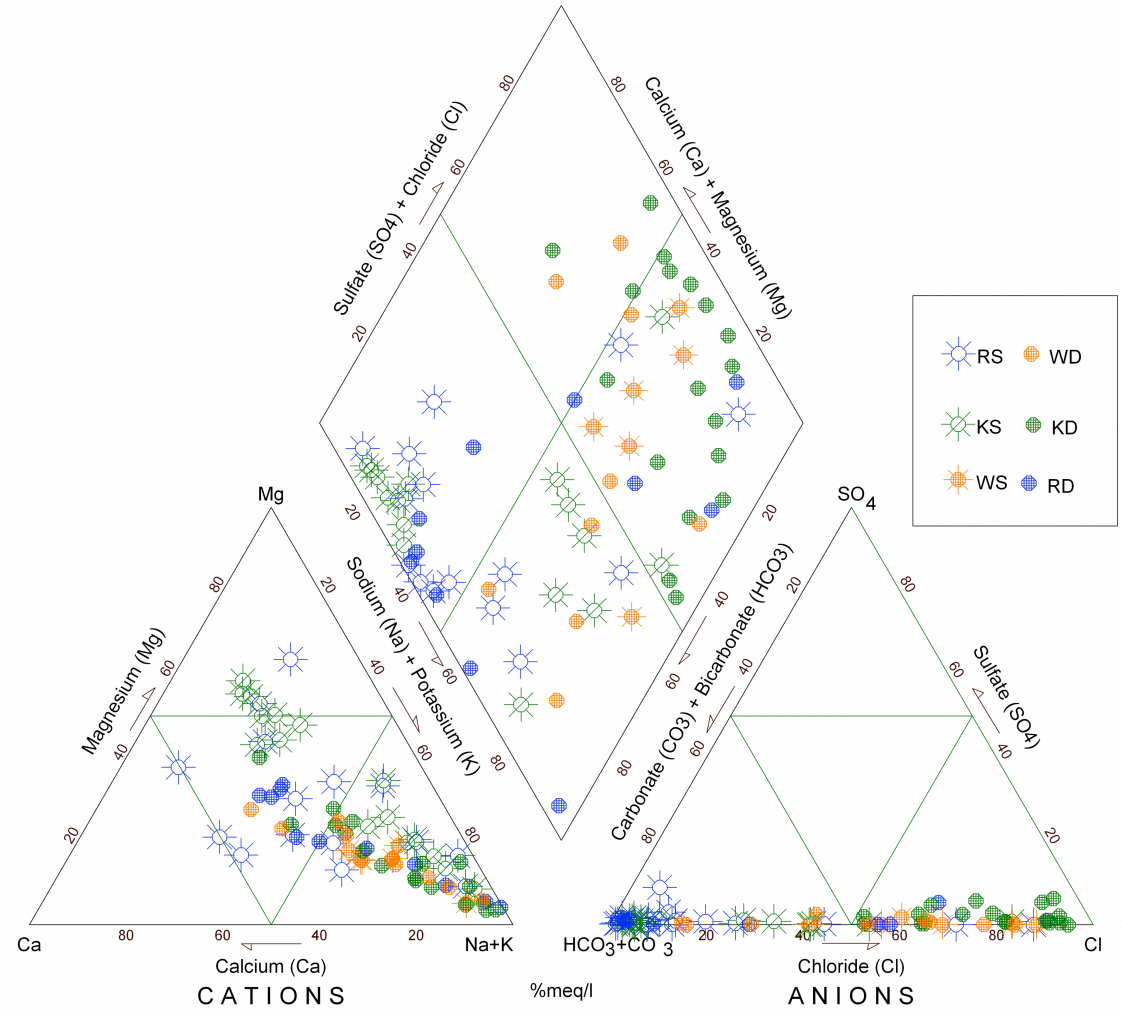

Figure 5-12: Piper plots of the samples indicate different water types. In the right rectangle 'RS' 'KS' 'WS' stand for Regional, Kachua, and Khulna shallow groundwater, while deep groundwater is indicated by by 'RD', 'KD', 'WD'.

5.3.1.3 Redox conditions: Arsenic and other redox sensitive elements

A number of parameters e. g., HCO_3, SO_4, As, Fe, Mn are sensitive to the aquifer redox state defined by ORP. A matrix plot of these parameters including depth (Figure 5-13) shows subtle vertical differences. ORP generally shows negative values throughout the depth profile indicating similar reducing condition. Arsenic (As), and HCO3 show a significant vertical trend. HCO_3 and As are found to be high in magnitude at shallower levels a result of the reducing condition of shallower system.

Sulphate concentrations are mostly low (<5 mg/L), but there are some samples (mostly >150 m depth-level) which contain higher SO_4 (5-40 mg/L). These high SO_4 samples generally have higher EC values where SO_4 has a positive a relationship with EC, a seawater influence is indicated. Fe and Mn do not show any visible vertical trend, and no significant correlation with As. The solubility of Fe and Mn minerals is strongly redox-controlled, particularly at near-neutral pH. Spatial and vertical variation in pH, and variation in initial content of the (Fe and Mn) minerals in the aquifer materials may be functional in determining the Fe and Mn concentrations. A good correlation between As, and Fe and Mn has however been reported in many parts of the basin, mostly in the shallow groundwater (*BGS/DPHE 2001; McArthur et al. 2001; Ahmed et al. 2004*).

In most shallow wells (<100 m) As concentrations are found to be above the Bangladesh drinking-water standard (50 µg/L) reaching a maximum of 754 µg/L, while deeper samples contain lower concentrations (<53 µg/L) (Figure 5-14). Five wells at >100 m out of 29 in the eastern region and 2 wells out of 9 in Khulna are found to contain arsenic above 10 µg/L (WHO guide-line for As in groundwater). Regionally the high As wells in the eastern region follow the pattern observed in the compiled data (see Figure 6-15).

5.3.2 Isotopic nature

5.3.2.1 Isotopic composition

50 groundwater samples (both deep and shallow) were analysed for O-H stable isotope analysis (Appendix 5.1). A summary of the analysed data is given in table 5-2. In general, shallow groundwater spans a wider range of values for both O and H.

Because of the isotopic range it is not possible to differentiate shallow (<100 m) and deep (>100 m) groundwater, though deep groundwater has a somewhat condensed range of values compared to shallow groundwater (Figure 5-15). All the groundwater samples fall sub-parallel to the World Meteoric Line (WML, $\delta^2H = 8\delta^{18}O+10$) *(Craig 1961)*, indicating meteoric sources of recharge. The linear fit for all groundwater samples is $\delta^2H = 6.0\delta^{18}O-0.19$ (n = 50, R^2 =0.81), the slope of which is lower than WML. The linear fit for shallow groundwater samples is $\delta^2H = 5.4\delta^{18}O-3.72$ (n = 24, R^2 =0.85), possibly indicating an evaporative trend. However, deep groundwater is

almost parallel to the WML, and has a linear fit ($\delta^2H = 7.7\delta^{18}O+7.84$ [n = 26, R^2 =0.86]) close to WML. Previous studies on groundwater from shallow and deeper aquifer in the basin indicated a linear fit to be $\delta^2H = 6.9\delta^{18}O+1.0$ (n = 53, R^2 =0.91) *(Aggarwal et al. 2000)*, and in the western part of the basin $\delta^2H = 5.8\delta^{18}O-3.0$ (n = 64, R^2 =0.82) (*Mukherjee et al. 2007a*).

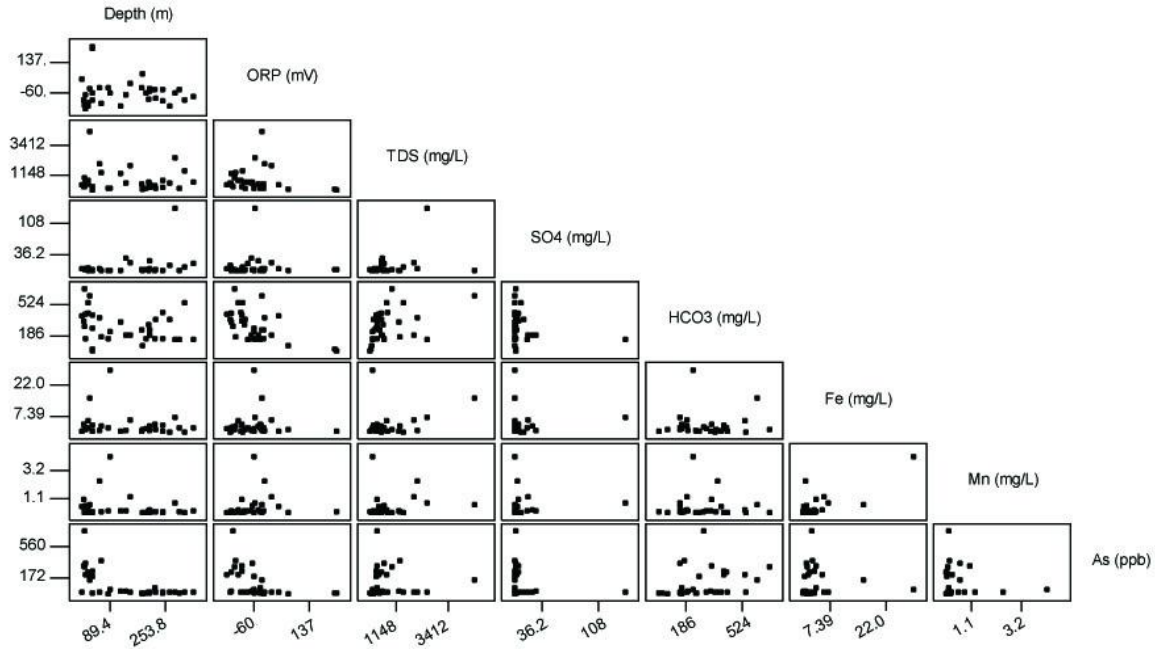

Figure 5-13: A matrix plot of redox sensitive parameters. Note 'depth' is included to show the depth-wise variation of the parameters.

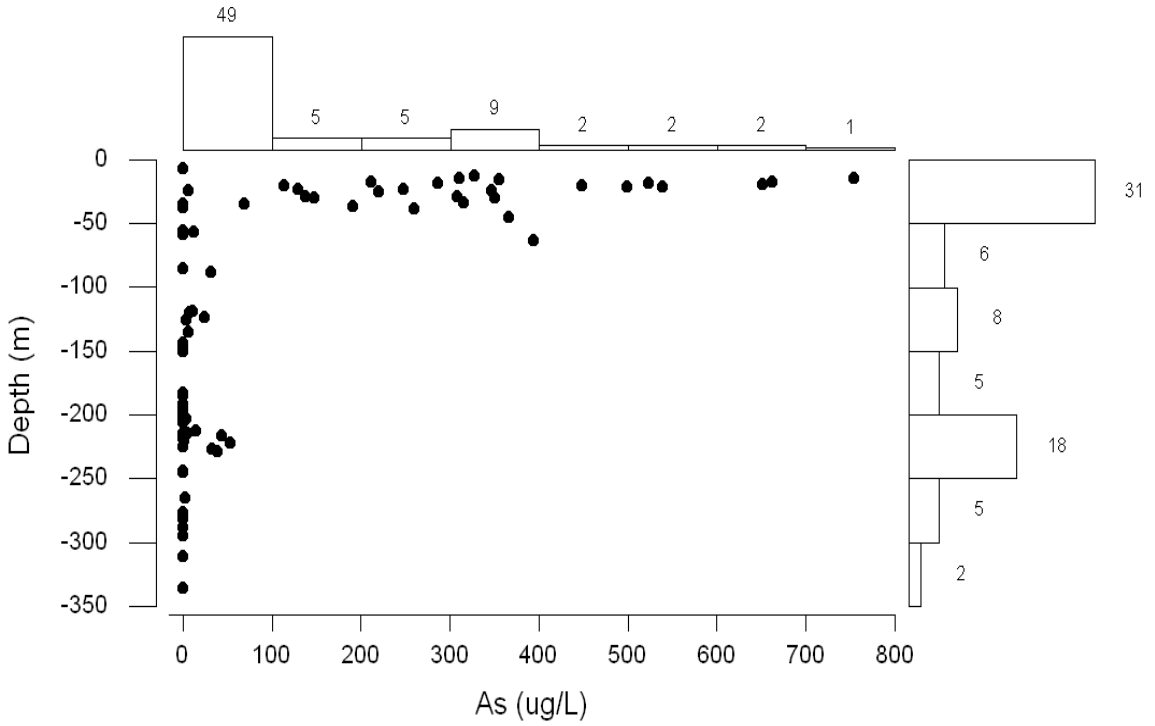

Figure 5-14: Depth vs arsenic (As) plot showing the vertical structure of As concentration.

Table 5-2: Statistical summary of stable isotope composition of the sampled groundwater.

Attributes	All, n=50		Shallow, n=24		Deep, n=26	
	$\delta^{18}O$ ‰	$\delta^{2}H$ ‰	$\delta^{18}O$ ‰	$\delta^{2}H$ ‰	$\delta^{18}O$ ‰	$\delta^{2}H$ ‰
Mean	-3.9	-23.4	-3.9	-25.0	-3.9	-22.0
Median	-3.7	-21.5	-3.8	-22.7	-3.6	-19.5
Maximum	0.7	-7.6	0.7	-7.6	-2.7	-12.3
Minimum	-6.7	-43.4	-6.7	-43.4	-5.5	-33.1
Standard deviation	1.2	8.0	1.5	9.0	0.8	6.8

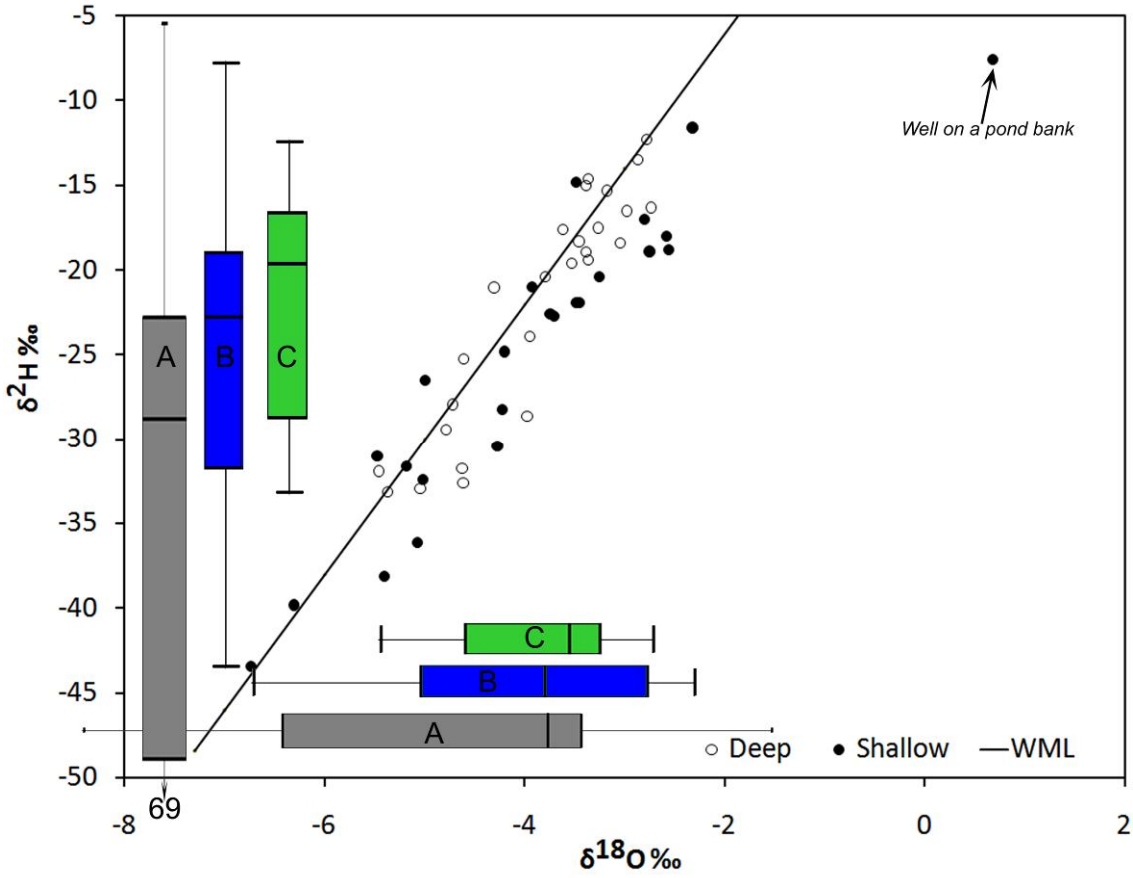

Figure 5-15: Isotopic composition of shallow and deep groundwater in the region shown on standard O-H plot along with world meteoric line (WML) *(Craig 1961)*. A, B, C indicate box plot representations of data: 'B' and 'C' represent shallow and deep groundwater respectively, and 'A' represents 6-year river (Buriganga) water isotope monitoring data (W. G. Burgess, personal communication). The data show the wide isotopic range of waters in the region. A similar range observed for the river water and the shallow groundwater indicates a potential relationship between the two.

Shallow groundwater isotopic composition shows a wider range of values. This may be indicative of surface water contribution to the shallow groundwater. River water isotopic composition shows great seasonal variability. A 6-year monitoring record (W. G. Burgess, Personal communication) for the Buriganga River, in the central part of the basin was used to show the range (Figure 5-15).

A highly enriched value (δ^2H -7.6 and $\delta^{18}O$ 0.68) of a shallow groundwater is observed (Figure 5-15). This sample was from a well at 14 mbgl, and located by the bank of a pond. The enriched value may be indicative of evaporated pond recharging the shallow aquifer.

5.3.2.2 Spatial pattern

The number of samples covering different parts of the basin is low in the current study. A landward trend of shallow groundwater isotopic composition associated with Rayleigh distillation effect has been reported in earlier work from the western part of the basin (*Mukherjee et al. 2007a*). In the current data set there is an indication of an E-W trend (Figure 5-16). Shallow groundwater from Khulna city is more depleted than from the study region further east. In the case of deep groundwater, regional differences appear negligible.

5.3.2.3 Vertical trend

By observation, there is no specific vertical trend in the isotopic composition of the groundwater. However, groundwater at depth (>100 m) has an isotopically condensed composition relative to shallower groundwater which has a wide isotopic range (Figure 5-17 and Table 5-2). Table 5-2 represents summary statistics of isotopic composition of shallow and deeper groundwater. Moreover, efforts have been made to look at the depth-wise isotopic variation at two particular sites at which multi-depth samples were collected. Identification of vertical trend in at those sites remains inconclusive because of resolution of the data, though at 'Titas site' a relatively depleted isotopic composition of deeper groundwater (>100 m) (Figure 5-18 and Figure 5-19) can be seen.

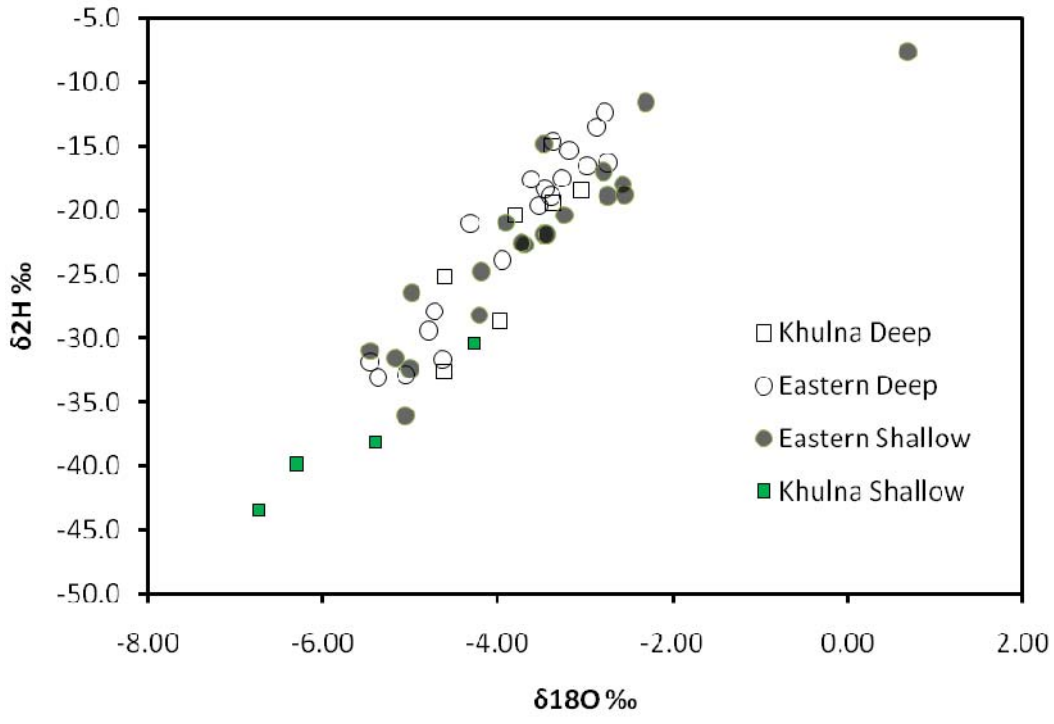

Figure 5-16: Delta plot of O-H in four groups, indicating the regional disparity. Note that Khulna is located in the middle-western part of the basin.

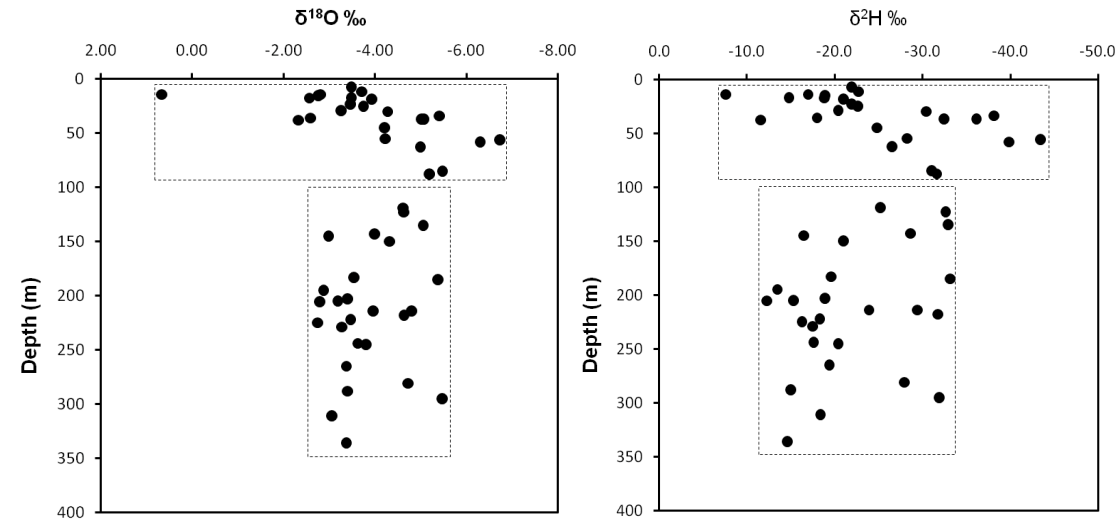

Figure 5-17: Plots of $\delta^{18}O$ ‰ and $\delta^{2}H$ ‰ against depth.

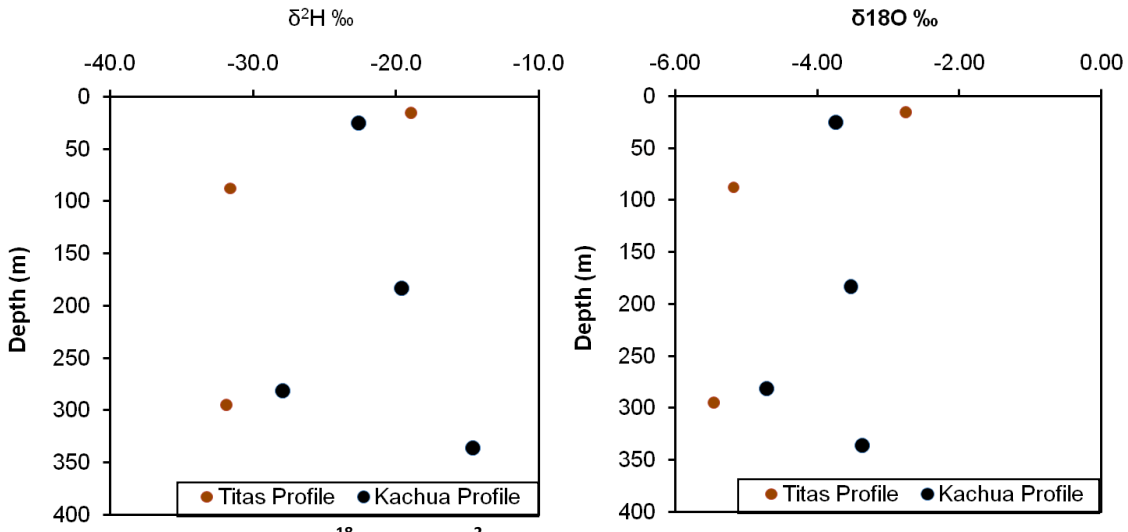

Figure 5-18: Depth profiles of $\delta^{18}O$ ‰ and $\delta^{2}H$ ‰ at two locations in the eastern region.

5.3.3 Radiocarbon analysis

5.3.3.1 Analysis outcome

A total of 23 groundwater samples were submitted for analysis of ^{14}C activity of dissolved inorganic carbon (DIC) (Table 5-3). The range of ^{14}C activity is similar to that found in earlier studies (*Aggarwal et al. 2000; BGS/DPHE 2001; Harvey et al. 2002b; Zheng et al. 2005*). The age is estimated based on the difference between the ^{14}C activity of DIC in an analysed groundwater and its ^{14}C activity at the time of recharge. But there are uncertainties in estimating the ^{14}C activity at recharge as well as subsequent dilution or enrichment of ^{14}C by water-rock interactions along the groundwater flow path *(Buckau et al. 2000)*. The better the understanding of the sources of uncertainties and their consideration in age estimation, the lesser the error will be in derived age.

Table 5-3: Results of radiocarbon analysis carried out in the current project. (pMC: Percent Modern carbon)

Sample ID	Depth (m)	Latitude	Longitude	$\delta^{13}C$ (‰)	CO2 (cc STP)	Uncorrected pMC	Corrected pMC
DT0114-11S	15.4	23.597	90.797	-19.10	5.30	105.98±0.66	104.71±0.65
KHOP4	25	23.341	90.923	-6.34	5.90	70.79±0.48	68.15±0.5
KCC-EdU-2	30	22.764	89.526	-9.60	4.80	88.77±0.59	86.03±0.57
CU0104-7	37	23.419	91.136	-11.42	3.40	124.37±0.78	120.98±0.76
SP0116-16	37	24.950	91.869	-21.82	5.10	88.62±0.59	88.05±0.59
DT0114-11M	87.78	23.597	90.797	-13.76	6.00	27.86±0.29	27.23±0.28
KCC-0127-22M	119	22.764	89.524	-6.73	5.90	12.97±0.18	12.5±0.18
DS0104-8D	135	23.606	91.053	-17.40	3.90	46.04±0.37	45.33±0.37
JB0105-10D	150	23.621	90.860	-38.57	5.40	6.88±0.13	7.07±0.14
KHOP5	183	23.340	90.923	-18.09	5.00	25.42±0.26	25.06±0.26
CG0103-5D	185	23.229	91.307	-19.72	5.90	82.69±0.61	81.8±0.61
LC0104-6D	195	23.174	91.006	-6.36	5.00	23.54±0.26	22.67±0.25
CL0102-2D	203	22.768	90.860	-11.46	4.80	2.6±0.09	2.53±0.09
KHNS98D	205	23.436	90.839	-10.44	4.20	22.42±0.26	21.76±0.25
FG0102-1D	205.5	23.126	90.756	-7.63	5.40	19.07±0.26	18.41±0.25
NN0105-9D	222	23.890	90.969	-12.60	4.50	27.29±0.27	26.61±0.26
DB0103-4D	225	22.984	91.337	-13.02	2.70	15.75±0.2	15.37±0.2
BJ0103-3D	244	22.993	91.091	-11.66	3.50	24.56±0.28	23.9±0.27
KCC-0128-26D	245	22.856	89.537	-5.79	6.00	12.04±0.17	11.58±0.16
KHOP1	281	23.340	90.923	-20.99	5.40	35.83±0.31	35.53±0.31
DT0114-11D	295	23.597	90.796	-18.86	5.40	26.75±0.27	26.41±0.26
KCC-ExD-2	311	22.764	89.526	-4.61	5.20	7.71±0.14	7.39±0.13
KHOP2	336	23.340	90.923	-13.09	5.20	23.68±0.27	23.11±0.26

Analysis indicates similar values of $\delta^{13}C$ for both shallow and deep groundwater. But ^{14}C activity shows distinct differences between shallow and deep groundwater (Table 5-4). Shallow groundwater generally has higher values of ^{14}C while deep groundwater contains lower values. There are exceptions in the groups, with some deep groundwater, particularly in areas in the foothills, with higher ^{14}C counts, possibly indicating more recent recharge. There are only 6 shallow groundwater samples in this study. One of these shows significantly lower counts, 27.23 pMC (percent modern carbon). In most cases, site specific information on the subsurface lithology is not available, however, in this case the sampled well is found to be tapping water from a layer covered by thick clay (Figure 5-19), and also it is relatively deeper than other shallow groundwater analysed in this study.

Table 5-4: Summary statistics of the radocarbon analysis.

Attribute	$\delta^{13}C$ (‰)		pMC	
	Shallow, n=6	Deep, n=17	Shallow, n=6	Deep, n=17
Mean	-13.67	-13.94	82.53	23.94
Median	-12.59	-12.60	87.04	22.67
Maximum	-6.34	-4.61	120.98	81.80
Minimum	-21.82	-38.57	27.23	2.53

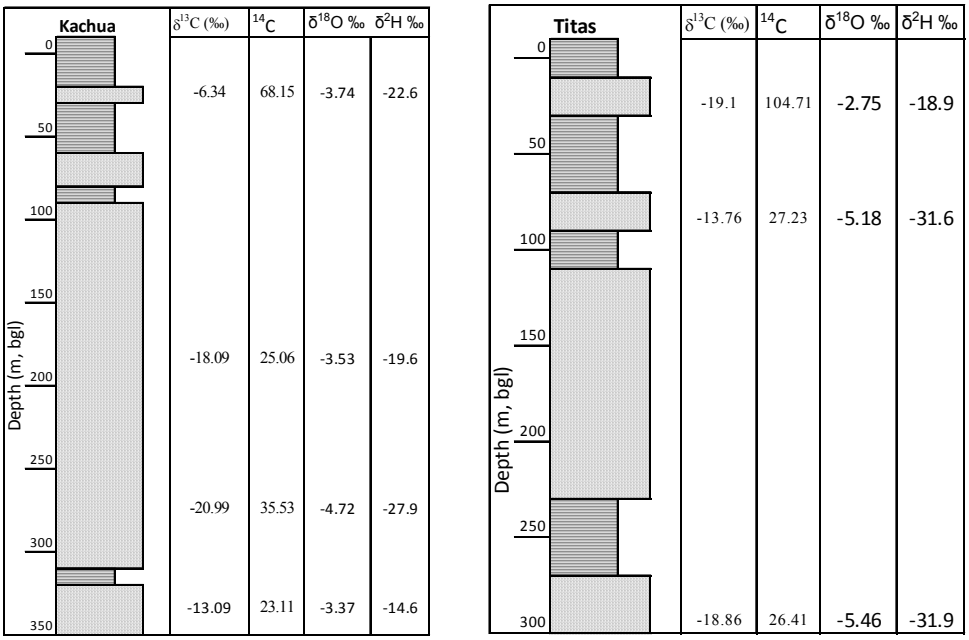

Figure 5-19: Profile of stable isotope composition and ^{14}C (activity in pMC). Lithologs are presented with standard symbols in terms of dual (sand and silt-clay) lithology.

5.3.3.2 Complications and limitations

^{14}C activity of groundwater has been applied to understanding groundwater recharge, movement, and sustainability of the resources, particularly of older groundwater *(e. g., Clark and Fritz 1997; Kazemi et al. 2008)*. There remains a great deal of uncertainty in the estimation of groundwater age based on ^{14}C due to lack of direct information on the recharging groundwater ^{14}C activity, and isotopic evolution by water-rock interaction along the flow path. Sources of uncertainty in age estimation have been discussed in many published papers (e. g., *Aravena et al. 1995; Clark and Fritz 1997; Buckau et al. 2000; Zhu 2000; Maduabuchi et al. 2006; Douglas et al. 2007; Kazemi et al. 2008; Coetsiers and Walraevens 2009*).

The ^{14}C concentration in DIC upon primary recharge is normally set to the level of atmospheric CO_2 prior to nuclear atmospheric testing, i. e., around 100 pMC (percent modern C referred to 94.9 % of the activity concentration of the NBS oxalic acid standard in 1950) (*Pearson and White 1967; Buckau et al. 2000*). This atmospheric ^{14}C concentration may have deviated from 100 pMC due to the changes in the earth's magnetic field over time, and thus deviate the groundwater age

estimated using this data *(Buckau et al. 2000)*. Atmospheric ^{14}C concentration was greatly influenced by atmospheric bomb tests in the 1960s, leading to a peak of ~200 pMC in the period 1963-1966. This makes age estimation of pre-bomb groundwater difficult. Moreover, atmospheric ^{14}C reaches the groundwater table by infiltrating through the soil root zone, where dissolution of soil-CO_2, derived from organic matter, occurs. The ^{14}C concentration of primary recharge, depends on the ^{14}C concentrations of such different sources and their contribution to DIC *(Buckau et al. 2000)*.

As the primary recharge DIC reaches the water-table and joins the groundwater flow system, a variety of processes may lead to its isotopic modification, especially by dilution and fractionation. Buckau et al. *(2000)* summarised the processes as follows:

- dissolution of sedimentary carbonate by the primary recharge carbonic acid
- on repeated dissolution and precipitation, the carbonate sediments may contain ^{14}C
- ion exchange of Ca^{2+} and Mg^{2+} for Na^{+} in clay minerals, leading to dissolution of ^{14}C-free $CaCO_3$
- incongruent dissolution of dolomite
- degassing of CO_2
- dissolution of $CaSO_4$ resulting in calcite precipitation through excess concentrations of Ca^{2+}
- changes in saturation concentrations via weathering of feldspar
- dissolution of sedimentary ^{14}C-free carbonate by organic acids, such as humic and fulvic acids
- admixing of volcanic or magmatic CO_2
- microbiologically mediated CH_4 generation
- microbiologically mediated oxidation of organic C via dissolved O_2, nitrate or SO_4

Most of the above mentioned sources of dilution of ^{14}C activity are possible in the Bengal Basin except admixing of volcanic or magmatic CO_2. In addition, loss of ^{14}C-bearing groundwater into intercalated clay layers *(Bethke and Johnson 2002)* may complicate the determination of actual age. Harvey et al. (*2002a*) have shown at a research site, Munshiganj in central Bangladesh, that radiocarbon ages of DOC are as old (3 to 5 ka) as aquifer sediments, while DIC-derived ages for groundwater may be much younger. They suggested that DIC cannot therefore be the oxidative product of the older DOC. This observation has not been tested for DOC-derived age estimates from other parts of the basin, but if it is true, organic matter oxidative dilutions of groundwater ^{14}C in DIC would not be significant. High $\delta^{13}C$ values corresponding with high HCO_3

concentrations (Figure 5-20) have been explained as the outcome of cation exchange coupled to a second stage of calcite dissolution *(Coetsiers and Walraevens 2009)*, which may be occurring in the Bengal Basin.

5.3.3.3 ^{14}C groundwater age corrections

Additional sources of carbon exist in most aquifers and can cause dilution of ^{14}C activity. In order to address the different sources leading to alteration of the isotopic carbon composition of DIC, models have been developed which consider relevant chemical processes and changes in the ^{13}C signatures (*Fontes and Garnier 1979; Plummer et al. 1994; Aravena et al. 1995; Clark and Fritz 1997; Buckau et al. 2000; Geyh 2000; Bethke and Johnson 2008; Mokrik et al. 2008; Coetsiers and Walraevens 2009*). Due to insufficient data on the chemical composition, the isotopic composition of dissolved carbon containing species, the mineralogy of the sediments, the isotopic nature of the sediments including the age of the aquifer materials, the current study avoids detailed corrections, particularly by isotope-exchange or reaction path models. In the current study a basic correction has been made for initial ^{14}C values, and another correction has been applied where dilution of the ^{14}C is reflected in the $\delta^{13}C$.

Knowing the ^{14}C activity of DIC in recharge is a prerequisite of groundwater age estimation. Many empirical approaches have been applied to estimate this initial activity *(Geyh 2000)*. Here, an ^{3}H vs ^{14}C diagram was used to estimate the initial ^{14}C activity in the DIC of groundwater following Verhagen et al. *(1974)*. Available ^{3}H and ^{14}C data from the different parts of the basin reported by earlier workers *(Aggarwal et al. 2000; Zheng et al. 2005)* were complied to generate an ^{3}H vs ^{14}C diagram (Figure 5-21), which was then used to estimate the initial activity of ^{14}C as 87 pMC, realistically close to 100 pMC. The estimated value of initial ^{14}C activity is close to the fixed correction value of 85 pMC as proposed by Vogel and Ehhalt (*1963*).

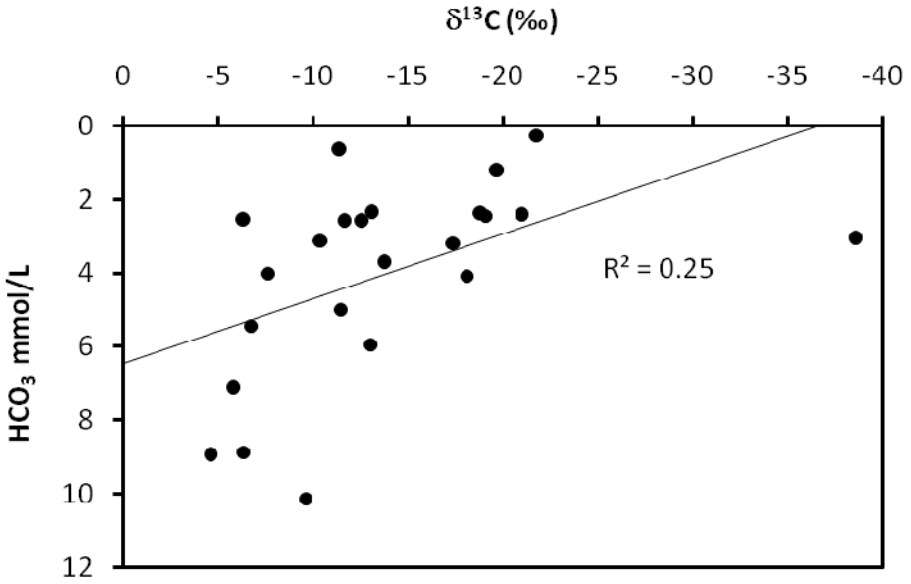

Figure 5-20: Graph shows high $\delta^{13}C$ values corresponding with high HCO_3 concentrations.

Much of the carbon in groundwater derives from gaseous CO_2 in the vadose zone, and its isotopic nature is altered due to addition of carbon from the root-zone and mineral dissolution. As the enriched inorganic $\delta^{13}C$ from the carbonate minerals mix with the isotopically depleted biogenic $\delta^{13}C$, the DIC becomes isotopically more enriched until the CO_2 is exhausted, the pH rises and the dissolution of carbonate minerals stops *(Mook et al. 1974)*. Carbonate minerals are found to occur throughout the aquifer sequence in Bangladesh in the form of siderite ($FeCO_3$) and ankerite [$Ca(Fe, Mg, Mn,)(CO_3)^2$], and the proportion of calcite and magnesite minerals varies between 2.1 and 6.9% *(Hasan 2008)*. Reactions that influence $\delta^{13}C$ (calcite dissolution, oxidation of organic matter and methanogenesis) also influence the ^{14}C activity measured in groundwater. The simplest isotopic mixing model utilizes different ^{13}C of DIC from primary recharge and the admixed DIC from carbonate sediments. Additional sources of carbon and the ^{14}C-free DIC from mineralization of SOC (sedimentary organic carbon) cannot be distinguished from each other by the ^{13}C content. An earlier study however, indicated that organic-matter oxidation contributes insignificantly in the dilution of ^{14}C activity. *Maduabuchi et al. (2006)* used the following equation (Eq. 5-2) to estimate groundwater age where initial ^{14}C activity is modified by dissolution of dead carbonates in the soil zone. In the equation they considered the initial concentration to be 100 pMC, where here it is considered to be 87 pMC. Here the stable isotope ratios of C in the aquifer matrix ($\delta^{13}C$ = 0‰) reflects the likelihood that detrital carbonate is derived from marine sediments in the Himalayan catchment, following Harvey (*2002b*). For soil gas a value of $\delta^{13}C$ = -25‰ was used, also following Harvey (*2002b*). Figure 5-20 demonstrates fractionation between DIC and solid phase carbonate during dynamic equilibration.

$$^{14}C_{age(yrs)} = 8267 \times \ln\left[\left(87/C_{14}\right) \times \left(\delta^{13}C/-25\right)\right] \quad \text{.....Eq. 5-2}$$

Where C_{14} is the ^{14}C activity measured in DIC expressed in pMC

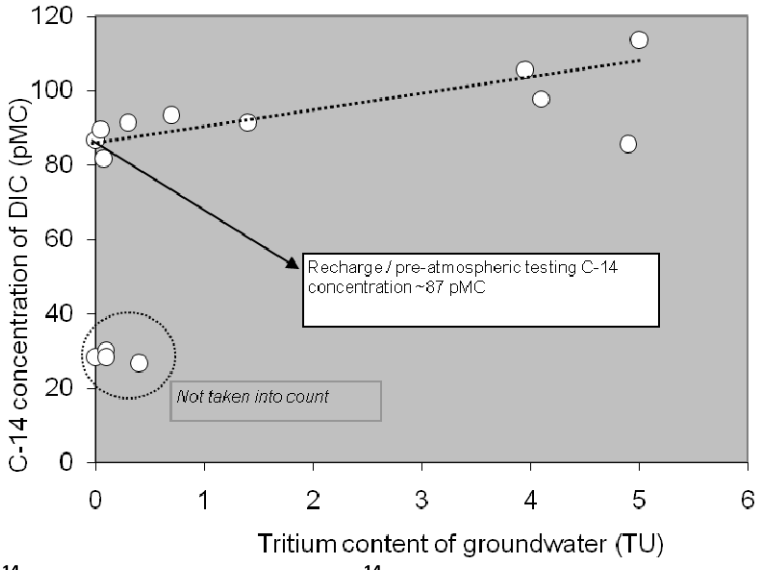

Figure 5-21: ^{3}H vs ^{14}C diagram indicating the initial ^{14}C activity around 87 pMC

5.3.3.4 Groundwater age

Groundwater ages from the measured ^{14}C activities have been estimated, and three age estimates are tabulated (Table 5-5) for each groundwater sample with respect to the correction procedures of section 5.3.3.3. In the first case it is assumed that initial ^{14}C activity was 100 pMC and no dilution occurs other than decay; this is the uncorrected apparent age (UC). In the second case, an initial value for ^{14}C activity was taken as 87 pMC, as derived from the $^{3}H/^{14}C$ plot, but with no dilution other than decay, and this is called the corrected age, C1. In the third case, the estimated value of initial activities along with dilution of ^{14}C is considered by reference to the $\delta^{13}C$ values; this is called the corrected age, C2.

As would be expected, the corrected ages are lower than the uncorrected apparent ages (Figure 5-22) showing a range 3000 to <10,000 years BP (Before Present). This indicates that groundwater at deeper levels was recharged under a climatic regime comparable to present day climate, as also indicated by the O and H isotopic signature (see section 5.3.2.1), even in respect of the pattern and intensity of rainfall *(Goodbred et al. 2003)*. Groundwater recharged during the last glacial maxima ~18 ka BP would be isotopically more depleted. Previous studies indicating deep groundwater in the Bengal Basin to be very old, 15 to 30 ka (*Aggarwal et al. 2000; Zheng et al. 2005; Michael and Voss 2009a*), make reference to uncorrected ages that are very close to the uncorrected ages estimated in the current study.

The groundwater uncorrected ages are found to increase with depth (R^2 = 0.33 and 0.32 for UC and C1; n=23), but the trend becomes insignificant (R^2 = 0.10, n=23) for the corrected ages (C2) (Figure 5-22). The depth ternd (for C2) becomes negligible (R^2 = 0.01, n=17) if samples >100 m deep are considered.

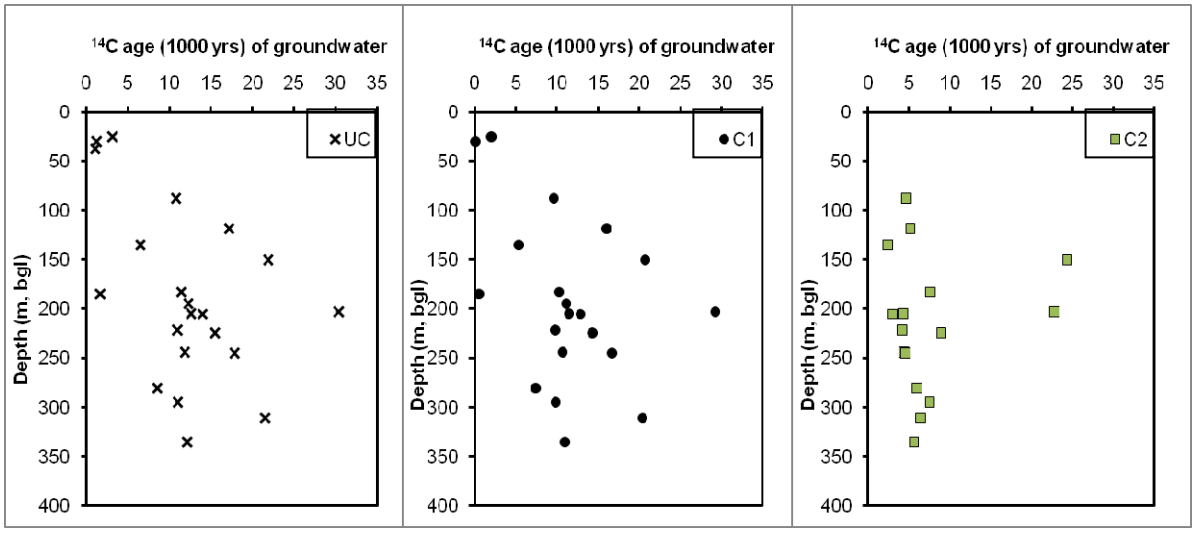

Figure 5-22: Age of groundwater versus depth in Bengal aquifer system. Here UC, C1 and C2 represent three different age estimates, see text. Note that modern groundwater are excluded from the plot.

A representative 2D basin-scale groundwater flow model was constructed (Figure 5-23) using MODFLOW -2000 (*Harbaugh et al. 2000*). Lateral and basal boundaries of the model were considered as no-flow. The top boundary was assigned a fixed head, to provide topographically driven groundwater flow. The natural condition with no abstraction was considered. The width (375 km) and depth (500 m) of the modelled aquifer approximates to 1/200, a similar aspect ratio as the Bengal Aquifer System. Topographic elevation differences across the basin were approximated in the same way. Effective hydraulic conductivity was taken as Kx = 35 m/d and two different hydraulic anisotropy values were considered. Modelling (Figure 5-23) demonstrates that in the highly-anisotropic aquifer (Chapter 4) deep groundwater recharges from the basin margin, leading to a groundwater age that is invariant with depth (as in the case of the corrected age (C2) trend, Figure 5-22). There is no prominent spatial pattern of groundwater age distribution (Figure 5-24); younger deep groundwater at the basin margin areas may be associated with enhanced infiltration at the basin margin due to higher relief.

Table 5-5: Estimated ages of groundwater (years BP). Here UC, C1 and C2 represent three different age estimates, see text. In the table negative values indicate modern groundwater in the aquifer. In the last column '±' indicates the standard deviation associate with the lab measurement.

Field ID	Depth (m)	UC	C1	C2	±
DT0114-11S	15.4	-380	-1532	-3757	51
DT0114-11M	87.78	10754	9603	4667	85
CU0104-7	37	-1574	-2726	-9203	52
SP0116-16	37	1052	-99	-1224	55
KHOP4	25	3170	2019	-9324	60
KCC-EdU-2	30	1244	93	-7820	55
DS0104-8D	135	6541	5390	2394	67
JB0105-10D	150	21902	20751	24335	162
LC0104-6D	195	12269	11118	-198	91
CL0102-2D	203	30397	29246	22798	289
FG0102-1D	205.5	13990	12839	3028	112
NN0105-9D	222	10945	9793	4129	80
DB0103-4D	225	15482	14331	8937	107
BJ0103-3D	244	11832	10681	4376	93
DT0114-11D	295	11007	9856	7526	81
CG0103-5D	185	1661	510	-1452	61
KHOP5	183	11441	10289	7615	85
KHNS98D	205	12608	11457	4238	94
KHOP1	281	8555	7403	5958	72
RKHOP2	336	12110	10959	5610	92
KCC-0127-22M	119	17191	16039	5191	118
KCC-0128-26D	245	17823	16671	4579	113
KCC-ExD-2	311	21536	20385	6408	144

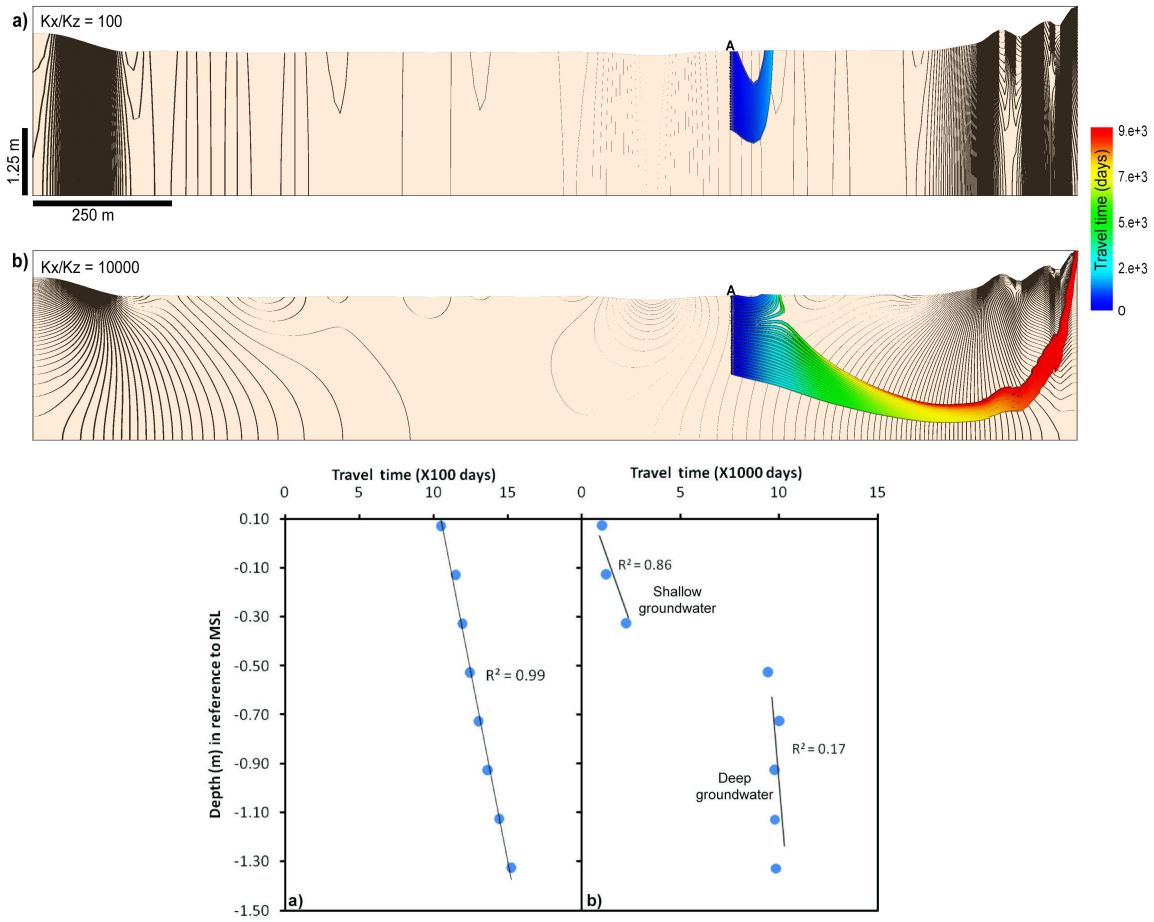

Figure 5-23: Numerical representation of groundwater flow-systems in a vertically anisotropic aquifer (K_x/K_z 100 and 10,000) and associated profiles of groundwater travel time at a location 'A'. (a) Local recharge leads to linearly increasing travel time with depth due to the increasing flow-path lengths. (b) The insignificant depth-wise trend observed if deep groundwater is considered follows from the fact that recharge derives from the distant basin margin.

5.4 Discussion

Consistent interpretations of groundwater isotopes and groundwater age indicate that the deep groundwater has originated as recharge at the basin margin. Interpretation of groundwater chemistry is inconclusive as discussed in the following sections.

5.4.1 Hydrochemical processes

The types of groundwater are mostly of Ca–Mg–HCO_3 and Na-Cl, with Cl, HCO_3, and Na as the dominant ions. The general hydrochemical nature of shallow and deep groundwater is as heterogeneous as the sediment lithology, influenced by processes including seawater mixing, anthropogenic contamination (particularly in shallow groundwater), and water-rock interaction as indicated by the wide range and high standard deviation of most hydrochemical parameters.

The mineralogy of the aquifer is dominated by quartz, K-feldspar (orthoclase) and plagioclase (anorthite and albite) with a substantial content of biotite and ferro-hornblende including

magnetite and rutile *(von Brömssen et al. 2007)*. Geochemical modelling *(Mukherjee and Fryar 2008)* indicates that groundwater in the basin is for the most part in equilibrium with kaolinite, and that primary feldspars are unstable. Also, groundwater is in equilibrium with quartz rather than with amorphous silica. The dissolved groundwater Al concentration is controlled by solubility of primary silicates weathering products, such as kaolinite or illlite. The slow dissolution kinetics of these clay minerals at near-neutral pH may be responsible for the small concentrations of Al (~0.1 mg/L) in groundwater (Figure 5-25a).

Ion exchange may also be in operation in the aquifer. As a consequence of Ca exchange for Na on the surface of clay minerals, such as kaolinite or illite, Na concentrations may increase preferentially compared with simple mixing as revealed by a Na/Cl ratio greater than 1.0, as Ca decreases (Figure 5-25b). Equally, a well-defined relationship between Na/Cl ratio and Ca concentration in groundwater is not possible due to the simultaneous occurrence of carbonate weathering *(Dowling et al. 2003)*. Isotopic depletion at higher EC may be an indication of the invasion of saline connate water of the aquifer by fresh water (Figure 5-26).

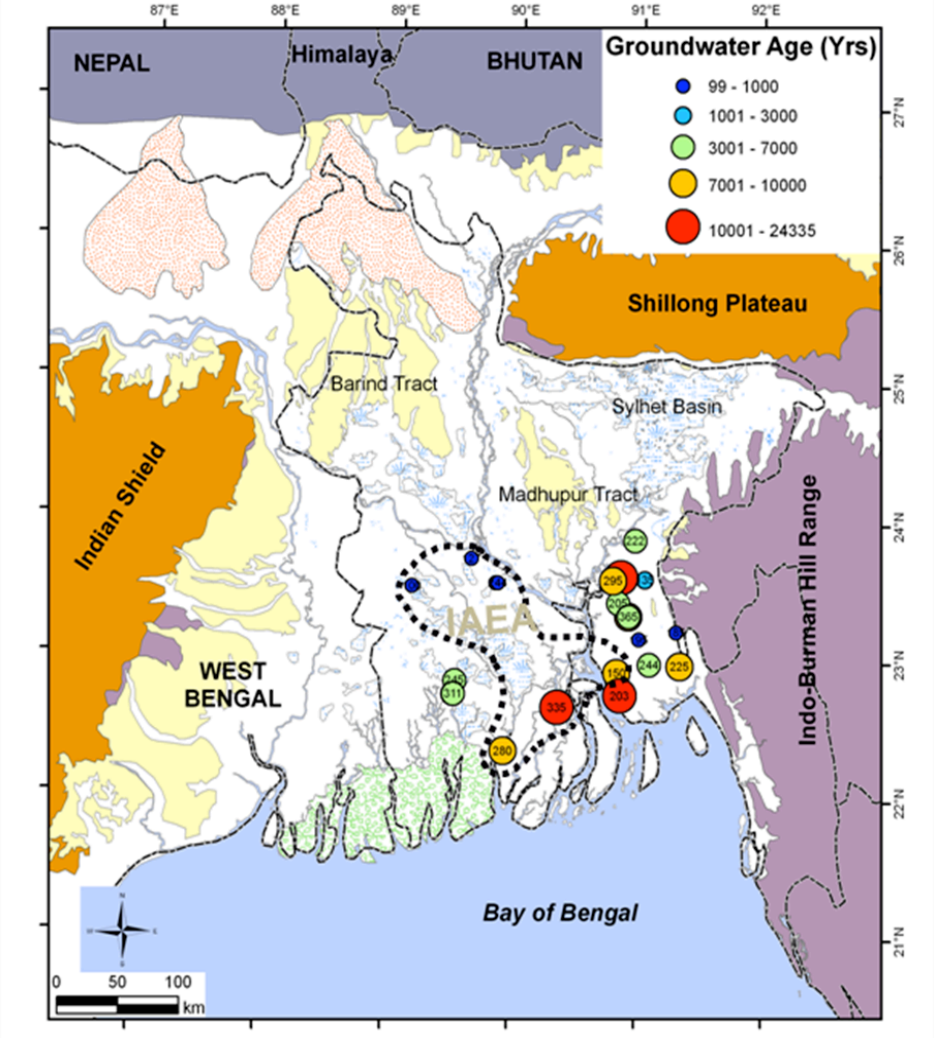

Figure 5-24: Spatial distribution of (C2) groundwater age of samples from wells deeper than 100 m bgl. Note the 6 dates estimated using Aggarwal et al. *(2000)* data included here marked as IAEA.

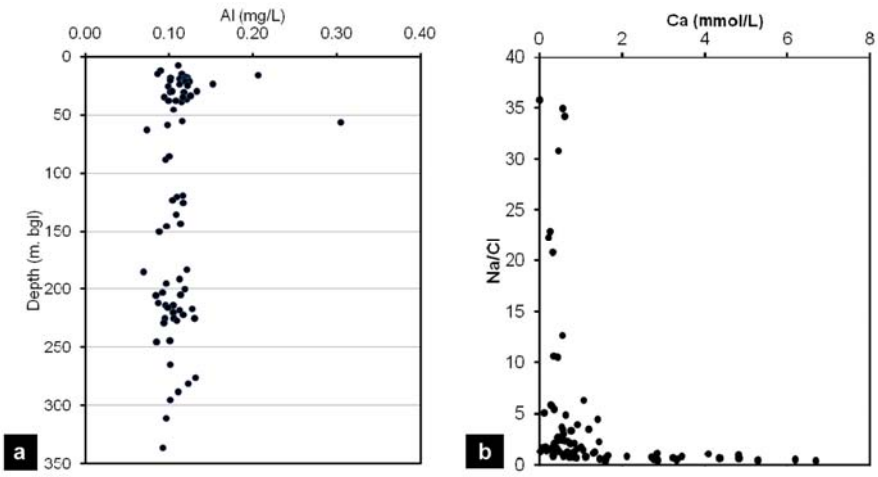

Figure 5-25: Al versus depth indicating similar rock-water interaction throughout the aquifer; (b) Na/Cl versus Ca indicating Na/Cl ratio greater than 1.0, as Ca decreases.

The hydrochemical pattern of groundwater on regional scale may be controlled by the flow system. Deeper groundwater is more commonly of Na-Cl type. This may be explained as sea water intrusion and mixing, or flushing of saline aquifer by fresh-water or old-water close to the end of a flow-path where Na-Cl type water dominates. Shallow groundwater has a wider range of concentration for almost all ions, and may be associated with low life-span of these flow-system and anthropogenic activities. In addition, shallow groundwater contains excessive levels of arsenic, associated with the reductive dissolution of FeOOH minerals *(Nickson et al. 1998)*. Similar reductive dissolution of Fe-OOH is found to be associated with high content of Fe in the deep aquifer without excessive arsenic *(Halim et al. 2010)*. This iron reduction may be an important processes controlling groundwater chemistry in the basin. Earlier work *(Mukherjee et al. 2008)* indicates the overlapping redox controls on groundwater chemistry in the basin.

5.4.2 Deep floodplain groundwater compared to Dupi Tila water

The deep aquifer of the Holocene floodplain is thought to be geologically equivalent to the Dupi Tila aquifer *(Ravenscroft 2003)*, which is composed of a similar lithology as the floodplain aquifers but contains alternating layers of brown and grey-coloured sediments (*Davies and Exley 1992; Burgess et al. 2010*). However, hydrochemical analyses indicate that the groundwaters of these two aquifers are different. In the Dupi Tila aquifer the water type is Ca-Mg-HCO_3 whereas Na-Cl dominates the deeper aquifer. Groundwater from the Dupi Tila aquifer is similar to that from the Pleistocene Tracts of western and central Bangladesh (the Madhuphur and Barind tracts) *(Hasan et al. 1998)*. The Dupi Tila sediments are extensively oxidised to about 150 m while at deeper levels it is reduced to slightly oxidised.

Hydrochemical differences between the Dupi Tila aquifer and the deep and shallow floodplain aquifers along a transect in eastern Bangladesh have been studied by Hasan *(2008)* who found a similar disparity. Lithologically, these aquifers may be similar but they have different redox histories (section 3.3.2.1). The Dupi Tila aquifer in the north and eastern part of the basin

experienced several cycles of sea-level low stand and consequent weathering and flushing by oxidising meteoric recharge while the deep aquifers of the current floodplain have not experienced this. The redox difference controls the hydrochemical characters in the two environments *(Stollenwerk et al. 2007)*.

5.4.3 Contrast between deep water of different hydrogeological contexts

The deep aquifer in the basin is discontinuously separated by low-permeability materials from the shallow levels. Deep groundwater in Kachua is not separated from the shallow groundwater by a low-permeability materials but the reverse is true in Khulna (section 5.1.2). Relatively high resolution sampling was carried out in these areas (Figure 5-1). Hydrochemical conditions are reducing in the deep aquifers, with more pronounced reduction at Khulna (Figure 5-27). The major-ion chemistry in both regions is complicated by salinity; deep groundwater at Khulna is $NaHCO_3$-NaCl type while at Kachua NaCl type water dominates (Figure 5-28) *(Hoque et al. 2008)*. Radiocarbon (^{14}C) activity is lower in the deeper groundwater at Khulna (7-12 pMC) than at Kachua (22-36 pMC). This may imply older groundwater in the Khulna deep aquifer despite the long history of groundwater abstraction there.

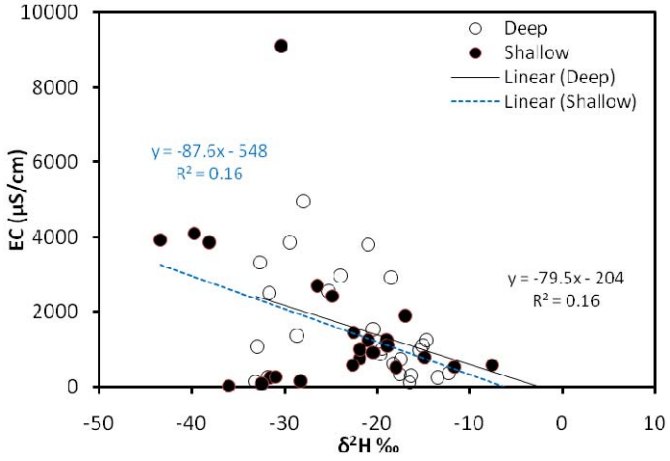

Figure 5-26: The EC vs δ^2H plot shows depleted groundwater has higher EC.

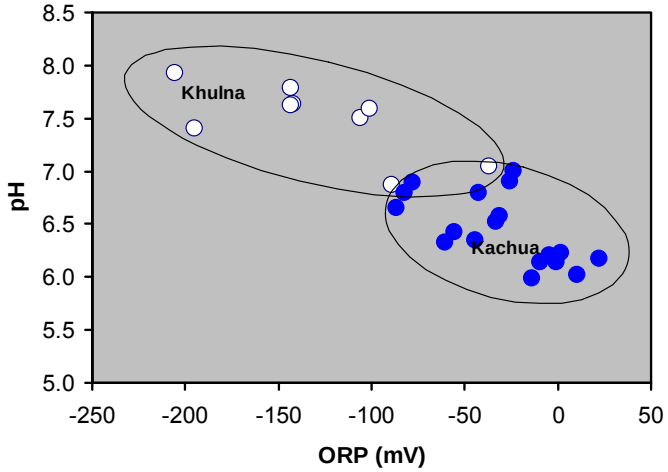

Figure 5-27: A simple plot of deep groundwater ORP and pH indicate pronounced reduction in Khulna deeper aquifer than that of Kachua.

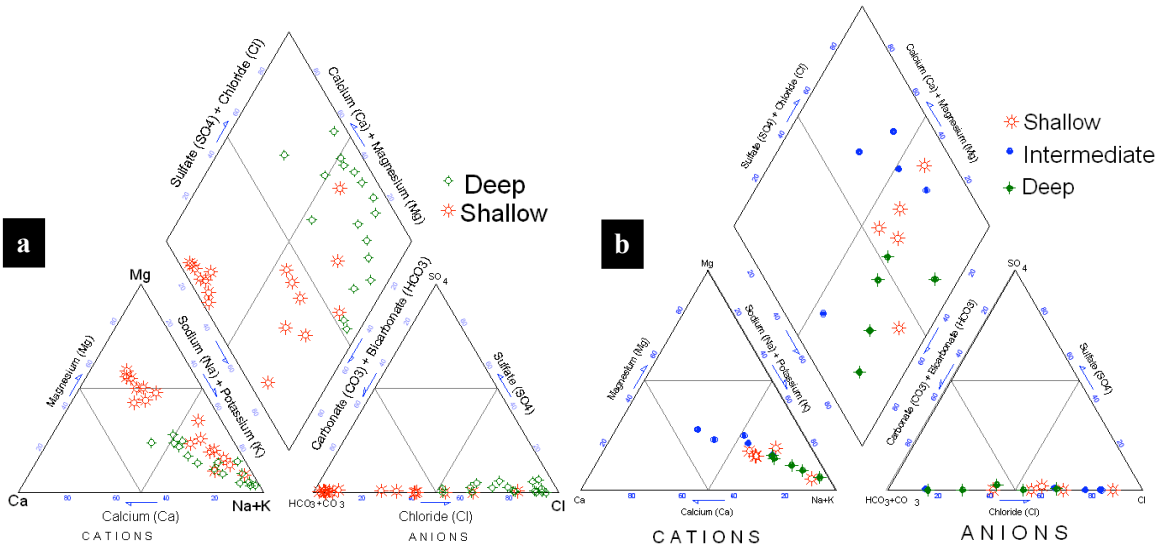

Figure 5-28: Piper plots indicate a mixing (fresh and saline) trend in Kachua (a) shallow and deep groundwater. In Khulna (b) shallow and intermediate water have the mixing trend but deep groundwater has no Cl end member.

5.4.4 Explaining the stable isotope depth profile: Recharge and paleo-climate

The δ^2H –$\delta^{18}O$ data plotted against ^{14}C derived ages may suggest subtle difference (mean $\delta^{18}O$ is -4.5 [n= 8] and -3.7 [n= 15] for younger and older groundwater respectively) in isotopic composition between younger (<10 ka) and older (>10 ka) groundwater, when considering uncorrected age (Figure 5-29). The O and H isotopic content would be expected to be lighter under a colder climate before 10 ka. Corrected groundwater ages, C2, (with two exceptions) indicate the groundwater to be younger than 10 ka and comply with similar δ^2H –$\delta^{18}O$ isotopic composition of range, associated with an effectively constant climatic condition over this time (cf. *Clark and Fritz 1997*). The isotopic nature of groundwater therefore supports the interpretation that the 'actual age' of groundwater in the region is much lower than the uncorrected age. An earlier study *(Aggarwal et al. 2000)* concluded that the stable isotopic signature of deeper water (at depths of 100–150 m and ~300 m) is different ($\delta^{18}O$ values >-3 and <-6) from that of shallower aquifers, suggesting paleorecharge during a different climatic regime between 3 and 30 ka ago. The groundwater age of the deeper aquifer has not been determined with confidence and current analysis indicates this to be younger than 10 ka. Groundwater modelling also supports the estimated age to be 10 ka or less (section 8.2).

Shallow groundwater in the region is much younger and contains a wider range of isotopic signature, indicating recharge from pre-monsoon rains (*Mukherjee et al. 2007a*) or partly evaporated surface water *(Zheng et al. 2005)*. In contrast, deep groundwater contains a narrower range of isotopic values (Figure 5-17) indicating recharge may have not happened from or through the shallow groundwater system. The slope of $\delta^{18}O$ vs. δ^2H reflects, approximately, the equilibrium fractionation associated with hydrogen and oxygen, and the intercept reflects the kinetic fractionation at the source regions *(Murad and Krishnamurthy 2008)*. Deviations of slope

and intercept from such 'average' behaviour gives useful information regarding secondary processes related to surface water-groundwater interaction. Shallow and deep groundwater in the basin have different slopes and intercepts (Figure 5-30). Shallow groundwater has a slope of 5.4 which is lower than the WML, indicating potential evaporation of recharging water prior to infiltration. In contrast, deep groundwater has a slope of 7.7, similar to WML, indicating limited or no enrichment of rain water prior to infiltration. Topography coupled with hydraulic anisotropy leads to a hierarchically nested flow system in the basin (Figure 5-23 and also section 6.2). Deep groundwater associated with regional flow system is originated from the basin margin hilly areas. Precipitation in the basin margin areas undergoes less evaporation prior to infiltration.

On the other hand, pre-monsoon rainwater which is isotopically enriched (*Mukherjee et al. 2007a*) is less likely to infiltrate due to the soil condition at the end of the dry season. An earlier study *(Ramesh and Sarin 1992)* shows that high altitude streams in the Himalaya have isotopic similarity with the WML. Similar streams in the basin margin hilly areas of the present study region may also provide a recharge source for the deep aquifer. These are possible reasons why deep groundwater has a narrow range of isotopic values compared to shallow groundwater in the basin.

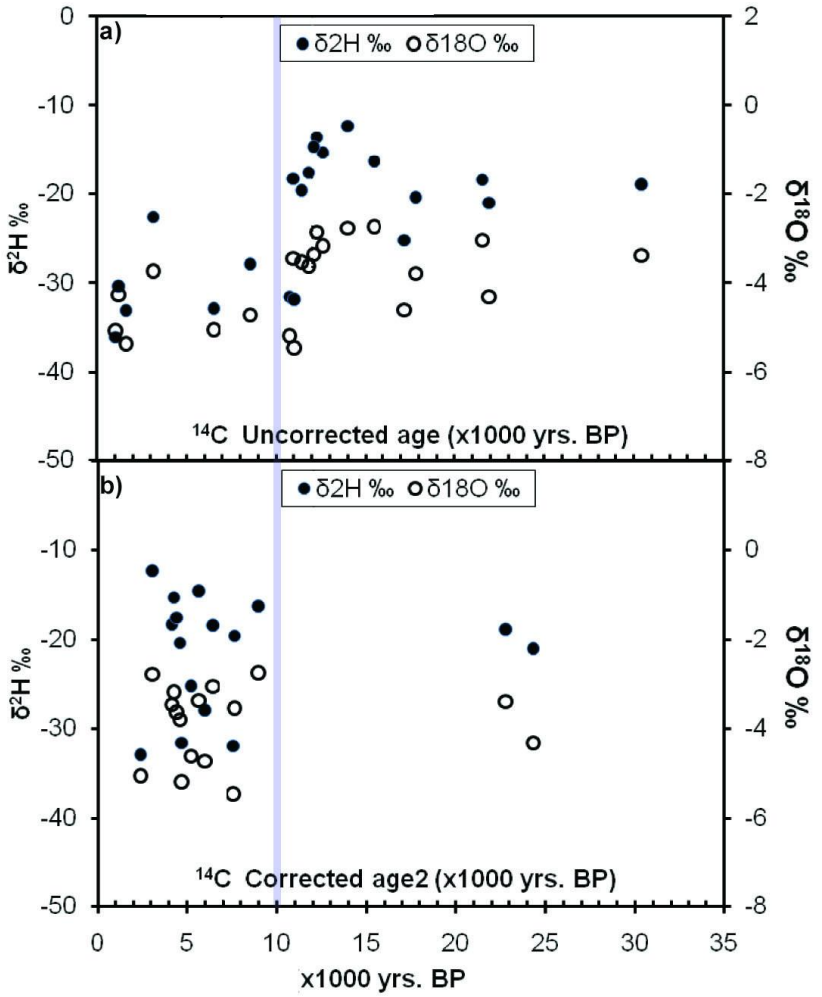

Figure 5-29: Plot of δ^2H –$\delta^{18}O$ versus ^{14}C age for groundwater, (a) uncorrected age, UC; (b) corrected age, C2. Note 10 ka BP is marked.

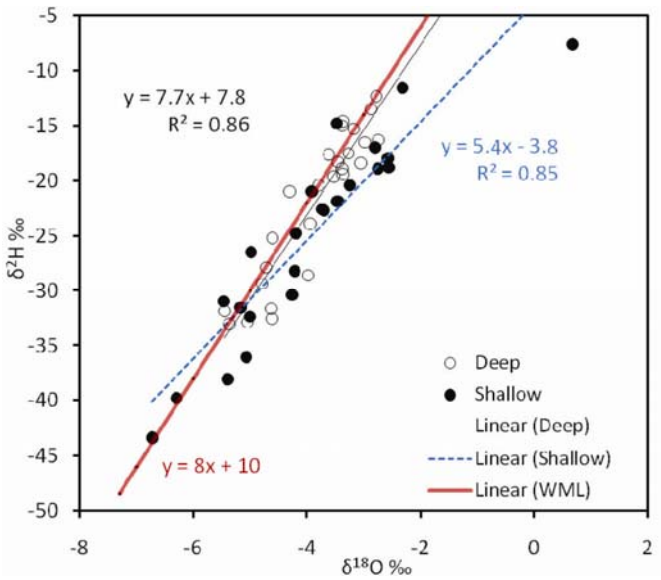

Figure 5-30: Delta plot showing best fit line and slope calculation for shallow and deep groundwater. Note that a much enriched $\delta^{18}O$ has affected the best-fit line for the shallower groundwater, if that is excluded interpretation based on the diagram still remain same; however magnitudes in slope and intercept become different.

Increasingly, attention is drawn to recharge of deep groundwater as a constraint on its long-term sustainability as a source of water, yet recharge estimations are non-existent. Radiocarbon-derived groundwater age can be used to estimate the rate of recharge to the deep aquifer in Bangladesh. A relationship between porosity (η), thickness of the aquifer (b) and groundwater age (T_t) to recharge rate (R) is proposed by Bouhlassa and Aiachi *(2002)* as following-

$$R = \eta b / T_t \quad \text{.....Eq. 5-3}$$

Recharge values were estimated using the uncorrected (UC) and corrected groundwater age (C2) (Table 5-6). In the estimation thickness (b) and porosity (η) of the deeper aquifer are taken to be 250 m and 25% respectively. The median of estimated recharge rate ranges between 5 and 11 mm/yr, which is comparable with basin-scale model (*Michael and Voss 2009a*) derived rate 17 mm/yr.

5.4.5 Controls on hydrochemistry and isotopic nature

The water chemistry of the Ganges-Brahmaputra drainage system is controlled by the presence of carbonates, the composition of silicates and the oxidative breakdown of sulphides (*Galy and France-Lanord 1999; Dowling et al. 2003*). Galy and France-Lanord *(1999)* observed that despite heavy monsoonal rainfall, chemical weathering is limited in the Ganges flood plains.

In general geochemical modifications occur progressively along groundwater flow-paths, following recharge; the longer the flow-path and the travel-time, the greater the hydrochemical

maturation. Systematic changes occur in the anion facies of groundwater, from HCO_3 through SO_4 to Cl, both along flow-path and with depth. Tóth *(1999)* summarised the geochemical changes along flow lines and in different flow-systems operating in thick unconfined aquifers as shown in figure 5-31.

In the Bengal Basin groundwater flow is controlled by topography and hydraulic anisotropy of the intercalated and discontinuous silt-clay layers. Flow-systems in operation in the Bengal Basin aquifer system are similar to those in figure 5-31 (see section 6.2). Flow-systems in nature are much more complicated in three dimensions, and hydrochemistry has a fourth dimension, time. However, topography and architecture of sub-surface silt-clay layers (section 4.3.8) ensure that shallow groundwater (<70-100 mbgl) is part of a shallow flow-system, while deeper water is part of the deep regional flow-system. Shallow groundwater circulates over less than hundreds of years, while deeper groundwater circulates over thousands of years. Complexities arise in the zone of groundwater discharge where deep groundwater and shallow water mix. This is why shallow groundwater has a more heterogeneous hydrochemical and isotopic character, with a more immature chemical character.

Table 5-6: Recharge rates (mm/yr) to the deep aquifer derived from groundwater age.

Sample ID	Depth (m)	Un-corrected age in yrs. (1)	Corrected Age, C2 in yrs. (2)	Recharge Rate for (1) mm/yr	Recharge Rate for (2) mm/yr
DS0104-8D	135	6541	2394	9.6	26.1
JB0105-10D	150	21902	24335	2.9	2.6
LC0104-6D	195	12269	Modern	5.1	-
CL0102-2D	203	30397	22798	2.1	2.7
FG0102-1D	205.5	13990	3028	4.5	20.6
NN0105-9D	222	10945	4129	5.7	15.1
DB0103-4D	225	15482	8937	4.0	7.0
BJ0103-3D	244	11832	4376	5.3	14.3
DT0114-11D	295	11007	7526	5.7	8.3
CG0103-5D	185	1661	Modern	37.6	-
KHOP5	183	11441	7615	5.5	8.2
KHNS98D	205	12608	4238	5.0	14.8
KHOP1	281	8555	5958	7.3	10.5
RKHOP2	336	12110	5610	5.2	11.1
KCC-0127-22M	119	17191	5191	3.6	12.0
KCC-0128-26D	245	17823	4579	3.5	13.7
KCC-ExD-2	311	21536	6408	2.9	9.8
Minimum (mm/yr)				2.1	2.6
Maximum (mm/yr)				37.6	26.1
Median (mm/yr)				5.1	11.1

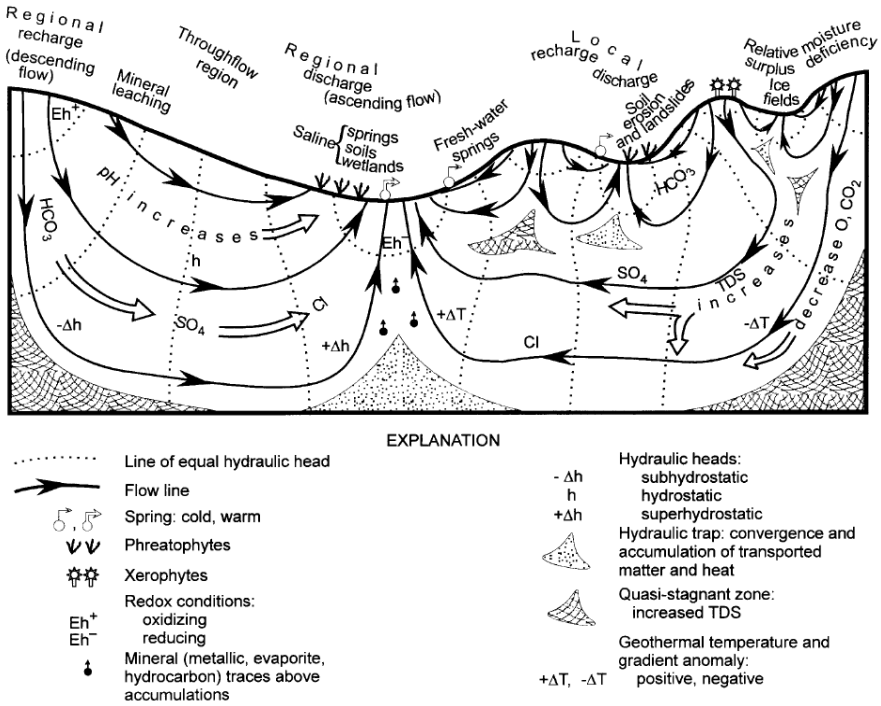

Figure 5-31: Hydrochemical condition of groundwater in different flow-systems and along flow-paths *(Tóth 1999)* in an unconfined aquifer.

In addition to the difference in flow-system, there are differences in the aquifer sediments of the shallower and deeper part of the basin. Shallow (<70 to 100 mbgl) sediments were deposited over the last eustatic cycle i. e., the Holocene period, while deeper sediments were deposited during earlier eustatic cycles of the Quaternary Period or even earlier (section 3.3.2.1). Moreover, older sediments at the surface have a different post-depositional weathering history leading to redox state of the aquifer zones, with implications for hydrochemical type of water (section 3.5).

5.5 Synthesis of the key points

In this chapter the distribution of chemical and stable isotopic characteristics of groundwater throughout the study region have been described. These distributions have been considered in relation to the groundwater flow pattern, and a deep groundwater flow system, probably recharged from the basin margins, has been identified.

Groundwater from 23 points across the study region has been dated by ^{14}C analysis of dissolved inorganic carbon. This provides a data-set for comparision against modelled groundwater travel times.

Part C: Representations & Modelling

Chapter 6
Groundwater Flow and Arsenic

This chapter investigates the patterns of groundwater flow in the basin and the relationship this has with groundwater arsenic. A new conceptual model 'SiHA (**S**ilt-clay layers **i**nfluence **H**ierarchical groundwater flow system and **A**rsenic progression in aquifer)' is developed and described. This chapter points out how conceptualisation of the flow-systems and the arsenic issue leads to specific modelling targets and approaches to modelling.

6.1 Previous modelling

Hydrological modelling including the examination of the groundwater component of the Bengal Basin started in the mid-1980s (*van Wonderen 2003; Mukherjee et al. 2007b*). Most modelling efforts were focussed on small portions of the basin, bounded by political borders, project boundary or hydro-morphic feature at the ground surface. Modelling efforts were solely directed at groundwater resource assessment for irrigation potential. MPO *(1990)* was possibly the first national scale model aimed to model groundwater recharge. Some modelling studies concentrated on the resource assessment of the Dhaka aquifer (*EPC/MMP 1991; Hasan et al. 1998; Hasan 1999; DWASA 2000*), from where groundwater was being withdraw at rate far in excess of recharge, leading to a 1.5-2.5 m decline on the water level per year (*Morris et al. 2003; Hoque et al. 2007; Shamsudduha et al. 2009a*).

In the mid-1990s, the discovery of excessive dissolved arsenic in shallow groundwater over much of Bangladesh led to a number of modelling activities within the Bengal Basin. The objectives of the modelling were centred on the fate of arsenic, ranging from understanding distribution of arsenic within the aquifer *(BGS/DPHE 2001)*, the pumping induced transport of arsenic from one zone to other zone within the shallow aquifer (*Cuthbert 1999; Cuthbert et al. 2002; Burgess et al. 2007*), the relation of As to groundwater dynamics *(Harvey et al. 2006; Klump et al. 2006;*

McArthur et al. 2008), and evaluation of the safety of the deeper arsenic-free aquifer zone (*Cheetham 2000; Bashar et al. 2002; GRG/HG 2002; JICA 2002; Mukherjee et al. 2007b; Shibasaki et al. 2007*). However, all this modelling was done on a local scale, restricted by either the local hydrological features or political boundaries.

Local-scale models may be suitable for understanding local, shallow flows, but they have limited success and cannot effectively simulate the deep flow. To understand the sustainability of the deep groundwater requires at least a regional-scale model, which should incorporate the recharge areas relevant to the depth of interest and which should not be restricted by a boundary which is close to the area of interest. Recent modelling studies (*Michael and Voss 2008; 2009b; 2009a*) comprise the entire basin including all unconsolidated aquifer sediments up to ~3000 m bgl, with the aim of understanding the controlling factors of the flow-system in the basin, and also the security of the deeper groundwater against arsenic migration from the shallower depth. Due to the large areal extent of the modelling domain, the basin-scale model has to sacrifice the details of the underlying geology. The base-case model of Michael and Voss *(2008)* considered the aquifer as a single anisotropic (Kh/Kv=10,000) aquifer for the whole basin. Basin-scale studies may be suitable for understanding the basinal flow-system, but omission of local details limits their applicability to the assessment of the sustainability of the deeper groundwater at any specific site. To assess the importance of the local geological details on the groundwater flow and sustainability of the deep groundwater, sub-basin scale modelling efforts which incorporate the local geological details are required. In addition, the single anisotropic representation (e. g., *Keating et al. 2005; Michael and Voss 2009a*) of fluvio-deltaic aquifers at basin scale may provide convincing results for regional flow dynamics due to regional uniform distribution of low conductivity materials. However, areas of dominant paleo-channel activity are characterised by sandy sediment (section 4.3.4), where anisotropy should be significantly lower and in this situation a single anisotropic representation may not be applicable.

6.2 Understanding groundwater flow-system

Groundwater flow in a sedimentary basin can be driven by gravity *(Tóth 1963; Tóth 2009)*, buoyancy *(Thornton and Wilson 2007)*, and compaction *(Kooi 1999)* depending on the hydro-mechanical context. In the Bengal Basin groundwater flow is generally driven by the topography, however in the coastal region density differences may come into effect, while at depth (in the same region), due to subsidence, sediment compaction may also have an impact.

In the current analysis it is considered that groundwater flow is driven by gravity. Nevertheless, in the modelling studies an attempt has been made to represent the effect of density in the seaward region by considering the equivalent fresh-water head for the seawater (section 7.6.3). On the contrary, compaction is considered to have lesser significance because of the shallower depth of interest (< 400 m) *(Barker 1990)*.

Although flow is driven by gravity, because of spatial topographic differences and the occurrence of low permeability materials, groundwater flow in this fluvio-deltaic terrain becomes compartmentalised *(Freeze and Witherspoon 1967; Ophori and Tóth 1990; Tóth 2009)*. Details of the factors controlling flow in fluvial-deltaic unconsolidated aquifers are described in chapter 3 of Tóth *(2009)*. The following section considers how topography and distribution pattern of low-permeability materials in the subsurface affect groundwater flow, and how this flow system is related to the distribution and progression of groundwater arsenic in the basin. The later part of this chapter outlines the implications for the modelling objectives.

Several simple demonstration models have been developed to investigate the groundwater flow systems in operation in the region. All the models were developed using the Hsieh *(2001)* model code 'Topodrive', a 2D vertical section steady state groundwater flow model. All boundaries of the models are considered as no-flow except the top boundary where a fixed head is assigned. Recharge is not assigned separately rather top fixed head boundary acted as source of recharge and points of discharge depending on the hydraulic head. Models are in a steady state, natural condition with no abstractions. Besides the aforesaid common features the geology and topography varies from model to model as outlined in each case description.

6.2.1 Topography, low permeability materials, and their coupling

The present landform of the Bengal Basin is made of alluvial-fluvio-deltaic sediments from north to south. The basin is bounded by hilly terrain in the east and north, and Precambrian shield area in the west. The elevation of the basin margin features ranges from approximately one hundred metres to several kilometres. Regional elevation within the basin decreases from <100 m in the northwest alluvial fan region to less than 1m in the coastal areas (Figure 3-1). In addition, there are three major rivers running to the Bay of Bengal in the south of this basin, and each has associated river valley depressions. As of gravitational principles of groundwater flow *(Tóth 1963; Tóth 2009)*, these regional topographical differences may generate a regional groundwater flow system between the basin margin high and the river valleys and the coastal region. In a homogeneous sub-surface, groundwater flow generated by such a topography would penetrate deeply *(Zijl 1999)* due to the flatness of the basin (note the regional rise is 1 m over 150 km towards the north). In reality, the subsurface is not homogeneous (section 4.3) and ground elevation increases northward with numerous ridges and sloughs (generic features of alluvial-fluvio-deltaic terrain) superimposed on the regional gradient. Moreover, observation reveals smaller scale hummock-depressions (a microtopograpy) overlying the ridges-sloughs. The subsurface of fluvio-deltaic terrain is composed of discontinuous layers of clay, silt, sand, and their mixture. Permeability and hydraulic anisotropy of these materials can vary by several orders of magnitude.

Three simple 2D steady-state groundwater flow simulations presented in figure 6-1 demonstrate possible patterns of groundwater flow across a transect representative of this basin. In these simple models the basin extent is assumed to be 15 km, and a topographic relief difference is approximated to be the in the same ratio as in the Bengal Basin. This is done as the flow-system is an issue of scale which behaves in the same way in larger dimensions. In the models, arbitrary topography is used to simulate the regional and some local features and it is assumed that the water table mimics the topography. The models demonstrate that flow is dominated by the sub-regional topography if the aquifer system is considered to be homogeneous with very low anisotropy (Kh/Kz=10). As previously described, aquifers in fluvio-deltaic terrain are very heterogeneous, which makes the hydraulic system behave anisotropically. Representation of the geological heterogeneities modelled using increased anisotropy ($Kh/Kz=10^4$) indicates that the flow-system is almost entirely dominated by the regional topographical differences, and all the groundwater, at least at some depth, originates from the basin margin. However, geological heterogeneities are localised in nature. A model with distribution of the low permeability materials (two order of magnitude lower permeability than sand) with hydraulic anisotropy ($Kh/Kz=10^4$) indicates that deeper flow is driven by regional topography and originates from the basin margin, whereas at shallow levels, flow is localised and influenced by local topographical differences (this is explained in section 6.2.2). These simple models indicate that groundwater flow-systems in the Bengal Basin are controlled by the coupling of topography and the presence of hydraulically anisotropic low permeability materials at depth.

The presence of high and low permeability materials, with hydraulic anisotropy, in the subsurface greatly influences the flow-system even in regions with low topographical variation, i. e., with subtle variation in water table *(*p. 35 in *Tóth 2009)*. Additional modelling indicates that the even very low topographical differences can generate hierarchically nested flow systems when there is sufficient anisotropy (section 6.2.3).

6.2.2 Relief and local flow

The regional scale topography and relief of the Bengal Basin is controlled by the tectonically generated hills and intra-basin uplifted blocks. Topographical features in the floodplain-deltaplain-channel setting consist of ridges and sloughs, and the spatial dimension (wave-length) varies from tens to hundreds of meters between the tops of ridges and the bottom of nearby sloughs *(Miall 1996)*. In addition, there exists a microtopography within the ridges and sloughs, at a smaller spatial dimension (1 m or less) between hummocks and depressions. The topographical relief differences are less than 1m to more than a few 10s of m in the ridges-slough settings, whilst it is in the range of few millimetres to few centimetres in the hummock-depressions. All these relief differences are significant for local groundwater flow, as groundwater flow is initiated by the gradient of the groundwater table, a mimic of the topographical relief.

One simple 2D steady-state groundwater flow model presented in figure 6-2 demonstrates the flow between two successive ridges and sloughs in a floodplain setting with arbitrary internal geological heterogeneities.

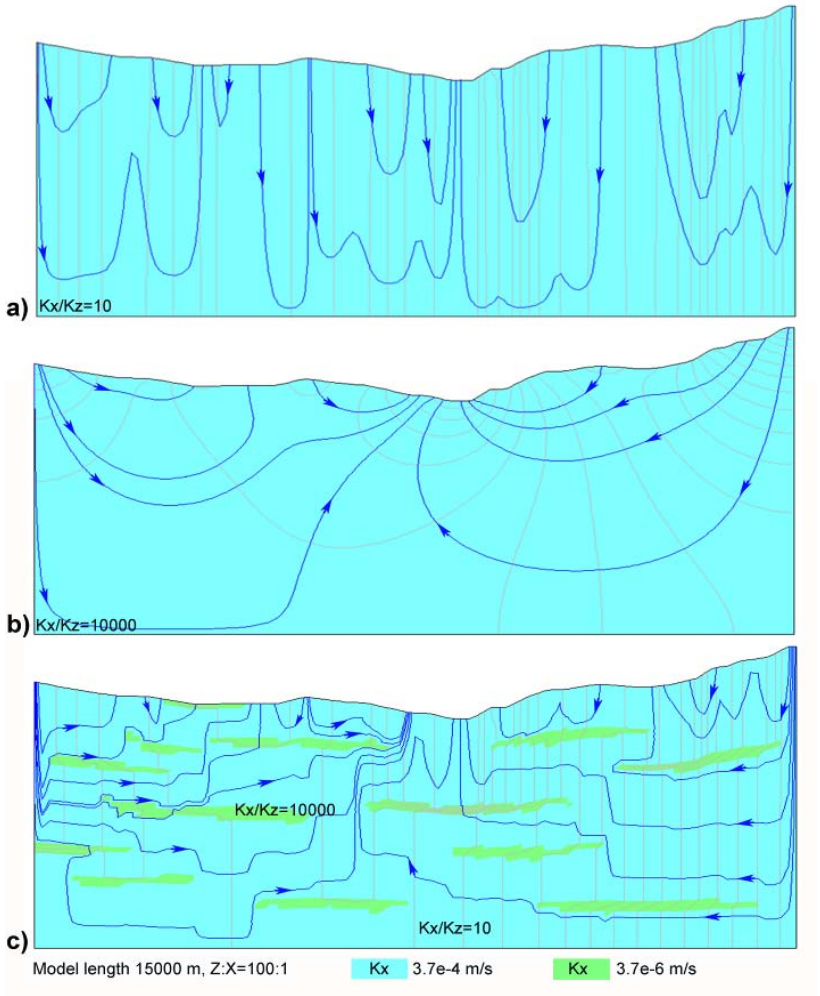

Figure 6-1: Regional flow system driven by only topography (a), geological heterogeneity as of statistical equivalent (b), and conceptual distribution of geological heterogeneities (c).

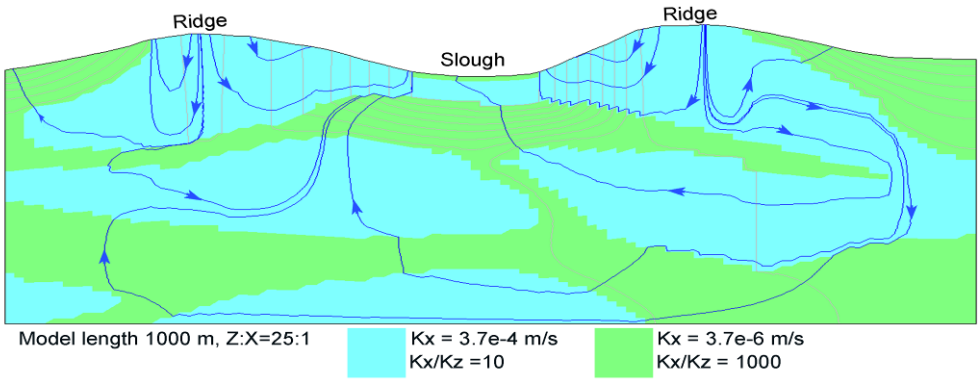

Figure 6-2: Local scale groundwater flow system between two successive ridges and sloughs in a floodplain setting with arbitrary silt-clay and sand distribution.

Groundwater flow at a shallow level within the aquifer is expected to be highly localised due to the combined effects of local topography (including microtopography) and geological heterogeneities, and may end at local streams or lakes. However, there is a regional gradient in the groundwater level of the shallow aquifer. The water level elevation is measured to be as high as ~100 m in the northwest and gradually decreases to the <1 m above the MSL (Figure 3-15). This regional gradient in shallow water level is often misinterpreted to infer long flow line towards the major rivers, even to the coast, which in fact may not be the case on account of the sediment heterogeneity. The regional gradient is just a reflection of the regional relief, whereas there are local topographic lows (local streams or lakes).

It is important to mention that in the current 3D modelling (Chapter 7) the flow induced by this local relief or microtopography will not be represented due to size of the model grids, which are much larger than these features (section 7.5.5). However, the sub-regional topography along with underlying hydraulic anisotropy is certain to result in a hierarchy of flow systems (section 6.2.3). The deep flow-system is expected to be dependent mostly on the anisotropy and regional topography.

6.2.3 Hydraulic (conductivity) anisotropy

In a basin with ubiquitous low permeability materials in the subsurface (even of limited areal extent) with the higher anisotropy (Kh>>Kv), the geometry and dimension of flow-systems are largely controlled by the anisotropy *(*p. 59 in *Tóth 2009)*. In general, geological porous materials on a highly local scale act as homogeneous isotropic media, which become heterogeneous and anisotropic with the increase in scale of consideration. The primary cause of anisotropy at the small scale is the orientation of clay minerals *(Freeze and Cherry 1979)*. On a larger scale, layered heterogeneity in the form of silt-clay and sandy or silty clay with intrinsic anisotropy contributes to the regional and basin-scale anisotropy. Ababou *(1996)* shows how the lateral dimension of layers of silt-clay and other fine materials contributes to the system anisotropy (see section 4.3.6.1).

Three sets of simple models were developed to understand the effect of anisotropy on groundwater flow in 2-dimensions (Figure 6-3). Two of the models have the same topography but with different internal distributions of anisotropic materials. One of these considers the system as a single anisotropic aquifer (Figure 6-3a), whilst the other has dispersed anisotropic low permeability materials within it (Figure 6-3c). These two differ from the third model which has topographical variation, but a single, anisotropic aquifer (Figure 6-3b). The modelling indicates that topography has a lesser influence on the generation of hierarchically nested flow systems in this highly anisotropic aquifer, where anisotropy plays the major role. The modelling also shows that horizontal conductivity differences (Kh) hardly affect the flow system; rather it is controlled by anisotropy. Naturally, sand and clay differ by several orders of magnitude in horizontal

hydraulic conductivity, and they also differ significantly in the vertical direction. It is estimated that sand has one order of magnitude less permeability in the vertical direction, but that low permeability materials (silt, clay, silty or sandy clay) have an anisotropy of 10^3 to 10^7 depending on the lithification, consolidation, compaction, and overburden pressure.

Different values of anisotropy can give hierarchically nested flow systems, for a single aquifer representation and / or in case of discrete representation of low permeability materials. With an increase of anisotropy, flow becomes much more regional and stretched, especially the deeper flow. Discrete representation of the low permeability material was found to be an adequate representation of discontinuous presence of the low permeability materials. Penetration depth of flowing groundwater is deeper where low permeability materials are absent. This indicates that discrete representation of localised low permeability materials is necessary in order to evaluate the groundwater flow system at local level.

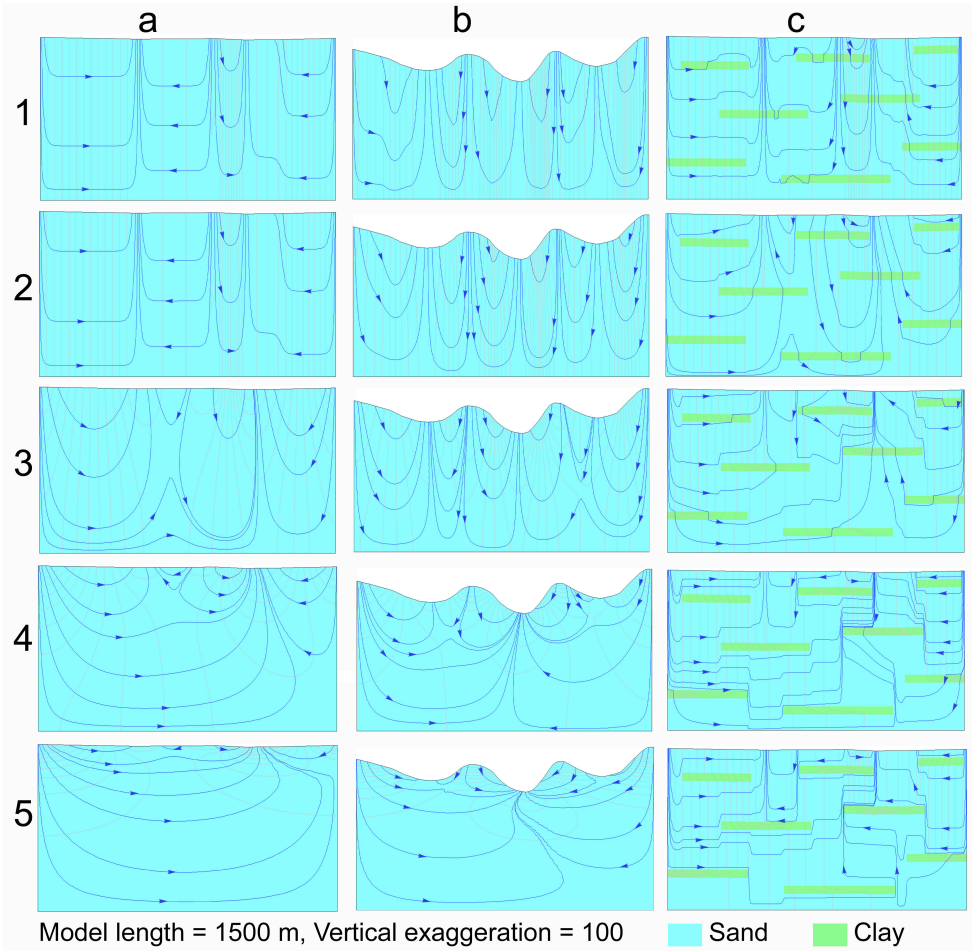

Figure 6-3: Matrix of models showing the affect of topography, bulk anisotropy and discrete anisotropic bodies (silt-clay layers) within the aquifer. In the models sand has hydraulic conductivity 3.7e-4 m/s, and clay is 3.7e-6 m/s. Vertical hydraulic anisotropy (Kx/Kz) increases from 10 to 100,000 in models '1a' to '5a' and models '1b' to '5b'; in model '1c' no anisotropy is given, sand has anisotropy of 10 in column 'c' and anisotropy of clay increases from 100 to 100,000 in model '2c' to '5c'. Models indicate that anisotropy dominates over topography in generating hierarchically nested flow systems in areas of relatively flat topographic relief.

6.2.4 Thickness and distribution patterns of low permeability materials

It is mentioned in the earlier section that low permeability materials are pervasive and lateral continuity is limited in fluvio-deltaic deposits. Their thickness also varies from place to place and also with depth. To check the effect of thickness and discontinuity of these low permeability materials, several 2D vertical section models were developed (Figure 6-4). The results indicate that thickness has only a nominal effect on the flow pattern. In areas where low permeability materials are absent, groundwater flow penetrates to a greater depth. In fact, in the absence of low permeability materials throughout the whole thickness in some areas a single flow system can exist depending on the intrinsic vertical hydraulic anisotropy of the sands and topography.

Characteristically, in fluvio-deltaic sequences low permeability materials are discontinuous but ubiquitous and 'random', their architecture is such that they form an effectively continuous layer if stacked as a single slab. This architecture of occurrence of low permeability layers is termed as '*stacked-mosaic-continuous'* hereinafter. This pattern of distribution of low permeability materials with anisotropy was tested in the modelling (Figure 6-4). It is found that even though the low permeability layers are discontinuous they are very effective in generating hierarchically-nested flow systems where they form a *stacked-mosaic-continuous* layer. This observation was tested with different anisotropy values of the low permeability materials. It is found that even a very low anisotropy (Kh/Kz=100) lead to the hierarchically nested flow systems.

The modelling reveals that shallow flows are generated from the local ground surface and remain at shallower depth (over the low permeability materials) if the '*stacked-mosaic-continuous'* condition prevailed, at least when the system is in an undisturbed state. In contrast, same condition leads the deeper flow system to generate at the boundary of the model and operates at the deeper level. The two flow systems do not come into contact at the point except where they discharge.

6.2.5 Model representation of low permeability materials

Due to the ubiquitous but discontinuous occurrence of the low permeability materials it is very difficult, if not impossible, to map them in 3D. This is why in modelling efforts statistical or representative descriptions must be used to incorporate the effect of the low permeability materials. Model predictions become uncertain due to the incompleteness of our knowledge and representation of real systems *(Watts et al. 1996)*. To investigate how different representations affect the flow field several simple models were employed (Figure 6-5).

Modelling indicates that a single anisotropic representation results in hierarchically nested flow systems (Figure 6-5 [1b]). However, if low permeability materials are locally absent the groundwater flow would penetrate more deeply. The effect of the local absence of low permeability materials can be incorporated if the effective hydraulic conductivity is estimated

based on site-specific data as a 'column-slab', or 'block-slabs' in vertical direction (Figure 6-5 [3a and 3b]).

Two other methods of representation (Figure 6-5 [2a and 2b]) were tested a) by making a thin mosaic of stacked-layer of low permeability materials, and b) by making two thin mosaics of stacked-layers of low permeability materials. These follow the concept of '*stacked-mosaic-continuous*' layer. It is found that in some areas stacking of discontinuous low permeability materials (for a certain depth-slab) form a continuous layer restricting the shallow flow system, at least in natural condition. This indicates *stacked-mosaic-continuous* representation could be an alternative approach to employing anisotropy for representing low permeability materials in groundwater models.

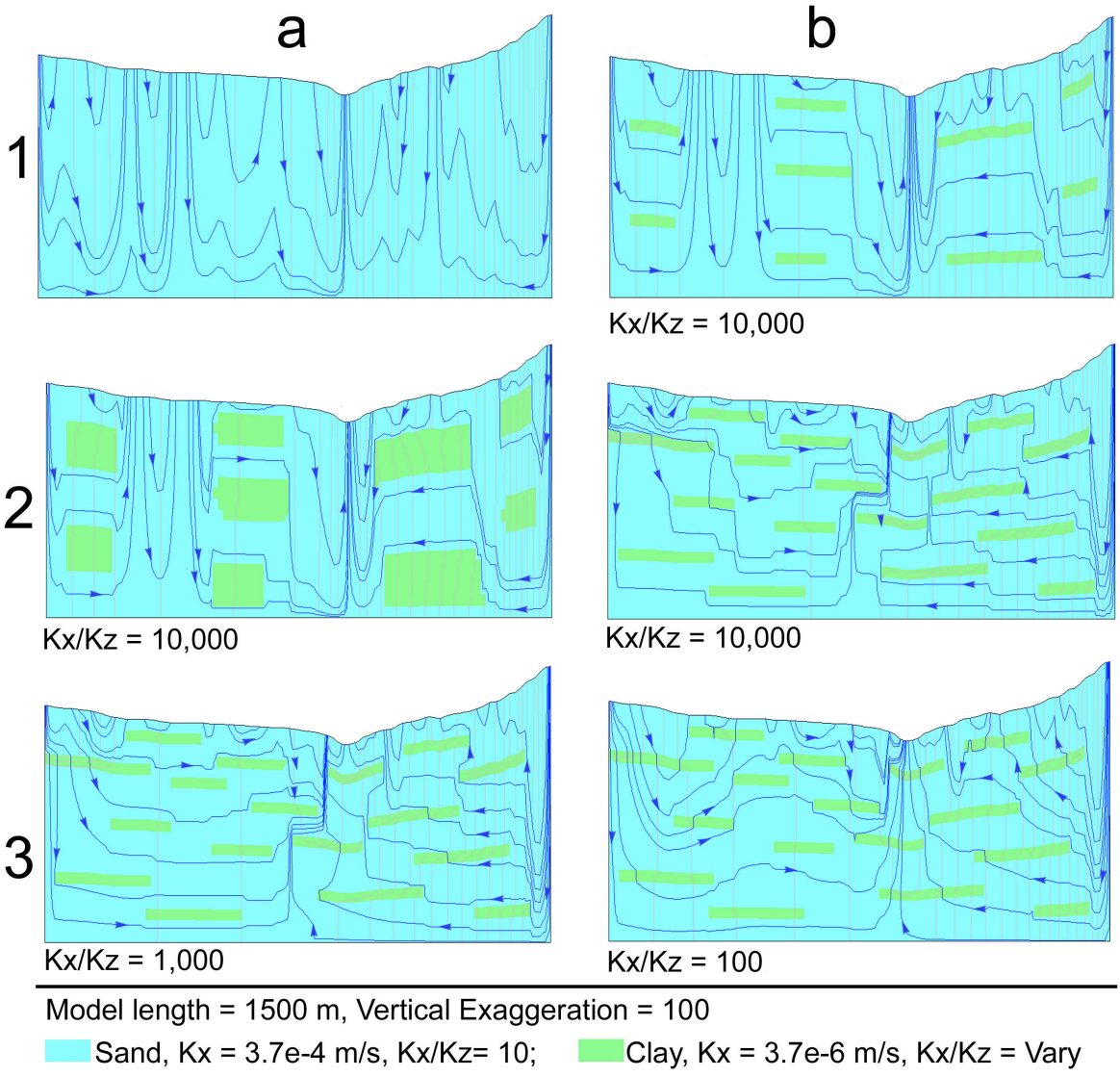

Figure 6-4: Matrix of models shows how dispersed and discontinuous silt-clay layers control groundwater flow-systems. Low anisotropy of silt-clay (3b) can nevertheless result in a hierarchically nested flow-system where the silt-clay architecture is '*stacked-mosaic-continuous*'.

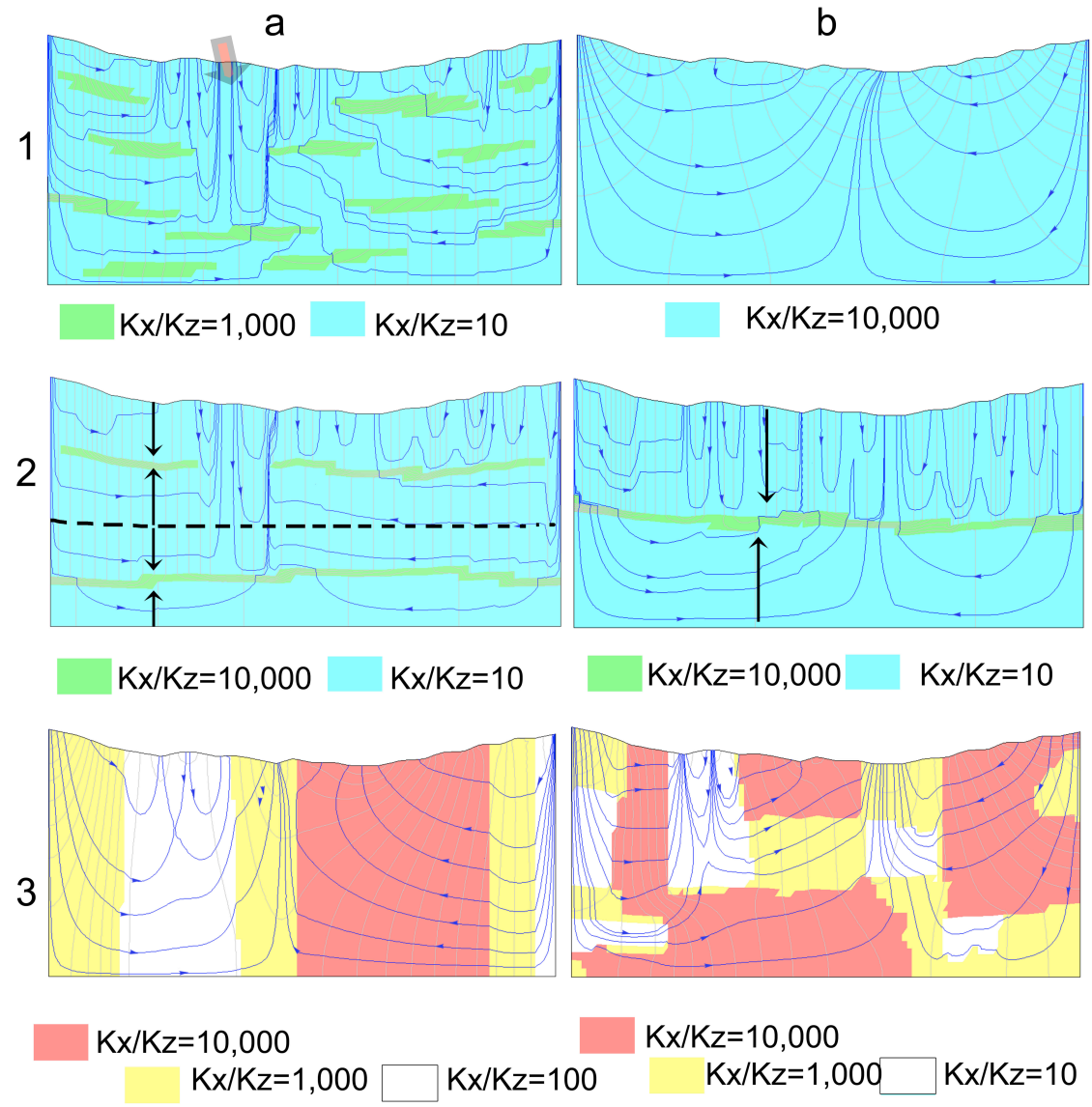

Figure 6-5: Matrix of models indicating different representations of dispersed silt-clay layers. Model '1a' shows the assumed natural distribution of silt-clay layers (indicated by green colour). The effect of these silt-clay layers has been represented in different ways; model '1b' is the single anisotropic aquifer representation. Note the local deeply penetrating flow (arrow in '1a') has not been simulated by the model '1b'. Model '2a' and '2b' are the representations where overlapped silt-clay layers are stacked as indicated by arrows, into a mosaic of thin layers. In model representations '3a' and '3b', the silt-clay layers are represented as effective hydraulic properties into column-slab and block-slab respectively.

6.3 Recharge processes and paleo-recharge

Groundwater recharge in fluvio-deltaic aquifers occurs mainly from rainfall and to some extent from surface water bodies. The recharging water joins the groundwater table, and becomes part of the dynamic flow-system of groundwater. The recharge mechanism for deeper groundwater is not clear but is believed to occur from the shallower part by vertical flow, and through regional flow

originating from highlands within or at the margin of the basin (*K. M. Ahmed, personal communication*).

Aforementioned modelling indicates that groundwater in the deeper part of the basin originates from the basin margin due to the presence of ubiquitous and overlapping (i. e., *stacked-mosaic-continuous)* low permeability materials with hydraulic anisotropy. The shallow flow system operates at shallow depth and remains isolated from the deep flow system. In this case recharge to the deeper level does not come by vertical flow from shallower levels.

In a thick aquifer, groundwater at deeper levels is found to be old i. e., this water was recharged during the geological past. In the Bengal Basin this deep groundwater was recharged around 3 to 7 ka ago, as indicated by radiometric dating (see section 5.3.3.4). At this time recharge to the deeper level is likely to have occurred at the basin margin. Due to the sediment anisotropy (section 4.3.8) multiple flow systems were likely in place, even during times of low rainfall and during the eustatic low stands. Seasonality in rainfall would have led to fluctuation in the water table but sea-level was around ~120 m below the present day level and rainfall was low in the Bengal Basin (*Kutzbach 1981; Goodbred and Kuehl 2000; Sarkar et al. 2009*). The water table may have dropped by tens of metres, but a shallow flow system and a deep flow system are expected to have existed throughout the time of delta formation. Deeper groundwater recharge was likely always, including in the geological past, from the basin margin. Water would only be derived from the overlying ground surface if anisotropic-low-permeability material were absent.

The stable isotopic nature of the shallow groundwater over the Bengal Basin (*Aggarwal et al. 2000; BGS/DPHE 2001; Mukherjee et al. 2007a; Stute et al. 2007; Sengupta et al. 2008*) indicates that shallow groundwater is mostly recharged from rainfall and surface water bodies (rivers, wetlands, flood-waters and ponds). Modelling of stable isotopic imprints of groundwater and surface water from western (West Bengal, India) and eastern (East-central Bangladesh) part of the basin indicate that surface water and groundwater have different ranges of characteristics *(Sengupta et al. 2008)*. The data imply that shallow groundwater in the Bengal Basin is predominantly recharged from rainfall and that the contribution made by other surface water bodies is minor.

Recharge into the shallow groundwater occurs from rainfall. As the monsoon proceeds the topographically lower regions become flooded and the flood-level and groundwater levels should equilibrate rapidly on account of the permeability of the surface sediments. As rainfall recharge occurs on the higher ground, the low lying flooded lands could act as local groundwater discharge zones for water recharged in the relatively higher ground. However, at the beginning of the monsoon rivers respond to the upstream rainfall rapidly and this may lead to indirect groundwater recharge locally in the close-vicinity of the river channel. River recharge water should not be expected to reach regions which are distant from the river due to the ubiquitous presence of silt-

clay layers of the aquifer. The anisotropic silt-clay layers compartmentalise the aquifer into smaller groundwater bodies, which recharge at local highs and discharge to the lows.

6.4 SiHA hypothesis: linking arsenic distribution and the groundwater flow-systems

Scientific research efforts over the past two decades have provided contradictory evidence regarding the sources, mechanisms of mobilization, and spatio-temporal variability of the dissolved As concentration in aquifers. Anaerobic reductive dissolution/desorption of the solid phases of As achieves a wider acceptance as a mechanism of As release (see section 3.7), however the role of geology, and factors controlling the heterogeneities and distribution of As in the aquifer remain unclear (*Nickson et al. 1998; van Geen et al. 2003b; Meharg et al. 2006; McArthur et al. 2008; Polizzotto et al. 2008; Seddique et al. 2008*). Arsenic distribution in the groundwater has rarely been linked with the groundwater flow-system at different depths. The distribution of As in groundwater has been investigated in recent times as a snapshot of a geological time, whereas the pattern of As occurrence in fact represents a redistribution of aqueous arsenic by moving groundwater on geological timescales. In this section an attempt is made to show that the coupled influence of topography and distribution of low permeability materials control groundwater flow, and also the distribution and mobility of dissolved As within the Bengal Aquifer System. It is hypothesised that '**S**ilt-clay layers **i**nfluence **H**ierarchical groundwater flow systems and **A**rsenic progression in aquifer' and named as '**SiHA**' hypothesis.

It is proposed that geological cyclicity due to rapid reworking of the depositional engine coupled with penecontemporaneous groundwater flow in the region has restricted As to the upper part of the aquifer system over geological timescales. The new hypothesis is not contradictory with the results of earlier studies, but explains a wide range of interrelated facts comprehensively (Table 6-1 and see also Figure 6-8).

Table 6-1: Summary of earlier observations, explanations of the As problem and explanation based on the SiHA hypothesis (see also Figure 6-8).

Observations	**Earlier Explanation(s)**	**SiHA Hypothesis**
Shallow groundwater in the south contains higher amount of dissolved As compare to that of northern region of the Bengal basin *(BGS/DPHE 2001)*.	Generally sediments in the south are finer and contain higher amount of organic carbon leading to reduction *(BGS/DPHE 2001; Ravenscroft et al. 2005)* and release of As; In addition low topography, and lower slope of the southern region causes slower flushing (*Ravenscroft et al. 2005; Shamsudduha et al. 2009b*) of As	In the south the deposition of As bearing sediments is relatively recent, and in the delta plain the finer sediments at the surface and the fine aquifer sediments makes flushing of As slower.

Table 6-1: Continued

Observations	Earlier Explanation(s)	SiHA Hypothesis
Deeper (>150 mbgl) part of the aquifer has low to no dissolved As (*Bhattacharya et al. 1997; BGS/DPHE 2001; van Geen et al. 2003b; Ravenscroft et al. 2005*)	Geochemical stability and lack of organic carbon at depth *(McArthur et al. 2004)*, and a higher amount of pyrite which acts as sink for As *(Lowers et al. 2007)*. During sea-level low stand As was flushed away from the deeper parts of the aquifer *(BGS/DPHE 2001; Ravenscroft et al. 2005)*	The maximum depth of As occurrence is limited by the depth of penetration of the shallow flow system. This has been so over geological development of the Bengal Basin. In addition, any deeper flow lines would have crossed an oxidised layer (at some depth) which would have sequestered aqueous As.
Excessive dissolved As is found at depth (>150 mbgl) in some areas of the basin (*Ravenscroft et al. 2009; Burgess et al. 2010*)	Not explained	Due to absence of silt-clay aquitard between shallower and deeper depth, or hydraulic short circuit of the shallow flow-system due to induced pumping. As at depth may also represent as trapped before being flushed, by a silt-clay layer being deposited above the As-bearing zone, and restricting the groundwater flow.
Groundwater in the Pleistocene oxidised inliers do not contain dissolved As (*BGS/DPHE 2001; Ravenscroft et al. 2001; van Geen et al. 2003b*)	Reactivity of the sediments and their adsorptive capacity (*Ravenscroft et al. 2001; McArthur et al. 2004*)	Flushing of As if originally present, because these sediments are >>10,000 years old, and adsorptive capacity leads groundwater remaining As-free even if invaded by a shallow flow-system bearing As.
Low topography and low slope associated with high As (*Ravenscroft et al. 2005; Shamsudduha et al. 2009b*)	Causing slower flushing and hence more As (*Ravenscroft et al. 2005; Shamsudduha et al. 2009b*)	Slow or no flushing; often these acted as discharge zone leading enrichment of As
Young groundwater has less dissolved As compare to relatively old groundwater *(Stute et al. 2007)*	Recently recharge water indicate flushing reduces As *(Stute et al. 2007)*	Flushing with the recharging water
Within the aquifer high As groundwater found to occur above the silt-clay or peat layer, not below (An observation of this study)	Peat or silt-clay increases the reducing capacity of the aquifer environment *(Ravenscroft et al. 2001; McArthur et al. 2004)* hence releasing more As, but does not explaining why the same process is not occurring below the layer.	Groundwater flow operates at shallower level above the silt-clay layers, leading As to be restricted above the silt-clay layer

Table 6-1: Continued to next page

Table 6-1: Continued

Observations	Earlier Explanation(s)	SiHA Hypothesis
Mixing of old and young water at ~30 mbgl has been occurring, and As maxima (bell-shape) is present around that depth (*Harvey et al. 2002b; Klump et al. 2006*)	No explanation but opined to be the cause of As release at that depth due to convection/convergence of flow *(Klump et al. 2006)*	The maximum depth of penetration of the shallow flow system is up to that depth, and below that the deeper, older regional flow occurs. Mixing of them has no effect on the As mobilisation, rather the flow system redistributes As in a way that As is at maximum around the base of the shallow flow system.
Re-infiltrated irrigation water bringing young carbon to depth (*Harvey et al. 2002b*)	Causing reduction of the aquifer, hence releasing As (*Harvey et al. 2002b*)	Shallow groundwater throughout the basin contains young carbon as this groundwater is recently recharged. These may promote the aquifer reducing condition.
Two nearby wells yielding water from the same depth contain As-free and high As-water *(Burgess et al. 2002; McArthur et al. 2004)*	The As source is depth specific and discontinuous *(Burgess et al. 2002)*	This is associated with the juxtaposed position of the well-flushed and ill-flushed zone of aquifer, due to position of the silt-clay layer.
Area covered by surface silt-clays reported to contain high As while aquifer zone overlain by sands has low As (*Aziz et al. 2008; Weinman et al. 2008; Hoque et al. 2009*).	Ease of surficial sand to be flushed by recharging water (*Aziz et al. 2008; Weinman et al. 2008; Hoque et al. 2009*)	Differential flushing; in the discharge zone, where wetland sediments are located, silt-clays reduce the flushing
Rise of As concentrations over decadal scale (*Ravenscroft et al. 2005; Burgess et al. 2007*)	Explained as delay in As transport from source zone within individual tube-well catchments *(Burgess et al. 2002)*.	This model says As concentration is variable ranging from decade to centuries, depending on the position of the silt-clay layer. In addition, As concentration in low-As-well will reduce over time, if the natural system is not interrupted
In sediments As is found to be associated with pyrite *(Lowers et al. 2007)*	Not explain but opined to be authigenic *(Lowers et al. 2007)*	This is sedimentological, and the higher the vertical rate of sedimentation the more authegenic pyrite there would be.

6.4.1 Arsenic release, mobilisation, and cyclicity

Excessive dissolved arsenic (As) in unconsolidated fluvio-deltaic aquifers in Asia is believed to be desorbed through reductive dissolution of Fe(III) (hydr)oxides of the aquifer sediments (Figure 3-23); one group has suggested that sediments within the aquifer contain the As (*Nickson et al. 1998; BGS/DPHE 2001; McArthur et al. 2001; Harvey et al. 2002b; Anawar et al. 2003; Ahmed et al. 2004; Meharg et al. 2006; Seddique et al. 2008*) whereas another proposed near-surface sediments as the source (*Swartz et al. 2004; Polizzotto et al. 2005; 2006; Kocar et al. 2008; Polizzotto et al. 2008*). Irrigation-induced groundwater flow and recharge is proposed as a means

to fuel the reductive capacity of the aquifer through the delivery of young carbon (*Harvey et al. 2002b; Neumann et al. 2010*); sedimentary organic matter is proposed by others (McArthur et al. 2004). Mixing of young and old water *(Klump et al. 2006)* at ~30 m depth, and recharge-facilitated flushing, has been proposed to lower As concentration in the upper part of the aquifer (*Stute et al. 2007; Hoque et al. 2009*). Very rarely has the As problem been seen in the light of groundwater flow on the regional to local scale, although fluvio-deltaic terrains generally support a very dynamic, hierarchically nested groundwater flow system *(Tóth 1995; Zijl 1999)*. Polizzotto *et al (2008)* reported a substantial hydrological role, coupled with geochemical processes, to control As in Asian groundwater at a small scale. A unified process is yet to be revealed that links the sources, mobility, spatio-vertical-temporal dimensions, and geological cyclicity of this substance in groundwater system, at a scale <1m to basin scale.

In the preceding sections the conceptual understanding of the groundwater flow-systems has been made with simple 2D vertical-section model analyses. The distribution of As within the aquifer can be linked to hierarchical groundwater flow system.

Polizzotto et al *(2005; 2006; 2008)* have asserted that As enters solution mostly from solid mineralogical phases of near surface sediments close to the water table, while others believe this to be happening within the aquifer (*Nickson et al. 1998; BGS/DPHE 2001; McArthur et al. 2001; Harvey et al. 2002b; Anawar et al. 2003; Ahmed et al. 2004; Meharg et al. 2006; Seddique et al. 2008*). Current work suggests that As adsorbed to the less stable Fe(III) (hydr)oxide should not be stable under anaerobic aquifer conditions, and should be dissolved simultaneously close to the water table under reducing conditions, freeing Fe and As into solution. Groundwater flow systems operate as conveyor belts which effectively serve as the mechanism for mobilization, and redistribution of ions, energy, heats etc in the aquifer *(Tóth 1999)*. However, free ions (Fe, As etc.) might undergo geochemical changes and be subject to a number of solid / liquid equilibrium. All dissolved ions in groundwater eventually reach the discharge zone. Immobilisation and concentration of As at the discharge zone redox interface may be happening through formation of metastable pyrite *(Wilkin and Barnes 1997),* which is later able to undergo oxidative breakdown (in favourable situations of geological reworking) to form FeOOH-As. In the discharge zones at the redox interface under oxidising conditions, As may also be sequestered to pre-existing or concomitantly formed Fe(III) *(Datta et al. 2009)* (Figure 6-6).

Recharge and discharge of shallow groundwater facilitate As accumulation at the redox boundary throughout basin. The widespread occurrence of accumulated arsenic and iron close to the surface (within 2-3 mbgl) *(Zahid et al. 2009)* may result from shallow groundwater discharge. The conceptual recharge mechanism explained in the preceding section can be related to delta-wide As accumulation at the redox boundary. Because of seasonal flooding and wide-spread rainfall almost the entire delta surface works as an alternating groundwater discharge and recharge zone depending on the condition of flooding. Groundwater discharge naturally occurs at

the flooded-bed near the flood-water and soil interface *(Trefry et al. 2007)*. This interface fluctuates according to the flood depth. As the position of the redox boundary fluctuates, the sequestration front of As and other redox sensitive species also moves. During flooding, under reducing conditions, solid-phase As is desorbed *(Roberts et al. 2010)*, but only penetrates the aquifer when recharge prevails. In contrast, relatively elevated areas rarely undergo flooding and act as persistent zones of recharge. Shallow groundwater in these regions would have low solute content (and low As content) due to the oxygenated condition and hence provide less As to the aquifer flow system. Due to episodic deltaic development over a 100 to 1000 yr time-scale recharging and discharging conditions alternate with topographic inversion and/or channel avulsion or migration. A newly activated recharge zone with higher As content at the interface could temporarily contribute As and other solutes to the aquifer flow system through reductive dissolution when the geochemical condition become reducing.

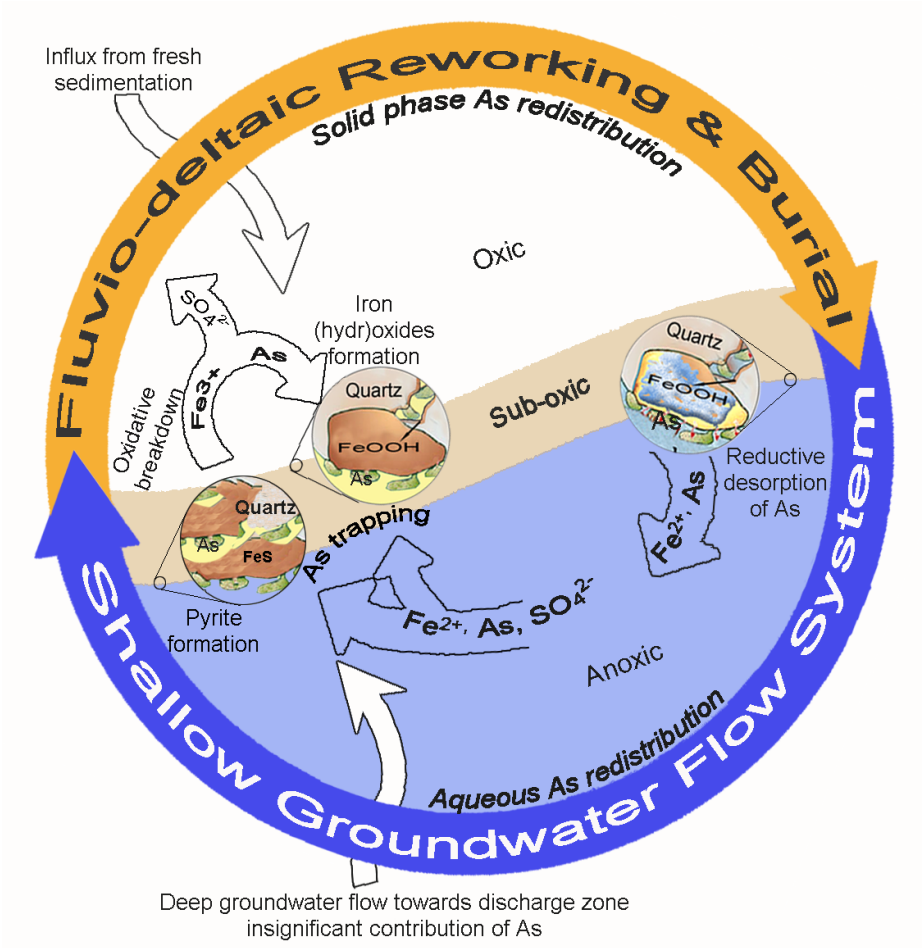

Figure 6-6: Geological cyclicity of As in reducing fluvio-deltaic aquifer system. This shows how As is released to groundwater in the shallow sub-surface at the recharge areas, under reducing aquifer conditions. The As is conveyed in solution in the groundwater flow field. In the regions of groundwater discharge dissolved As is sequestered in meta-stable pyrite or on the Fe(III)oxides depending on the redox condition. These mineral phases along with sediments are later reworked and redeposited, and under suitable conditions As may be released again into the groundwater flow-field. The occurrence of As in the aquifer largely reflects the redistribution of As by groundwater flow. Anisotropic silt-clay layers restrict dissolved As to the shallow groundwater flow field.

Arsenic accumulation and land surface inversion can be linked with the sequence development during Holocene time, and particularly with the high-stand system tract, during periods of slackening sea-level rise. In the shoreline and shelf strata this interval is bounded at its base by a maximum flooding surface, normally a clay-rich silt, and at its top by a sequence boundary *(*e. g., *Catuneanu et al. 2009)*. Early high-stand fluvial deposits may be indistinguishable from the facies of the late transgressive system tract. During the late high-stand, reductions in flood basin accommodation space may result in an increased lateral, rather than vertical, accretion and the formation of laterally-interconnected and amalgamating channel and meander belt systems with poorly preserved flood-plain deposits *(Shanley and McCabe 1993)*. This lateral accretion phase is most likely associated with the release of As in groundwater in the deltaic environment. This lateral accretion would have had two folds geochemical role: (1) solid-phase geochemical breakdown and formation of less stable FeOOH (with As) because of geological reworking, (2) organic matters may have had leached to the water-table from the organic-rich-sediments deposited across the floodplains.

Trapping of As in the discharge zone may explain why organic-rich, fine-grained materials in the aquifer sediments contain more pyrite and As *(Lowers et al. 2007)*, as these organic-rich fine materials are expected in the syn-depositional topographic depressions i. e., at groundwater discharge zones. In addition, detrital grains with sorbed As may be deposited in this environment. Rapid burial allows FeS-As minerals to stay in the solid phase as they quickly enter the reduced zone. This may be the reason for a higher content of FeS-As in the deeper sediments of Bangladesh *(Lowers et al. 2007),* which were deposited in transgressive settings during earlier eustatic cycles of Quaternary time (section 3.3.2.1).

The Fe(III) hydroxides are susceptible to reductive dissolution if not transformed into a more crystalline state with areal exposure and with time. During the reductive dissolution of Fe(III), biogenic magnetite may be produced though mediation by magnotobacteria *(Karlin et al. 1987)*. Occurrences of magnetitite at shallow depth have been reported by earlier investigators *(Horneman et al. 2004; Swartz et al. 2004)*. Erosion, reworking and redeposition of surficial sediments enrich the less stable Fe(III) (hydr)oxide in As and hence facilitate the potential for release of As from the newly formed settings. But if the geological situation favours neoformation of more crystalline Fe(III) oxide through long-time aerobic exposure, As will become sequestered in a more stable form of iron oxides. This is the case in the Pleistocene oxidised aquifers (*McArthur et al. 2001; van Geen et al. 2003b*) and in the piedmont alluvial sediments *(BGS/DPHE 2001)*.

This geological cyclicity affecting As has operated for the whole duration of fluvio-deltaic activities. On account of the penecontemporaneous groundwater flow-system operating at shallow depths, As remains in the top part of the aquifer in the long-term. However, a small component of dissolved As will be released to the surface water system and ultimately to sea via groundwater

discharge. In the case of older i. e., pre-Quaternary deltas and deltaic sediments, arsenic is not present in groundwater because these have had sufficient time to flush all of the dissolved arsenic from their system. In the case of the Bengal delta, which has been developing over the whole Quaternary Period, input of As has possibly stopped or decreased in most parts of the basin but groundwater flushing is ongoing and additional time will be required to complete the flushing of the As from the groundwater system.

6.4.2 Flow-system and distribution of arsenic in aquifer

Groundwater flow, reworking and redeposition of the sediments may have played a vital role in As cyclicity in the aquifer. This is why in some areas, As is flushed away whereas others contain As. On a basin scale, in the northwest of the Bengal Basin, aquifers contain insignificant level of aqueous As while in the south As concentration reaches up to several hundreds of µg/l. In a recent study *(Winkel et al. 2008)* this high As related to the deltaic deposits across the Asian deltas. The deltaic deposits can be seen as deposits of repeated reworking. This process of deposition facilitates formation of less stable Fe(III) (hydr)oxide leading to increased As in the aqueous pool through reduction. In the Bengal Basin, prolonged and comparatively younger deltaic processes *(Allison et al. 2003)* are found to occur in the high arsenic region (Figure 6-7), indicating the link between As release and deltaic processes. In contrast, in coastal areas, low As concentration in groundwater may be due to the abundance of marine sulphur sources which facilitate As sequestration *(Lowers et al. 2007; Shamsudduha and Uddin 2007)*, and also to higher rates of burial.

Vertical distribution of As in the aquifer is believed to be limited in the Holocene sediments *(BGS/DPHE 2001; Harvey et al. 2002b; van Geen et al. 2003b; Horneman et al. 2004; McArthur et al. 2004; Polizzotto et al. 2005; Zheng et al. 2005; Harvey et al. 2006; Klump et al. 2006; Polizzotto et al. 2006; Polizzotto et al. 2008),* and the model proposed here explains this as the vertical limit of the shallow flow system. However, if the shallow groundwater flow system passes through an oxic sediment layer, As would be sequestered at the interface, and this is why oxic aquifer zones in the Bengal Basin are safe in terms of As at whatever depth they occur. A higher concentration of As at the redox interface has been reported at a study site in the eastern part of Bangladesh *(Breit et al. 2004)*. In some parts of the country (particularly in the western region) As is found to occur at greater depths than 100 m, and this may be related to the absence of a silt-clay layer, i. e., possibly due to large gap in the overlapping silt-clay layers. However, mildly elevated As may also occur at greater depth below a silt-clay cover in other parts (see section 6.4.5). This may have been cut-off from the active (shallow) flow-system due to deposition of a silt-clay layer before complete flushing of As occurred. In the majority of Bangladesh, the available drillers' logs show a stacking of silt-clay layers at depths <150 m, and their mosaic forms an effectively continuous layer (section 4.3.8 and Figure 4-17), which restricts the shallow flow-system to above the depth of the silt-clay layers.

The northwest part of the country is a regionally extensive alluvial fan which has no As except at the local scale, where flood basins are present and As is present locally in shallow groundwater. This is likely to occur as a result of the cyclicity of As through groundwater flow and redeposition. This reworking, remodification and reprecipitation may also be happening in other enclosed hilly areas, like Nepal (*van Geen et al. 2008a; Pokhrel et al. 2009*), Tripura of India *(Chakraborti et al. 2008)*, and upstream valley areas of the Ganges and Brahmaputra *(Ravenscroft et al. 2009)*. However, regionally in these types of geological terrain (alluvial fan, piedmont and high-gradient upstream regions) reworked sediments are transported out of the region and redeposition does not occur. This means that the contribution of As to the aqueous pool is limited or has ceased in these areas, and flushing of aqueous As is acting to remove As on a geological time scale.

In the delta region, a shallow flow system associated with micro to local topographic differences may be active during the drier part of the year, mostly in the wetland areas, and hence may actively be redistributing As in the very upper part of the aquifer. During the wet season, due to flooding or an elevated water table, reductive dissolution of the solid phase As may be induced. Seasonal peaks in As concentration at shallow depth have been reported from a similar deltaic setting in Cambodia *(Polizzotto et al. 2008)*. Shallow As release may not significantly contribute to the main aquifer as shallow groundwater flow is mostly to the local wetlands, which are discharge areas for the local flow system. However, some wetlands do act as recharge ponds during the early part of the monsoon and may therefore contribute As to the aquifer at a very local scale due to the compartmentalisation of the aquifer induced by the silt-clay layering.

In Bangladesh the profile of groundwater As concentration has been found to peak between depths of 28 and 45 mbgl in the Holocene aquifer (*Harvey et al. 2002b; Horneman et al. 2004; Klump et al. 2006*), and close observation of the data reveals that the peak is just above a clay layer or below a surface clay layer in each case (see section 6.4.4). Moreover, Klump et al *(2006)* reported a contrast in groundwater age i. e., juxtaposition of young and old water, close to the depth of the As peak, but without explanation. By the proposed conceptual model, a shallow groundwater system operates at the shallow level (~30 m), where it may be restricted above a silt-clay layer, below which deeper groundwater flows with longer flowpaths, leading to this juxtaposition of young and old water. The comparatively young flow system controls the arsenic distribution here as it does in other parts of the basin. Around the aforementioned depth fine sediments occur throughout the delta which may be associated with the Holocene high-stand *(Goodbred and Kuehl 1999)*. This silt-clay rich zone often forms the base of the shallow locally derived flow system, and hence determines the maximum penetration of dissolved As, and shallow groundwater is then directed to the discharge zone.

Some studies (*Aziz et al. 2008; Weinman et al. 2008; Hoque et al. 2009*) indicate that beneath surface sandy layers there are lower groundwater As concentration than below surficial clays.

This distribution can be explained where sandy higher ground acts as a recharge area, while clays occur in depressions which act as groundwater discharge zones. Over the past several ~100 years, due to lack of reworking under the conditions of a stable or prograding delta As is flushed and redistributed in such a way that the recharge areas have low As and the discharge areas have elevated As. Above the silt-clay layers As is at higher concentration due to the focussing of shallow groundwater flow. In general at a recharge zone one would expect low Fe, high Eh, high DO, and low As and there would reverse as the flow progresses to the discharge zone (*Tóth 1999*). This general distribution is overprinted by the distribution of silt-clay layers. These low permeability materials render the sediments anisotropic and compartmentalise the groundwater flow system in the aquifer.

6.4.3 Representative simulation of spatio-vertical As distribution

Arsenic has cycled between solution and the solid mineral phases in the sediments throughout the geological evolution of the area. The distribution of As currently seen in the aquifer is in fact partially redistributed, representing a snap-shot of geological time. A simple 2D model was created using MODFLOW-2000 *(Harbaugh et al. 2000)* and MT3DMS *(Zheng and Wang 1999)* to understand how this redistribution occurs over geological time (Figure 6-8). The modelling considers only advective transport. An initial concentration of As is assumed in the upper part of the aquifer and no new release is considered. The model demonstrates how As is redistributed with the flowing water. Elevated As concentrations develop in the discharge zone, and lower As concentrations in the recharge zone. If the penetration depth of the flow system is limited by a silt-clay layer, elevated As is found just above the silt-clay layer, due to the lower groundwater flow rate leading to slower flushing in those depths. This simple modelling explains the bell shape distribution of As commonly observed in groundwater depth profiles. Also it is seen that As is retained in the shallower part of the aquifer due to the flow-system being limited to at this depth.

A simple zone budget analysis *(Harbaugh 1990)* indicates that aquifer sediments bounded by silt-clay layers are flushed more slowly (Figure 6-8c). The use of zone budget analysis therefore illustrates the implications of lower flushing rates in areas bounded or covered by silt-clay layers (Figure 6-9). This demonstrates how differential rates of flushing can result in the observed spatial distribution of As in the aquifer.

6.4.4 Field evidence in support of the hypothesis

6.4.4.1 Vertical profiles of groundwater arsenic

Vertical profiles of groundwater As have been described at many sites of investigation (*Harvey et al. 2002b; Dhar et al. 2008; Itai et al. 2008; Liβner 2008; McArthur et al. 2008*) and at a national level (*DPHE/BGS/MML 1999; BGS/DPHE 2001*). The national level survey data show that wells >150 m in depth generally have low As content while shallow wells have a variable range of As

concentration. The spatial variability is highest at the shallower level, and a generalisation would be that the concentrations form a bell-shape distribution with a maximum As concentration around 20 to 45 mbgl. The maximum point of this distribution of arsenic was reported to vary from region to region *(*e. g., *Harvey et al. 2006)*.

A few of the site-specific vertical As profiles and the corresponding lithological profiles have been compiled (Figure 6-10 to 6-14). These demonstrate a strong linkage between the position of the silt-clay layer, and high groundwater As concentrations. In every case an As maximum occurs above the silt-clay layer. The present hypothesis considers that this distribution can be explained by the patterns of groundwater flow, but this could not be proven by modelling because of the lack of spatial data on the silt-clay layers. The vertical As profile does not always conform to a bell-shape, but may be spiky if a number of silt-clay intercalations occur (Figure 6-14 (c)).

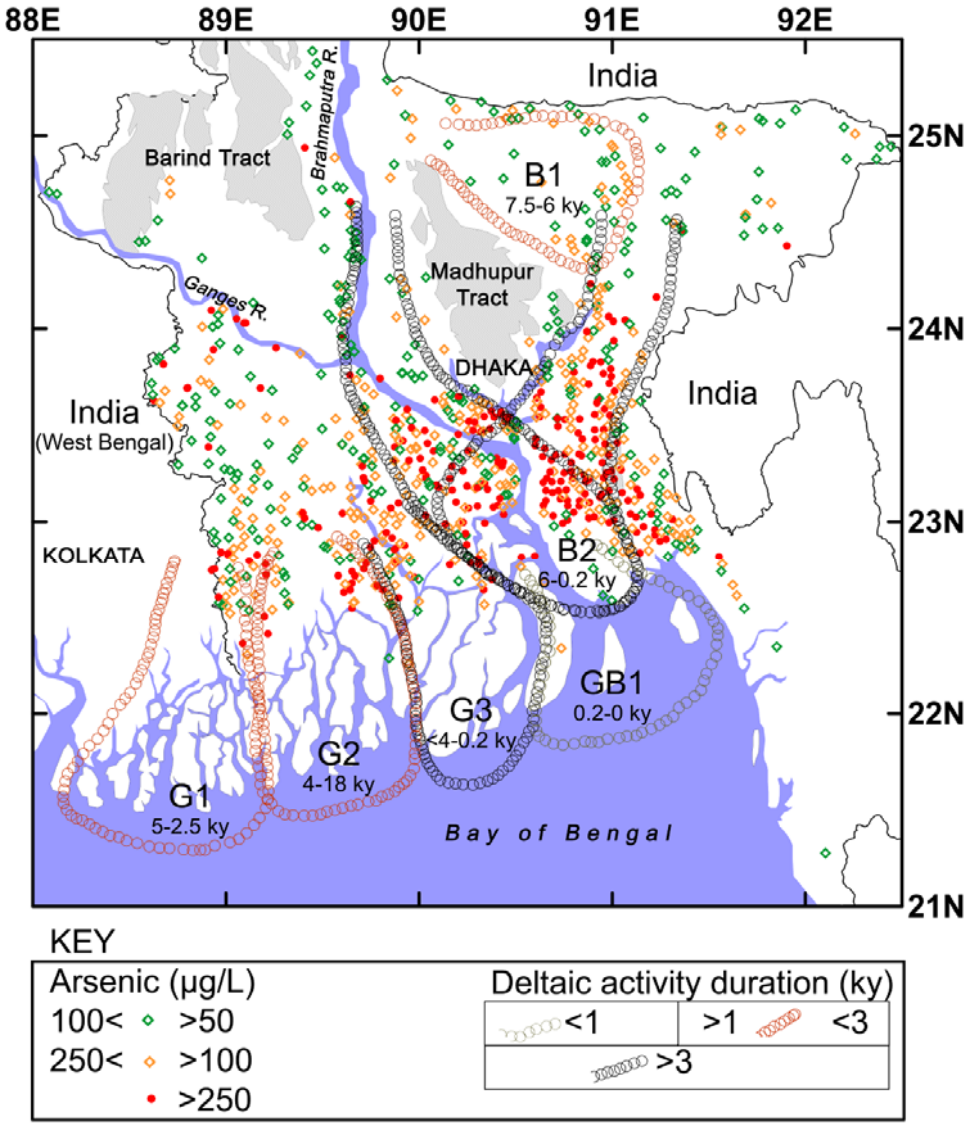

Figure 6-7: Groundwater dissolved As hot spots and deltaic activity lobes in southern Bangladesh. Deltaic lobes were taken from Allison et al. *(2003)* and As data by BGS/DPHE *(2001)* were used. Map demonstrates that high As areas are where prolonged deltaic activity took place

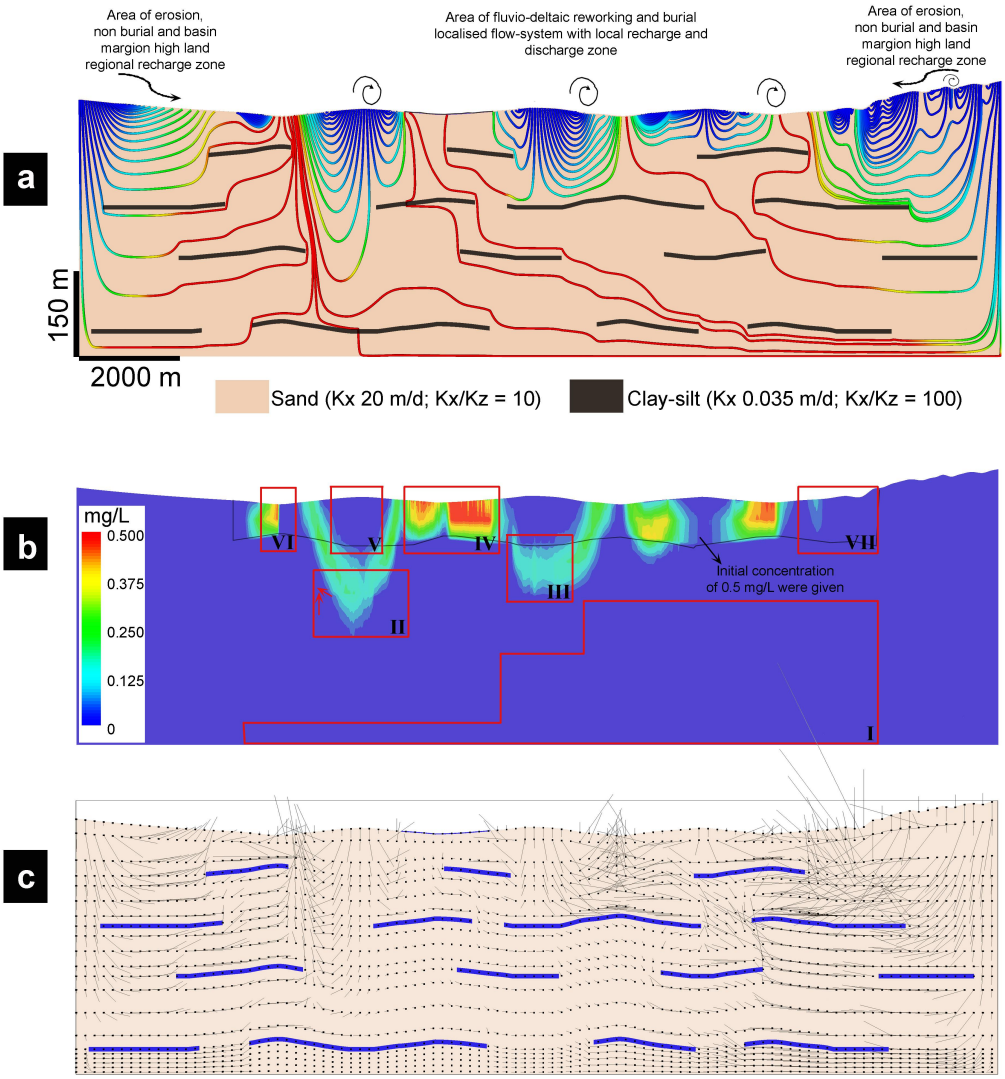

Figure 6-8: Groundwater flow and redistribution of aqueous As on geological time scale. (a) Geological framework of the 2D model which was developed using the MODFLOW code with no-flow along all three sides except the top boundary where a fixed head is set at the level of the topography to replicate recharge. Blue (young) to red (old) colours indicate groundwater flow lines from recharge to discharge zone. Major geological and hydrological processes are indicated. (b) Arsenic concentration of 0.5 mg/l from the top layer as redistributed by groundwater flow simulated using MT3DMS for advective transport over 5000 years. This illustrates how As is restricted to the shallower part of the aquifer keeping deeper levels As-free [I]; higher penetration of shallow flow can penetrate deeper where a silt-clay layer is absent [II]; arsenic is found to be restricted above the silt-clay layer [III] due to flow deviation by the silt-clay layer, but surface silt-clay layers slow the rate of flushing and hence maintain higher concentration in those areas [IV]; flushing reduces the concentration in the zone of local recharge [v]; but the position of the sub-surface clay layer is found to juxtapose contrasting As concentrations [VI]; under higher topographic gradients As is flushed relatively faster [VII]. The double arrow in box II indicates a location where 'regional' old water comes close to 'shallow' young water, not previously explained. (c) A vector plot, the length of the line is proportional to the vector magnitude of groundwater flow, illustrating the aquifer compartmentalisation induced by the distribution of silt-clay layers.

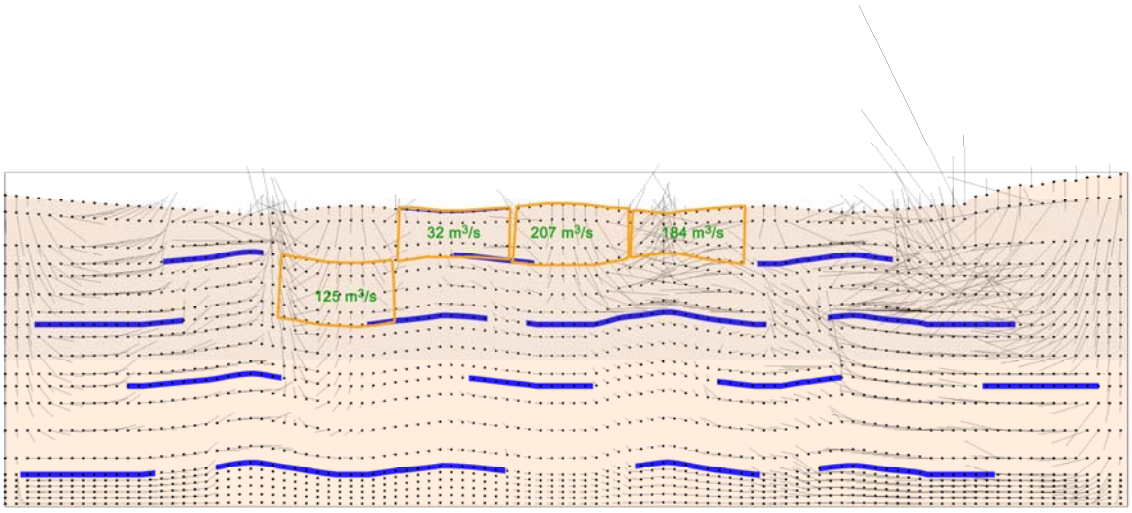

Figure 6-9: Volumetric flushing rate in different regions of the aquifer indicating the differential rate.

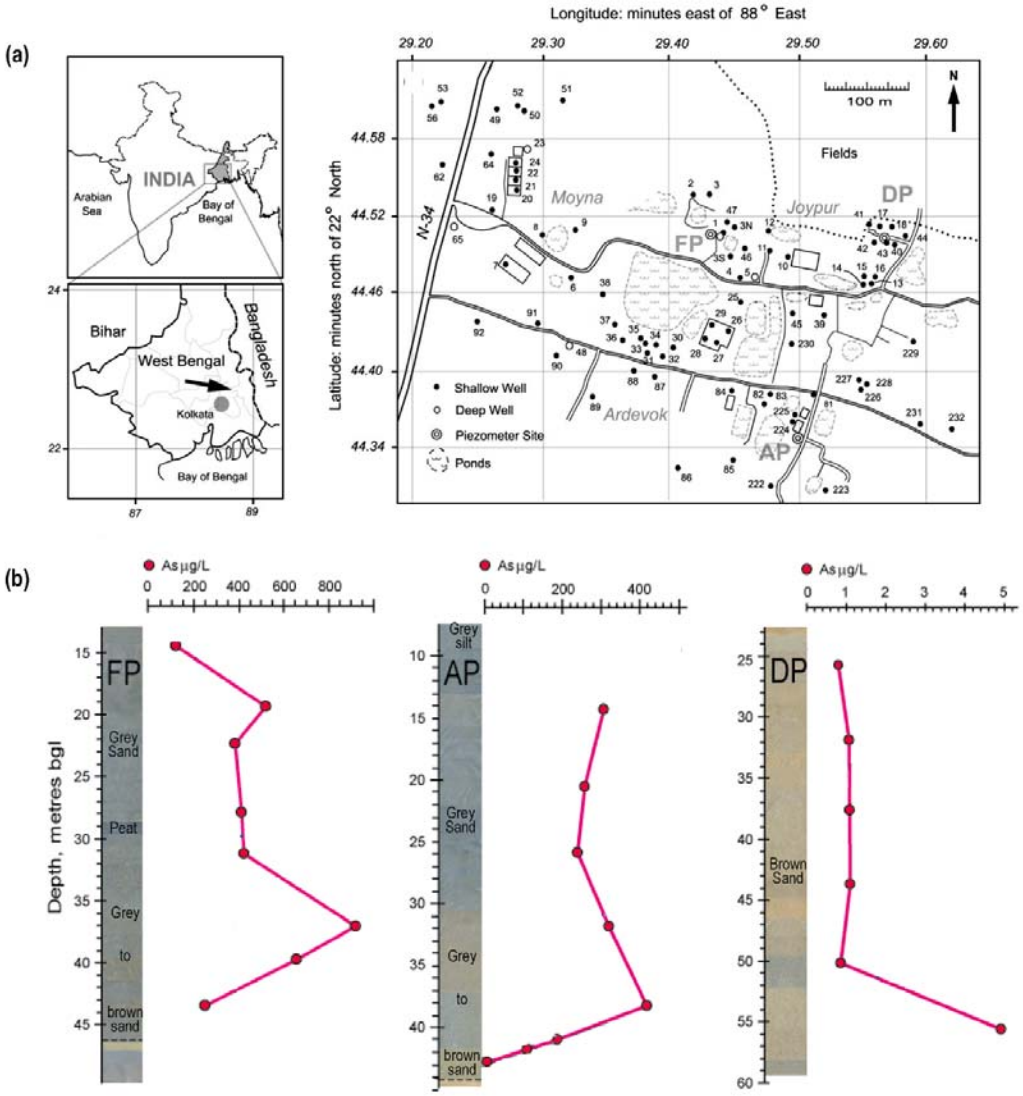

Figure 6-10: Vertical profile of groundwater arsenic from closely-spaced nests wells at Barasat from West Bengal, India *(McArthur et al. 2008)*. (a) Location of 3 nests wells, location map adapted from McArthur et al. *(2004)*. (b) Profiles of groundwater arsenic concentration.

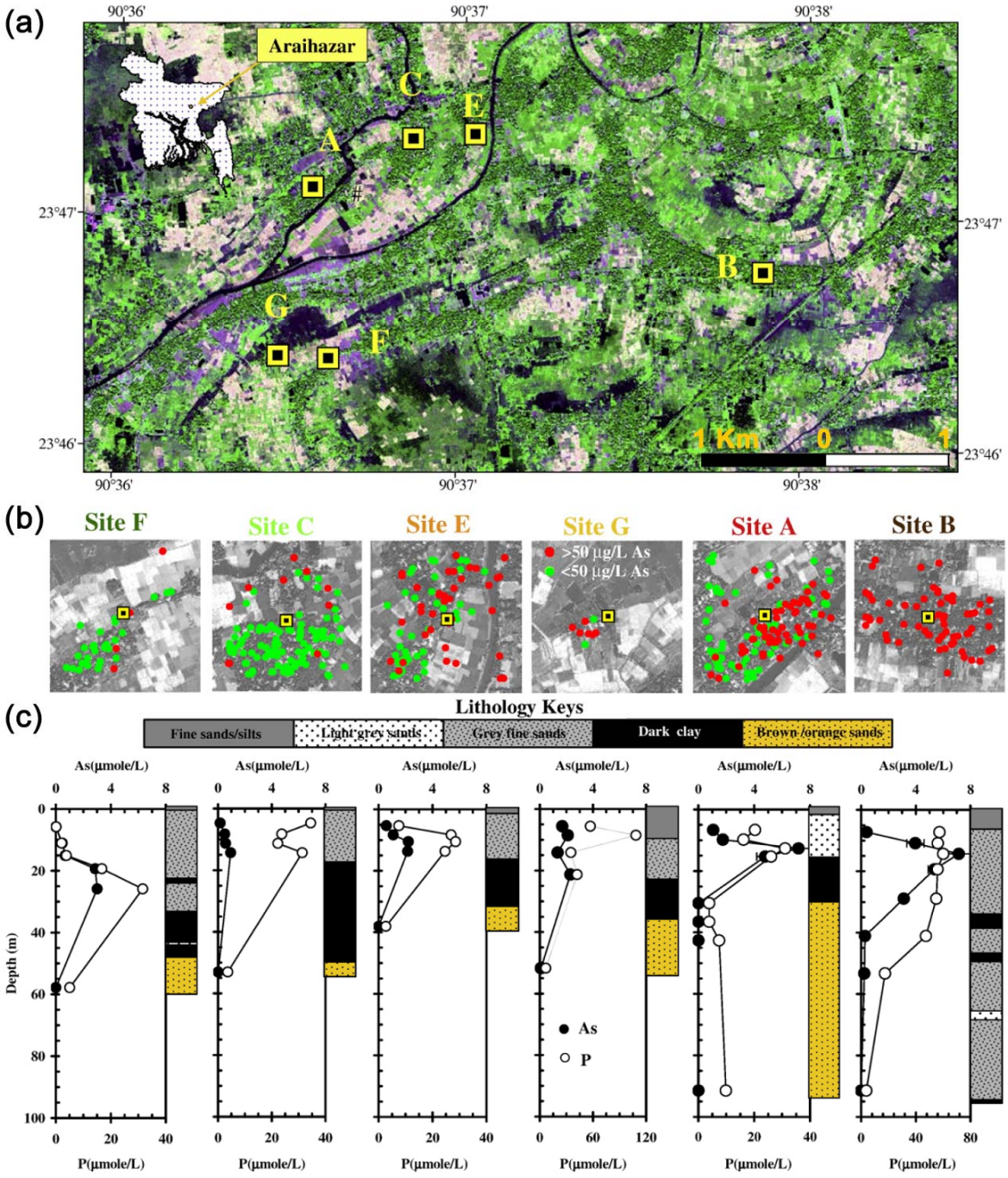

Figure 6-11: Vertical profile of groundwater arsenic from closely spaced nests wells over a 25 km^2 area at Araihazar in central Bangladesh *(Dhar et al. 2008)*. (a) Locations of six nests of wells were plotted on an IKONOS image of Araihazar study area in central part of Bangladesh (inset). (b) The 400 m × 400 m squares represent an enlarged view of the spatial distribution of As in existing wells surrounding the 6 well nests. Green and red solid circles indicate the As level <50 µg/L, and ≥50 µg/L, respectively. Sites F, C, E, G, A, and B are arranged from left to right and colour coded with increasing average As concentration in the surrounding wells. (c) The depth profiles of average groundwater As and P concentration for all sites. The scales for P concentration were different for Sites G and B.

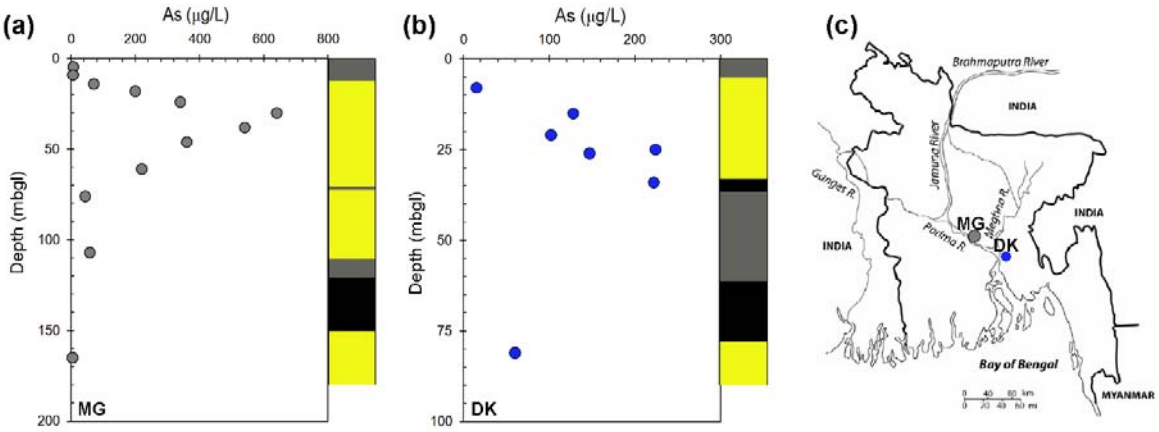

Figure 6-12: Vertical profile of groundwater arsenic from closely spaced nests wells from Munshiganj (MG) and Daudkandi (DK) at south central Bangladesh. (a) MG indicates the site investigated by many researchers (e. g., *Harvey et al. 2002b; Swartz et al. 2004; Klump et al. 2006; Polizzotto et al. 2006; Neumann et al. 2010*), Arsenic and lithological data used here to reconstruct the profile are from Swartz et al. *(2004)*. Grey and black indicate silt and clay respectively, while yellow is sand. (b) DK site data from Liβner *(2008)*, lithological symbols are same of 'b'. (c) Location of the sites in Bangladesh.

The As concentrations, and the distribution of silt-clay layers are very heterogeneous at depth. It is reported that nearby wells may have significantly different As concentration (*Burgess et al. 2002; Harvey et al. 2002a; Horneman et al. 2004; McArthur et al. 2004*). But in all these studies, construction of the vertical profile of As concentration is from measurements made at a number of piezometers in close vicinity. There must be uncertainty as to whether these profiles are truely representative of the vertical arsenic distribution, as the distribution of silt-clay layers may varies at a spatial scale smaller than the scatter of measurement points.

6.4.4.2 Spatio-vertical transects of groundwater arsenic distribution

Two recent studies (*van Geen et al. 2006b; Metral et al. 2008*) determined vertical profiles of As concentration along transects in the western (Chakdaha, West Bengal) and eastern (Araihazar, Bangladesh) parts of the basin. The spatial resolution was >5 per km, and >1 per 2.5 m in the vertical. These are the most high resolution determinations of the spatio-vertical heterogeneity of As along transects in the Bengal Basin. Consideration of the observations with the lithological layering reveals the relationship between As concentration in groundwater and the silt-clay layer distribution (Figure 6-13 and Figure 6-14). It is seen that high As concentrations occur above silt-clay layers and decrease upward if the ground surface is sandy, but remain constant if the surface is itself silt-clay rich (Figure 6-13). In contrast, if silt-clay intercalations segment the aquifer, high As concentration are found at depth in the region bounded by silt-clay layers (Figure 6-14). It should be mentioned that groundwater flow is a function of topography and the distribution of silt-clay layers, which impose anisotropy in three dimensions (section 6.2). So a single phrase 'differential flushing' may be appropriate to explain the spatio-vertical variability of groundwater As concentration in the aquifer.

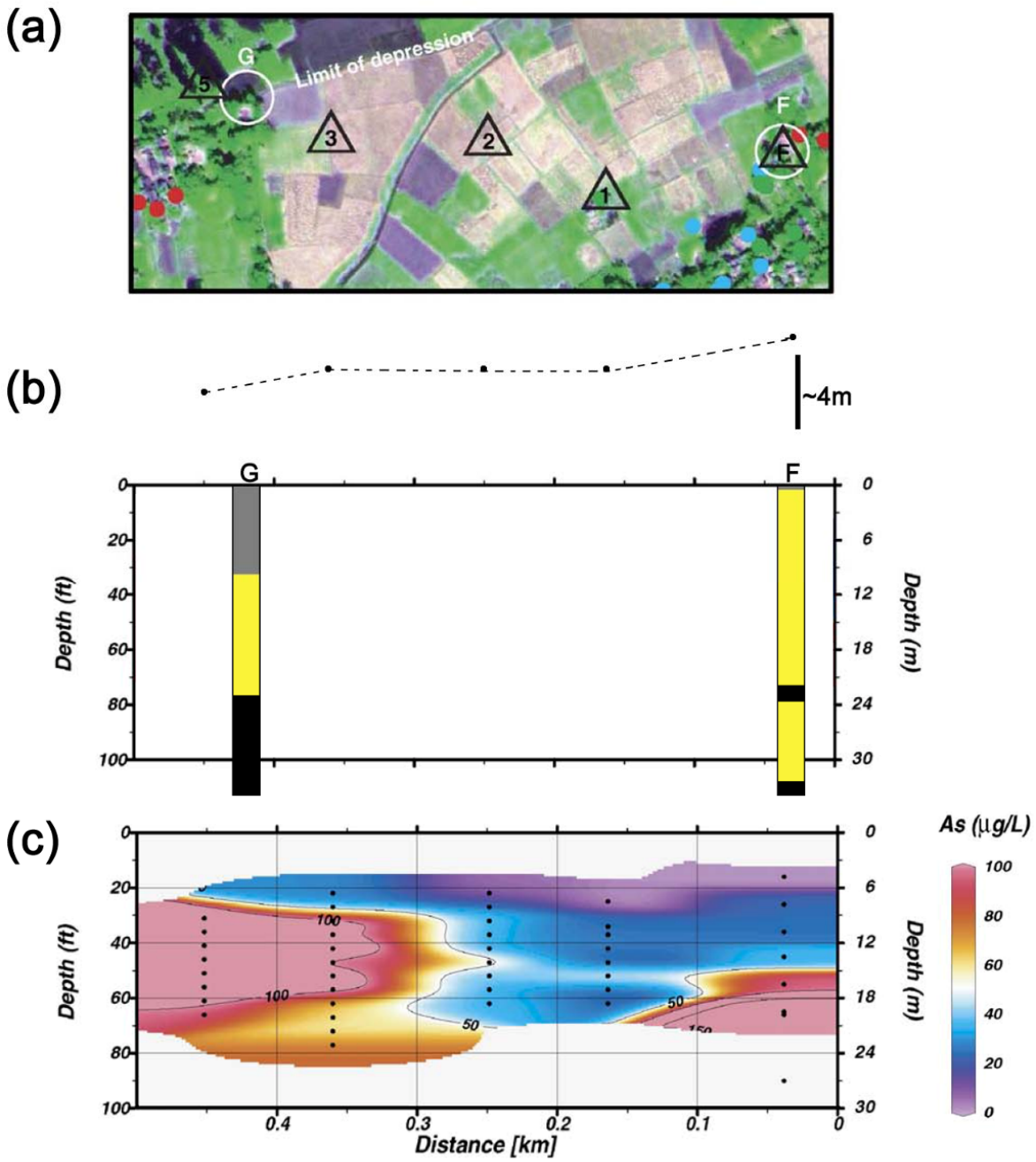

Figure 6-13: Spatial variation of groundwater arsenic concentration along a ~ 500 m transect at Araihazar in central Bangladesh (*van Geen et al. 2006b*). (a) Location of the sites where high resolution vertical groundwater sampling were carried out. Note that sites G and H are indicated as of figure 6-11. (b) Relative elevation as extracted from the global Digital Elevation Model *(EROS 2002)*. Lithological information at the specific sampling sites are not available, but lithologs (symbols as of figure 6-12) at site G and F are shown as of Dhar et al. *(2008)*. (c) Groundwater As concentration, contoured (after *van Geen et al. 2006b*), dots represent sampling points.

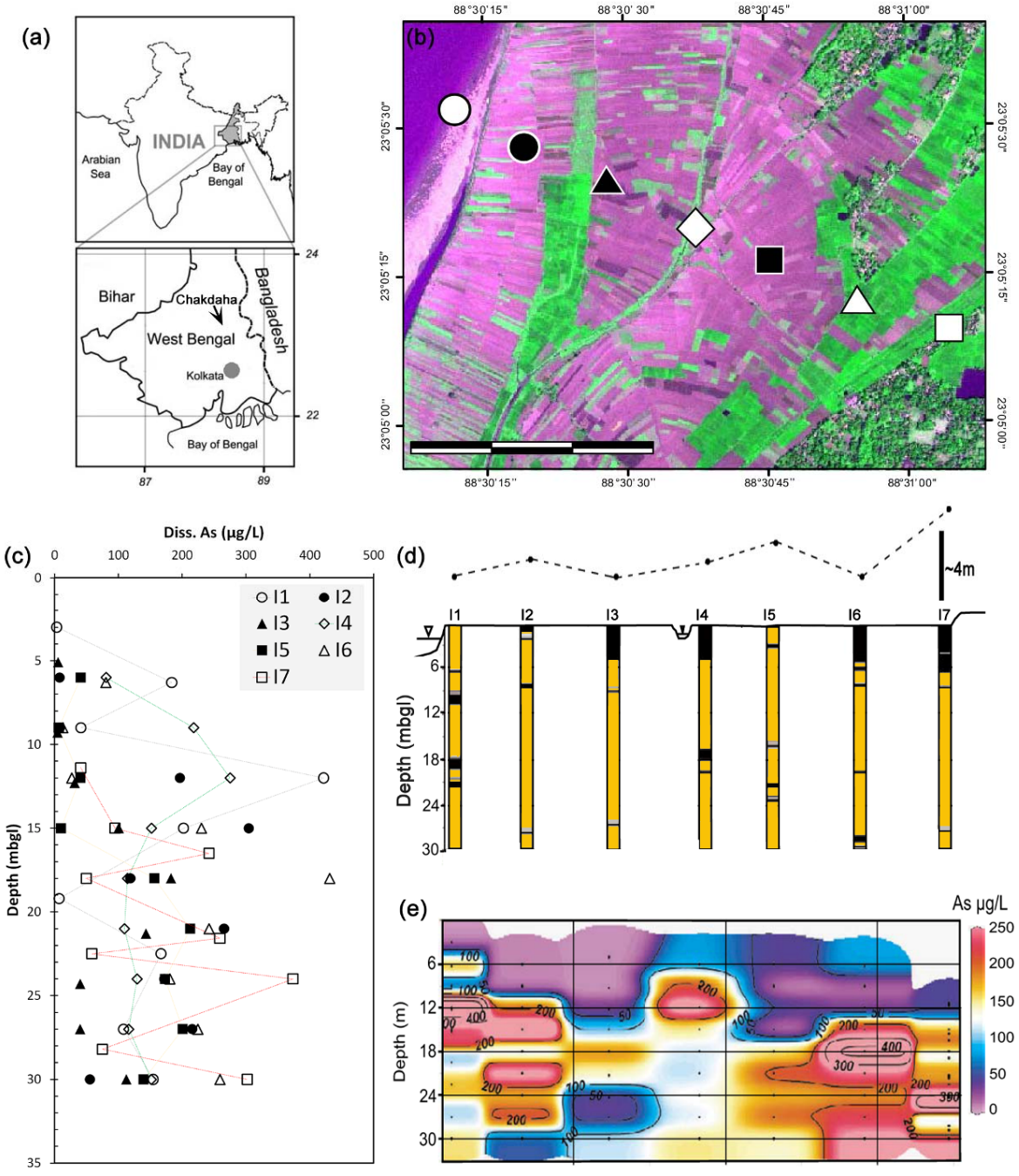

Figure 6-14: Spatial variation of groundwater arsenic concentration along a ~ 1500 m transect in Chakdaha, West Bengal *(Metral et al. 2008)*. (a-b) Location of the sites where high resolution vertical groundwater sampling was undertaken along a transect. (c) Depth profiles As concentration. (d) Relative elevation as extracted from the global Digital Elevation Model *(EROS 2002)*. Lithological information at the specific sampling sites (symbols as of figure 6-12). (e) Groundwater As concentration, contoured *(*after *Metral et al. 2008)*.

6.4.5 An explanation for the deep groundwater arsenic

A compilation (Figure 6-15) of basin-wide surveys *(BGS/DPHE 2001; DPHE/DFID/JICA 2006; Mukherjee 2006; Van Geen et al. 2007)* indicates that groundwater As exceeds 10 µg/l in 18% of the deep hand-pumped wells (n=1165), and that <2% of these exceed 50 µg/l, the regulatory limit of Bangladesh and West Bengal, but whether this is as a result of breached well casings or occurs as a hydrological response to pumping remains uncertain. However, there is a pattern to the distribution of the high As deep tube-wells. They follow paleochannels of the Ganges in the west *(*see *Sarkar et al. 2009)* and centre *(Umitsu 1993)* and a plaeo-channel of the river Gumti (Figure 4-12) in the east. Along the paleo-channels, sandy sediments were deposited and during the early stage of the Holocene delta development, the sedimentation rate was ~10 time higher than the current rate *(Sarkar et al. 2009)*. If the rate of sedimentation was too great for groundwater to flush paleochannel deposits, As-rich groundwater could have been trapped. There deposits may also have become cut-off from the active (shallow) flow-system due to deposition of a silt-clay layer before complete flushing of As. In addition, the patterns of As distribution at depth at these locations are similar to the shallow As situation, although absolute concentrations are lower. The As distribution appears to be associated with the silt-clay layers and by implication to the differential groundwater flushing rate.

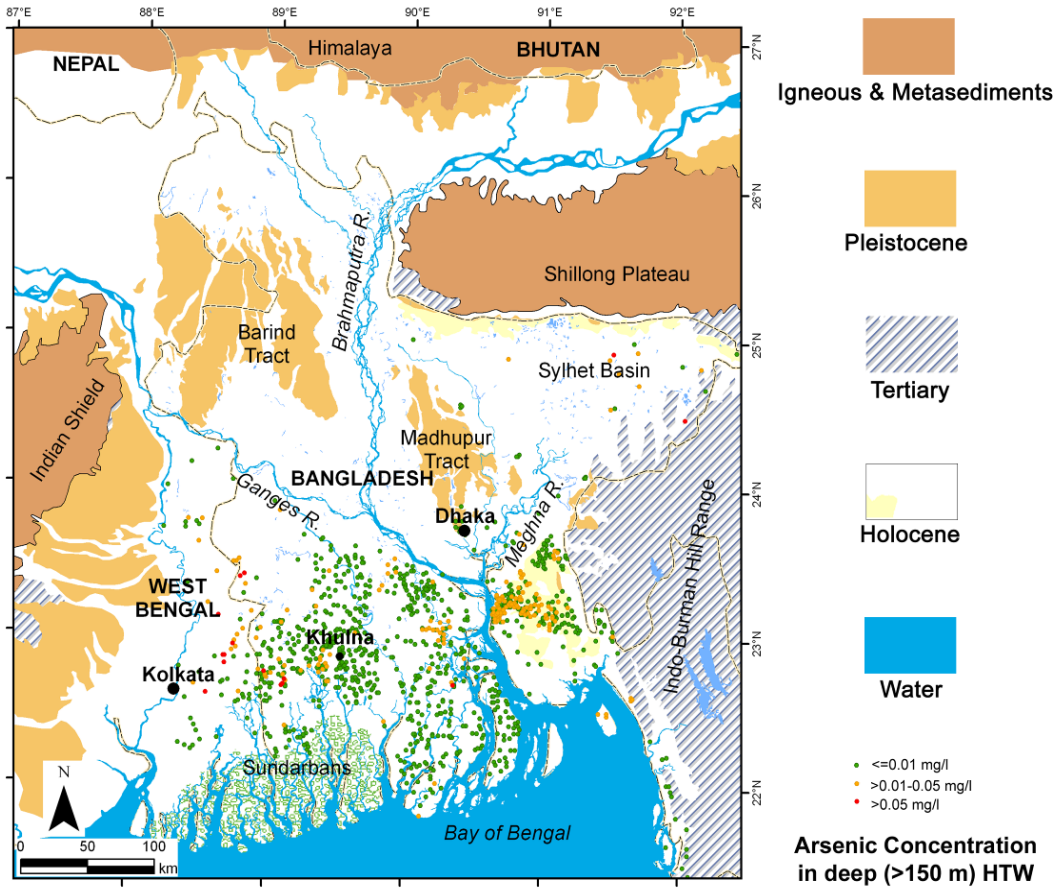

Figure 6-15: Arsenic concentration at hand-pumped wells (with exception in West Bengal, India where long-screen public supply wells were sampled) in the Bengal Basin, depth >150 m. Data (1165 records) from various sources see text. Generalised geology and structural elements are indicated.

An alternative explanation requires further investigation: it may be that due to the high proportion of sand in these regions, groundwater at this depth may be under the influence of shallow flow-system. This alternative is considered less likely because silt-clay layers, even if at a lesser frequency, would tend to inhibit penetration of shallow flow-system to such depths.

6.4.6 Temporal trends in groundwater As concentration

The hypothesis suggests how groundwater flow controls the geological mobilisation and progression of As in sedimentary basins of southern Asia. The interplay of climate, tectonics and eustatic changes in sea level cause the delta to shift its location to the south or north accordingly. Penecontemporaneous deltaic reworking and groundwater flow have operated episodically to keep As at shallower levels of the aquifer in the deltaic region over much of Quaternary time. Current conditions may have been initiated following delta development during the last episode of eustatic transgression in the early Holocene. Groundwater As occurrences in upland settings such as Tripura, Nepal, are suggested to be associated with reworking of sediments in a closed basin setting with shallow circulating groundwater. In addition to regional delta-building activities, landscape modification at a local scale is common in these settings, and topographic changes alter the groundwater flow field. This changing groundwater flow field is responsible for the redistribution of aqueous As within the aquifer, and slow desorption of As from the solid phase mineralogical sources at the redox boundary (in the area of reworking and redeposition) contributes As to the aqueous pool. Arsenic release may be greater in deltaic or closed basin than in fluvial settings. In fluvial regions flushing is dominant, which is why in northern Bangladesh groundwater As is generally lower than in the south. Heterogeneity in the distribution of As is proposed to be a product of the heterogeneity of sub-surface silt-clay layers, the strength of differential groundwater flushing, and chemical kinetics in the shallow flow system.

Release and flushing of As occurs over geological time. However, if groundwater pumping occurs, the flow system is modified and rapid transport of As may be induced. Monitoring data is available only for 3 years *(Cheng et al. 2005)* in central parts of the country, and no temporal changes is apparent over this time. A proxy with tube-well age has indicated that older wells contain higher As (*Ravenscroft et al. 2005; Burgess et al. 2007*) (Figure 6-16). However, there may be sample bias in favour of older wells with high As. Earlier practice of installing wells at a comparatively deeper level may have resulted in those older tube-wells having generally higher As concentration. Moreover, older wells may be installed above a silt-clay layer, where it has been shown that As is naturally high (section 6.4.4). Also the older, deeper, wells may be concentrated in southern Bangladesh where groundwater As concentrations are generally higher. Therefore it is difficult to demonstrate how As concentration changes over time at tube-wells. The hypothesis presented here gives some hope that understanding and mapping the discontinuous silt-clay layers may be a basis for locating As-safe tube-wells in the shallow

system. However, this would assume the stability of the flow system, which is by now greatly affected by groundwater abstraction.

Another recent study in Araihazar *(Dhar et al. 2008)* reported 3-year monitoring for a number (n=37) of piezometers to a depth of 90 m. These data show some minor increase and decrease in some wells but no significant trend in As concentration over time. The authors could not explain the observations. The hypothesis presented here can however explain the observations of Dhar et al *(2008)*, particularly the increasing trend that can be related to As transport induced by irrigation abstraction.

Naturally, As concentration should decrease over time due to groundwater flushing. Where As concentration is low at a tube-well it should decrease with time because the well is located in a favourable zone (Figure 6-8) where As has naturally been flushed away over time. Pumping (for irrigation or other purposes) should facilitate the flushing further. Where As concentration is low but the tube-well is screened between a high-As region (local groundwater discharged area, or areas covered by silt-clay layers) and an irrigation pumping well, the As concentration in the tube-well discharge may increase with time. The increase should be slow however because groundwater will (mostly) flow to the tube-well through the higher permeability aquifer zones which will naturally allow a higher flow rate contain less As. Therefore it is considered according to the hypothesis presented here that As concentration in tube-wells with low As concentration will, in general, decrease over time or remain low for a long duration. Understanding the flow-system would help to identify the wells which might be under greater threat due to irrigation or such pumping. Note that a prevalent belief is that As concentration will increase in most tube-wells with time (*Ravenscroft et al. 2005; Burgess et al. 2007*). Currently, >70% of shallow tube-wells are found to contain As below <50 µg/l, Bangladesh regulatory limit *(BGS/DPHE 2001; Ravenscroft et al. 2009)*.

As arsenic occurrence and distribution in groundwater is associated with deltaic sedimentary processes and groundwater flow, it is expected to have been present since the initiation of the delta itself. By the hypothesis presented here the maximum occurrence of As in groundwater would have been in the south during sea level low stands and further north during high stands (Figure 6-17). The delta has a history of eustatic changes throughout the Quaternary Period, and a thick sedimentary sequence which can support a groundwater flow-system which would concentrate As in the shallow aquifer. Deltas with a lesser thickness of sediments, and a sloping bed rock at shallow depth would give rise to sustained groundwater flow which would more rapidly flush As from the system.

6.5 SiHA hypothesis and flow modelling

The main uncertainty concerning the groundwater flow-system is the hydraulic anisotropy imposed by the low permeability materials; however it is this anisotropy which controls

groundwater flow in the region. Simple 2D modelling (Figure 6-4) has shown that anisotropy can lead to a hierarchy of groundwater flow systems. Anisotropy has previously been shown to determine the hydraulic resistance *(Rushton 1986)*, and to control the strength/stability of the flow-system *(Vissers and van der Perk 2008)*. Moreover, anisotropy will also determine the sustainability of deeper groundwater against perturbation of the groundwater flow-regime i. e., its vulnerability to short circuit flow from shallow levels.

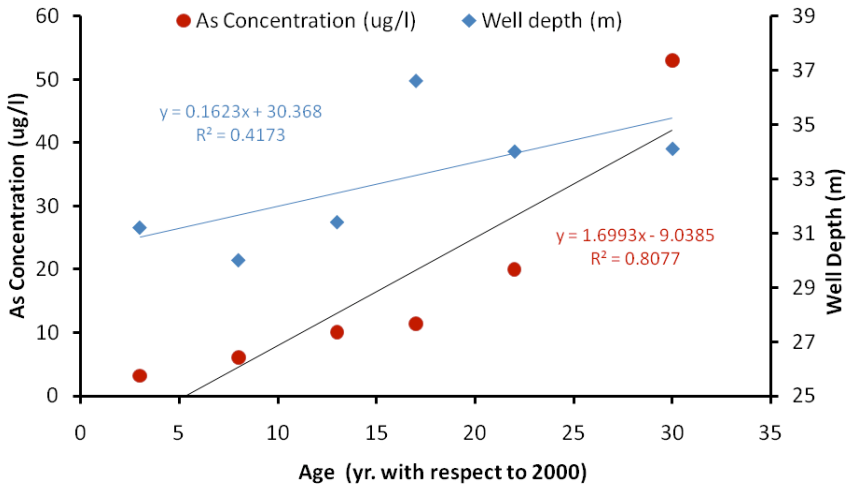

Figure 6-16: Median As concentration and tube-well depth versus tube-well age (calclulated from BGS/DPHE, 2001 dataset). This graph indicates increasing As concentration and tube-well age, previously used as proxy for temporal increase of arsenic with time. The data also show that older wells were deeper (see text).

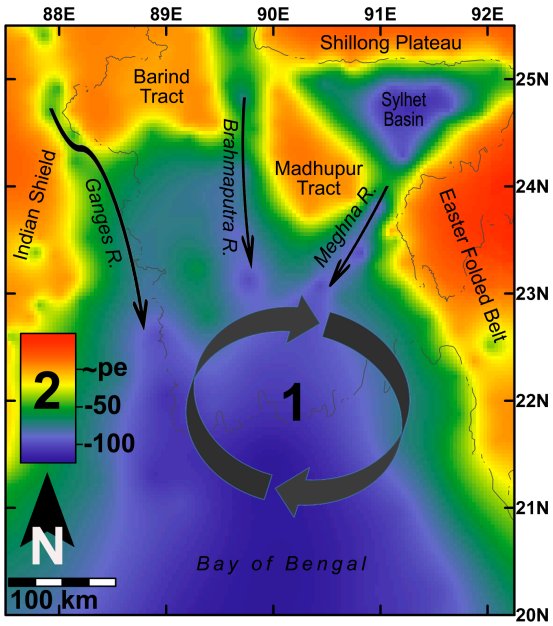

Figure 6-17: Estimated pre-Holocene land surface elevation based on the known thickness of the Holocene sediments. Elevation scale (2) indicates elevation in metres below approximate present elevation (~pe). In the map '1' indicates the pathway of the position of the maximum occurrences of As in groundwater, with the falling and rising of sea-level, and the associated deltaic sedimentation front.

Discontinuous lenses of low-permeability sediments occur ubiquitously throughout the basin. Representation of the basin as a single anisotropic aquifer provides one view of the flow systems, but in reality anisotropy comes from these low permeability materials (Figure 6-5). Flow in the aquifer at smaller scales is disrupted by the presence and absence of specific low permeability layers. According to the SiHA hypothesis As has been present in the groundwater system of the Bengal basin since the early stages of delta development, and will remain indefinitely in the shallower part of the aquifer if natural condition is undisturbed. It is however, the aquifer system is not in natural condition, and abstraction of groundwater from the deeper part of the aquifer has been increasing. The vulnerability of the deeper level of the aquifer to invasion by As will therefore be determined by the stability of the natural flow-systems. Again, 'stability of the natural flow-systems' is a balance between the anisotropy imposed to the system by silt-clay layers and amount of pumping. Yet again, finding and characterising the effective anisotropy at the scale of a model grid and also for individual silt-clay layer involves uncertainties. Models with different representations of the anisotropy may reproduce similar patterns of hydraulic head, but the groundwater flow pathways and travel-times would be expected to be different. Comparing the results of model using different methods of aquifer representation against independently-derived groundwater age estimates could be a basis for judging how best to represent 'effective anisotropy' of the aquifer system and hence to investigate the stability of flow system. In the current project a range of different representations of the aquifer were considered in this manner.

Chapter 7
Development of Models

A range of groundwater flow models were developed. The difference in the models was the mode of representation of geological heterogeneity in terms of hydraulic conductivity. This chapter describes the details of the models' development including specific modelling targets and approaches to modelling. All the model representations share common features i. e., model domain, overall geometry, recharge distribution and also certain hyadulic parametres (S_y, S_s, n). These common features are described first, and then the features specific to each representation at increasing level of complexity.

7.1 Modelling targets and test of model performance

7.1.1 Modelling targets

The general purpose of model building is to assist in the understanding of physical systems, and / or to provide a predictive tool. The aim of the current modelling is to develop models which would assist the study of sustainability of the deep groundwater in Bangladesh. However, the objective is to investigate the ways in which the hydrogeological framework can best be represented in a groundwater model, to increase confidence in model results. This was done using a multi-model approach as outlined in the following section (7.2).

A recent model study (*Michael and Voss 2008; 2009b; 2009a*) incorporated hydrogeological heterogeneity in single homogeneous, anisotropic aquifer representation (in terms of hydraulic conductivity) at the basin-scale. The current research tests the significance of incorporating local detail in representation of the aquifer system by applying increasing steps of complexity, i. e., by incorporating heterogeneity, anisotropy and hydrostratigraphical layering.

7.1.2 Tests of the quality of the model representations

Bangladesh Water Development Board (BWDB) has established a network of >1200 piezometers to monitor water level at national scale (*Shamsudduha et al. 2009a*). These piezometers monitor water level at a shallow depth (median depth of piezometers <30 m). Lack of data on deep groundwater heads limits the applicability of conventional model calibration. However, multi-level hydraulic head data is available at one location (Kachua, K on Figure 7-1) which was used for comparison with simulated heads at those depths. In addition, a national-scale map of depth to water table (Figure 3-17) at intermediate depths (depth of measurement, ~90 mbgl) is available *(BADC 2004)*. This map converted to water-table elevation (Figure 7-1) was used for qualitative comparison with the spatial variation of head simulated by the models.

Moreover, the current modelling objectives are related to transport of As from shallow to deep levels and therefore conventional calibration against head alone would be insufficient. Also, models with distinct hydrogeological representation may produce similar head distribution, but dissimilar groundwater flowpaths and travel-times to a particular location.

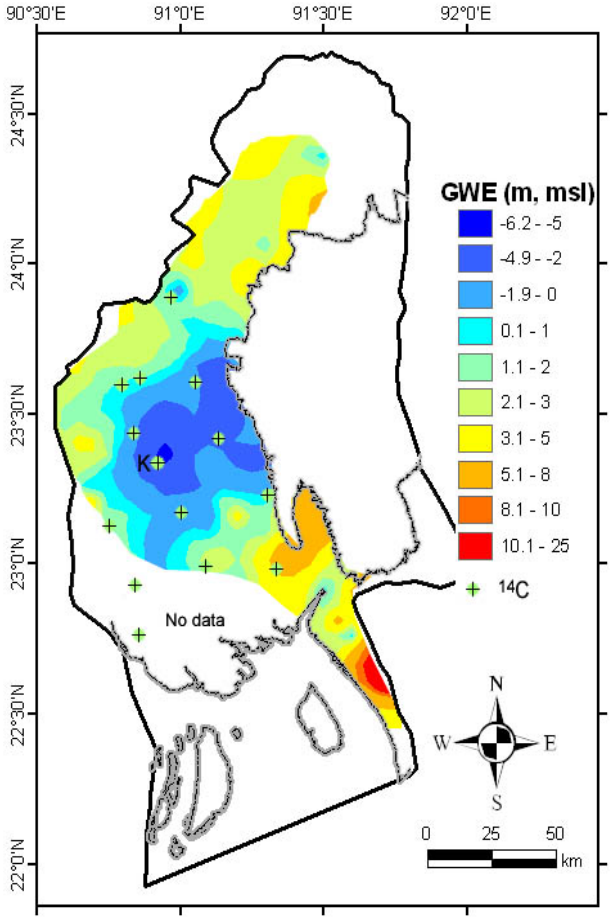

Figure 7-1: Elevation of groundwater table (GWE) (measurement depth ~90 mbgl) in reference to MSL calculated for the model area based on water-table configuration of figure 3-17, and SRTM elevation *(EROS 2002)*. An intermediate magnitude water-table depression in the central part of the model area can be observed. Locations of well indicated for which ^{14}C derived groundwater age has been estimated. In addition, at 'K' monitored head profiles are available for comparison.

Therefore, in the current modelling, all the models were compared to independent estimates of groundwater age (section 5.3.3) specific to 14 points in the model region (Figure 7-1). In this way models could be judged to see which one represented the reality most closely.

7.1.3 Uncertainties

As models are simplified representations of the reality, and there are many sources of uncertainty in groundwater modelling. Uncertainties arise firstly from incomplete definition of the conceptual framework that determines model structure; from spatial and temporal variations in hydrological variables that are either not fully captured by the available data or not fully resolved by the model; and also from the scale of effective hydrogeological variables *(Nilsson et al. 2007)*. All modelling efforts pay attention to minimise the effect of uncertainties and try to capture the important aspects of the flow regime.

Uncertainties in the model structure are mainly associated with how the mechanics of groundwater flow is related to the geological structure. In most mathematical models of subsurface flow and transport, the conceptual framework is assumed to be given, accurate and unique *(Dagan et al. 2003)*. In the current modelling effort attention has been given to encompassing the structural uncertainties (section 7.2) within the constraints of model scale. Each (effective) model grid is 1 km × 1 km. Elevation differences vary on a scale of 100 m or less and so spatial representation of the water table is limited. The spatial extent of the anisotropic litho-units are often less than the scale of a 1 km × 1 km model grid and so cannot be represented explicitly in the model, although they may affect the flow field. Absence of local topography affects only the shallow flow-system, while the focus of this research lies with the deep system. To encompass uncertainty in the representation of heterogeneities a multi-model approach has been considered (section 7.2).

Parameter estimation is another source of uncertainty. Previous modelling studies in this aquifer show that for reasonable values of other hydraulic parameters, groundwater model results are most sensitive to the hydraulic conductivity values (e. g., *Michael and Voss 2009b*). In the current study alternative models were developed using hydraulic conductivity as the only parameter defining hydrogeological structure (section 7.2). Here hydraulic conductivity includes both horizontal (Kh) and vertical (Kv) conductivity. Parameter values have been estimated on the effective values at the scale of the model grid.

Errors in groundwater abstractions, and also by incomplete spatial coverage of other attributes may lead to additional uncertainty. Boundary conditions present another source of uncertainty. In the current modelling an effort has been made to reduce the uncertainties involved with the boundary condition (section 7.6).

7.2 Conceptual models and multi-modelling approaches

The conceptualisation of the geological model structure of the region was derived from the analysis of 1573 drillers' log, around a dozen petroleum exploration logs, and 12 geophysical logs along with geological structural data. Analysis of the drillers' logs indicates that low permeability materials are ubiquitous throughout the region. There are also alignments of more pervasively coarse sand bodies, which are interpreted as stacked paleo-channel sands and stacked interfluves with finer dominence (Figure 7-2). Nearly all boreholes intersect multiple layers of sands and silt-clays. Hydrogeological framework is similar throughout the southern part of the basin with ubiquitous silt-clay layers and regions of stacked paleo-channel-sands and fine-dominated interfluves.

Low permeability materials, due to their anisotropic hydraulic nature and overlapping distribution, control groundwater flow in the region (section 6.2). Conceptualisation of their distribution for model representation was found to be very difficult due to their pervasive occurrences but discontinuous areal extent. Although for the model area 589 (1573 in total) logs were available, this is on average only 1 in 5 km^2 and heterogeneities in this fluvio-deltaic terrain occur at much smaller scale.

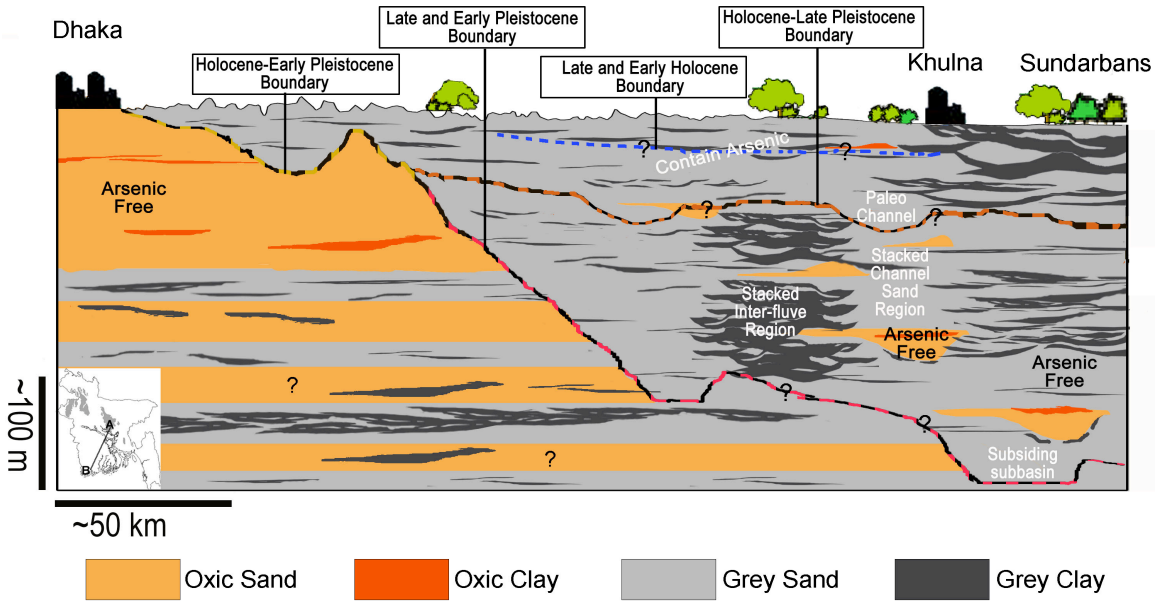

Figure 7-2: Aquifer hydrogeological framework– a conceptual bi-modal (sand-clay) representation of the aquifer environments in the Bengal Basin along a line A-B (see index map). Episodes of sustained weathering during eustatic sea level low stands from the Early Pleistocene are reflected in the regionally extensive oxididation of sediments of the central and northern part of the basin. Holocene sands, silts and silty-clays beneath the active floodplains overlie Pleistocene sediments to a depth generally of about 100 m in the south. Stacking of stable channel sands and adjacent interfluve deposits produced by repeated eustatic cycles resulted in the occurrence of belts of thick sands, and finer materials with limited lateral extents across the southern part of the basin. Note that oxic (brown) and reduced (grey) lithologies of equivalent grain size have similar hydraulic properties.

There are three levels of complexity (Figure 7-3) by which the effects of the low permeability materials have been incorporated into groundwater models: (1) using single anisotropy: the entire model domain is considered a single homogeneous anisotropic aquifer, (2) spatial heterogeneity is applied, to the single anisotropic aquifer, (3) a hydrostratigraphy is applied, envisaging a layered aquifer system which is both heterogeneous and anisotropic. These complexities were realised using two different modes of representation (R1 and R2 in Table 7-1). An alternative representation, the *stacked-mosaic-continuous* method, incorporates the effect of discrete distribution of silt-clay layers (R3 in).

For each of the three modes of representing lithological heterogeneity, steady state (pre-development) and /or transient state models were developed. Parameter estimation for each mode of representation is described in chapter 4. The resulting matrix of groundwater flow models is summarised in table 7-1. Using the Ababou method, a number of models was developed under R1 representation, which differ in terms of the 'correlation length' applied.

7.3 Model code and pre- & post-processor

To carry out this analysis the modular, three-dimensional, finite difference numerical model MODFLOW-2000 *(Harbaugh et al. 2000)* was used for simulations, the MODFLOW-GUI graphical user interface *(Winston 2000)* for setting up simulations, the MODFLOW post-processors MODPATH *(Pollock 1994)* for tracing groundwater flow paths, and ZoneBudget *(Harbaugh 1990)* for calculating water budgets. Argus ONE (Open Numeric Environment) (www.argusone.com and Argus Interware Inc, Herzelia, Israel) a model-independent Geographical Information System for numerical modelling, is used in the modelling work to incorporate input data, and produce output. The Plug-in Extension (PIE) technology of Argus enables a two-way communication between external programs, here MODFLOW and Argus ONE.

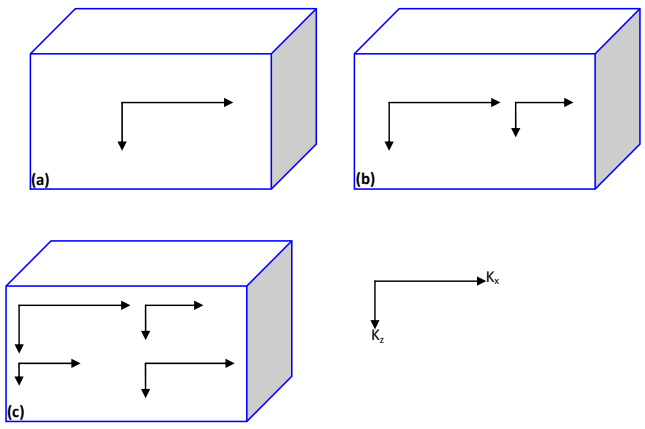

Figure 7-3: Level of geological complexities considered in model representations: (a) homogeneous single anisotropic aquifer, (b) spatially heterogeneous, anisotropic aquifer, (c) spatially heterogeneous anisotropic, multi-layered aquifer (i. e., has hydrostratigraphy).

Table 7-1: Matrix of aquifer representations developed to encompass the uncertainty in the lithological heterogeneity.

Limited extent of lithofacies: applying the method of Ababou (1996) (Section 4.2.7.1) (R1)	A **method based on sand and clay fraction** (Section 4.2.7.2) (R2)	***Stacked-mosaic-continuous*** representation (R3)
Equilibrium models		
Single, homogeneous, anisotropic (Kh/Kv = 10^4) aquifer; Pre-development (nM1), Post-development (nM2)		
4-layer anisotropic aquifer with spatially variable K based on variable l= 100 m (layer 1), 500 m (layer 2), 1000 m (layer 3) Pre-development (nM3), Post-development (nM4)		
Transient models		
Single, homogeneous, anisotropic (Kh/Kv = 10^4) aquifer (nM5)		9-layer anisotropic aquifer, the upper 300 m divided into 4 slabs (0-50-100-200-300), with a 5 metre thick layer taken at the bottom of each slab as another layer. This way the upper 300 m is discretised in 8 layers and bottom layer similar to 4th layer in other model, for detail please see section 7.8.3 (LS1).
4-layer anisotropic aquifer with spatially variable K based on variable l= 100 m (layer 1), 500 m (layer 2), 1000 m (layer 3) Pre-development (nB6)		
Single anisotropic aquifer with spatially variable K based on l = 500 m (nM8)	Single anisotropic aquifer with spatially variable Kh and Kz (SC2)	
4-layer anisotropic aquifer with spatially variable K based on variable l= 500 m (layer 1), 500 m (layer 2), 500 m (layer 3) (nM11)	4-layer anisotropic aquifer with spatially variable Kh and Kz based on silt-clay and sand content on different slabs (SC3)	
4-layer anisotropic aquifer with spatially variable K based on variable l= 100 m (layer 1), 100 m (layer 2), 100 m (layer 3) (nM13)		
'*l*' *stands for correlation length which was considered to be similar in X and Y dimension* *Boundary conditions are similar in all models*		

7.4 Model domain

7.4.1 Geographical boundaries

Models were developed for the eastern part of Bangladesh, and for hydrogeological purposes (section 7.6) the eastern boundary of the model was expanded into the Indian state of Tripura (Figure 7-4). The eastern boundary follows the north-south aligned hills in Tripura, while the western and northern boundaries follow alignment of major rivers. The southern boundary of the model is set around 50 km from the coast in the Bay of Bengal.

7.4.2 Rationale for choosing the model area

Model boundaries were chosen based on the concept of hydrogeological unit basin *(Anning and Konieczki 2005)*. The hydrogeological unit basin is defined to have coincident groundwater and surface-water basins. The model region is elevated in the eastern part, and slopes westward toward bounding rivers and the coast (Figure 7-4). The NNW-SSE aligned hills in Tripura form the surface water drainage divide between east and west. There are several smaller-scale (interconnected) surface-water drainage catchments, but they all are embedded in the bigger region and ultimately drain to the bounding rivers and to the sea in the west and southwest. The Google Earth (http://earth.google.com/) satellite images were carefully observed (under several order of magnification) for the patterns of rivers-streams to render surface water drainage in the region.

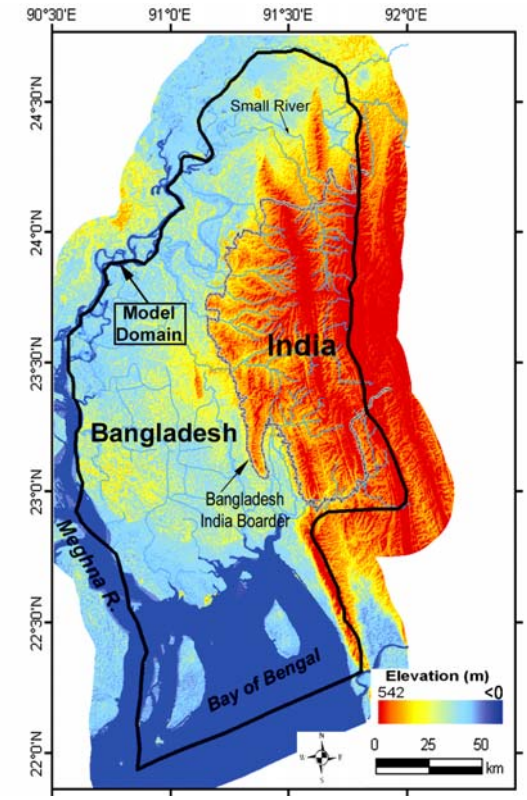

Figure 7-4: Geographical boundary of the model area over digital elevation model (DEM) *(EROS 2002)* of the area.

The region was targeted because it contains the highest number of shallow tube-wells with excessive dissolved arsenic, and in addition to that, thousands of deep tube-well has been installed in the region over the past decade for arsenic-free water. These two sets of wells made this area an appropriate and important region for modelling studies, towards the objective of assisting the study of vulnerability of the deeper aquifer to arsenic breakthrough from shallower depth.

It is likely that groundwater flow occurs under topographic influence (at least at the deeper level) from east to west and is discharged to rivers and at the coast. At the shallower level (<75 mbgl) groundwater flow may be localised due to hydraulic anisotropy *(*e. g., *Tóth 1963)*. Nevertheless, it remains unresolved about how representative the western river boundary is for deep groundwater conditions. Considering the physiography of the eastern hills, and the anisotropic nature *(*e. g., *Zijl 1999)* of fluvio-deltaic deposits in the sub-surface, the Meghna river (the lowest topographical element in the basin) in the west of the modelled region should act as line of discharge for deep groundwater flow (at least to a depth of several hundred metres below the ground). On the seaward side, groundwater discharge should be occurring within a few kilometres of the coast *(*e. g., *Taniguchi et al. 2008)*, however the coastal boundary was extended up to ~50 km offshore. In the east groundwater does not enter the model area in the subsurface as the boundary is a low-permeability mud-rich layer (i. e., UMS) deepening westward, which is found at ~2000 mbgl around the western boundary region of the model (section 4.2.4). This low permeability layer formed the bottom boundary of the model (section 7.5.2).

7.5 Model geometry and discretisation

7.5.1 Lateral extent

Laterally the model area is extended beyond Bangladesh territory, although the area of most interest lies within Bangladesh border. The model region is extensive, ~28,000 km^2. To achieve consistency with plausible natural boundaries (section 7.6) for the deep groundwater flow system, the Tripura Hills in the east, and the Meghna River in the west were chosen as boundaries for the model area (Figure 7-4).

7.5.2 Base of the model

The deep sedimentary sequence over the underlying hard-rock basement at ~20 km bgl *(Alam 1989)* may host a slow-moving groundwater flow system(s), which might also be under the influence of subduction related tectonic processes (see section 3.2.5) operating in the deepest parts of the region *(Ingebritsen et al. 2006)*, but this is not relevant to the flow system(s) of interest operating in the uppermost 300 to 500 m. Inclusion of this deepest flow system(s) in the model would be computationally costly and unnecessary. Moreover, basin-scale model analysis (*Michael and Voss 2009a*) shows that groundwater flux below the depth of 1000 m is <1% of the recharge.

In addition, the stratigraphy of the region up to ~2000 mbgl is made of fluvial-deltaic sediments *(Burgess et al. 2010)* which are hydraulically very anisotropic which reduces the penetration depth of recharging water (*Zijl 1999; Tóth 2009*). Below the fluvio-deltaic sequences a low permeability marine clay, the UMS (section 3.3) is considered the bottom boundary of the model. The depth to the UMS from the ground surface varies in the region due geo-tectonic modification. Considering the structural attributes of the area, and available exploratory drilling records, a digital elevation model (with respect to sea level) for the top surface of UMS was created (see sections 4.2.4 and 4.3.1). The UMS is taken to be impermeable to groundwater flow.

7.5.3 Upper limit of the model

The top of the model is set according to the topography of the region. The topography of the region was created from the Shuttle Radar Topography Mission (SRTM) digital elevation model data *(EROS 2002)* of 90 m resolution. The model grid varies from 1000 to 5000 m^2 so resampling of elevation data was undertaken with average elevation calculated based on all data points in each model grid. A potential problem with the use of this data, mentioned by Michael and Voss (*2009a*), is that where there is vegetation, the SRTM data reflect the elevation of top of vegetation. This was not a problem for most of the current model area as vegetation is primarily near the ground surface and dense tree cover is rare. However, in the eastern part of the model where the topography is hilly elevation over some grids may be influenced by canopy height instead of land-elevation. But as the grid size in that area is 5000 m^2, averaging of the data points would minimise this influence. The area in question is away from the main region of interest in the model. The model contains more than 5000 km^2 area of sea and some island masses. For this marine zone, bathymetry data was taken from Al-Salek *(1998)*, and in the west the river bottom elevation data for the river Meghna were estimated from Rahman et al. *(2004)*.

7.5.4 Vertical stratification

Geologically the entire domain is composed of heterogeneous and discontinuous fluvio-deltaic sediments, and in the model this is represented in the form of variable hydraulic conductivity with anisotropy, with or without spatial heterogeneity. The discontinuous anisotropic silt-clay layers (with particular pattern of occurrence - Figure 4-17) together with the topographical variations in the water-table support a hierarchy of groundwater flow-system. To comply with the depth dependence of abstraction points the models have 8 vertical units subdivided further (Table 7-2), but in order to incorporate the lithological attributes (see chapter 4), those units considered to be 4 layers (see Table 7-4). Note the difference in model LS1 (section 7.8.3).

7.5.5 Discretisation

The total model is ~28,000 km^2 in areal extent and vertically it is >2000 m deep in some areas. The entire model volume was discretised into a number of 3-D blocks.

7.5.5.1 Spatio-vertical discretisation

The model contains a principal area of interest with an areal extent of ~10,000 km^2 and vertically up to 350 to 500 m deep. To comply with the need to detail spatial modelling attributes (pumping, hydraulic properties etc), and minimise computational time, lateral grid discretisation was set to 1000 m in the area of interest, while it is 5000 m in areas beyond (Figure 7-5). In a transition zone a grid smoothing factor of 1.5 *(Harbaugh et al. 2000)* is maintained for computational stability.

Vertically, there are eight units in the model which have varying thicknesses and vertical discretisation (Figure 7-5). These are listed in table 7-2. Units are thin where the depth to the bottom boundary decreases. The grid discretisations remain the same for all the models, except one model based on 'lithological generalisation (section 7.8.3)', which has 13 units with number of dicretised layers in each. In all models the top unit is only one metre thick, so as to incorporate surface processes (rivers, lakes etc.) most effectively.

7.5.5.2 Time discretisation

Groundwater flow in nature is transient, and shows seasonality in response to recharge. Moreover, long-term climatic variability also affects the behaviour of groundwater. On top of the natural processes, the groundwater system is increasingly coming under anthropogenic influences. These interventions have an increasing long-term trend and seasonal variations. To incorporate the increasing groundwater use and seasonal variations the model considered 1960 to 2008 as a period of groundwater development (Table 7-3). Groundwater development prior to 1960s was limited to dug-wells for drinking water purposes only and was insignificant compared with development during recent decades.

The modelling covers a total simulation period of 48045 BC to 2008. This long duration of time was considered in order to derive the backward travel time of deep-water in the region, some of which is reported *(Aggarwal et al. 2000)* to be 10 to 20 ka years old. It is assumed that the geology of the area remains as of today throughout this time, which in reality is not the case. Only one stress period was assigned for the period prior to 1955, when there was no groundwater development. The historical period, 1956 to 2008, was simulated with 53 stress periods ranging in length from 5 years up to 1980, then to 1/3 year for the subsequent time (Table 7-3). Modelling was also carried-out in steady state for both pre-development conditions and development conditions (with 2008 abstraction scenario).

7.6 Boundary conditions

Numerical solution of a set of differential equations requires boundary conditions to be specified *(Harbaugh et al. 2000)*. Lateral boundaries in all models are set as no-flow along the lateral boundaries of the model domain, with justification explained below.

Table 7-2: Model units and vertical discretization (units are listed from top of the model to bottom)

Unit	Maximum thickness (m)	Number of vertical cells
1	1	1
2	49	4
3	50	5
4	100	10
5	100	10
6	100	10
7	100	10
8	2000	20

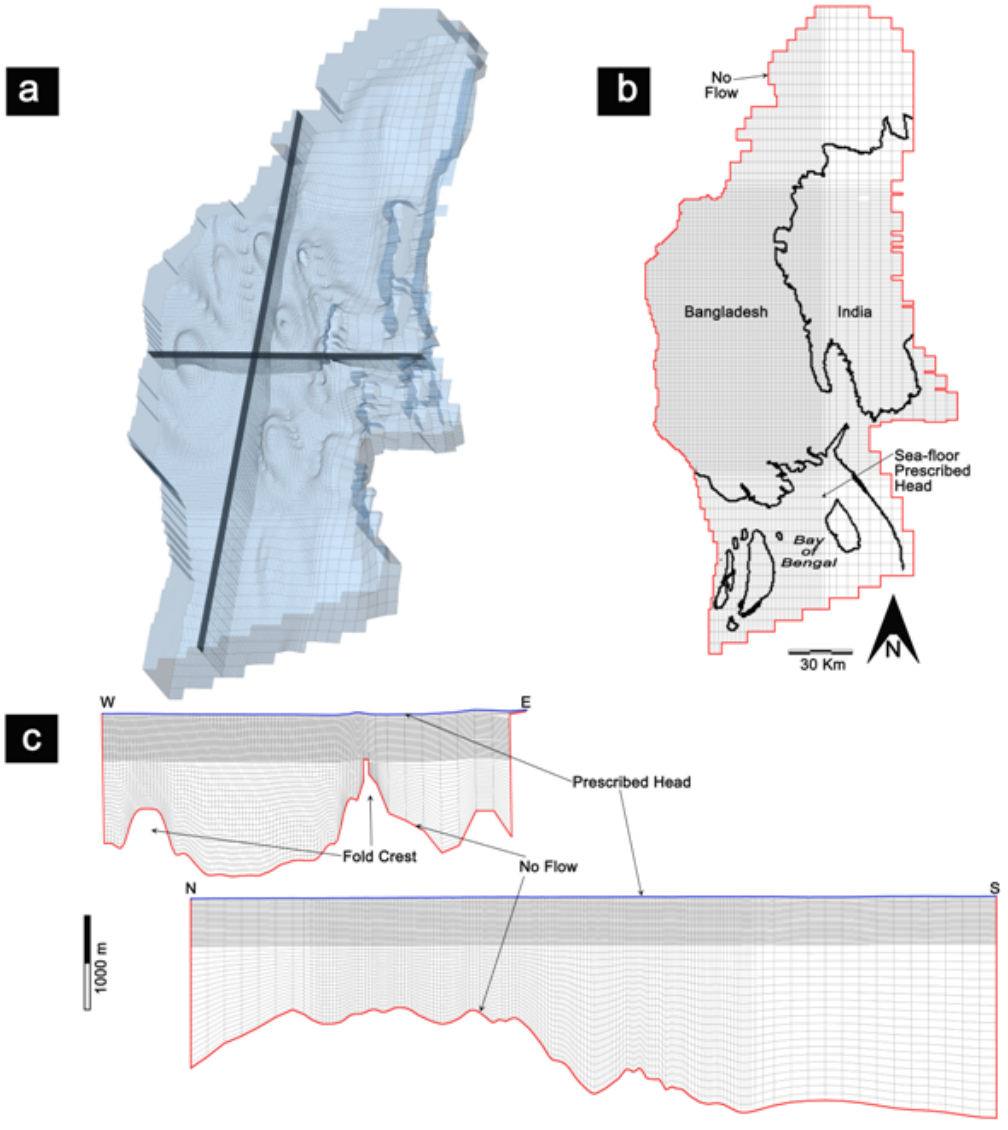

Figure 7-5: Model geometry, grid, and boundary conditions locations shown in (a). Three-dimensional view of model domain. Vertical exaggeration is 20x. Bottom elevation of the model is associated with the folding-induced, uneven distribution of the UMS. b) Top view of model grid. Boundary between India and Bangladesh, and coast-line are shown for reference. c. Vertical cross-sections; note grid discretization decreases with depth.

Table 7-3: Time discretisation and stress periods considered in the modelling

Stress Period	Time in stress period		No. of step	Calendar year
	(yrs)	(sec)		
1	50000.0	1.57788E+12	1	48045BC-1955
2	5.0	157788000	5	1956-1960
3	5.0	157788000	5	1961-1965
4	5.0	157788000	5	1966-1970
5	5.0	157788000	5	1971-1975
6	5.0	157788000	5	1976-1980
7	1.0	31557600	2	1981
8	1.0	31557600	2	1982
9	1.0	31557600	2	1983
10	1.0	31557600	2	1984
11	1.0	31557600	2	1985
12	1.0	31557600	2	1986
13	1.0	31557600	2	1987
14	1.0	31557600	2	1988
15	1.0	31557600	2	1989
16	1.0	31557600	2	1990
17	1.0	31557600	2	1991
18	1.0	31557600	2	1992
19	1.0	31557600	2	1993
20	1.0	31557600	2	1994
21	0.8	26287200	2	1995 (Jan-Oct)
22	0.5	15778800	3	Nov 1995-Apr 1996
23	0.5	15778800	3	May 1995-Oct 1996
24	0.5	15778800	3	Nov 1996-Apr 1997
25	0.5	15778800	3	May 1997-Oct 1997
26	0.5	15778800	3	Nov 1997-Apr 1998
27	0.5	15778800	3	May 1998-Oct 1998
28	0.5	15778800	3	Nov 1998-Apr 1999
29	0.5	15778800	3	May 1999-Oct 1999
30	0.5	15778800	3	Nov 1999-Apr 2000
31	0.5	15778800	3	May 2000-Oct 2000
32	0.3	10519200	4	Nov 2000-Feb 2001
33	0.3	10519200	4	Mar 2001-Jun2001
34	0.3	10519200	4	Jul2001-Oct2001
35	0.3	10519200	4	Nov 2001-Feb2002
36	0.3	10519200	4	Mar 2002-Jun2002
37	0.3	10519200	4	Jul2002-Oct2002
38	0.3	10519200	4	Nov 2002-Feb2003
39	0.3	10519200	4	Mar 2003-Jun2003
40	0.3	10519200	4	Jul2003-Oct2003
41	0.3	10519200	4	Nov 2003-Feb2004
42	0.3	10519200	4	Mar 2004-Jun2004
43	0.3	10519200	4	Jul2004-Oct2004
44	0.3	10519200	4	Nov 2004-Feb2005
45	0.3	10519200	4	Mar 2005-Jun2005
46	0.3	10519200	4	Jul2005-Oct2005
47	0.3	10519200	4	Nov 2005-Feb2006
48	0.3	10519200	4	Mar 2006-Jun2006
49	0.3	10519200	4	Jul2006-Oct2006
50	0.3	10519200	4	Nov 2006-Feb2007
51	0.3	10519200	4	Mar 2007-Jun2007
52	0.3	10519200	4	Jul2007-Oct2007
53	0.3	10519200	4	Nov 2007-Feb2008
54	0.3	10519200	4	Mar 2008-Jun2008

7.6.1 Eastern boundary

The eastern boundary coincides with a surface water-divide, and is taken as a groundwater divide as the impervious clay (UMS) is reported to be exposed along the fold-crest (section 4.3.1). Moreover, the UMS likely acts as a barrier to large-scale horizontal flow across the model boundary. Therefore this boundary was treated as 'no–flow'. In addition, this boundary was set more than 50 km east of the area of principal interest.

7.6.2 West and North boundaries

The boundary in the west is demarcated by a major river, the Meghna, which is one of the lowest topographic elements in the basin. It is considered to be a discharge region for flow-paths of interest because of its low topography and its perennial occurrence. In the north a tributary of the Meghna River originating from the eastern hills is taken as a boundary. Flow is assumed not to cross this geomorphological boundary, which is taken as a no-flow boundary at depth.

7.6.3 Southern boundary

The southern boundary of the model is in the Bay of Bengal, more than 50 km offshore. Representation of this boundary is difficult, and strictly requires a variable-density model. However, the current modelling effort principally considered fresh inland groundwater, and the density of seawater was taken into account to secure the southern boundary condition. The southern boundary over the sea region was set as a prescribed head along the seafloor, with a no-flow boundary at the southernmost edge of the model. Head at the seafloor was set to the equivalent freshwater head calculated as '1.025 x bathymetry' at that point. In the deeper part of the bay very low permeability sediments have been reported (*Michael and Voss 2009a*), which would restrict flow into or out of the sea-floor. *Michael and Voss* (*2009a*) used a very low hydraulic conductivity (1×10^{-12} m/s) to the model seafloor, which had the effect of reducing the impact of the sub-bay boundary on the interior of the model. A similar measure is taken in the current modelling to tackle the seaward boundary of the model.

7.6.4 Base and top boundary

The bottom boundary in MODFLOW by default is a no-flow boundary. In the current modelling the base of the model rests on low-permeability marine clay (UMS) at a variable depth across the region, and so a no-flow boundary is realistic. The top boundary is critical and is taken as a prescribed head defined by the topography to represent recharge (see section 7.9.1).

7.7 Hydrogeological parameterisation

Hydrogeological properties representing the aquifer-system in groundwater-flow models are hydraulic conductivity (horizontal and vertical), specific storage, specific capacity, and porosity.

These properties are specified in the model using the LPF (Layer Property Flow) package of MODFLOW-2000 *(Harbaugh et al. 2000)*.

7.7.1 Hydraulic conductivity

Groundwater flow in aquifers is controlled by hydraulic attributes of the constituents of the aquifers. Among the attributes (hydraulic conductivity, specific storage, specific capacity, and porosity) hydraulic conductivity plays the vital role (e. g., *Johnson and Dreiss 1989; Wen and Hernandez 1996; Fogg et al. 1998; Ritzi 2000; Zhang et al. 2006*). Hydraulic conductivity indicates the ease of water passing through a material. Hydraulically, sedimentary strata are grouped into multiple layers and designated as aquifers or aquitards according to their hydraulic conductivity, and a generalised numerical conversion may be applied for modelling purposes to achieve the effective hydraulic representation. But in a fluvial-deltaic terrain like the Bengal Basin heterogeneity and spatial discontinuity of the layers complicate the procedure. In this case the hydraulic conductivity of a depth slice can vary spatially over several orders of magnitude, so heterogeneity is a major control on the bulk aquifer 'effective' properties on a regional scale.

In a fluvio-deltaic terrain on a local scale the subsurface extent of the low permeability materials controls groundwater flow. A regional flow-system originates from the basin-margin as a separate flow at depth as a consequence of the presence of those low permeability materials in a particular pattern of occurrence (i. e., *stacked-mosaic-continuous*, see sections 4.3.8 and 6.2). For a sub-basinal model, as in the present case, acknowledging these low permeability materials in a deterministic way in the model at scales ranging from stratigraphical features (m scale) to basin fill (river basin) is computationally expensive, if not impossible. However, it is also a difficulty to map the distribution of these because of the wide spacing of data points. Characterizing the distribution of the low permeability materials statistically is one of the options. Sections 4.3.6 and 7.8 describe different ways applied to incorporate the effect of low permeability materials in the current modelling efforts.

7.7.2 Specific yield, specific storage and porosity

Specific yield (S_y) is determined by the drainable porosity of an unconfined aquifer in the region of water table fluctuation, while specific storage (S_s) is controlled by the bulk compressive properties of the matrix in the region of head change. Values of S_s generally range from 10^{-5} m^{-1} (sandy gravel) to 10^{-2} m^{-1} (tight clay) *(Domenico and Schwartz 1998)*. Confined storativity, S, is the product of S_s and aquifer thickness. Earlier pumping tests in the study region found S to be in the range of 0.00087-0.0019 *(BWDB 2005)* at depths greater than 200 m. Specific yield values range from 0.02–0.05 over much of the Basin *(MPO 1987)*. The spatial variability of S_y and S_s in this sand-dominated terrain is not expected to be great. Therefore, a single value of S_y and S_s is used for individual model layers as of table 7-4. In the current modelling studies S_y is unimportant because recharge is simulated as a fixed head at the top layer of model.

Porosity represents the amount of void space in the aquifer materials. This property, as effective porosity, is required in estimation of groundwater velocity and travel-times. In the current study MODPATH *(Pollock 1994)* is used to calculate the groundwater travel time and flow-paths between points of interest and their recharge location. Effective porosity values are taken relatively higher for finer grained materials compared to coarse grained, and not to vary spatially within the layer (Table 7-4).

7.8 Effective hydraulic conductivity: range of representation of 'K' field

There are many approaches to representing geological heterogeneities in groundwater models (see section 4.2.7). Twelve different 3-D model representations were developed in this thesis (section 7.2), some with similar hydraulic conductivity fields but different modes of representing stresses (steady state vs. Transient, pre- or post-development). Eight of the models are transient, and have identical stress representations but different representations of heterogeneity in hydraulic conductivity. Hydraulic conductivity was varied in order to explore the uncertainties associated with geological representation in groundwater models of the Bengal Basin.

Geological heterogeneities were characterised by hydrostratigraphical analysis within which the extent of individual lithological units and also the silt-clay and sand fractions were considered (chapter 4). These attributes (the extent of lithological units and fraction of silt-clay to sand) were transformed from geological descriptions to numerical characterisations of the hydraulic conductivity (see section 4.2.7). The different hydraulic conductivity fields included plausible and more extreme representations.

7.8.1 The dimension of homogeneities and heterogeneities

Many investigators have recognized the importance of low-permeability silt-clays in controlling flow (*Novakovic et al. 2002*). However, it is difficult to include realistic distributions of silt-clay layers in groundwater models because of the wide spacing of data, the limited vertical resolution and also the poor quality of the data. As the spatial extent of the silt-clay layers plays a critical role, the effects of alternative lateral dimensions of the lithological layers were tested. These different representations were described in section 4.2.7. The alternative dimensions may not represent the actual physical dimension in the field, but relate to the scale of statistical homogeneity. One or some of these may be effective representations of the real world, and can be judged against independently derived data of head and groundwater age.

7.8.2 Sand-clay ratio effects on flow

The fraction of sand and silt-clay in a log can be used as indicative of the lateral continuity of lithological units in alluvial aquifers. The sand and silt-clay fraction data were linked with values of hydraulic conductivity derived from pump-test data. The effective hydraulic conductivity is estimated at the drillers' log points in two different ways, described in section 4.2.7.

7.8.3 'Stacked-mosaic-continuous' representation

The inclusion of discrete silt-clay layers as individual layers results in a pattern of groundwater flow that is taken to be the actual flow pattern (see section 6.2). It is not however credible to include actual distributions of silt-clays in groundwater models due to their numbers and complexity. Simple modelling (see section 6.2) showed that depth-wise stacking of the low permeability materials can generate the same flow-pattern as in the case of discrete distribution of the individual layers of low permeability materials. The depth-wise '*stacked-mosaic-continuous'* (see section 6.2.4) representation loses some of the detail in the flow pattern but is correct at the regional and sub-regional scale and includes locally-generated deeply penetrating flow.

To test this in 3-D regional model, the upper 300 m depth slab was divided into 4 sub-slabs (0-50-100-200-300 m), and for each sub-slab a basal 5-m was considered an additional unit. The uppermost 300 metres was therefore discretised to 9 units (including an uppermost 1 m unit as is all 3D models). The full model then becomes a 12-unit model. In terms of hydrostratigraphical or effective hydraulic conductivity layering this model is 9 layers (Table 7-4). From the drillers' log for each depth slice the silt-clay content was calculated, and those beds with >5% silt-clay, hydraulic properties of silt-clay were assigned to the appropriate 5-m unit. In the case of the silt-clay content >75% silt-clay hydraulic properties are assigned to the entire sub-slab at that location. Equations 4-7 (in all cases) and 4-8 (only if silt-clay content was >50%) were used to estimate the effective horizontal and vertical hydraulic conductivity at the drillers' log points for each unit. Vertical hydraulic conductivity for the 5-m thick unit was derived from the silt-clay content at a fixed ratio to the horizontal hydraulic conductivity i. e., 1/1000 for silt-clay content >75%, 1/500 for silt-clay content >10%, 1/100 for silt-clay content >5%, and 1/10 for silt-clay content <5%. After estimating the hydraulic conductivity at the drillers' log points a 'nearest neighbour' algorithm (e. g., *Kitanidis 1997*) was used to generate the hydraulic conductivity field for each unit. The resulting overall effective hydraulic conductivity field is illustrated in figure 7-6.

7.9 Stresses: recharge and groundwater withdrawal

Stresses represent the water designed to enter or be drained from the model domain. In natural condition, water enters the groundwater system as recharge, and discharges into rivers, lakes, sea, and by evapotranspiration (ET). This natural setting is disrupted by water abstraction at wells. Groundwater is discharged from the aquifer both by natural means and through water-well abstraction. Natural discharges are allowed from the model by reference to prescribed heads along the rivers, stream, and sea boundary. No water was allowed to leave the model domain below the top layer i. e., boundaries below the top layer were all set to be no-flow. Discharge via abstraction wells was assigned as a negative flux at locations described in section 7.9.2. The top layer of the model is a prescribed head assigned to represent recharge and areas of natural discharge.

Table 7-4: Specific yield (S_y) and specific storage (S_s) values used in the models

Unit	Hydrostratigraphy/ hydraulic layer	Specific Yield (S_y)	Specific Storage (S_s) m^{-1}	Effective Porosity (n)	*Model SL1	
					Units	Hydraulic layer
1	Layer 1	0.06	1E-3	0.30	1	Layer 1
2		0.06	1E-4	0.25	2	
					3	Layer2
3		0.06	1E-4	0.25	4	Layer3
					5	Layer4
4	Layer 2	0.06	1E-4	0.25	6	Layer5
					7	Layer6
5	Layer 3	0.1	1E-5	0.20	8	Layer7
					9	Layer8
6	Layer 4	0.1	1E-5	0.20	10	Layer9
7		0.1	1E-5	0.20	11	
8		0.1	1E-5	0.20	12	

** Model based on stacked silt-clay layers is compared to the other models, only units (5 m thick units are shaded) and hydraulic layers are compared.*

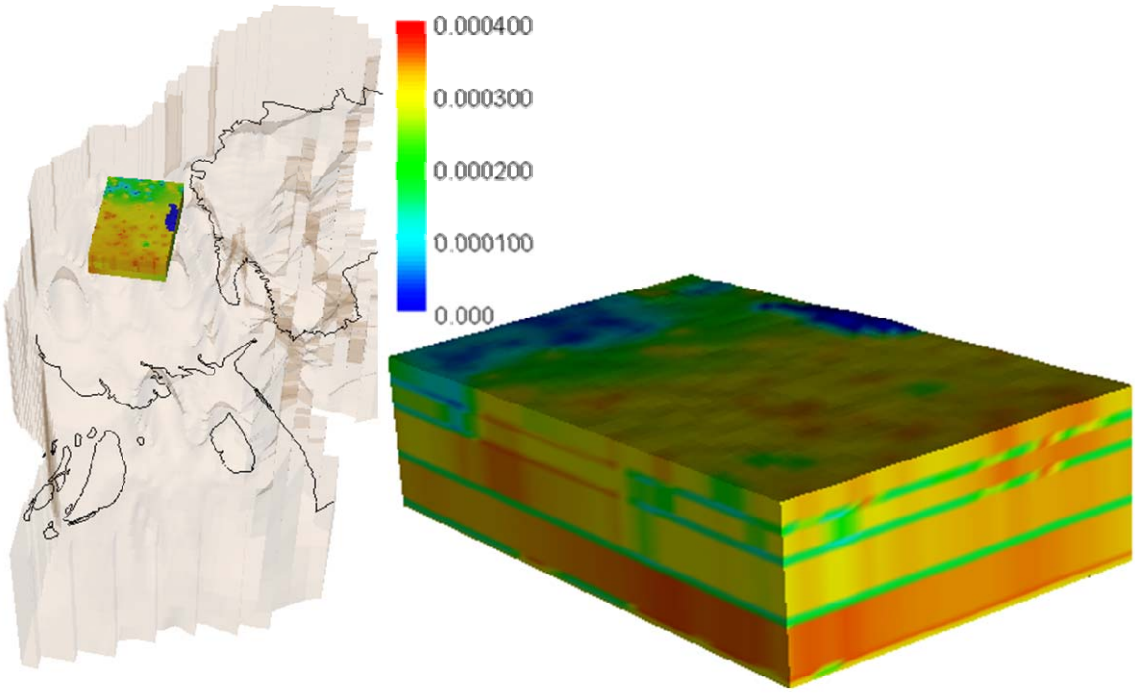

Figure 7-6: Effective horizontal hydraulic conductivity field sampled from stacked silt-clay layer model. Colour bar indicates the hydraulic conductivity in m/s.

7.9.1 Recharge

Representation of recharge in a groundwater model in a fluvio-deltaic terrain with monsoon climate is difficult *(Sanford 2002)* because the availability of recharging water and its control by the accommodation-storage capacity defined by the water-level in the shallow aquifer environment. Actual recharge (R_a) becomes a function of discharges (G_d) (both natural and abstraction via water-well), where R_a is proportional to G_d. There is no existing map on the spatial distribution of actual recharge over time in Bangladesh. There is information on the spatial variation of potential recharge, which is (in most parts) higher than the actual recharge *(MPO 1987)*. Sanford *(2002)* suggested that a prescribed head at the top boundary of the model in such a setting would be a better representation of recharge. This approach was applied in a previous basin-scale model in the region (*Michael and Voss 2009a*).

In reality, Bengal Basin aquifers derive recharge from rainfall (mostly during June-September) and from the surface water bodies which remain full during and beyond the rainy season. During the dry season (November to March) a large amount of groundwater is withdrawn for irrigation, in addition to the millions of low-yield hand-pump well abstractions and the high-yielding industrial abstraction which occurs throughout the year. Groundwater also leaves the aquifer as ET from crops during the dry season at an annual rate estimated to be 608 mm *(WARPO 2000)*. Water-table fluctuations in the shallow aquifer throughout Bangladesh are reported to be 2 to 6 m (with respect to sea-level), depending on the elevation of land-surface (higher in elevated, and lower in low areas) and the amount of irrigation abstraction (*Shamsudduha et al. 2009a*). In the model area, seasonal water-table fluctuations are is in the lower range as the area is less elevated; however in the hilly area in the east the fluctuation may be higher. No data are available to support this. In the rainy season, most part of the delta is flooded i. e., the water-table rises above the ground. Due to extensive irrigation, land over the delta fields remains flooded during the dry season as well. In addition, there are plentiful perennial surface-water bodies even in the hilly areas. All of the above emphasises the availability of water at the surface throughout the year, to enter the groundwater system whenever storage is available. In reality the water-table fluctuates seasonally indicating a lag time in the availability of water for recharge during parts of the year. However, given the current modelling interest in the deeper level of the aquifer and widespread availability of water near the surface throughout the year, representation of recharge as prescribed head at the model top boundary is considered appropriate. A sensitivity analysis of the previous basin-scale model by Michael and Voss (*2009a*) indicates that this representation does not alter the modelling results much in comparison to other ways of representing recharge.

7.9.2 Groundwater withdrawal

Groundwater withdrawal in Bangladesh is an ever increasing hunt for a natural resource. Bangladesh has highest population density (947/km^2) on earth, but it is self sufficient in food

production. Food self-sufficiency was achieved through the application of irrigated agricultures in the 1960s. At the moment, 90% of the irrigation is based on the groundwater resource (*Bhuiyan 1984; BADC 2003*). Millions of hand-pumped tube-wells are in use in Bangladesh meeting the household demand of water, as do high-yielding wells in the urban and industrial locations. There is no monitoring database available on groundwater abstractions, and abstractions are occurring outside of any central control. In the following sub-sections a description is made how these abstractions were estimated for the current modelling effort.

7.9.2.1 Irrigation abstractions

The large number of wells and sub-basinal coverage of the model make it impossible to treat individual irrigation wells in the model. There is no spatial data on the well location and on the amount of pumping. Moreover, pumping occurs in different wells in different time and the amount also varies. The net amounts of pumping at different depths were assigned as rate per area or rate per person or rate per well as described below. Depths of the pumping were estimated from available spatial data.

7.9.2.1.1 Data used

A limited amount of data is available on the amount of water withdrawn for irrigation both spatially and over time due to lack of central control and monitoring. In recent years Bangladesh Agricultural Development Corporation *(BADC 2003)* started surveys to make an inventory of how much land is under irrigation in each sub-district, and some analyses are available on the growth of irrigation. These two lines of information along with crop-water requirements were used to make an estimate on the irrigation withdrawal over time.

7.9.2.1.2 Estimation

Areas of irrigated land data were compiled from the BADC *(2003)* for individual upazila (sub-district) under the model area. It is mentioned before that the model requires time-series data on this from the 1960s i. e., from the inception of groundwater irrigation in the region. To estimate the amount of irrigation abstraction for different years, data for 2003 from BADC was taken as a base-year dataset. This base-year data were projected backward and forward to estimate temporal irrigation abstraction based on generalised trend as of figure 7-7.

From the history of groundwater development in the region (*Bhuiyan 1984; WARPO 2000; BADC 2003; Rahman and Ravenscroft 2003; Wahid et al. 2007, and also http://www.brri.gov.bd/ accessed 21 July 2008*) a generalised in trend of groundwater-based irrigation (Figure 7-7) was established. It is assumed that spatial distribution of irrigated land was similar (of 2003) throughout the time and only areal extents in those upazilas have changed over time. Based on this assumption and trend, groundwater irrigated areas in different years were estimated with respect to year 2003.

In Bangladesh during the irrigation season about 1 to 1.5 m equivalent depth of water is abstracted depending on the surface geology of the area (*WARPO 2000; Harvey et al. 2006; Wahid et al. 2007*). Generally, in the north-west it is higher while in the south and southeast it is lower. In the current modelling, irrigation abstraction is considered to be 1 m/year equivalent depth of water. On this basis, an amount of total irrigation abstraction is estimated for different years. These abstractions are then matched with different stress periods of the model, due to the seasonal nature of abstraction, particularly for irrigation. The amount of groundwater abstraction in 2003 was converted into a rate per area by dividing by the total area of the upazila. For simplicity, the amount of abstraction in different stresses periods was converted into a fraction of the 2003 abstraction. Finally, for individual stress periods, it becomes

$$Q_{sp} = \left(\frac{q_r \times q_{2003}}{t_{sp}} \right) \quad \text{.....Eq. 7-1}$$

In the equation Q_{sp} is abstraction rate (m/sec); q_r is the areal rate (i .e. areal flux) of abstraction in 2003; q_{2003} is the fraction with respect to 2003; and t_{sp} is the time is seconds in the respective stress period.

These estimates on the groundwater abstraction for irrigation were then converted into spatial data with temporal attribute in GIS. Conversion of data into GIS facilitates easy handling and later conversion into model-grids. An example for 2005 is given in figure 7-8. An estimate is also made based on the aforesaid literature for the variation of areal extent over time as of figure 7-7. Irrigation data for Tripura, India, state were not available. It is known that irrigation in that area is mostly from surface water *(WWF and DoA 2007)*, and hence no irrigation abstraction from groundwater was applied in those areas.

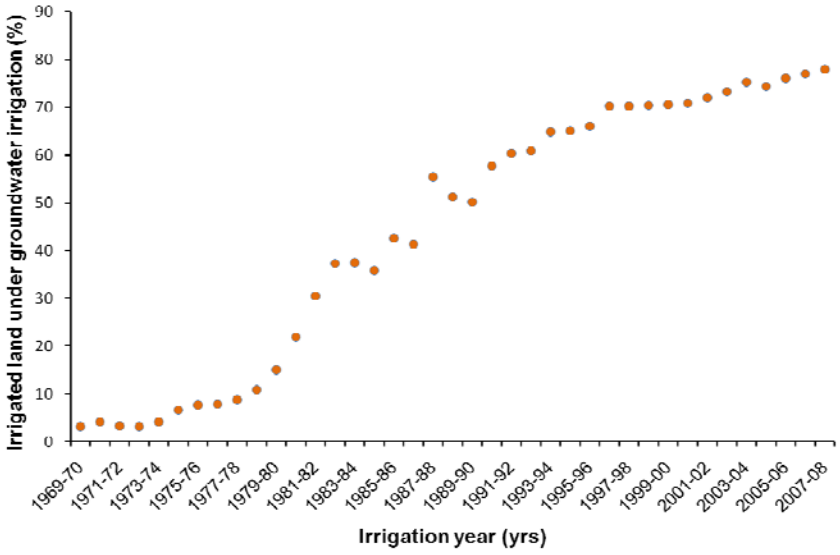

Figure 7-7: Estimated irrigated land (%) under groundwater-irrigation scheme in south-east Bangladesh over time.

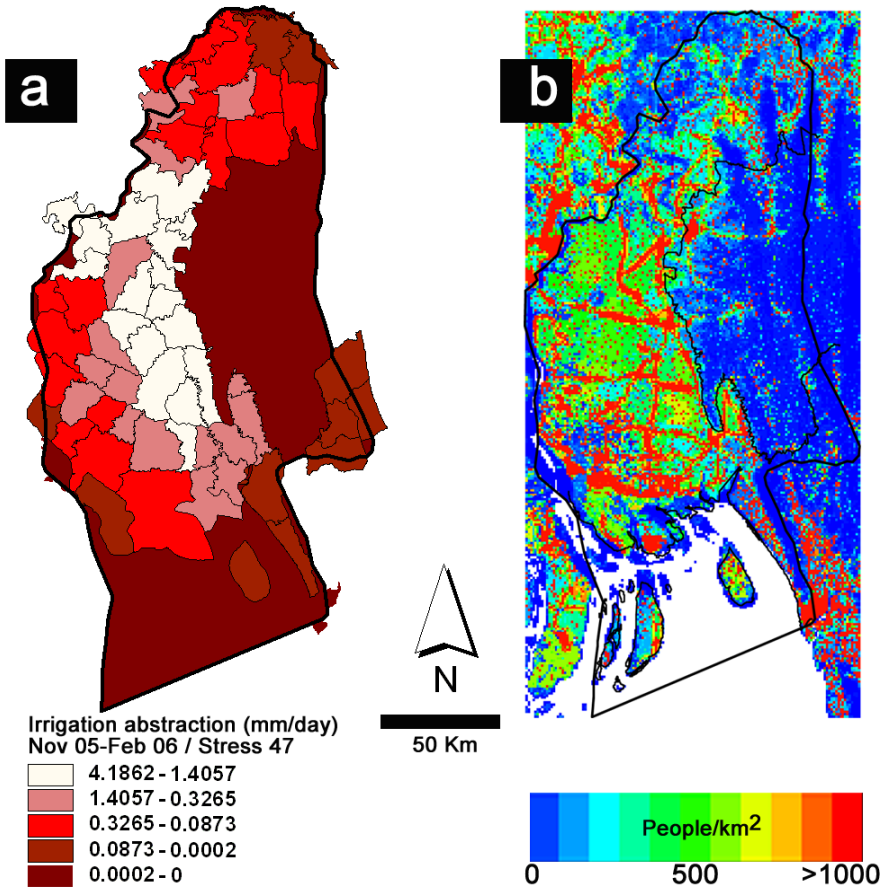

Figure 7-8: Estimated irrigation abstraction (mm/day) for the stress period 47 (peak irrigation time of the year 2005-2006) (a), and LandScan global population-model derived population distribution in the area used for estimation of groundwater abstraction from shallower depth of the aquifer (b).

The depth of the irrigation-well was found to vary spatially in the study area possibly due to suitability of the aquifer zone for this heavy abstraction. To comply with the depth variations a contour of spatial well-depth variation was generated from the available data to guide the abstraction depth in the model.

7.9.2.2 Household and industrial abstraction

There are no reasonable statistics on the number and locations of the millions of the hand pumped tube wells operating in the region. These wells operated historically at shallower depth (<100 mbgl). However, with the discovery of groundwater arsenic at these shallow wells attention turned to the deeper level, which is essentially arsenic-safe. In Bangladesh, >75,000 deep hand-pumped wells had been installed by 2007 *(Ravenscroft et al. 2009)*. Among those >20,000 tube wells were installed in the model region under the arsenic mitigation plan at depths >150 mbgl (*DPHE, Personal communication, 2008*). In addition to these low yielding wells, there are numbers of high-yielding wells which operate in the local towns to meet the urban water demand. There are some abstractions in the area for industrial purposes as well. All these abstraction have been considered for their respective depths.

7.9.2.2.1 Data used

Household abstractions were estimated based on per-capita consumption using population data. Population data were extracted from the global population model, LandScan 2006 *(ORNL 2008)* (Figure 7-8). These data are assumed to be the true distribution of population in 2006. Information on the growth of population in the region is available from the Bangladesh Bureau of Statistics *(BBS 2004)*, which are used to estimate the total household, industrial, and drinking water abstractions over time.

Data on the number of high-yielding wells in operation at the local towns were collected from the Department of Public Health Engineering (DPHE), Dhaka, including the temporal growth in the number of wells. Abstraction by these wells was estimated using average operation time multiplied by the discharge capacity of the well. These are simulated as point abstractions in the model. Deep hand-pumped well locations are available for about 600 wells in the model area *(DPHE/DFID/JICA 2006)*, and these are included as abstraction points in the model. As the number of wells increases with time and data for those are not available, the rate of abstraction for these wells was increased to accommodate increased withdrawal from the respective depths.

7.9.2.2.2 Estimation

In the model area (and also other parts of Bangladesh) nearly 100% of the population rely on groundwater for their drinking water. The dependency on groundwater started to grow in the 1960s and in the 1990s the figure reached 100%. Domestic, non-drinking use is still under 30% from these resources (http://faostat.fao.org/ accessed on 21 July 2008). Most, if not all, of these demands are meet by the shallow hand tube wells operated at shallow depth (<100 m) bgl. The per-capita amount of water consumption per day (C_{pc}) was estimated for individual year as Eq. 7.2.

$$C_{pc} = \left(\frac{\left(d \times p_{dgw}\right) + \left(h \times h_{hgw}\right)}{p_{tot}} \right) \quad \text{.....Eq. 7-2}$$

In the equation,

d = drinking water use, 5 l/day/person (http://faostat.fao.org/ accessed on 21 July 2008)

P_{dgw} = population count depended on groundwater for drinking

h=domestic water use, 70 l/day/person (http://faostat.fao.org/ accessed on 21 July 2008)

h_{hgw}= population count depended on groundwater for household purpose

P_{tot} = total population

The drinking water requirement was taken as 5 l/day. This estimated per-capita abstraction rate was then used to estimate the total abstraction of water in different years based on population in the respective year. These abstraction volumes then converted into rate of abstraction in different year by dividing total population of particular year. Finally, these different abstraction rates were converted to a rate with respect to 2006, for which the population density dataset (Figure 7-8) can be applied to distribute the domestic groundwater abstraction throughout the model domain for different stress periods.

It is considered that deep aquifer development in the region had started in the middle of the 1990s with deep hand-pumped tube-wells. It is assumed that each deep tube-well meets the demand of drinking water for 30 families with 5 members in each i. e., 750 litre/day. This is a conservative estimate, as in a densely populated area in central Bangladesh it is found to be ~2500 litre/day (*van Geen et al. 2003a*). There is no actual data on the number of deep tube-wells in operation in the region. In the current modelling effort 1600 wells are considered to start operation during 1996 (K. M. Ahmed, personal communication). From that number with a 10% increment for the following years (up to 2008), deep groundwater abstraction was estimated. However, abstractions are applied to the model as point abstraction through 600 wells by increasing the rate of abstraction at those points to accommodate the greater number of wells (Figure 7-9). There is no abstraction from deeper level in the eastern Hilly area as there the geology is complex, most of the wells are shallow and in some cases people depend on dug wells *(WWF and DoA 2007)*.

For urban areas, abstraction is considered to be by high yielding, motorised pumps. The number of wells in operation in different years in different local urban townships was collected from DPHE (Figure 7-9). For individual wells a 20 l/sec rate is taken to estimate abstraction. The capacity of the wells is 56 l/s but in the model this is reduced to reflect the operation time (~10 hours in a day) of the wells.

Separate estimates are not made for industrial abstraction, as the area is not much industrialised. There are some minor industrial activities in the area where population density is also high. Here industries are usually close to or within the local towns, and get water from the urban supply. For these two reasons abstraction for industrial activities have not been considered separately.

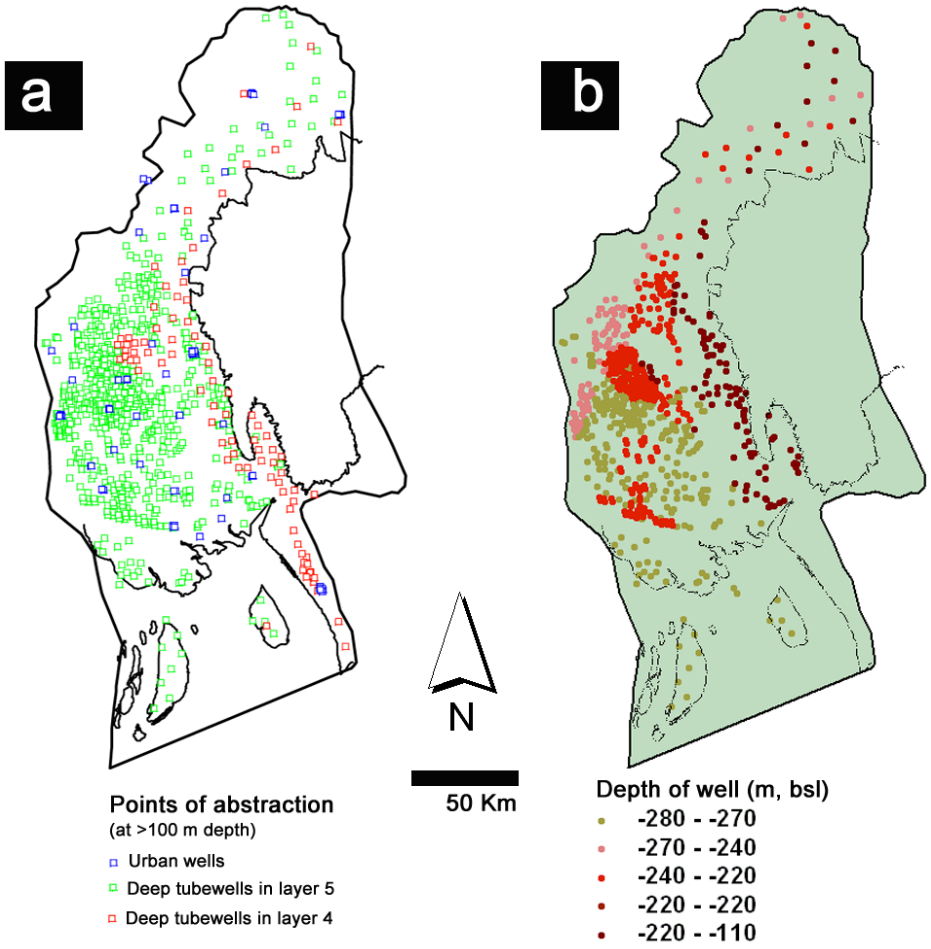

Figure 7-9: Points of abstraction used in the model and depth of the wells.

Chapter 8
Model Results

Models contribute to understanding groundwater flow-systems and assist management planning for groundwater resources. The range of models (Table 7-1) developed under the current project might have a range of applications, such as evaluating the effects of geological representation on the simulation of groundwater flow, evaluating arsenic breakthrough from the shallower to the deeper part of the aquifer, estimating the magnitude of submarine groundwater discharge, evaluating the sustainability of the deep groundwater resource, and trans-boundary groundwater studies. The objective of the current research requires evaluation of the models against a set of observations and independently-derived groundwater age estimates. The models have been ranked according to their performances against these criteria. This chapter presents and describes the model results and their comparison against the field observations of head and groundwater age.

8.1 Hydraulic comparison

Hydraulic heads are conventionally used for groundwater model calibration *(e. g., Freeze and Cherry 1979; Kresic 2007)*. The BWDB has established a network of >1200 piezometers to monitor water level at national scale (section 3.4.1) but this network is restricted to the shallower part of the aquifer system (median depth <30 m). The Bangladesh Agricultural Development Corporation (BADC) has a network (at much lower resolution) for monitoring groundwater head at the depths of irrigation abstraction, which at 30 to 90 mbgl is still in the shallower part of the aquifer system. As there are no widespread monitoring data available for deeper levels, the magnitude and spatial pattern of monitored hydraulic head at 90 mbgl (Figure 7-1) were used for comparison with the simulated heads at the same depth. Due to representation of the recharge as a prescribed head at the top layer of the model (section 7.5.3 and 7.9.1) simulated head at shallow levels should be expected to be slightly higher than the observed head. One multi-level nest of 5 wells over the depth range 25 to 355 mbgl at the centre of the study area (Figure 7-1) has been

monitored during 2003 to 2005 by BWDB, and these data have been available to the current project for comparison with the model-simulated head profile across those depths.

8.1.1 Spatial distribution of head at 90 mbgl

A visual comparison of the spatial pattern and magnitude of the head observed at 90 mbgl (see Figure 7-1) was made for the different aquifer representations (Table 8-1, Figure 8-1 and Appendix A8.1). All the model representations simulated the spatial pattern of the hydraulic head adequately. This is thought to be because the head distribution is mostly controlled by the distribution of irrigation pumping which is the same in all the models. The magnitude of hydraulic head was considered adequate if the simulated head was in the range of observed head +/- half of observed head; in effect the maximum allowed error was ± 3 m. The magnitude of hydraulic head is a function of hydraulic properties and pumping. All models gave a reasonable magnitude of the head, except model nM5 (single anisotropic homogeneous aquifer representation) which resulted in a very low hydraulic head throughout (Figure 8-1). Model representation nM5 failed to simulate the head magnitude correctly as a consequence of its single value of high hydraulic anisotropy.

8.1.2 Vertical head profile at Kachua

Only the transient models were used to simulate head at depths 25, 180, 335, and 352 mbgl. The simulated heads were compared with the average of the monthly head derived from the weekly field measurements (Figure 8-2 and Appendix A8.2) at a location 'Kachua', in the central part of the study area. A simple pass-fail test was applied to the different models by comparison to the vertical head profile and the magnitude of the water-level observed at different depths (Table 8-1). All the transient models were found to simulate the observed pattern adequately but the magnitude was found to be grossly in error in the case of model nM5, and model LS1 too low and too high respectively. However, for all models, the simulated hydraulic head annual minimum occurs around February while the observed minimum is around March-April. This is thought due to the representation of recharge as a fixed head at the ground surface in all the models, allowing the aquifer system to take water whenever it needs, while in reality the hydraulic minimum falls during the driest time of the year, coupled with the irrigation abstraction. The simulated minimum represents the irrigation-induced drawdown in the water-table.

8.2 Comparison with measured groundwater ages

Previous investigations (e. g., *Harrar et al. 2003; Zyvoloski et al. 2003; Troldborg et al. 2007*) have emphasized that alternative models of an area with different geological conceptualisations can generate a similar pattern of hydraulic head and in some cases also the correct magnitude of head, but may lead to very different simulations of flow path and travel time to particular locations. A model may be acceptable by reference to heads but inadequate by reference to travel

times. In the current project all the models were used to calculate travel time to 19 grid-blocks (4 of them are <100 m deep), equivalent to positions where groundwater age was estimated independently by ^{14}C activity (see section 5.3.3). Comparisons between the 'goodness of fit' achieved by the different aquifer representations were made through (i) a correlation between groundwater age and travel time, (ii) the median of (groundwater age / travel-time), and (iii) the number of simulated travel times that were equal to the groundwater age determinations.

Table 8-1: Check between simulated and observed hydraulic heads

Models (Aquifer representations)	Head profile		Spatial head	
	Pattern	Magnitude	Pattern	Magnitude
nM1-nM4	Steady state models (no comparison was made)			
nM5	✓	× (too low)	✓	× (too low)
nB6	✓	✓	✓	✓
nM8	✓	✓	✓	✓
nM11	✓	✓	✓	✓
nM13	✓	✓	✓	✓
SC2	✓	✓	✓	✓
SC3	✓	✓	✓	✓
LS1	✓	× too high	Not extracted (computationally expensive)	

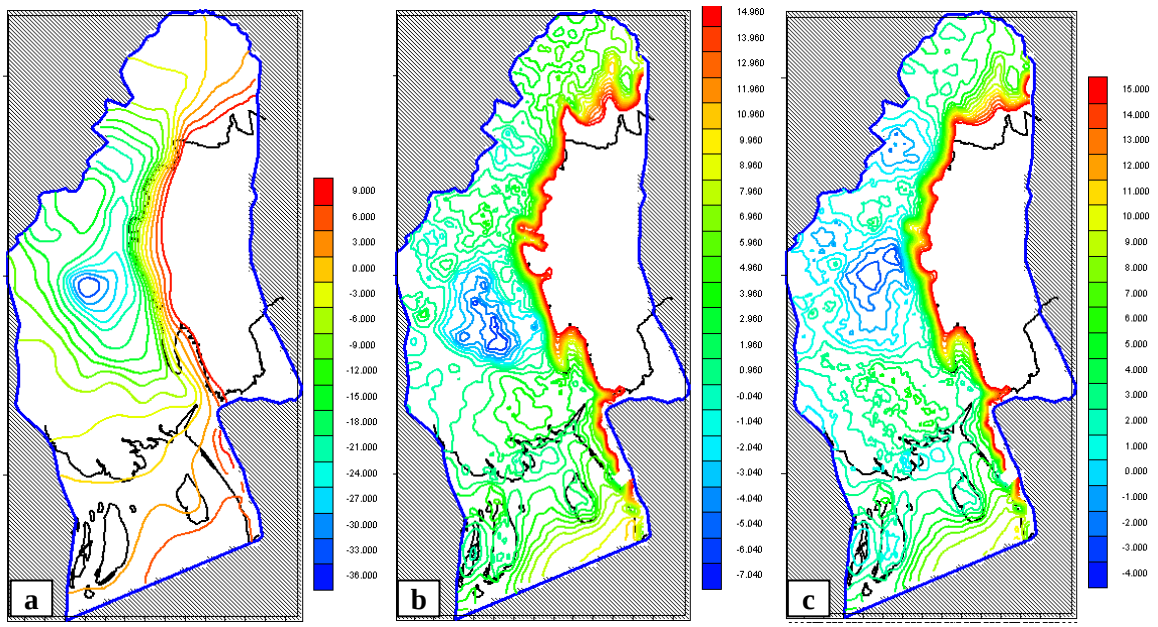

Figure 8-1: Simulated spatial head variation (Feb 2004) at 90 mbgl depth, (a) Model representation nM5 (single layer anisotropic homogeneous aquifer), (b) Model representations nM8 (single layer anisotropic heterogeneous aquifer), (c) Model representation nM11 (4-layer anisotropic and heterogeneous aquifer).

Uncertainties are involved with ^{14}C estimates of groundwater age (section 5.3.3.3); however, some corrections were made with other isotopic constraints towards a better estimate of groundwater age (C2) (section 5.3.3.4). It is found that groundwater at depths >100 mbgl in the model area is less than 8 ka old, with two exceptions where an age greater than 20 ka is derived. The exceptionally old groundwater shows a similar environmental isotopic signature to the 8 ka groundwater. It is to mention that the corrections used to derive the C2 age (section 5.3.3.3) did not consider ^{14}C dilution due to oxidation of organic matter. The corrected age estimates C2 were used in the comparison of the model travel time simulations, and hereinafter groundwater age estimate C2 is used as 'groundwater age'.

8.2.1 Correlation and regression analysis

Pearson correlation analysis was carried out to find the extent of linear relationship between the groundwater age determination and the modelled travel-time. It was found that all the model representations give a positive correlation, however, model representation nM4 (single anisotropic homogeneous steady-state post-development condition) gives a poor correlation (<0.1) (Figure 8-3). Among the transient models all representations give significant ($r \geq 0.5$) correlation except nB6 (4-layer anisotropic and heterogeneous aquifer with a specific correlation length applied to each layer). Model representation nM11 (4-layer anisotropic and heterogeneous aquifer, with correlation length 500 m in each layer) gives the best correlation between groundwater age determination and modelled travel time, followed by model representation nM8 (single layer anisotropic and heterogeneous aquifer). This result demonstrates that heterogeneity is a critical feature in consideration of flow path details in groundwater models of the Bengal Basin.

A linear regression analysis by using the least squares method to fit for groundwater age determination versus modelled travel time was carried out (Figure 8-4). Model representation nM11 (4-layer anisotropic and heterogeneous aquifer) shows a value of 0.44 for R^2 (a measure of fit between the data sets), where other representations have R^2 value less than this. The low agreement between the data sets may be influenced by several issues (see section 8.2.2).

In every model representation the best fit line was compared with the 1:1 line of the data sets. It is found that model representations nM5 (single layer anisotropic and homogeneous aquifer) and nM8 (single layer anisotropic and heterogeneous aquifer) have good agreement (slope, m>0.9), and are parallel to but non-coincident with the 1:1 line. In contrast, model representations based on sand and silt-clay fractions SC2 (single layer anisotropic and heterogeneous aquifer) and SC3 (4-layer anisotropic and heterogeneous aquifer), and the *stacked-mosaic-continuous* silt-clay layer representation LS1 (9-layer anisotropic and heterogeneous aquifer) have a good agreement (m>0.7) with 1:1 line and are approximately coincident with the 1:1 line. The close proximity of best fit lines to the 1:1 line with reasonable slope values indicates the quality of the model

representations. This result demonstrates that an element of hydrostratigraphy is beneficial in consideration of flow path detail in groundwater models of the Bengal Basin.

In every case groundwater age determinations were divided by the model estimated travel time leading to 19 values for every model. The median values of these were calculated for each model (Table 8-2 and Figure 8-5). A median value close to or equal to 1 (hereinafter 'unity') is expected. The median values also indicate if a model over- or under-estimates the simulated travel time compared to groundwater age determinations. A median value greater than unity indicates under-estimation of travel time, while a value less than unity represents over-estimation. By this method it is apparent that model representations with higher values of anisotropy (nM5) over-estimate the travel time, while representations incorporating extreme heterogeneity with spatially varied anisotropy (nM13) under-estimate the travel-time. More moderate values of anisotropy and heterogeneity, and a degree of hydrostratigraphy are more successful in reproducing the groundwater ages.

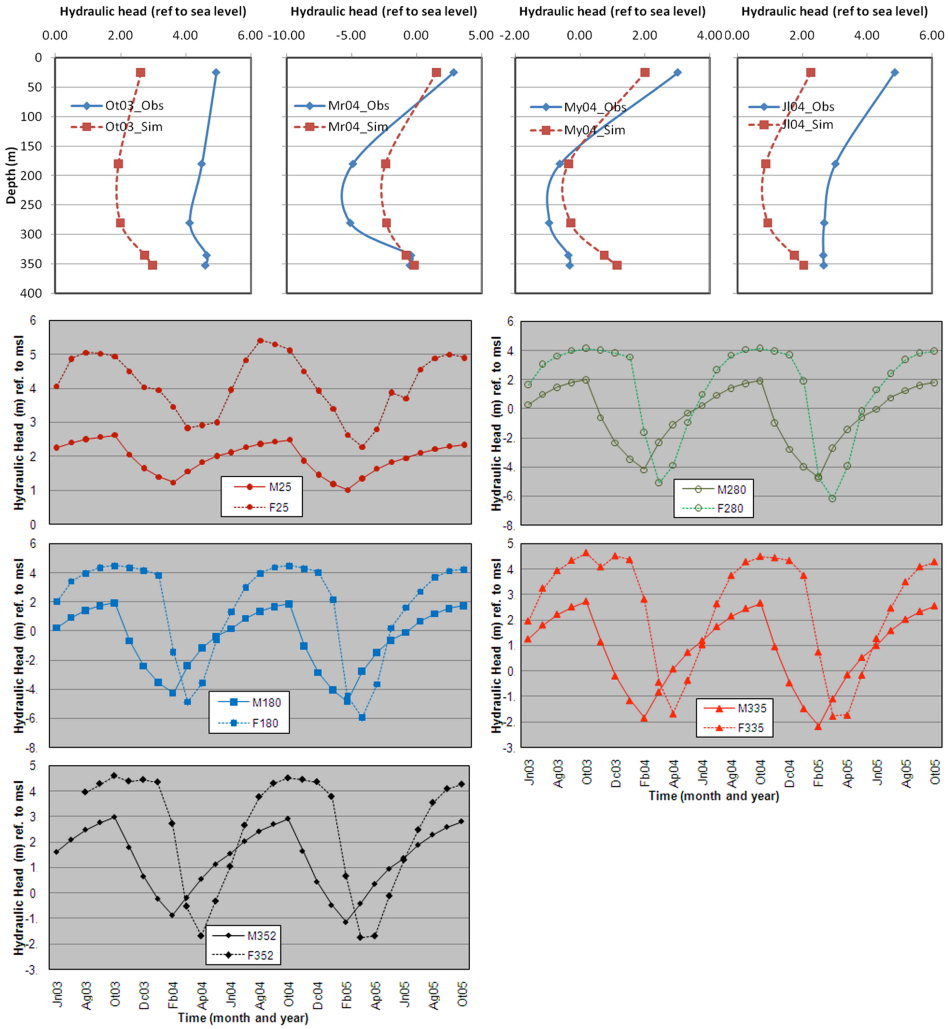

Figure 8-2: Comparison of observed and simulated hydraulic head profile over different months (upper panels) and observed and simulated hydrograph for Model nM11 (lower panels). In the lower panels legend 'M' indicate simulated while 'F' indicate monthly average of observed field data, and number in association indicates the depth in mbgl.

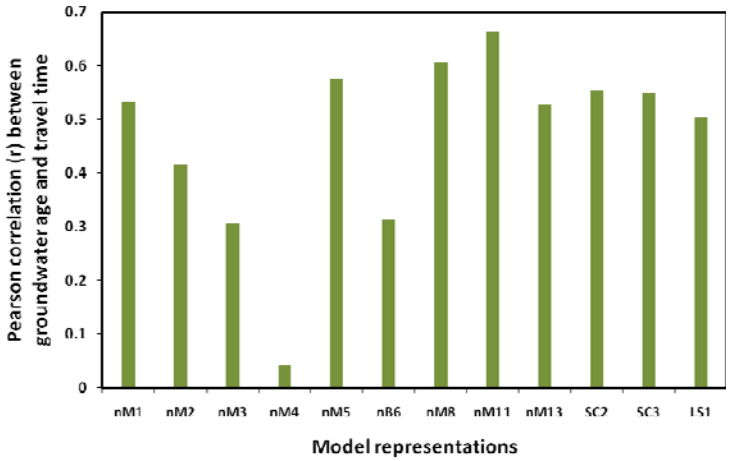

Figure 8-3: Pearson correlation coefficient (r) between models estimated travel times and groundwater ages.

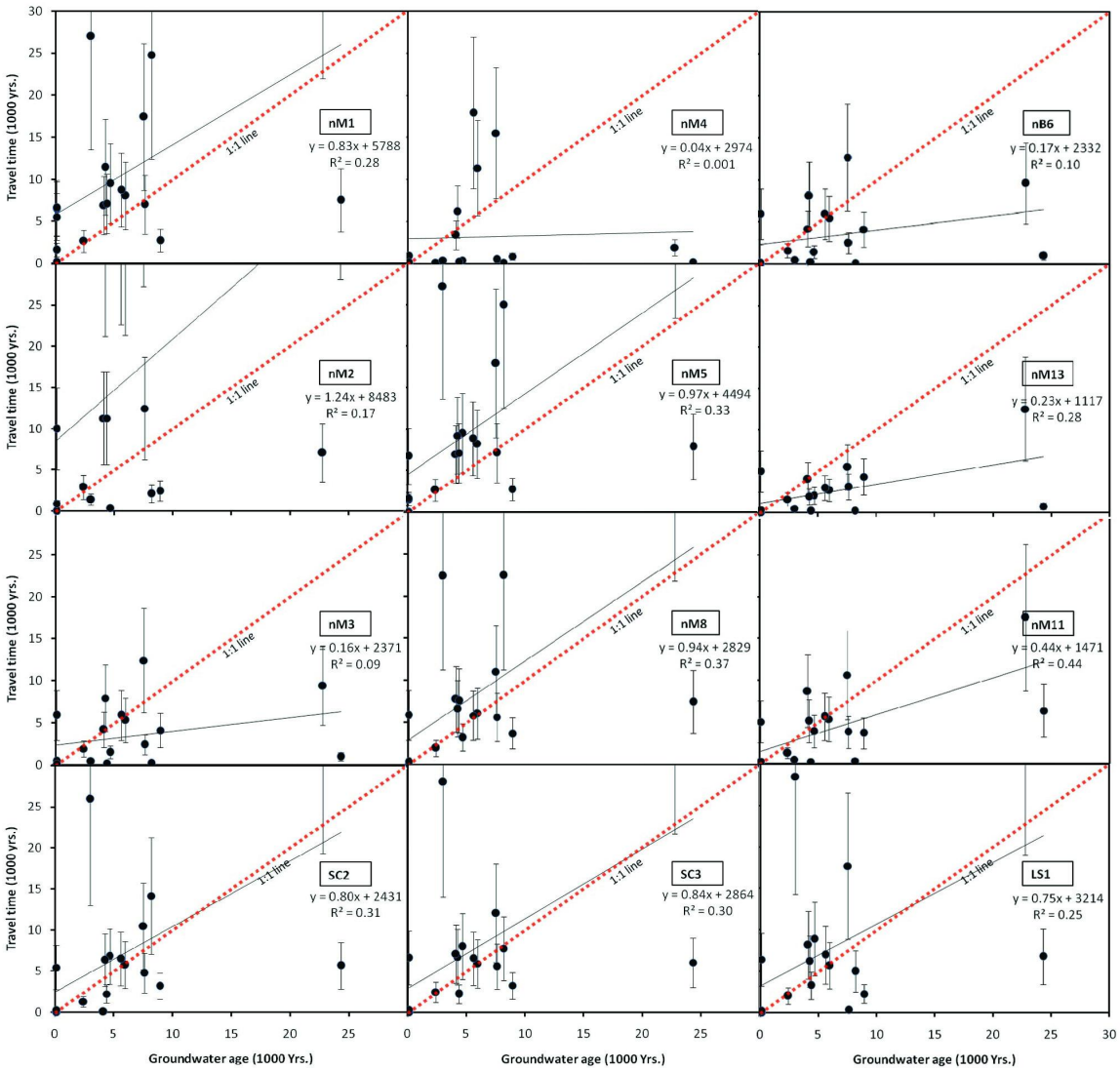

Figure 8-4: Scattered plot of groundwater age vs travel time. In the graphs best fit line (black line) and 1:1 line are shown. Note the ±50% error bar in travel time axis. There are some travel times in some model representations greater than 30 ka and there are not shown on the graph but are included in the analysis.

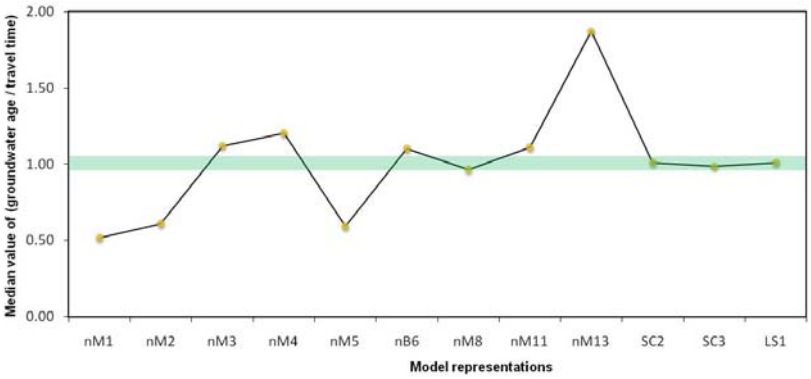

Figure 8-5: Median of (groundwater age / travel time) for each model representation (n=19 for each).

8.2.2 Number of correct age estimations by the models

A close look at the individual wells, however, reveals that the model does not reproduce individual sample ages correctly. The plots of groundwater ages vs. the simulated travel-time show a great amount of scatter about the 1:1 line (Figure 8-4). These discrepancies are compounded by the fact that travel-time at a point in space is an integration of the upstream velocity field, so that errors in calculated velocities can accumulate along a modelled flow path *(Sanford et al. 2004)*.

Factors that could contribute to the discrepancies between the simulated travel-times and groundwater age determinations are:

(1) Groundwater ages were determined for samples collected from a tube-well, screen volume 0.03 m^3, while simulated travel time is the mean-travel time of no less than a 1.00E7 m^3 model grid volume. Groundwater age in an alluvial aquifer is found to vary over the length of a well screen *(Weissmann et al. 2002; Sanford et al. 2004),* however studies on the travel-time variation on the scale of a model grid which could be substantial, are rare. Sanford and Buapeng *(1996)* discussed the importance of model discretization of the individual sand and clay layers to capture the travel-time variability, though this is not possible in complex alluvial aquifers.

(2) Although ^{13}C data were used in this study to "correct" the ^{14}C ages, other carbonate reactions can give age variations of a few to several thousand years *(Plummer et al. 1994)*. Another potential source of error is the loss of ^{14}C along the flow path by diffusion into clay layers (*Sudicky and Frind 1981; Sanford and Buapeng 1996; Sanford 1997*) which has not been considered in this study, although it may lead to a significant over-estimation of groundwater age in a multi-layered alluvial aquifer systems (*Sanford and Buapeng 1996; Sanford 1997*).

(3) Ages of groundwater at depth in the study area, which range between 3,000 and 8,000 years, indicate that these would have been affected by changes in the flow regime over this time. In this study sea-level is considered at its present day level throughout, although it has mostly been above the current level in the recent past (Figure 3-6). A detailed paleo-flow simulation would be required to capture the effect of sea-level changes, which is not justified by the uncertainty in the

data. Sea-level induced gradient changes would not have affected the deep flow system as much as the shallow system due to delayed adjustment *(see Tóth 1995; 2009)*.

The relative contribution of these factors cannot be quantified for individual points on account of the heterogeneity of the aquifer system. However, the points sampled for C-14 dating are located in the southern part of the modelled region (Figure A8.3 in appendix) where lithological data density are less; the low density of data may have influenced the homogeneity scale used in the models.

Comparisons have however been made to judge which model representation gives the greatest number of correct travel-time estimates, relative to the groundwater age determination. 'Correct' is taken as ± 50% of the travel time simulation. This large range was allowed to compensate the effect of aforesaid errors. In numerical analysis a value of '100 years' has been assigned to the 'modern' groundwater (in terms of ^{14}C activity). It is found that model representations SC3 (4-layer anisotropic and heterogeneous aquifer) and nM8 (single layer anisotropic and heterogeneous aquifer) simulate travel times successfully most frequently (Figure 8-6). It follows that where supportable by data, both hydrostratigraphy and heterogeneity should be described in order to optimize model representation for simulation of solute transport.

8.3 Ranking the models

The different model representations have been ranked according to their performance as judged by simulation of hydraulic head, and replication of groundwater ages as travel time (Figure 8-7). The model representations nM8, nM11, SC2 and SC3 all give travel times close to the determined groundwater ages. Among these successful model representations nM8 and SC2 are single layer anisotropic and heterogeneous aquifer representation. The difference between nM8 and SC2 is the method of assigning effective hydraulic conductivity. In nM8 hydraulic conductivity is calculated assuming the homogeneity of the lithological units persists over 500 m^2 spatially, while the SC2 calculation is based on the fraction of sand and silt-clay. Models nM11 and SC3 are 4-layer, anisotropic heterogeneous aquifer representations, and effective hydraulic conductivity was calculated as for nM8 and SC2 respectively, but for four vertical layers in each case.

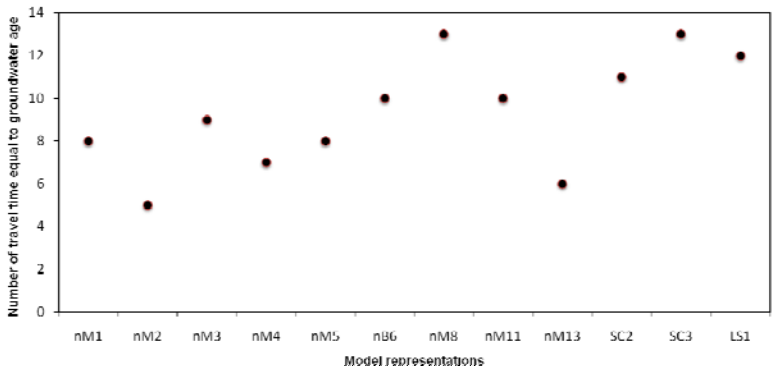

Figure 8-6: Number of travel time equal to groundwater age simulated by different model representations out of 19 (see text).

Model representations nM8 and SC3 are found to be superior among the successful models because they can simulate the greater number (13) of groundwater ages as travel times, with a median of (groundwater age / travel time) value close to 1 (Figure 8-4 and section 8.2.2). All the model representations, nM1-SC3, incorporate lithological heterogeneities in a particular way over a certain thickness leading to anisotropy at every depth of the aquifer, restricting groundwater flow in the vertical direction. In reality, groundwater flow responds to the individual silt-clay layers, and flow lines can penetrate as far as the top of a silt-clay layer, as determined by topography. Model representation LS1 (9-layer anisotropic and heterogeneous aquifer) was designed in a way to address this limitation. The spatial hydraulic head outcome could not be extracted for this representation due to computational limitations of the data-viewing program, however the pattern of the simulated vertical head profile was reasonable (Appendix A8.2). The magnitude of head was too high, possibly because of sand and silt-clay isolations, and the inadequate resolution of layering in respect of the hydraulic effect of sand and silt-clay isolation. The model LS1 successfully simulates a significant number (12) of groundwater age determinations as travel times, but some simulated travel times were very long compared to the groundwater ages. This model representation may be improved further with a larger number of layers, but computational limitations would need to be overcome. Consideration of heterogeneity (both in spatial and vertical directions) in greater detail improves the performance of groundwater models of the Bengal Basin.

Table 8-2: Comparison of groundwater age and simulated travel-time

Models (aquifer representations)	Correlation between groundwater age and travel time	Median value of (groundwater age / travel time)	Number of travel time equal to groundwater age
nM1	0.53	0.52	8
nM2	0.42	0.61	5
nM3	0.31	1.12	9
nM4	0.04	1.20	7
nM5	0.57	0.59	8
nB6	0.31	1.10	10
nM8	0.61	0.97	13
nM11	0.66	1.11	10
nM13	0.53	1.87	6
SC2	0.55	1.01	11
SC3	0.55	0.99	13
LS1	0.50	1.01	12

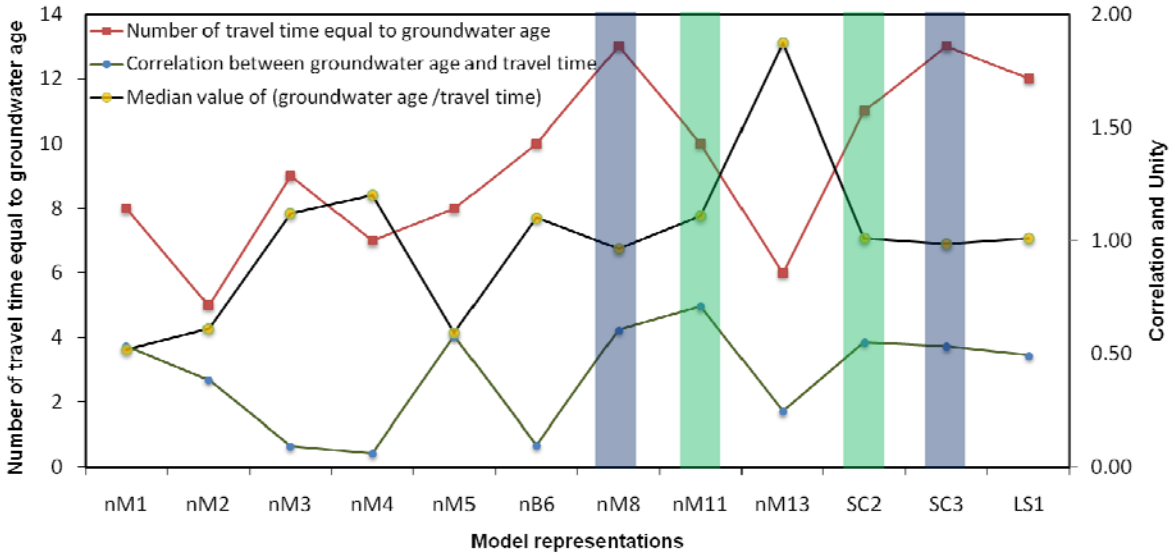

Figure 8-7: Summary of comparison of groundwater age and travel time simulated by different model representations. Note colour bars represent the different good model representations of aquifer.

8.4 Water balances of the models

ZONEBUDGET is a program that uses flow results from MODFLOW to construct the water budgets of individual zones *(Harbaugh et al. 2000)*. The total model area was sub-divided into three zones (Figure 8-8). Water balances were estimated for all the transient models (except LS1) and one pre-development steady state model (nM3) (Table 8-3). The main items of the flow budget are the sub-marine groundwater discharge (SGD), flow to wells, flow to greater depths (which ultimately discharge to wells or sea), and recharge for every sub-basins / zones in the form of flux of water. These components of the water budget were found to change over time as the development history has been changed; however, for simplicity the budget analysis is described for the year 2003.

Recharge to the groundwater model domain is represented by prescribed head at the top boundary, which is why amount of water contributing to the water-table is determined as a modelling result. It is here defined as the total volume of water that enters from the constant head upper boundary over a period of time to the first layer divided by the area of land within the model domain. It is found that the amount of recharge is dependent on the hydraulic conductivity and the pumping; both have a proportional relationship to the amount of recharge. Recharge to the water table ranges from around 300 to 500 mm/year over the different geological representations for the year 2003. Pre-development models indicate this to be <200 mm/year when there is no abstraction. Under natural conditions the amount of water recharged is balanced by discharge to the sea or local topographic low points, but when pumped abstractions occur recharge is increased if there is the water availability at the surface. Higher ground is found to contribute more to the recharge than the lower ground. Potential recharge over large portions of the region has been estimated as 300–600 mm/year and greater by several methods considering precipitation,

evapotranspiration, and seasonal water-table fluctuation *(MPO 1987; WARPO 2000)*. The model simulated values fall within this range.

Water-well discharge is found to be mostly from the shallower depth (<100 m) where abstraction was around 100 times than that of deeper abstraction in the year 2003. Recharge to groundwater below 100 m and 200 m was estimated to be greater from the hilly areas than the floodplain due to the influences of the topographic gradient and aquifer anisotropy. However, amount of water calculated as contributing to those depths is influenced by the representation of the lithology in the models. It is found that models with higher anisotropy and large-scale upscalling of heterogeneity provide less recharge to depths >100 m. Model representations SC3 (4-layer anisotropic and heterogeneous aquifer) and nM8 (single layer anisotropic and heterogeneous aquifer) simulated a recharge rate 23 mm/yr and 46 mm/yr per unit of total-land-area respectively at depth greater than 200 m (Table 8-3). These range are comparable with earlier estimate 17 mm/yr derived from a basin scale model (*Michael and Voss 2009a*), and also radiocarbon derived estimates 2-26 mm/yr (section 5.4.4). Submarine groundwater discharge (SGD) is found to decrease sharply with groundwater development, and also varies between model representations. It is to note that the estimated range (0.3 and 0.6 cm/yr per unit of total-land-area for models SC3 and nM8 respectively) of SGD (Table 8-3) has similarity with earlier model investigations, 0.4 cm/yr per unit of land area (*Michael and Voss 2009a*) but not with Basu et al *(2001)* who determined SGD from the marine strontium isotope record to be 81 cm/yr per unit of land area. Harvey (*2002a*) argued this 'strontium derived' SGD to be unrealistically a high value.

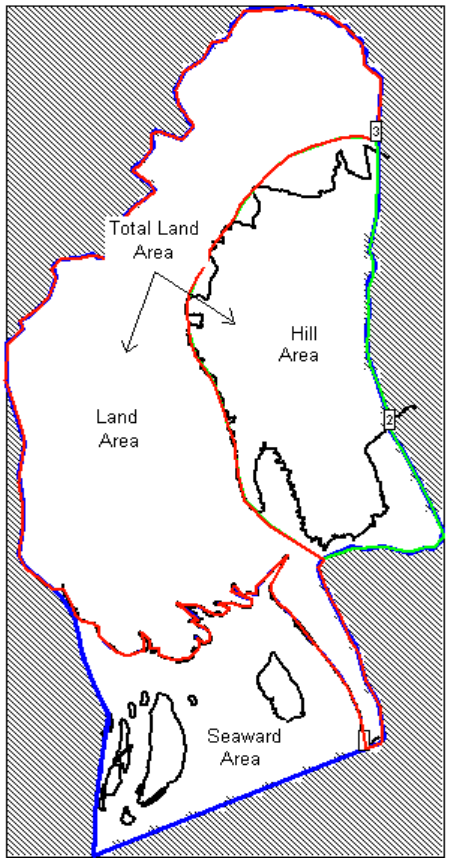

Figure 8-8: Zones of water balance analysis.

Table 8-3: Water balance analysis for 2003 for different model representations (all values as cm/yr.)

Model →		nM3	nM5	nB6	nM11	nM8	nM13	SC2	SC3
γSGD^	Flux over land area	1.3	0.1	0.6	0.6	0.6	0.7	1.0	0.3
Groundwater Abstraction*	Shallow (<100m)	0.0	40						
	Deep (>100 m)	0.0	0.4						
Flux below >100 m	Land$	6.1	0.7	7.0	6.0	4.5	7.2	3.8	2.7
	Hill†	22	4.8	22	18	17	31	15	10
	Average^	12	2.2	12	10	8.9	16	7.9	5.3
Flux below >200 m	Land$	3.0	0.1	3.4	2.9	1.7	5.1	1.2	0.7
	Hill†	13	3.1	13	11	9.9	27	8.4	5.3
	Average^	6.7	1.2	6.8	5.8	4.6	13	3.8	2.3
Recharge	Land$	9.2	35	39	40	40	36	42	38
	Hill†	34	39	51	52	57	60	60	47
	Average^	18	37	43	33	46	44	48	41

Note:

'SGD' stands for Submarine Groundwater Discharge

γ = Estimated as the net discharge to the constant head in the sea-ward side of the model

^= calculated as flux over total land area 2.2 x 10^{10} m^2

†= Calculated as flux over the eastern hilly area 7.9 x 10^9 m^2

$= Calculated as flux over western plain-land, 1.4 x 10^{10} m^2

8.5 Recharge zone delineation

The models were applied to describe the flow-paths of groundwater from recharge to the point in the aquifer system where groundwater age has been determined. This was achieved by backward particle tracking from the points of interest to the source of recharge. All the model representations indicate that shallow (<100 m deep) groundwater comes from local recharge. In their differences with respect to points in the deep groundwater flow system, the illustrations (Figure 8-9 and for others see appendix A8.3) demonstrate the significance of adequate representation of the aquifer heterogeneity, as simulated recharge origin is seen to vary from local to distant at some points between the different representations. Local origin of deep groundwater occurs when model structure allows (Figure 8-9 and for full illustration of results see appendix A8.3). It is apparent that simulated flow-path is dependent on the degree of representation of geological detail, and hence upscaling of small-scale heterogeneity increases the confidence in the model results. On the contrary, upscaling of small-scale-heterogeneity taking smaller correlation length than the representative of real homogeneity-dimension leads to an unrealistic hydraulic continuity.

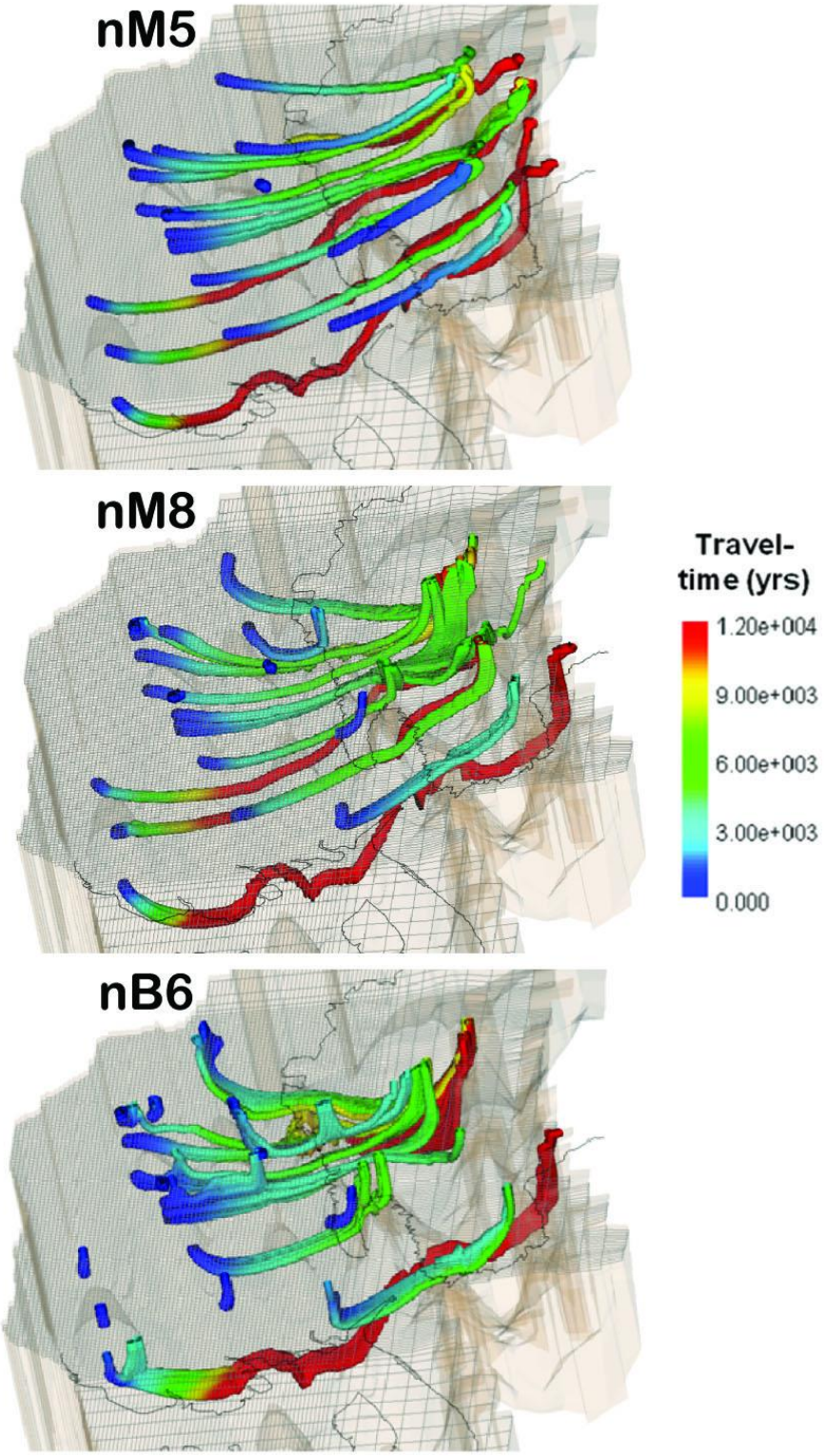

Figure 8-9: Flow-paths to the grid-locations of ^{14}C groundwater age estimates. In model representation nM5 (single layer anisotropic homogeneous aquifer) all deep groundwater derives from the eastern hilly areas. In model representation nM8 which incorporates heterogeneity in a single layer anisotropic aquifer, deep groundwater at some points is derived locally from recharge closer to the deep tube-well sampled. In model representation nB6 (4-layer anisotropic and heterogeneous aquifer) deep water comes from shallower depth in the local area at a number of points. Note that the model domain is cropped in the north and south to zoom-in on the area of interest, and for reference the international boundary and the coastal boundary of Bangladesh are marked. Colour bar indicates the travel-time in years.

For the model representations nM8, SC3, nM11, and LS1, the successful representations for groundwater age simulation, flow-paths from many points between 210 to 250 m depths in a high resolution grid were simulated back towards their recharge location. All models indicate water at depth comes predominantly from the basin margin hilly areas in the east (Figure 8-10). However, there are some locations in the south where water at depth originates in part from the shallower depth in the local area. This shallow contribution may be associated with the poor representation of the geology due to low density of data. Otherwise, the modelling is indicating that induced recharge from these local regions would carry arsenic from the shallow regions and ultimately compromise the arsenic security of deep groundwater abstraction at these points.

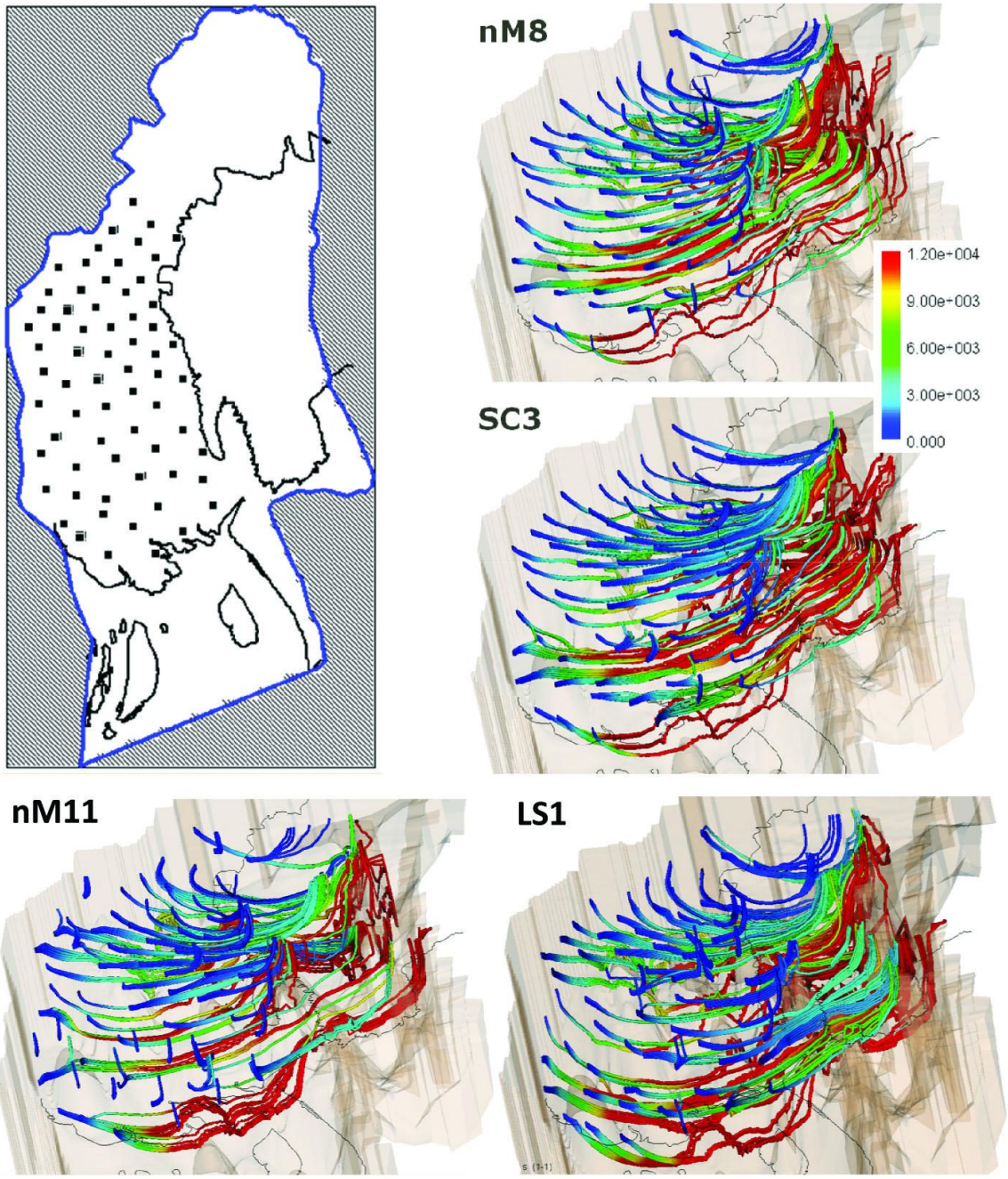

Figure 8-10: Flow-path tracked backward from the grid-location marked on the left figure at 210 to 250 m depth for model representations nM8, SC3, nM11, and LS1. The flow-paths show that almost entire groundwater at depths comes from eastern hilly areas. Colour bar indicates the travel-time in years.

8.6 Synthesis of key points

In this chapter, the range of model representations of the hydrostratigraphy has been applied to simulate head variation throughout the study region, and to derive recharge zones and groundwater travel time to the points where groundwater ages were determined by ^{14}C analysis.

A comparison was made of the ability of the seven aquifer representations used for groundwater flow modelling to reproduce the observed spatial and vertical variation in hydraulic head, and groundwater travel times. The most successful representations were nM8, nM11, SC2 and SC3. All these representations incorporate anisotropy and spatial heterogenety. Representations nM8 and SC2, being single-layer representations, are the more simple. Incorporation of layered hydrostratigraphy is not justified on the basis of the independent tests provided by the groundwater age determinations presented here. There remains the possibility that where there is a greater density of lithological data than in the current research, it may become important to include hydrostratigraphy.

Chapter 9
Addressing the Research Objectives

The enormous scale of As contamination of shallow tube-wells emerged gradually during the 1980s in West Bengal *(Mazumder et al. 1988)* and was recognised in Bangladesh in the 1990s *(BADC/MMI/HTS 1992)*. Since then, no solutions have been implemented that provide As-free water to the majority of the affected population leading to world's largest mass poisoning *(Smith et al. 2000)*. Of the mitigation options *(Ahmed et al. 2006)* (domestic water treatment using iron oxide filters, well-switching, installation of deep tube-wells to 'As-free' parts of the aquifer, and others), deep tube-wells, usually taken to be >150 m *(Bhattacharya et al. 1997)*, offer the most popular, practical and economic solution *(Ravenscroft et al. 2009)*. Deep groundwater continues to be targeted, yet there is limited understanding of the variety of environments that host As-free groundwater, found at depths ranging from <30 m to >200 m *(Ahmed et al. 2006; DPHE/DFID/JICA 2006)* depending on the geological context, and there are concerns (*DPHE/DFID/JICA 2006; Michael and Voss 2008; Burgess et al. 2010*) that deep groundwater may in time become vulnerable to invasion of As from shallow depths.

The research was aimed at an improved understanding of the hydrogeology of the deeper regions of the alluvial aquifer in southern Bangladesh, and hence to develop tools (here, computer models) to be used for assessing the security of the deep (essentially arsenic-free) groundwater resources against invasion by arsenic from the shallower part. This chapter is designed to discuss the extent to which those objectives were met and to draw conclusions. The objectives of the research as mentioned in section 1.2 are reiterated here for clarity. The research addressed several research questions as follows -

- How can the deeper aquifers best be represented, in order to investigate their vulnerability to vertical leakage?

- There are several sources of uncertainty - how can uncertainty be incorporated?
- How is arsenic distribution linked to groundwater flow at local to regional scale, from shallow to deeper region of the aquifer?
- Can hydrochemical and isotopic profiles be used to constrain the hydrostratigraphy as reproduced in groundwater models?
- What further research is needed in order to develop useful guidelines for sustainable development of the deeper aquifers?

9.1 Aquifer representation in groundwater models

How can the deeper aquifers best be represented, in order to investigate their vulnerability to vertical leakage?

There are many ways (and more; including stochastic realisations) testable against independent data:

- Through anisotropy- e. g., a single layer homogeneous anisotropic aquifer
- Through heterogeneity – e. g., a single layer vertically homogeneous but spatially heterogeneous anisotropic aquifer
- Through hydrostratigraphy – e. g., a multi-layer heterogeneous aquifer with spatially-vertically varied anisotropy; scale of homogeneities could be varied in spatial direction as well as in vertical layers (see section 4.3.6)

It is found that aquifer heterogeneities are better represented in spatially and vertically varied anisotropic representations than in homogeneous representation of the whole aquifer system.

Some studies of hydrostratigraphy at local to sub-regional scale in the Bengal Basin have found that the shallow floodplain aquifer is separated from deeper groundwater by a silt-clay aquitard eg in West Bengal (*Mukherjee et al. 2007b; McArthur et al. 2008*), western Bangladesh (*JICA 2002; Burgess et al. 2007*), and Khulna in the south-west *(LGED/BRGM 2005)*, and the coastal region *(DPHE/DANIDA 2001)*. The aquitard has additionally been reported as regionally persistent across central *(BADC/MMI/HTS 1992)* and south-east Bangladesh *(Ravenscroft and McArthur 2004)*. Here compilation of data from >2,000 deep boreholes *(DPHE/DFID/JICA 2006)* has led to a better-constrained interpretation. The reanalysis of 1573 drillers' log from the southern part of Bangladesh (Figure 3-5) indicates the discontinuous nature of the sediments at basin scale. This discontinuous nature of the sedimentary units should be expected due to the fluvio-deltaic nature of sedimentation throughout the region over the past one millions years (see chapter 3). This research subsumes the basin-scale aquifer as a single aquifer-system, locally containing less-

extensive aquifers at a sub-basin scale, but acting as a single mega-aquifer at basin scale. The aquifer system is named 'the Bengal Aquifer System', and rests on the Upper Marine Shale (see chapter 4).

Representation of geological observations in groundwater models is an issue of conceptualisation of lithological heterogeneity in the aquifer. This issue is complicated, in fluvial-deltaic aquifers, where heterogeneities occur at a much smaller scale than to the model grid, and the spatial availability of data is sparse. Carrera et al. *(1993)* state that "accurate characterization of geological media sounds absurdly utopic". However, the reliability and usefulness of models in guiding development strategies is determined by the scale over which sediment heterogeneities are properly represented in the models.

The effective anisotropy provided by multiple discontinuous layers of silty-clay has been used in a description of a single, anisotropic aquifer at the scale of the entire Bengal Basin by *Michael and Voss (2008)*. In the current project a sub-basinal (south-east part of the basin) model area (Figure 1-1) has been considered, and in addition to making one single representations of the aquifer, several other representations were developed. 589 drillers' logs were used to characterise the hydrogeological framework including 11 petroleum exploration logs, for understanding the deeper geology of the model area (for details see chapter 4). Analysis reveals that in 3D the aquifer can be treated as comprising areas of sand dominance and silt-clay dominance. These were interpreted as stacking of paleo-channels and paleo-interfluves. It is known that the spatial dimension of silt-clays influences the hydraulic properties *(Ababou 1996)* and hence control groundwater flow. In fluvial-deltaic terrain the occurrence of silt-clay units may be random, and so their extent may lead to errors. To address this, several representations of the hydraulic conductivity field were generated (section 7.8) using the drillers' log information, taking different spatial dimensions of the silt-clay units. It is found that increasing the spatial dimension of the silt-clay units increases the effective horizontal hydraulic conductivity and also the effective vertical anisotropy. There is a small number of field hydraulic test (pump test) data available for the region, and attempts were made to relate these to sand-clay fraction of the sequence. Empirical equations were formulated to estimate the effective hydraulic conductivity from the sand-clay percentages. In one approach all silt-clays occurring in a sequence were stacked into a single thin layer leading areas of missing silt-clay zone of aquifer in groundwater models (section 7.8.3).

In the current modelling even the successful model representations fail to simulate adequately groundwater ages at some points in the model domain, and spatially these points are located in areas where lithological data density are less. The low density of data may have influenced the homogeneity scale which was preferentially determined for the areas where data density is relatively high. Model nM8, a single layer model with spatially varied hydraulic conductivity and

anisotropy successfully simulated a larger number of groundwater ages than nM11 (a four-layer model with spatio-vertically varied hydraulic conductivity and anisotropy).

9.2 Sources of uncertainty

There are several sources of uncertainty - how can uncertainty be incorporated?

The research has applied a multi-model approach as advocated by the International Ground Water Modeling Center (IGWMC).

Groundwater models are the simplified numerical representation of natural groundwater systems and by origin contain uncertainties rooted in the numerous assumptions of the mathematical description of the natural system. This question is closely linked to the first, because heterogeneity is a major source of uncertainty. But there exit others, namely: correctness of the conceptual model, accuracy of model parameters; and uncertainties in future stresses *(Carrera et al. 1993)*. This research tried to characterise the uncertainties associated with conceptualisation and model parameters linking both to heterogeneities in a multi-model approach *(*e. g., *Poeter and Anderson 2005)*.

Uncertainties associated with conceptualisation are rooted in the heterogeneities within the aquifer materials (at variety of scale), and boundary conditions. Heterogeneities in the case of a fluvial-deltaic terrain are complex to conceptualise as they occur at smaller scale than the scale of data availability, and they cannot be incorporated explicitly because they are much smaller than the grid size of a model. In the current project, uncertainty due to heterogeneities has been estimated by developing a range of plausible model representations including a range of value for the for silt-clay layer length dimension. Modelling has shown that the smaller the length dimension of silt-clay layers the more the hydraulic-connection. The actual anisotropy of the silt-clay layer is unknown, and a higher resolution of data is desirable. Model validation against groundwater age determinations provided a method of ranking the most appropriate representation (see section 9.3).

To reduce the impact of boundary condition uncertainty, boundaries were extended far away from the area of interest. This extension is done through several critical analyses (for detail see section). The Meghna river in the western boundary of the model was set as a prescribed head in the top model layer but as no flow below. It remains unresolved whether groundwater flow from the eastern hills or elsewhere crosses this line or not in reality. Basin scale modelling (*Michael and Voss 2009a*) indicates this boundary to be potentially a no-flow boundary for reasonable anisotropy, but alternative anisotropy representations and indeed the actual natural condition of the aquifer may allow flow to cross the river at depth. Flow and field observations and future modelling are required to resolve this issue.

Hydraulic conductivity is considered to be the parameter of most influence in controlling groundwater flow. So it was chosen as the means for incorporating heterogeneities into the groundwater models (see section 4.2.7). However, other hydraulic parameters (e. g., storativity, porosity) may also carry significant heterogeneities, and remain as uncertainties unincorporated in the modelling. Recharge has been represented as prescribed head at the top layer of the model, but in reality has a strong seasonality. This as source of uncertainty is thought to be insignificant for the deeper regions of the basin.

9.3 Model constraining by hydrochemical signature

Can hydrochemical and isotopic profiles be used to constrain the hydrostratigraphy as reproduced in groundwater models?

Groundwater models are conventionally constrained by observation of hydraulic head. Here, groundwater chemistry and particularly groundwater age has been successfully used as an additional constraint.

In the current research field samplings (>70 samples) was carried at thirty five locations to develop an understanding of the hydrochemical isotopic variability, and to estimate groundwater age (see chapter 5). Hydrochemical and isotopic data were used to understand their linkage to flow-system. Isotopic observations were of value in understanding of flow system at a large scale. The groundwater models were successfully constrained using comparison of groundwater age estimates against model derived travel-time. The method is limited by uncertainties with the estimation of age using carbon-14. Two different correction methods were used. Although uncertainties remain, this provided a valuable indicator for use in ranking the quality of the different representations of geological heterogeneity.

9.4 Groundwater flow and arsenic

How is arsenic distribution linked to groundwater flow at local to regional scale, from shallow to deeper region of the aquifer?

(1) A causal link between arsenic distribution and the groundwater flow-system, and geological evolution over the last one million years, has been presented which explains all the main characteristics of As distribution including its progression in the reducing fluvial-deltaic aquifer system over geological time. (2) By this hypothesis As is dominantly controlled by groundwater flow with geochemical interaction imposing second-order control. (3) This new analysis sheds light on the overlooked contribution of individual silt-clay layers on the flow-field where previous (*Michael and Voss 2009a*) emphasis has been on evaluating the effective properties of the fluvio-deltaic terrain.

Hydrostratigraphical analysis (chapter 4) shows that the study area is composed of heterogeneous fluvio-deltaic materials, highly discontinuous laterally. Discontinuous clay-silt layers form an effective continuous mosaic layer when stacked (i. e., '*stacked-mosaic-continuous'* defined in section 6.2.1.4), and behaves like a continuous aquitard in terms of its effect on flow-path geometry on a regional scale and hydraulically support a hierarchical flow systems i. e., shallow and deep (Section 6.2.1). The lithological architecture of the basin determined that deep groundwater was recharged from the basin margin throughout Plio-Quaternary time, and hence generally As-free.

Chapter 6 describes 'SiHA (**S**ilt-clay layers **i**nfluence **H**ierarchical groundwater flow systems and **A**rsenic progression in aquifer)' hypothesis which determines that the present distribution of arsenic at local and regional-scale in the Bengal Basin aquifer system is an inevitable result of dynamic equilibrium between two interacting processes, (1) topographically-driven groundwater flow in the aquifer controlled by the distribution of silt-clay layers, and (2) geochemical cycling of arsenic between the solid and aqueous phases. Arsenic is released from the shallower depth and conveyed by the shallow flow-system which restricts it within the shallower level of the aquifer system. The hypothesis explains how arsenic has been present in the groundwater system since the early stages of basin development, and will remain indefinitely, but that groundwater in parts of the basin should be free of arsenic and could be developed cautiously as a sustainable 'arsenic-safe' water supply. It explains all the observed patterns of heterogeneity in arsenic concentration within the aquifer through a single process 'differential flushing' controlled by the architecture of discontinuous silt-clay layers in the aquifer. The hypothesis is developed for the Bengal Basin, but is applicable to all modern fluvial-deltaic regions, whether coastal or not, anywhere in the world.

9.5 Implications for sustainable development

What further research is needed in order to develop useful guidelines for sustainable development of the deeper aquifers?

A higher density of data is required to calculate effective hydraulic conductivity values if smaller measurement volumes is considered *(Schulze-Makuch et al. 1999)*. In case of multi-layer representations nM11, SC3, and nB6 a higher density of lithological data may be needed to get better results because measurement volume are much smaller compare to single-layer model representations nM5 and nM8. Detailed discrete model representation such as LS1 should be able to simulate the flow-pattern and travel-time more realistically upscaled-models, but these detailed models are computationally expensive, and sufficient data are often not available. These representations may be improved by applying finite element modelling where a different homogeneity scale may be used in different areas according to the different grid/element size and the density of data.

The multi-model approach presented can be applied to identify areas of potentially sustainable groundwater development. The best model representations (see section 8.3) should be used for prediction and guiding future strategies for development. However, these models could be improved in consideration of further groundwater ages, particularly, in areas where there is no current agreement with the model travel-time. For this purpose model parameter could be calibrated further, with respect to ^{14}C dates. In addition, more dating and additional lithological data could be used to improve the model parameterisation. There are thousands of tube-wells in operation for which lithological data may be available, to increase the data density. Note that the analysis presented here demonstrates that groundwater flow at depth in the Bengal Basin has always been recharged from the basin margin, and models should therefore be careful to represent this geo-hydrogeological fact.

References

Ababou R (1996) Random porous media flow on large 3-D grids: numerics, performance, & application to homogenization. In: Wheeler MF (ed) Mathematics & application: Environmental studies - mathematical, computational and statistical analysis, IMA volume in Mathematics & its application 79:1-25.

Acharyya SK, Chakraborty P, Lahiri S, Raymahashay BC, Guha S, Bhowmik A (1999) Arsenic poisoning in the Ganges delta. Nature 401: 545-545

Acharyya SK, Lahiri S, Raymahashay BC, Bhowmik A (2000) Arsenic toxicity of groundwater of the Bengal basin in India and Bangladesh: the role of Quaternary stratigraphy and Holocene sea-level fluctuation. Environmental Geology 39: 1127-1137

Acharyya SK, Shah BA (2007) Groundwater arsenic contamination affecting different geologic domains in India - a review: influence of geological setting, fluvial geomorphology and Quaternary stratigraphy. Journal of Environmental Science and Health, Part A 42: 1795 - 1805

Aggarwal PK, Basu AR, Poreda RJ, Kulkarni KM, Froehlich K, Tarafder SA, Ali M, Ahmed N, Hossain A, Rahman M, Ahmed SR (2000) A report on isotope hydrology of groundwater in Bangladesh: implications for characterization and mitigation of arsenic in groundwater, IAEA TC Project BGD/8/016, International Atomic Energy Agency (IAEA), Vienna, pp. 61.

Ahmad J, Misra S, Goldar B (2006) Rural communities' preferences for arsenic mitigation options in Bangladesh. Journal of Water and Health 04: 463-477

Ahmed KM, 1994. Hydrogeology of the Dupi Tila sand aquifer of Barind Tract, NW Bangladesh, Unpublished Ph. D. thesis, University College London, UK, 317 pp.

Ahmed KM (2003) Constraints and issues of sustainable groundwater exploitation in BangladeshProceedings of the International Symposium on Safe and Sustainable Exploitation of Soil & Groundwater Resources in Asia, Okayama University, Japan, pp. 44-52.

Ahmed KM, Bhattacharya P, Hasan MA, Akhter SH, Alam SMM, Bhuyian MAH, Imam MB, Khan AA, Sracek O (2004) Arsenic enrichment in groundwater of the alluvial aquifers in Bangladesh : an overview. Applied Geochemistry 19: 181-200

Ahmed KM, Burgess WG (2003) Surface water and groundwater interaction in Bangladesh hydrogeology. In: Rahman AA, Ravenscroft P (eds) Groundwater resources and development in Bangladesh - background to the arsenic crisis, agricultural potential and the environment:275-295.

Ahmed MF, Ahuja S, Alauddin M, Hug SJ, Lloyd JR, Pfaff A, Pichler T, Saltikov C, Stute M, van Geen A (2006) Ensuring safe drinking water in Bangladesh. Science 314: 1687-1688. DOI 10.1126/science.1133146

Al-Salek JA (1998) Coastal trapping and funneling effects on storm surges in the Meghna estuary in relation to cyclones hittin Noakhali-Cox's Bazar coast of Bangladesh. Journal of Physical Oceanography 28: 227-249

Alam M (1989) Geology and depositional history of Cenozoic sediments of the Bengal Basin of Bangladesh. Palaeogeography, Palaeoclimatology, Palaeoecology 69: 125-139

Alam M, Alam MM, Curray JR, Chowdhury MLR, Gani MR (2003) An overview of the sedimentary geology of the Bengal basin in relation to the regional tectonic framework and basin-fill history. Sedimentary Geology 155: 179-208

Alam MK, Hasan AKMS, Khan MR, Whitney JW (1990) Geological map of Bangladesh, First edn Geological Survey of Bangladesh, Dhaka.

Allison MA, Khan SR, Goodbred SL, Jr., Kuehl SA (2003) Stratigraphic evolution of the late Holocene Ganges–Brahmaputra lower delta plain. Sedimentary Geology 155: 317-342

Anawar HM, Akai J, Komaki K, Terao H, Yoshioka T, Ishizuka T, Safiullah S, Kato K (2003) Geochemical occurrence of arsenic in groundwater of Bangladesh: sources and mobilization processes. Journal of Geochemical Exploration 77: 109-131

Anawar HM, Akai J, Sakugawa H (2004) Mobilization of arsenic from subsurface sediments by effect of bicarbonate ions in groundwater. Chemosphere 54: 753-762

Anawar HM, Mihaljevic M (2009) Comment on "Arsenic release from biotite into a Holocene groundwater aquifer in Bangladesh" by A.A. Seddique, H. Masuda, M. Mitamura, K. Shinoda, T. Yamanaka, T. Itai, T. Maruoka, K. Uesugi, K.M. Ahmed, D.K. Biswas. Applied Geochemistry 24: 483-485

Anderson MP (1989) Hydrogeologic facies models to delineate large-scale spatial trends in glacial and glacio-fluvial sediments. Geological Society of America Bulletin 101: 501-511

Anning DW, Konieczki AD (2005) Classification of hydrogeologic areas and hydrogeologic flow systems in the basin and range physiographic province, southwestern United States Professional Paper 1702 U. S. Geological Survey, Reston, pp. 44.

Aravena R, Wassenaar LI, Plummer LN (1995) Estimating 14C groundwater ages in a methanogenic aquifer. Water Resources Research 31: 2307-2317

Aziz Z, van Geen A, Stute M, Versteeg R, Horneman A, Zheng Y, Goodbred S, Steckler M, Weinman B, Gavrieli I, Hoque MA, Shamsudduha M, Ahmed KM (2008) Impact of local recharge on arsenic concentrations in shallow aquifers inferred from the electromagnetic conductivity of soils in Araihazar, Bangladesh. Water Resources Research 44: W07416. DOI 10.1029/2007WR006000

BADC (2003) Survey report on irrigation equipment and irrigated area in Boro 2003 season Survey and Monitoring Project for Development of Minor Irrigation, Bangladesh Agricultural Development Corporation (BADC), Dhaka.

BADC (2004) Ground water zoning map, Bangladesh Agricultural Development Corporation (BADC), Dhaka.

BADC/MMI/HTS (1992) Deep Tubewell II Project, esp. vol 2.1 Natural Resources Mott MacDonald International (MMI) and Hunting Technical Services (HTS) for the Bangladesh Agricultural Development Corporation (BADC) under the assignment to the Overseas Development Administration (UK), Dhaka.

BARC (1988) Agro Ecological Zones (AEZ) 515 inventory map, scale 1:250,000 Bangladesh Agricultural Research Council (BARC), Dhaka.

Barker JA (1990) A brief theoretical study of fluid migration mechanism in sedimentary basinsTechnical Report: Hydrogeology Series British Geological Survey, Keyworth, Nottingham, pp. 47.

Bashar K, Hafizul I, Ahmed N (2002) Modelling of the groundwater system of Nawabganj Upazila, Dhaka, for determining arsenic transport and the development potentiality of lower aquifer. Bangladesh Geoscience Journal 8: 1-16

Basu AR, Jacobsen SB, Poreda RJ, Dowling CB, Aggarwal PK (2001) Large groundwater strontium flux to the oceans from the Bengal basin and the marine strontitum isotope record. Science 293: 1470-1473

BBS (2004) Statistical year book of Bangladesh Bangladesh Bureau of Statistics (BBS), Ministry of Planning, GoB, Dhaka.

Bethke CM, Johnson TM (2002) Ground Water Age. Ground Water 40: 337-339

Bethke CM, Johnson TM (2008) Groundwater age and groundwater age dating. Annual Review of Earth and Planetary Science 36: 121-152. DOI 10.1146/annurev.earth.36.031207.124210

BGS/DPHE (2001) Arsenic contamination of groundwater in Bangladesh. In: Kinniburgh DG, Smedley PL (eds) BGS Technical Report WC/00/19 British Geological Survey, Keyworth, pp. 267.

Bhattacharya P, Chatterjee D, Jacks G (1997) Occurrence of arsenic-contaminated groundwater in alluvial aquifers from the Delta Plains, eastern India: Options for safe drinking water supply. Water Resources Development 13: 79-92

Bhattacharyya T, Sehgal J, Sarkar D (1996) Tripura Soils (Sheet 1&2). In: Bhattacharyya T (ed) National Bureau of Soil Survey (NBSS) and Land Use Planning (LUP), Nagpur.

Bhuiyan SI (1984) Groundwater use for irrigation in Bangladesh: the prospects and some emerging issues. Agricultural Administration 16: 181-207

Bilham R, England P (2001) Plateau pop-up during the great 1897 Assam earthquake. Nature 410: 806-809

Bouhlassa S, Aiachi A (2002) Groundwater dating with radiocarbon: application to an aquifer under semi-arid conditions in the south of Morocco (Guelmime). Applied Radiation and Isotopes 56: 637-647

Brammer H (1967) Soil Survey Project of Pakistan: Samples from East Pakistan for 14C dating.

Breit GN, Foster AL, Perkins RB, Yount JC, King T, Welch AH, Whitney JW, Uddin N, Muneem AA, Alam M (2004) As-rich Ferric oxyhydroxide enrichments in the shallow subsurface of Bangladesh. In: Wanty RB, Seal RR (eds) 11th International Symposium Water-Rock Interaction, 27 June-2 July, 2004, Saratoga Springs, NY Balkema, New York, pp. 1457-1461.

Buckau G, Artinger R, Geyer S, Wolf M, Fritz P, Kim JI (2000) 14C dating of Gorleben groundwater. Applied Geochemistry 15: 583-597

Burgess WG, Ahmed KM, Carruthers A, Cheetham H, Cobbing J, Cuthbert M, Mather S, McCarthy E (2007) Trends in arsenic concentration at tubewells in Bangladesh: conceptual models, numerical models, and monitoring proxies. In: Bhattacharya P, Mukherjee AB, Bundschuh J, Zevenhoven R, Loeppert RH (eds) Trace Metals and other Contaminants in the Environment, 9:63-84.

Burgess WG, Burren M, Perrin J, Ahmed KM (2002) Constraints on the sustainable development of arsenic-bearing aquifers in southern Bangladesh. Part 1: A conceptual model of arsenic in the aquifer. In: Hiscock KM, Rivett MO, Davison RM (eds) Sustainable groundwater development, Special Publication 193 Geological Society, London, pp. 145–163.

Burgess WG, Hoque MA, Michael HA, Voss CI, Breit GN, Ahmed KM (2010) Vulnerability of deep groundwater in the Bengal Aquifer System to contamination by arsenic. Nature Geoscience 3: 83-87. DOI 10.1038/ngeo750

BWDB (2005) Report on deep aquifer characterization and mapping project, phase I (Kachua, Chandpur) Ground Water Hydrology Division-I, Bangladesh Water Development Board (BWDB), Dhaka.

Caputo R (2007) Sea-level curves: Perplexities of an end-user in morphotectonic applications. Global and Planetary Change 57: 417-423

Carrera J, Mousavi SF, Usunoff EJ, Sánchez-Vila X, Galarza G (1993) A discussion on validation of hydrogeological models. Reliability Engineering & System Safety 42: 201-216

Catuneanu O (2002) Sequence stratigraphy of clastic systems: concepts, merits, and pitfalls. Journal of African Earth Sciences 35: 1-43

Catuneanu O, Abreu V, Bhattacharya JP, Blum MD, Dalrymple RW, Eriksson PG, Fielding CR, Fisher WL, Galloway WE, Gibling MR, Giles KA, Holbrook JM, Jordan R, Kendall CGSC, Macurda B, Martinsen OJ, Miall AD, Neal JE, Nummedal D, Pomar L, Posamentier HW, Pratt BR, Sarg JF, Shanley KW, Steel RJ, Strasser A, Tucker ME, Winker C (2009) Towards the standardization of sequence stratigraphy. Earth-Science Reviews 92: 1-33

Chakraborti D, Singh EJ, Das B, Shah BA, Hossain MA, Nayak B, Ahamed S, Singh NR (2008) Groundwater arsenic contamination in Manipur, one of the seven north-eastern hill states of India: A future danger. Environmental Geology 56: 381-390. DOI 10.1007/s00254-007-1176-x

Cheetham H, 2000. Modelling the movement of arsenic to public water supply wells in the deep alluvial aquifer, southern Bangladesh, Unpublished M. Sc. thesis, University College London, London, 73 pp.

Cheng Z, vanGeen A, Seddique AA, Ahmed KM (2005) Limited Temporal Variability of Arsenic Concentrations in 20 Wells Monitored for 3 Years in Araihazar, Bangladesh. Environmental Science & Technology 39: 4759-4766

Clark DI, Fritz P (1997) Environmental isotopes in hydrogeology Lewis Publishers, New York

Coetsiers M, Walraevens K (2009) A new correction model for 14C ages in aquifers with complex geochemistry - Application to the Neogene Aquifer, Belgium. Applied Geochemistry 24: 768-776

Coleman JM (1969) Brahmaputra river: channel processes and sedimentation. Sedimentary Geology 3: 129-239

Craig H (1961) Isotopic variations in meteoric waters. Science 133: 1702-1703

Curray JR (1991) Geological history of the Bengal geosyncline. Journal Association of Exploration Geophysics 12: 209-219

Curray JR (1994) Sediment volume and mass beneath the Bay of Bengal. Earth and Planetary Science Letters 125: 371-383

Curray JR, Emmel FJ, Moore DG, Raitt RW (1982) Structure, tectonics and geological history of the northern Indian Ocean. In: Nairn AE, Stehli FG (eds) The Ocean Basins and Margins:107-112.

Cuthbert M, 1999. Modelling the transport of arsenic to hand tubewells in the Holocene alluvial aquifer of Bangladesh, Unpublished M. Sc. thesis, University College London.

Cuthbert M, Burgess WG, Connell L (2002) Constraints on the sustainable development of arsenic-bearing aquifers in southern Bangladesh. Part 2: Preliminary models of arsenic variability in groundwater. In: Hiscock KM, Rivett MO, Davison RM (eds) Sustainable groundwater development, Special Publication 193 Geological Society, London, pp. 165-179.

Dagan G, Fiori A, Jankovic´ I (2003) Flow and transport in highly heterogeneous formations:1. Conceptual framework and validity of first-order approximations. Water Resources Research 39: 1268. DOI 10.1029/2002WR001717

Das B, Rahman MM, Nayak B, Pal A, Chowdhury UK, Mukherjee SC, Saha KC, Pati S, Quamruzzaman Q, Chakraborti D (2009) Groundwater arsenic contamination, its health effects and approach for mitigation in West Bengal, India and Bangladesh. Water Quality, Exposure and Health 1: 5-21. DOI 10.1007/s12403-008-0002-3

Dasgupta AK, Ghose A, Chakraborty KK (1993) Geological map of India Geological Survey of India, Hyderabad.

Datta S, Mailloux B, Hoque MA, Jung HB, Stute M, Ahmed KM, Zheng Y (2009) Enrichment of arsenic in sediments from the Meghna river bank in Bangladesh: Implication for recycling of arsenic. PNAS (Physical Science, Geology). DOI 10.1073 pnas.0908168106

Davies J (1989) The pilot study into optimum well design: IDA 4000 Deep Tubewell II Project. Volume 2 The geology of the alluvial aquifers of Central Bangladesh. Technical Report WD/89/9, British Geological Survey, Keyworth, Nottinghamshire, UK.

Davies J, Exley C (1992) Short term BGS pilot project to assess the "Hydrochemical character of the main aquifer units of central and north-eastern Bangladesh and possible toxicity of groundwater to fish and human". Final Report. Technical Report WD/92/43R, British Geological Survey, Keyworth, Nottinghamshire, UK.

Davis SN (1969) Porosity and permeability of natural materials. In: de Wiest RJM (ed) Flow Through Porous Media Academic Press, New York, pp. 54-86.

de Marsily G, Delay F, Goncalves J, Renard P, Teles V, Violette S (2005) Dealing with spatial heterogeneity. Hydrogeology Journal 13: 161-183. DOI 10.1007/s10040-004-0432-3

Desbarats AJ, Bachu S (1994) Geostatistical analysis of aquifer heterogeneity from the core scale to the basin scale: a case study. Water Resources Research 30: 673-684

Dhar RK, Biswas BK, Samanta G, Mandal BK, Chakraborti D, Roy S, Jafar A, Islam A, Ara G, Kabir S, Khan AW, Ahmed SA, Hadi SA (1997) Groundwater arsenic calamity in Bangladesh. Current Science 73: 48-59

Dhar RK, Zheng Y, Stute M, van Geen A, Cheng Z, Shanewaz M, Shamsudduha M, Hoque MA, Rahman MW, Ahmed KM (2008) Temporal variability of groundwater chemistry in shallow and deep aquifers of Araihazar, Bangladesh. Journal of Contaminant Hydrology 99: 97-111

Domenico PA, Schwartz FW (1998) Physical and Chemical Hydrogeology, 2nd edn John Wiley & Sons, New York

Douglas AA, Osiensky JL, Keller CK (2007) Carbon-14 dating of ground water in the Palouse basin of the Columbia river basalts. Journal of Hydrology 334: 502-512. DOI 10.1016/j.jhydrol.2006.10.028

Dowling CB, Poreda RJ, Basu AR (2003) The groundwater geochemistry of the Bengal Basin: Weathering, chemsorption, and trace metal flux to the oceans. Geochimica et Cosmochimica Acta 67: 2117–2136. DOI 10.1016/S0016-7037(02)01306-6

DPHE/BGS/MML (1999) Groundwater studies for Arsenic contamination in Bangladesh. Phase I: Rapid Investigation. British Geological Survey (BGS) and Mott MacDonald Ltd (UK).

DPHE/DANIDA (2001) Hydrogeology summary report, Five Districts Water Supply and Sanitation Group (5DWSG), DPHE-DANIDA Water Supply and Sanitation Components, Bangladesh, Department of Public Health Engineering (DPHE) and Danish International Development Assistance (DANIDA), Dhaka, pp. 128.

DPHE/DFID/JICA (2006) Development of deep aquifer database and preliminary deep aquifer map, Final report of first phase, Department of Public Health Engineering (DPHE), GoB and Arsenic Policy Support Unit (APSU), Japan International Cooperation Agency (JICA) Bangladesh, Dhaka, pp. 165.

DPHE/JICA (2008) Evaluation of the performance, village piped water supply system (120 schemes) Department of Public Health Engineering (DPHE) and JICA Bangladesh, Dhaka, pp. 83.

DWASA (2000) Updating of existing groundwater and land subsidence project, Final report, Volume 1, Department of Water Resources Engineering and Institute of Flood Control and Drainage Research, Bangladesh University of Engineering and Technology (BUET), Dhaka Water Supply and Sewerage Authority (DWASA), Dhaka, Bangladesh.

Eaton TT (2006) On the importance of geological heterogeneity for flow simulation. Sedimentary Geology 184: 187-201. DOI 10.1016/j.sedgeo.2005.11.002

EPC/MMP (1991) Dhaka region groundwater and subsidence study Engineering and Planning Consultants (EPC) in association with Sir Mott MacDonald and Partners (MMP). Dhaka Water Supply and Sewerage Authority, Dhaka, Bangladesh.

EROS (2002) Shuttle Radar Topography Mission (SRTM) Elevation Data Set. National Aeronautics and Space Administration (NASA), German Aerospace Center (DLR), Italian Space Agency (ASI). The National Center for Earth Resources Observations and Science (EROS), United State Geological Survey (USGS) Sioux Falls, USA.

Ezzy TR, Cox ME, O'Rourke AJ, Huftile GJ (2006) Groundwater flow modelling within a coastal alluvial plain setting using a high-resolution hydrofacies approach; Bells Creek plain, Australia. Hydrogeology Journal 14: 675-688. DOI 10.1007/s10040-005-0470-5

Fogg GE (1986) Groundwater flow and sand body interconnectedness in a thick, multiple-aquifer system. Water Resources Research 22: 679-694

Fogg GE, Noyes CD, Carle SF (1998) Geologically based model of heterogeneous hydraulic conductivity in an alluvial setting. Hydrogeology Journal 6: 131-143

Fontes J-C, Garnier J-M (1979) Determination of the Initial 14C Activity of the Total Dissolved Carbon: A Review of the Existing Models and a New Approach. Water Resources Research 15: 399–413. DOI 10.1029/WR015i002p00399

Freeze RA, Cherry AJ (1979) Groundwater Prentice-Hall International (UK) Limited, London

Freeze RA, Witherspoon PA (1967) Theoritical analysis of regional groundwater flow. 2. Effect of water-table configuration and subsurface permeability variation. Water Resources Research 3: 623-634

Galy A, France-Lanord C (1999) Weathering processes in the Ganges-Brahmaputra basin and the riverine alkalinity budget. Chemical Geology 159: 31−60

Gani MR, Alam MM (1999) Trench-slope controlled deep-sea clastics in the exposed lower Surma Group in the southeastern fold belt of the Bengal Basin, Bangladesh. Sedimentary Geology 127: 221-236

Gani MR, Alam MM (2004) Fluvial facies architechture in small-scale river systems in the Upper Dupi Tila Formation, northest Bengal Basin, Bangladesh. Journal of Asian Earth Sciences 24: 225-236

Geyh MA (2000) An overview of 14C analysis in the study of groundwater. Radiocarbon 42: 99-114

Glezen WH, Lerche I (1985) A model of regional fluid flow: sand concentration factors and effective lateral and vertical permiabilities. Mathematical Geology 17: 297-315

Goodbred SL, Jr., Kuehl SA (1999) Holocene and modern sediment budgets for the Ganges-Brahmaputra river system: evidence for highstand dispersal to floodplain, shelf and deep-sea depocenters. Geology 27: 559-562

Goodbred SL, Jr., Kuehl SA (2000) The significance of large sediment supply, active tectonism, and eustasy on margin sequence development: Late Quaternary stratigraphy and evolution of the Ganges-Brahmaputra delta. Sedimentary Geology 133: 227-248

Goodbred SL, Jr., Kuehl SA, Steckler MS, Sarker MH (2003) Controls on facies distribution and stratigraphic preservation in the Ganges-Brahmaputra delta sequence. Sedimentary Geology 155: 301-316

GRG/HG (2002) The status of arsenic transport in the deep wells at Manikganj district townFinal Report for Research and Development, DPHE, Water and Environmental Sanitation Section, UCICEF, Bangladesh Geohazard Research Group (GRG), Department of Geology, University of Dhaka, and Hydrogeology Group (HG), University College London, pp. 67.

Gupta SPD (1981) National Atlas of India, Eastern India (Plate 202) Soil Regions. In: Gupta SPD (ed) National Atlas of India National Atlas & Thematic Mapping Organisation. Department of Science & Technology. Government of India, Calcutta.

GWTF (2002) Report of the Ground Water Task Force (GWTF) Local Government Division, Ministry of LGRD & Cooperatives, GoB, Dhaka, pp. 77.

Hait AK, Das JK, Goshi S, Ray AK, Saha AK, Chanda S (1996) New dates of Pleisto-Holocene subcrop samples from south Bengal, India. Indian Journal of Earth Sciences 23: 79-82

Halim MA, Majumder RK, Nessa SA, Hiroshiro Y, Sasaki K, Saha BB, Saepuloh A, Jinno K (2010) Evaluation of processes controlling the geochemical constituents in deep groundwater in Bangladesh: Spatial variability on arsenic and boron enrichment. Journal of Hazardous Materials In Press. DOI 10.1016/j.jhazmat.2010.01.008

Haq BU, Hardenbol J, Vail PR (1987) Chronology of fluctuating sea levels since the Triassic. Science 235: 1156-1167

Haque SJ, 2006. Hydrogelogical characterization of the lower Dupi Tila aquifer of Dhaka city, Unpublished M. S. thesis, University of Dhaka, Dhaka, 51 pp.

Harbaugh AW (1990) A computer program for calculating subregional water budgets using results from the U. S. Geological Survey modular three-dimensional ground-water flow model U. S. Geological Survey, Reston, Virginia, pp. 46.

Harbaugh AW, Banta ER, Hill MC, McDonald MG (2000) MODFLOW-2000, the US Geological Survey modular ground-water model—user guide to modularization concepts and the ground-water flow processOpen File Report 00-92 U. S. Geological Survey, Reston, Virginia, pp. 121.

Harrar WG, Sonnenborg TO, Henriksen HJ (2003) Capture zone, travel time, and solute-transport predictions using inverse modeling and different geological models. Hydrogeology Journal 11: 536–548

Harvey CF, Ashfaque KN, Yu W, Badruzzaman ABM, Ali MA, Oates PM, Michael HA, Neumann RB, Beckie R, Islam S, Ahmed MF (2006) Groundwater dynamics and arsenic contamination in Bangladesh. Chemical Geology 228: 112-136. DOI 10.1016/j.chemgeo.2005.11.025

Harvey CF, Basu AR, Jacobsen SB, Poreda RJ, Dowling CB, Aggarwal PK (2002a) Groundwater Flow in the Ganges Delta. Science 296: 1563a-. DOI 10.1126/science.296.5573.1563a

Harvey CF, Swartz CH, Badruzzaman ABM, Keon-Blute N, Yu W, Ali MA, Jay J, Beckie R, Nieden V, Brabander D, Oates PM, Ashfaque KN, Islam S, Hemond HF, Ahmed MF (2002b) Arsenic mobility and groundwater extraction in Bangladesh. Science 298: 1602-1606

Hasan MA, 2008. Arsenic in alluvial aquifers in the Meghna basin, southeastern Bangladesh: hydrogeological and geochemical characterisation, Unpublished Ph. D. thesis, Royal Institute of Technology, Stockholm, Sweden.

Hasan MA, Ahmed KM, Sracek O, Bhattacharya P, von Brömssen M, Broms S, Fogelstrom J, Mazumder ML, Jacks G (2007) Arsenic in shallow groundwater of Banhladesh: investigations from three different physiographic settings. Hydrogeology Journal 15. DOI 10.1007/s10040-007-0203-z

Hasan MK, 1999. The Vulnerability of the Dupi Tila Aquifer, Dhaka, Bangladesh, Unpublished Ph. D. thesis, University College London, London.

Hasan MK, Ahmed KM, Burgess WG, Dottridge J, Asaduzzaman M (1998) Limits on the sustainable development of the Dupi Tila aquifer, Bangladesh. In: Wheater H, Kirby C (eds) Hydrology in a changing environment - Proceedings of the British Hydrological Society International Conference, Exeter, July 1998:185 -194.

Hoque MA, 2001. Geophysical and geochemical signatures and its geotectonic significance of the Eastern Folded Belt (EFB) of the Bengal basin, Unpublished M. Sc. thesis, University of Dhaka, Dhaka, 113 pp.

Hoque MA, Burgess WG, Ahmed KM (2008) Is the 'Khulna Experience' a Useful Indication of the Sustainability of Groundwater Abstraction from Deep Aquifers in Arsenic-Affected Southern Bangladesh? Paper presented at the 2008 Joint Annual Meeting, Houston, Texas, 5-9 October 2008

Hoque MA, Hoque MM, Ahmed KM (2007) Declining groundwater level and aquifer dewatering in Dhaka metropolitan area, Bangladesh: causes and quantification. Hydrogeology Journal 15: 1523-1534. DOI 10.1007/s10040-007-0226-5

Hoque MA, Khan AA (2005) Crustal dynamics, seismicity and seismotectonics of the Bengal basin, Proceedings First Bangladesh Earthquake Symposium, BES & BUET, BUET, Dhaka, pp. 45-54.

Hoque MA, Khan AA, Ahmed KM, Newaz MGN, Hoque M (under review) Arsenic mitigation in rural Bangladesh: level of public awareness and use of groundwater. Oriental Geographer

Hoque MA, Khan AA, Shamsudduha M, Hossain MS, Islam T, Chowdhury TH (2009) Near surface lithology and spatial variation of arsenic concentration in the shallow groundwater of Bangladesh. Environmental Geology 56: 1687-1695. DOI 10.1007/s00254-008-1267-3

Horneman A, van Geen A, Kent DV, Mathe PE, Zheng Y, Dhar RK, O'Connell SM, Hoque MA, Aziz Z, Shamsudduha M, Seddique AA, Ahmed KM (2004) Decoupling of As and Fe release to Bangladesh groundwater under reducing conditions: Part I. Evidence from sediment profiles. Geochimica et Cosmochimica Acta 68: 3459-3473

Hossain ME, Khan MA, Sikder MNI, Block M (2001) Seismic sequence stratigraphy and structural development in the Lalmai area, Eastern Bangladesh. Bangladesh Journal of Geology 20: 67-76

Hossain MS, Zaman MF (2003) Fluvial Architecture of Tista Fan. Dhaka University Journal of Science 51

Hounslow AW (1995) Water quality data analysis and interpretation Lewis Publishers, New York, USA

Hsieh AP (2001) Topodrive and partcleflow - two computer models for simulation and visualization of groundwater flow and transport of fluide particles in two dimensions U. S. Geological Survey, Menlo Park, California, pp. Open File Report 01-286.

HU/NPD (2001) Bangladesh petroleum potential and resources assessment 2001. Hydrocarbon Unit (HU), Ministry of Energy and Mineral Resources, GoB and Norwegian Petroleum Directorate (NPD), Dhaka, pp. 197.

Imam MB, Hussain M (2002) A review of hydrocarbon habitats in Bangladesh. Journal of Petroleum Geology 25: 31-52

Imam MB, Shaw HF (1985) The diagenesis of Neogene clastic sediments from Bengal basin, Bangladesh. Journal of Sedimentary Research 55: 665−671

Ingebritsen SE, Sanford WE, Neuzil CE (2006) Groundwater in geologic processes, Second edn Cambridge University Press, Cambridge

Ingersoll RV, Graham SA, Dickinson WR (1995) Remnant ocean basin. In: Busby CJ, Ingersoll RV (eds) Tectonics of sedimentary basins:363-391, Blackwell Science, Cambridge, UK.

Islam FS, Gault AG, Boothman C, Polya DA, Charnock JM, Chatterjee D, Lloyd JR (2004) Role of metal-reducing bacteria in As release from Bengal delta sediments. Nature 430: 68-71

Itai T, Masuda H, Seddique AA, Mitamura M, Maruoka T, Li X, Kusakabe M, Dipak BK, Farooqi A, Yamanaka T, Nakaya S, Matsuda J-i, Ahmed KM (2008) Hydrological and geochemical constraints on the mechanism of formation of arsenic contaminated groundwater in Sonargaon, Bangladesh. Applied Geochemistry 23: 3155-3176

Jakariya MD, Bhattacharya P (2007) Use of GIS in local level participatory planning for arsenic mitigation: A case study from Matlab Upazila, Bangladesh. Journal of Environmental Science and Health, Part A 42: 1933 - 1944

Jessica L, Rahman MM, Kazi MA, Brian M, Alexander van G (2010) Contrasting influence of geology on E. coli and arsenic in aquifers of Bangladesh. Ground Water Online

JICA (2002) The study on groundwater development of deep aquifers for safe drinking water supply to arsenic affected areas in Western Bangladesh, Final report, Japan International Cooperation Agency (JICA) Bangladesh, Dhaka.

Johnson NM (1995) Characterization of alluvial hydrostratigraphy with indicator semivariograms. Water Resources Research 31: 3217-3227

Johnson NM, Dreiss SJ (1989) Hydrostratigraphic interpretation using indicator geostatistics. Water Resources Research 25: 2501-2510

Johnston RB, Sarker MH (2007) Arsenic mitigation in Bangladesh: National screening data and case studies in three upazilas. Journal of Environmental Science and Health, Part A 42: 1889 - 1896

Jones PH (1985) Geology and groundwater resources of Bangladesh, Technical Report, P. H. Jones Hydrogeology Inc., Baton Rouge, LA, USA.

Karlin R, Lyle M, Heath GR (1987) Authigenic magnetite formation in suboxic marine sediments. Nature 326: 490-493

Kazemi AG, Lehr JH, Perrochet P (2008) Groundwater age Wiley-Interscience, New York

Keating EH, Robinson BA, Vesselinov VV (2005) Development and Application of Numerical Models to Estimate Fluxes through the Regional Aquifer beneath the Pajarito Plateau. Vadose Zone J 4: 653-671. DOI 10.2136/vzj2004.0101

Khan AA, Hoque MA, Ali M, Hassan MA (2003) Morpho-tectonic depressions and Early Holocene Land-Ocean interaction for transition metals adsorption in sediment and groundwater contamination – a case study from the Bengal delta, Bangladesh. Journal De-Physique IV 107: 691-694

Khan AA, Hoque MA, Shahriar KM, Akhter SH, Hoque M (2002) Convergent Tectonics and sedimentation in the eastern collision margin with emphasis to Bengal basin. Bangladesh Journal of Geology 21: 9-21

Khan FH (1991) Geology of Bangladesh The University Press Limited, Dhaka

Khandoker RA (1987) Origin of elevated Barind-Madhupur areas, Bengal basin: result of neotectonic activities. Bangladesh Journal of Geology 6: 1-9

Kitanidis PK (1997) Introduction to Geostatistics - Applications in Hydrogeology Cambridge University Press, Cambridge

Klingbeil R, Kleineidam S, Asprion U, Aigner T, Teutsch G (1999) Relating lithofacies to hydrofacies: outcrop-based hydrogeological characterisation of Quaternary gravel deposits. Sedimentary Geology 129: 299-310

Klump S, Kipfer R, Cirpka OA, Harvey CF, Brennwald MS, Ashfaque KN, Badruzzaman ABM, Hug SJ, Imboden DM (2006) Groundwater Dynamics and Arsenic Mobilization in Bangladesh Assessed Using Noble Gases and Tritium. Environmental Science & Technology 40: 243-250. DOI doi:10.1021/es051284w

Kocar BD, Polizzotto ML, Benner SG, Ying SC, Ung M, Ouch K, Samreth S, Suy B, Phan K, Sampson M, Fendorf S (2008) Integrated biogeochemical and hydrologic processes driving arsenic release from shallow sediments to groundwaters of the Mekong delta. Applied Geochemistry 23: 3059-3071

Koltermann CE, Gorelick SM (1996) Heterogeneity in sedimentary deposits: a review of stucture-imitating, process-imitating, and descriptive approaches. Water Resources Research 32: 2617-2658

Kooi H (1999) Competition between topography- and compaction-driven flow in a confined aquifer: Some analytical results. Hydrogeology Journal 7: 245-250

Kopera J (2006) A new way of looking at, and mapping, bedrock: the hydrostructural domain map of the Ayer Quadrangle, Northeastern Massachusetts. Paper presented at the The Geological Society of America (GSA) Philadelphia Annual Meeting Pennsylvania Convention Center: Exhibit Hall C, 22-25 October 2006 2006

Koss JE, Etridge FG, Schumm SA (1994) An experimental study of the effects of base-level change on fluvial, coastal plain and shelf systems. Journal of Sedimentary Research B64: 90-98

Kraus MJ (1999) Paleosols in clastic sedimentary rocks: Their geologic applications. Earth Science Review 47: 41-70. DOI 10.1016/S0012-8252(99)00026-4

Kresic N (2007) Hydrogeology and Groundwater Modeling CRS Press, Taylor & Francis Group, Boca Raton

Kutzbach JE (1981) Monsoon Climate of the Early Holocene: Climate Experiment with the Earth's Orbital Parameters for 9000 Years Ago. Science 214: 59-61. DOI 10.1126/science.214.4516.59

Laney RL, Davidson CR (1986) Aquifer-nomenclature guidelines, Open-file Report 86-534, U. S. Geological Survey, Reston, Virginia, pp. 46.

LGED/BRGM (2005) Groundwater resources & hydro-geological investigations in and around Khulna City Local Government Engineering Department (LGED), Volume 4 (Drilling), Dhaka.

Libner H (2008) Column Experiments Simulating Various Scenarios for Arsenic Mobilisation in Bangladesh Trent University and University of Dhaka, pp. 108.

Lindsay JF, Holiday DW, Hulbert AG (1991) Sequence stratigraphy and the evolution of the Ganges-Brahmaputra complex. American Association of Petroleum Geologist Bulletin 75: 1233-1254

Lisiecki LE, Raymo ME (2005) A Pliocene-Pleistocene stack of 57 globally distributed benthic δ18O records. Paleoceanography 20: PA1003. DOI 10.1029/2004PA001071

Lowers HA, Breit GN, Foster AL, Whitney J, Yount J, Uddin MN, Muneem AA (2007) Arsenic incorporation into authigenic pyrite, Bengal Basin sediment, Bangladesh. Geochimica et Cosmochimica Acta 71: 2699-2717

Maduabuchi C, Faye S, Maloszewski P (2006) Isotope evidence of palaeorecharge and palaeoclimate in the deep confined aquifers of the Chad Basin, NE Nigeria. Science of the Total Environment 370: 467-479. DOI 10.1016/j.scitotenv.2006.08.015

Mallick S, Rajagopal NR (1996) Groundwater development in the arsenic-affected alluvial belt of West Bengal—Some questions. Current Science 70: 956-958

Mannan A, 2002. Stratigraphic evolution and geochemistry of the Neogene Surma Group, Surma Basin, Sylhet, Bangladesh, Unpublished PhD thesis, University of Oulu, Oulu, Finland, 162 pp.

Maxey GB (1964) Hydrostratigraphic units. Journal of Hydrology 2: 124-129

Mazumder DNG, Chakroborty AK, Ghose A, Gupta JD, Chakroborti D, Dey SB, Chattopadhaya N (1988) Chronic arsenic toxicity from drinking tubewell water in rural West Bengal. Bulletin of the World Health Organization 64: 499-506

McArthur JM, Banerjee DM, Hudson-Edwards KA, Mishra R, Purohit R, Ravenscroft P, Cronin A, Howarth RJ, Chatterjee A, Talkdar T, Lowry D, Houghton S, Chadha DK (2004) Natural organic matter in sedimentary basins and its relation to arsenic in anoxic groundwater: the example of West Bengal and its worldwide implications. Applied Geochemistry 19: 1255-1293

McArthur JM, Ravenscroft P, Banerjee DM, Milsom J, Hudson-Edwards KA, Sengupta S, Bristow C, Sarkar A, Tonkin S, Purohit R (2008) How paleosols influence groundwater flow and arsenic pollution: A model from the Bengal Basin and its worldwide implication. Water Resources Research 44: W11411. DOI 10.1029/2007WR006552

McArthur JM, Ravenscroft P, Safiullah S, Thirlwall MF (2001) Arsenic in groundwater: testing pollution mechanisms for sedimentary aquifers in Bangladesh. Water Resources Research 37: 109-117

Meetei LI, Pattanayak SK, Bhaskar A, Pandit MK, Tandon SK (2007) Climatic imprints in Quaternary valley fill deposits of the middle Teesta valley, Sikkim Himalaya. Quaternary International 159: 32-46

Meharg AA, Rahman MM (2003) Arsenic contamination of Bangladesh paddy field soils: implications for rice contribution to arsenic consumption. Environmental Science & Technology 37: 229-234

Meharg AA, Scrimgeour C, Hossain SA, Fuller K, Cruickshank K, Williams PN, Kinniburgh DG (2006) Codeposition of Organic Carbon and Arsenic in Bengal Delta Aquifers. Environmental Science & Technology 40: 4928-4935. DOI doi:10.1021/es060722b

Metral J, Charlet L, Bureau S, Mallik S, Chakraborty S, Ahmed KM, Rahman MW, Cheng Z, van Geen A (2008) Comparison of dissolved and particulate arsenic distributions in shallow aquifers of Chakdaha, India, and Araihazar, Bangladesh. Geochemical Transactions 9: 1

Miall AD (1985) Architectural-element analysis: A new method of facies analysis applied to fluvial deposits. Earth-Science Reviews 22: 261-308

Miall AD (1996) The Geology of fluvial deposits: sedimentary facies, basin analysis, and petroleum geology, First edn Springer, Berlin

Michael H, Voss C (2009a) Controls on groundwater flow in the Bengal Basin of India and Bangladesh: regional modeling analysis. Hydrogeology Journal 17: 1561-1577. DOI 10.1007/s10040-008-0429-4

Michael H, Voss C (2009b) Estimation of regional-scale groundwater flow properties in the Bengal Basin of India and Bangladesh. Hydrogeology Journal 17: 1329-1346. DOI 10.1007/s10040-009-0443-1

Michael HA, Voss CI (2008) Evaluation of the sustainability of deep groundwater as an arsenic-safe resource in the Bengal Basin. PNAS 105: 8531-8536

Mikes D, Geel CR (2006) Standard facies models to incorporate all heterogeneity levels in a reservoir model. Marine and Petroleum Geology 23: 943-959. DOI 10.1016/j.marpetgeo.2005.06.007

Milliman JD, Meade RH (1983) World-wide delivery of river sediment to the oceans. Journal of Geology 91: 1-21

MMP/HTS (1982) ADB second phase tubewell project. Volume 3: Groundwater. Feasibility study for Asian Development Bank (ADB) Sir Mott MacDonald & Partners, and Hunting Technical Services, U. K.

Mokrik R, Mažeika J, Baublytė A, Martma T (2008) The groundwater age in the Middle-Upper Devonian aquifer system, Lithuania. Hydrogeology Journal online. DOI 10.1007/s10040-008-0403-1

Monsur MH, Tooley MJ, Ghatak GS, Chandra PR, Roy RK, Adhikari PC, Akhter SH (2001) A review and correlation of Quaternary deposits exposed in the Bengal Basin and its surrounding areas. Bangladesh Journal of Geology 20: 33-54

Mook WG, Bommerson JC, Staverman WH (1974) Carbon fractionation between dissolved bicarbonate and gaseous carbon dioxide. Earth and Planetary Science Letters 22: 169-176

Moore WS (1997) High fluxes of radium and barium from the mouth of the Ganges-Brahmaputra River during low river discharge suggest a large groundwater source. Earth and Planetary Science Letters 150: 141-150

Morgan JP, McIntire WG (1959) Quaternary geology of the Bengal Basin, East Pakistan and India. Geological Society of America Bulletin 70: 319-342

Morris BL, Seddique AA, Ahmed KM (2003) Response of the Dupi Tila aquifer to intensive pumping in Dhaka, Bangladesh. Hydrogeology Journal 11: 496-503

Mostafa R, 2005. Aquifer delineations in Kachua, Chandpur, S-W Bangladesh by bore hole logging, Unpublished M. S. thesis, University of Dhaka, Dhaka, 122 pp.

MPO (1987) The groundwater resources and its availability for development, Technical report no 5, Master Plan Organization (MPO), Ministry of Water Resources, GoB, Harza Engineering USA in association with Sir MacDonald and Partners, UK, Met Consultant, USA and EPC Ltd., Dhaka.

MPO (1990) Description of Groundwater Model Programs. National Water Plan Project Phase II Master Plan Organization (MPO), Dhaka, Harza Engineering, USA, Sir M MacDonald & Partners, UK, Meta Consultants, USA and EPC Ltd, Dhaka.

Mukherjee A, 2006. Deeper groundwater flow and chemistry in the arsenic affected western Bengal basin, West Bengal, India, Unpublished Ph. D. thesis, University of Kentucky Lexington, Kentucky, USA.

Mukherjee A, Fryar AE (2008) Deeper groundwater chemistry and geochemical modeling of the arsenic affected western Bengal basin, West Bengal, India. Applied Geochemistry 23: 863-894

Mukherjee A, Fryar AE, Rowe HD (2007a) Regional-scale stable isotopic signatures of recharge and deep groundwater in the arsenic affected areas of West Bengal. Journal of Hydrology 334: 151-161

Mukherjee A, Fryar AE, Rowe HD (2007b) Regional hydrostratigraphy and groundwater flow modeling of the arsenic affected western Bengal basin, West Bengal, India. Hydrogeology Journal 15: 1397-1418. DOI 10.1007/s10040-007-0208-7

Mukherjee A, von Brömssen M, Scanlon BR, Bhattacharya P, Fryar AE, Hasan MA, Ahmed KM, Chatterjee D, Jacks G, Sracek O (2008) Hydrogeochemical comparison and effects of overlapping redox zones on groundwater arsenic near the Western (Bhagirathi sub-basin, India) and Eastern (Meghna sub-basin, Bangladesh) margins of the Bengal Basin. Journal of Contaminant Hydrology 99: 31-48

Mukhopadhyay SC (1982) The Tista Basin: A Study in Fluvial Geomorphology K.P. Bagchi and Company, Calcutta

Müller RD, Sdrolias M, Gaina C, Steinberger B, Heine C (2008) Long-term sea-level fluctuations driven by ocean basin dynamics. Science 319: 1357-1362. DOI 10.1126/science.1151540

Murad AA, Krishnamurthy RV (2008) Factors controlling stable oxygen, hydrogen and carbon isotope ratios in regional groundwater of the eastern United Arab Emirates (UAE). Hydrological Processes 22: 1922-1931

NACSN (1983) North American stratigraphic code, North American Commission on Stratigraphic Nomenclature (NACSN). American Association of Petroleum Geologist Bulletin 67: 841-875

NACSN (2005) North American stratigraphic code, North American Commission on Stratigraphic Nomenclature (NACSN). American Association of Petroleum Geologist Bulletin 89: 1547-1591. DOI 10.1306/07050504129

Neumann RB, Ashfaque KN, Badruzzaman ABM, Ashraf Ali M, Shoemaker JK, Harvey CF (2010) Anthropogenic influences on groundwater arsenic concentrations in Bangladesh. Nature Geoscience 3: xx. DOI 10.1038/ngeo685

Nickson R, McArthur JM, Burgess WG, Ahmed KM, Ravenscroft P, Rahman M (1998) Arsenic poisoning in Bangladesh groundwater. Nature 395: 338

Nickson R, McArthur JM, Ravenscroft P, Burgess WG, Ahmed KM (2000) Mechanism of arsenic release to groundwater, Bangladesh and West Bengal. Applied Geochemistry 15: 403-413

Nilsson B, Højberg AL, Refsgaard JC, Troldborg L (2007) Uncertainty in geological and hydrogeological data. Hydrology and Earth System Sciences 11: 1551–1561

Niyogi D (1972) Quaternary mapping in plains of West Bengal. Program of the seminar on Geomorphology, Geohydrology and Geotechnics of the lower Ganga basin, Indian Institute of Technology.

Norrman J, Sparrenbom CJ, Berg M, Nhan DD, Nhan PQ, Rosqvist H, Jacks G, Sigvardsson E, Baric D, Moreskog J, Harms-Ringdahl P, Hoan NV (2008) Arsenic mobilisation in a new well field for drinking water production along the Red River, Nam Du, Hanoi. Applied Geochemistry 23: 3127-3142

North CP, Warwick GL (2007) Fluvial fans: Myths, misconceptions, and the end of the terminal-fan model. Journal of Sedimentary Research 77: 693-701. DOI 10.2110/jsr.2007.072

Novakovic D, White CD, Corbeanu RM, Hammon III WS, Bhattacharya JP, McMechan GA (2002) Hydraulic effects of shales in fluvial-deltaic deposits: ground-penetrating radar, outcrop observations, geostatistics, and three-dimensional flow modeling for Ferron Sandstone, Utah. Mathematical Geology 34: 857-893

Opar A, Pfaff A, Seddique AA, Ahmed KM, Graziano JH, van Geen A (2007) Responses of 6500 households to arsenic mitigation in Araihazar, Bangladesh. Health & Place 13: 164-172

Ophori D, Tóth J (1990) Relationship in regional groundwater discharge to stream: an analysis by numerical simulation. Journal of Hydrology 119: 215-244

ORNL (2008) LandScanTM 2006 Global Population Dataset - compiled on a 30" X 30" latitude/longitude grid. Oak Ridge National Laboratory (ORNL), U.S. Department of Energy, Oak Ridge, TN 37831, USA, www.ornl.gov/landscan.

Pearson FJ, Jr., White DE (1967) Carbon 14 Ages and Flow Rates of Water in Carrizo Sand, Atascosa County, Texas. Water Resources Research 3: 251–261. DOI 10.1029/WR003i001p00251

Peizhen Z, Molnar P, Downs WR (2001) Increased sedimentation rates and grain sizes 2–4 Myr ago due to the influence of climate change on erosion rates Nature 410: 891-897

PHED (1993) National Drinking Water Mission project on Arsenic pollution on groundwater in West Bengal, Final report. Steering Committee on arsenic investigation, Public Health Engineering Department (PHED), Govt. of West Bengal, India.

Pirazzoli PA (1993) Global sea-level changes and their measurement. Global and Planetary Change 8: 135-148

Plummer LN, Preston EC, Parkhurst DL (1994) An interactive code (NETPATH) for modelling net geochemical reactions along a fow-path, Version 2.0 US Geological Survey pp. 130.

Poeter E, Anderson D (2005) Multimodel ranking and inference in ground water modeling. Ground Water 43: 597-605

Poeter E, Gaylord DR (1990) Influence of Aquifer Heterogeneity on Contaminant Transport at the Hanford Site. Ground Water 28: 900-909

Pokhrel D, Bhandari BS, Viraraghavan T (2009) Arsenic contamination of groundwater in the Terai region of Nepal: An overview of health concerns and treatment options. Environment International 35: 157-161

Poland JF, Lofgren BE, Riley FS (1972) Glossary of selected terms useful in studies of the mechanics of aquifer systems and land subsidence due to fluid withdrawal, Water Supply Paper 2025 U. S. Geological Survey, Reston, Virginia, pp. 9.

Polizzotto ML, Harvey CF, Sutton SR, Fendorf S (2005) Processes conducive to the release and transport of arsenic into aquifers of Bangladesh. PNAS 102 18819-18823

Polizzotto ML, Hervey CF, Li G, Badruzzman B, Ali A, Newville M, Sutton S, Fendorf S (2006) Soild-phases and desorption processes of arsenic within Bangladesh sediments. Chemical Geology 228: 97-111

Polizzotto ML, Kocar BD, Benner SG, Sampson ML, Fendorf S (2008) Near-surface wetland sediments as a source of arsenic release to ground water in Asia. Nature 454: 505-509

Pollock DW (1994) User's guide for MODPATH/MODPATHPLOT, version 3: a particle tracking post-processing package for MODFLOW, the US Geological Survey finite-difference ground-water flow model U. S. Geological Survey Open-File Report 94-464.

Potter CJ, Sweetkind DS, Dickerson RP, Killgore ML (2002) Hydostructural maps of the Death Valley regional flow system, Nevada and California U. S. Geological Survey, Reston, Virginia, pp. 12.

Raghunath HM (1996) Ground Water, Second edn New Age Publications, Delhi

Rahman AA, Ravenscroft P (2003) Groundwater resources and development in Bangladesh - background to the arsenic crisis, agricultural potential and the environment Bangladesh Centre for Advanced Studies, University Press Ltd., Dhaka, pp. 446.

Rahman MM, Hussain MA, Islam GMT, Haque MA, Hoque MM (2004) Hydro-morphological characteristics around the Meghna bridge site in the Meghna riverJapan Bangladesh Joint Study Project on Floods Institute of Water & Flood Modelling (IWFM), Bangladesh University of Engineering & Technology (BUET), Dhaka.

Ramesh R, Sarin MM (1992) Stable isotope study of the Ganga (Ganges) river system. Journal of Hydrology 139: 49-62

Ravenscroft P (2003) Overview of the hydrogeology of Bangladesh. In: Rahman AA, Ravenscroft P (eds) Groundwater resources and development in Bangladesh - background to the arsenic crisis, agricultural potential and the environment:43-86.

Ravenscroft P, Brammer H, Richards KS (2009) Arsenic pollution: a global synthesis, First edn Wiley-Blackwell, U. K.

Ravenscroft P, Burgess WG, Ahmed KM, Burren M, Perrin J (2005) Arsenic in groundwater of the Bengal Basin, Bangladesh: Distribution, field relations, and hydrogeological setting. Hydrogeology Journal 13: 727–751. DOI 10.1007/s10040-003-0314-0

Ravenscroft P, McArthur JM (2004) Mechanism of regional scale enrichment of groundwater by boron: the examples of Bangladesh and Michigan, USA. Applied Geochemistry 19: 1413-1430

Ravenscroft P, McArthur JM, Hoque BA (2001) Geochemical and palaeohydrological controls on pollution of groundwater by arsenic. In: Chappell WR, Abernathy CO, Calderon RL (eds) Arsenic Exposure and Health Effects:53-77.

Reimann K-U (1993) Geology of Bangladesh Gebruder Borntreger, Berlin-Stuttgart

Renard P, de Marsily G (1997) Calculating equivalent permiability: a review. Advances in Water Resources 20: 253-278

RGlogging (2000) Robertson geologging manual, First edn Robertson Geologging Limited, Deganwy, Conwy, Gwynedd, LL31 9PX, U. K.

Rider MH (1996) The geological interpretation of well logs, Second edn Whittles Publishing, Caithness

Ritzi RW, Jr. (2000) Behavior of indicator variograms and transition probabilities in relation to variance in lengths of hydrofacies. Water Resources Research 36: 3375-3381

Ritzi RW, Jr., Dominic DF, Brown NR, Kausch KW, McAlenney PJ, Basial MJ (1995) Hydrofacies distribution and correlation in Miami Valley aquifer system. Water Resources Research 31: 3271-3281

Roberts LC, Hug SJ, Dittmar J, Voegelin A, Kretzschmar R, Wehrli B, Cirpka OA, Saha GC, Ashraf Ali M, Badruzzaman ABM (2010) Arsenic release from paddy soils during monsoon flooding. Nature Geoscience 3: 53-59

Roy RK, Chattopadhyay GS (1997) Quaternary geology of the environs of Ganga Delta, West Bengal and Bihar. Indian Journal of Geology 69: 177-209

Rushton KR (1986) Vertical flow in heavily exploited hard rock and alluvial aquifers. Ground Water 24: 601-608

Saha KC (1984) Melanokeratosis from arsenical contamination of tubewell water. Indian Journal of Dermatology 29: 37-46

Sanderson M, Ahmed R (1979) Pre-monsoon rainfall and its variability in Bangladesh: a trend surface analysis. Hydrological Sciences - Bulletin-des Sciences Hydrologiques 24: 277-287

Sanford W (2002) Recharge and groundwater models: an overview. Hydrogeology Journal 10: 110-120

Sanford WE (1997) Correcting for diffusion in carbon14 dating of ground water. Ground Water 35: 357-361

Sanford WE, Buapeng S (1996) Assessment Of A Groundwater Flow Model Of The Bangkok Basin, Thailand, Using Carbon-14-Based Ages And Paleohydrology. Hydrogeology Journal 4: 26-40

Sanford WE, Plummer LN, McAda DP, Bexfield LM, Anderholm SK (2004) Hydrochemical tracers in the middle Rio Grande Basin, USA: 2. Calibration of a groundwater-flow model. Hydrogeology Journal 12: 389-407. DOI 10.1007/s10040-004-0326-4

Sarkar A, Sengupta S, McArthur JM, Ravenscroft P, Bera MK, Bhushan R, Samanta A, Agrawal S (2009) Evolution of Ganges-Brahmaputra western delta plain: Clues from sedimentology and carbon isotopes. Quaternary Science Reviews 28: 2564-2581

Sarris TS, Paleologos EK (2004) Numerical investigation of the anisotropic hydraulic conductivity behavior in heterogeneous porous media. Stochastic Environmental Research 18: 188-197. DOI 10.1007/s0047-0030171-3

Schulze-Makuch D, Carlson DA, Cherkauer DS, Malik P (1999) Scale dependency of hydraulic conductivity in heterogeneous media. Ground Water 37: 904-919

Seaber PR (1986) Evolution of classification and nomenclature of hydrogeologic units. EOS 67

Seddique AA, Masuda H, Mitamura M, Shinoda K, Yamanaka T, Itai T, Maruoka T, Uesugi K, Ahmed KM, Biswas DK (2008) Arsenic release from biotite into a Holocene groundwater aquifer in Bangladesh. Applied Geochemistry 23: 2236-2248

Sengupta S, McArthur JM, Sarkar AK, Leng M, Ravenscroft P, Howarth RJ, Banerjee D (2008) Do ponds cause arsenic-pollution of groundwater in the Bengal Basin?: an answer from West Bengal. Environmental Science & Technology 42: 5156-5164. DOI 10.1021/es702988m

Shamsudduha M, 2007. Mineralogical and geochemical profiling of arsenic-contaminated alluvial aquifers in the Ganges-Brahmaputra floodplain Manikganj, Bangladesh, Unpublished M. Sc. thesis, Auburn University, Alabama, USA, 183 pp.

Shamsudduha M, Chandler RE, Taylor RG, Ahmed KM (2009a) Recent trends in groundwater levels in a highly seasonal hydrological system: the Ganges-Brahmaputra-Meghna Delta. Hydrology and Earth System Sciences Discussions 6: 4125-4154

Shamsudduha M, Marzen LJ, Uddin A, Lee M-K, Saunders JA (2009b) Spatial relationship of groundwater arsenic distribution with regional topography and water-table fluctuations in the shallow aquifers in Bangladesh. Environmental Geology. DOI 10.1007/s00254-008-1429-3

Shamsudduha M, Taylor RG, Chandler RE, Ahmed KM (2008) Basin-scale variations in shallow groundwater levels in Bangladesh over the last 40 years: assessing the impacts of groundwater-fed irrigationWater scarcity and water security seminar Geological Society, London, U. K.

Shamsudduha M, Uddin A (2007) Quaternary shoreline shifting and hydrogeologic influence on the distribution of groundwater arsenic in aquifers of the Bengal basin. Journal of Asian Earth Sciences 31: 177-194 DOI 10.1016/j.jseaes.2007.07.001

Shanley KW, McCabe PJ (1993) Alluvial architecture in a sequence stratigraphic framework: a case history from the Upper Cretaceous of Southern Utah, USA. In: Flint S, Bryant ID (eds)

Quantitative description and modeling of clastic hydrocarbon reservoirs and outcrop analogues:21-56.

Shepard D (1968) A two-dimensional interpolation function for irregularly-spaced data Proceedings of the 1968 ACM National Conference, pp. 517-524.

Shibasaki N, Lei P, Kamata A (2007) Evaluation of deep groundwater development for arsenic mitigation in western Bangladesh. Journal of Environmental Science and Health, Part A 42: 1919 - 1932

Smith AH, Lingas EO, Rahman M (2000) Contamination of drinking water by arsenic in Bangladesh: a public health emergency. Bulletin of the World Health Organization 78: 1093-1103

Sohel A, Kabir S, Hossain D (2009) Geophysical interpretation of the Rashidpur structure Surma Basin, Bangladesh. Journal of the Geological Society of India 74: 39-48

Steckler M, Akhter SH, Seeber L, Armbruster J (2007) GPS in Bangladesh: Delta subsidence, monsoonal loading and continental collision. In: UNAVCO (ed) 2008-2012 UNAVCO community and facility proposal: geodesy advancing earth ecience research:3-41.

Steckler MS, Akhter SH, Seeber L (2008) Collision of the Ganges-Brahmaputra Delta with the Burma Arc: Implications for earthquake hazard. Earth and Planetary Science Letters 273: 367-378

Stollenwerk KG, Breit GN, Welch AH, Yount JC, Whitney JW, Foster AL, Uddin MN, Majumder RK, Ahmed N (2007) Arsenic attenuation by oxidized aquifer sediments in Bangladesh. Science of the Total Environment 379: 133-150. DOI 10.1016/j.scitotenv.2006.11.029

Stute M, Zheng Y, Schlosser P, Horneman A, Dhar RK, Hoque MA, Seddique AA, Shamsudduha M, Ahmed KM, van Geen A (2007) Hydrological control of As concentrations in Bangladesh groundwater. Water Resources Research 43. DOI 10.1029/2005WR004499

Sudicky EA, Frind EO (1981) Carbon-14 dating of groundwater in confined aquifers: Implications of aquitard diffusion. Water Resources Research 17: 1060-1064

Sutton NB, van der Kraan GM, van Loosdrecht MCM, Muyzer G, Bruining J, Schotting RJ (2009) Characterization of geochemical constituents and bacterial populations associated with As mobilization in deep and shallow tube wells in Bangladesh. Water Research 43: 1720-1730

Swartz CH, Blute NK, Badruzzman B, Ali A, Brabander D, Jay J, Besancon J, Islam S, Hemond HF, Harvey CF (2004) Mobility of arsenic in a Bangladesh aquifer: Inferences from geochemical profiles, leaching data, and mineralogical characterization. Geochimica et Cosmochimica Acta 68: 4539-4557

Taniguchi M, Ishitobi T, Chen J, Onodera S-i, Miyaoka K, Burnett WC, Peterson R, Liu G, Fukushima Y (2008) Submarine groundwater discharge from the Yellow River Delta to the Bohai Sea, China. Journal of Geophysical Research 113. DOI 10.1029/2007jc004498

Tellam JH, Lloyd JW (1981) A review of the hydrogeology of British onshore non-carbonate mudrocks. Quarterly Journal of Engineering Geology and Hydrogeology 14: 347-355. DOI 10.1144/gsl.qjeg.1981.014.04.11

Thornton MM, Wilson AM (2007) Topography-driven flow versus buoyancy-driven flow in the U.S. midcontinent: implications for the residence time of brines. Geofluids 7: 69-78

Tóth J (1963) A theoretical analysis of groundwater flow in small drainage basins. Journal of Geophysical Research 68: 4795-4812

Tóth J (1995) Hydraulic Continuity In Large Sedimentary Basins. Hydrogeology Journal 3: 4-16

Tóth J (1999) Groundwater as a geologic agent: An overview of the causes, processes, and manifestations. Hydrogeology Journal 7: 1-14

Tóth J (2009) Gravitational systems of groundwater flow: theory, evaluation, utilization, First edn Cambridge University Press, Cambridge

Trefry MG, Svensson TJA, Davis GB (2007) Hypoaigic influences on groundwater flux to a seasonally saline river. Journal of Hydrology 335: 330-353

Troldborg L, Refsgaard JC, Jensen KH, Engesgaard P (2007) The importance of alternative conceptual models for simulation of concentrations in a multi-aquifer system. Hydrogeology Journal 15: 843-860. DOI 10.1007/s10040-007-0192-y

Uddin A, Lundberg N (1999) A paleo-Brahmaputra? Subsurface lithofacies analysis of Miocene deltaic sediments in the Himalayan-Bengal system, Bangladesh. Sedimentary Geology 123: 239-254

Uddin A, Lundberg N (2004) Miocene sedimentation and subsidence during continent–continent collision, Bengal basin, Bangladesh. Sedimentary Geology 164: 131–146

Umitsu M (1993) Late Quaternary sedimentary environments and landforms in the Ganges Delta. Sedimentary Geology 83: 177-186

UNDP (1982) The hydrogeological conditions of Bangladesh, Technical report DP/UN/BGD-74-009/1 United Nations Development Programme (UNDP), Dhaka.

van den Berg EH, de Vries JJ (2003) Influence of grain fabric and lamination on the anisotropy of hydraulic conductivity in unconsolidated dune sands. Journal of Hydrology 283: 244-266. DOI 10.1016/S0022-1694(03)00272-5

van Geen A, Ahmed KM, Seddique AA, Shamsudduha M (2003a) Community wells to mitigate the current arsenic crisis in Bangladesh. Bulletin of the World Health Organization 81: 632-638

van Geen A, Ahsan H, Horneman AH, Dhar RK, Zheng Y, Hussain I, Ahmed KM, Gelman A, Stute M, Simpson HJ, Wallace S, Small C, Parvez F, Slavkovich V, LoIacono NJ, Becker M, Cheng Z, Momotaj H, Shahnewaz M, Seddique AA, Graziano JH (2002) Promotion of well-switching to mitigate the current arsenic crisis in Bangladesh. Bulletin of the World Health Organization 80: 732-737

van Geen A, Aziz Z, Horneman A, Weinman B, Dhar RK, Zheng Y, Goodbred S, Versteeg R, Seddique AA, Hoque MA, Ahmed KM (2006a) Preliminary evidence of a link between surface soil properties and the arsenic content of shallow groundwater in Bangladesh. Journal of Geochemical Exploration 88: 157-161. DOI 10.1016/j.gexplo.2005.08.106

Van Geen A, Cheng Z, Jia Q, Seddique AA, Rahman MW, Rahman MM, Ahmed KM (2007) Monitoring 51 community wells in Araihazar, Bangladesh, for up to 5 years: Implications for arsenic mitigation. Journal of Environmental Science and Health, Part A 42: 1729 - 1740

van Geen A, Radloff K, Aziz Z, Cheng Z, Huq MR, Ahmed KM, Weinman B, Goodbred S, Jung HB, Zheng Y, Berg M, Trang PTK, Charlet L, Metral J, Tisserand D, Guillot S, Chakraborty S,

Gajurel AP, Upreti BN (2008a) Comparison of arsenic concentrations in simultaneously-collected groundwater and aquifer particles from Bangladesh, India, Vietnam, and Nepal. Applied Geochemistry In Press

van Geen A, Zhang Y, Goodbred S, Horneman A, Aziz Z, Cheng Z, Stute M, Mailloux B, Weinman B, Hoque MA, Seddique AA, Hossain MS, Chowdhury SH, Ahmed KM (2008b) Flushing history as a hydrogeological control on the regional distribution of arsenic in shallow groundwater of the Bengal basin. Environmental Science & Technology 42: 2283–2288

van Geen A, Zheng Y, Cheng Z, Aziz Z, Horneman A, Dhar RK, Mailloux B, Stute M, Weinman B, Goodbred S, Seddique AA, Hoque MA, Ahmed KM (2006b) A transect of groundwater and sediment properties in Araihazar, Bangladesh: Further evidence of decoupling between As and Fe mobilization. Chemical Geology 228: 85-96. DOI 10.1016/j.chemgeo.2005.11.024

van Geen A, Zheng Y, Versteeg R, Stute M, Horneman A, Dhar R, Steckler M, Gelman A, Small C, Ahsan H, Graziano J, Hussein I, Ahmed KM (2003b) Spatial variability of arsenic in 6000 tube wells in a 25 km2 area of Bangladesh. Water Resources Research 39: 1140-1155. DOI 10.1029/2002WR001617

Van Houten FB (1973) Origin of red beds: a review –1961–1972. Annual Review of Earth and Planetary Science 1: 39-61

van Wonderen JJ (2003) The use of groundwater models for resource assesment in Bangladesh. In: Rahman AA, Ravenscroft P (eds) Groundwater resources and development in Bangladesh - background to the arsenic crisis, agricultural potential and the environment:115-139.

Vengosh A, Rosenthal E (1994) Saline groundwater in Israel: its bearing on the water crisis in the country. Journal of Hydrology 156: 389-430

Verhagen BT, Mazer E, Sellshop JPF (1974) Radiocarbon and tritium evidence for direct recharge to groundwaters in the Northern Kalahari. Nature 249: 643-644

Vissers MJM, van der Perk M (2008) The stability of groundwater flow systems in unconfined sandy aquifers in the Netherlands. Journal of Hydrology 348: 292-304

Vogel JC, Ehhalt D (1963) The use of the carbon isotopes in groundwater studies. Radioisotopes in hydrology:383-395.

von Brömssen M, Jakariya M, Bhattacharya P, Ahmed KM, Hasan MA, Sracek O, Jonsson L, Lundell L, Jacks G (2007) Targeting low-arsenic aquifers in Matlab Upazila, southeastern Bangladesh. Science of the Total Environment 379: 121–132. DOI 10.1016/j.scitotenv.2006.06.028

von Brömssen M, Larsson SH, Bhattacharya P, Hasan MA, Ahmed KM, Jakariya M, Sikder MA, Sracek O, Bivén A, Doušová B, Patriarca C, Thunvik R, Jacks G (2008) Geochemical characterisation of shallow aquifer sediments of Matlab Upazila, Southeastern Bangladesh — Implications for targeting low-As aquifers. Journal of Contaminant Hydrology 99: 137-149

Wahid SM, Babel MS, Gupta AD, Clemente RS (2007) Spatial assessment of groundwater use potential for irrigation in Teesta Barrage Project in Bangladesh. Hydrogeology Journal. DOI 10.1007/s10040-006-0143-z

WARPO (2000) National Water Management Plan (NWMP) - draft development strategy report, Water Resources Planning Organization (WARPO), Ministry of Water Resources, GoB, Dhaka.

Warren JE, Price HS (1961) Flow in heterogeneous Porous Media. Society of Petroleum Engineers Journal 1: 153-169

Watts L, Samuel J, McGarry R, Silver A (1996) A methodology for estimating predictive uncertainty in groundwater contaminant modelling using the hydrogeochemical transport code, TRAFFICModelCARE 96, Calibration and Reliability in Groundwater Modelling, IAHS Publ no 237 IAHS, Golden, Colorado, USA, pp. 571-578.

Weber D, Englund E (1994) Evaluation and comparison of spatial interpolators II. Mathematical Geology 26: 589-603

Weinman B, Goodbred SL, Jr., Zheng Y, Aziz Z, Steckler M, van Geen A, Singhvi AK, Nagar YC (2008) Contributions of floodplain stratigraphy and evolution to the spatial patterns of groundwater arsenic in Araihazar, Bangladesh. Geological Society of America Bulletin 120: 1567-1580. DOI 10.1130/B26209.1

Weissmann GS, Fogg GE (1999) Multi-scale alluvial fan heterogeneity modeled with transition probability geostatistics in a sequence stratigraphic framework. Journal of Hydrology 226: 48-65

Weissmann GS, Zhang Y, LaBolle EM, Fogg GE (2002) Dispersion of groundwater age in an alluvial aquifer system. Water Resources Research 38: 1198-1210. DOI 10.1029/2001WR000907

Wen XH, Hernandez JJG (1996) Upscalling hydraulic conductivities in heterogeneous media: an overview. Journal of Hydrology 183: ix-xxxii

Whitney JW, Pavich MJ, Huq MA, Alam AKMK (1999) The age and isolation of the Madhupur and Barind Land Tracts, Ganges-Brahmaputra delta, BangladeshInternational Seminar on Quaternary development and coastal hydrodynamics of the Ganges delta in Bangladesh, Geological Survey of Bangladesh, Dhaka, 20-21 September 1999, Abstract Volume, p11.

Wilkin RT, Barnes HL (1997) Formation processes of framboidal pyrite. Geochimica et Cosmochimica Acta 61: 323-339

Williams MAJ, Dunkerley DL, De Deckker P, Kershaw AP, Stokes TJ (1993) Quaternary Environments. Edward Arnold, London.

Winkel L, Berg M, Amini M, Hug SJ, Annette Johnson C (2008) Predicting groundwater arsenic contamination in Southeast Asia from surface parameters. Nature Geoscience 1: 536-542

Worm H-U, Ahmed AMM, Islam HO, Huq MM, Hambach U, Lietz J (1998) Large sedimentation rate in the Bengal Delta: Magnetostratigraphic dating of Cenozoic sediments from northeastern Bangladesh. Geology 26: 487–490

WWF, DoA (2007) More rice, less water – small state, big results - experience of SRI in Tripura, India WWF International, Gland, Switzerland, and Department of Agriculture (DoA), Government of Tripura, Agartala - 799 003, Tripura, India, pp. 34.

Zahid A, Hassan M, Breit G, Balke KD, Flegr M (2009) Accumulation of iron and arsenic in the Chandina alluvium of the lower delta plain, Southeastern Bangladesh. Environmental Geochemistry and Health 31: 69-84

Zahid A, Hassan MQ, Balke KD, Flegr M, Clark DW (2008) Groundwater chemistry and occurrence of arsenic in the Meghna floodplain aquifer, southeastern Bangladesh. Environmental Geology 54: 1247-1260. DOI 10.1007/s00254-007-0907-3

Zhang Y, Gable CW, Person M (2006) Equivalent hydraulic conductivity of an experimental stratigraphy: Implications for basin-scale flow simulations. Water Resources Research 42. DOI 10.1029/2005WR004720

Zheng C, Wang PP (1999) MT3DMS: A Modular Three-Dimensional Multispecies Transport Model for Simulation of Advection, Dispersion and Chemical Reactions of Contaminants in Groundwater Systems; Documentation and User's Guide, Contract Report SERDP-99-1 U.S. Army Engineer Research and Development Center, Vicksburg, MS.

Zheng Y, Anderson RF, Froelich PN, Beck W, McNichol AP, Guilderson T (2002) Challenges in radiocarbon dating organic carbon in opal-rich marine sediments. Radiocarbon 44: 123-136

Zheng Y, Stute M, van Geen A, Gavrieli I, Dhar R, Simpson HJ, Schlosser P, Ahmed KM (2004) Redox control of arsenic mobilization in Bangladesh groundwater. Applied Geochemistry 19: 201-214

Zheng Y, van Geen A, Stute M, Dhar RK, Mo Z, Cheng Z, Horneman A, Gavrieli I, Simpson HJ, Versteeg R, Steckler M, Grazioli-Venier A, Goodbred S, Shahnewaz M, Shamsudduha M, Hoque MA, Ahmed KM (2005) Geochemical and hydrogeological contrasts between shallow and deeper aquifers in the two villages of Araihazar, Bangladesh: Implications for deeper aquifers as drinking water sources. Geochimica et Cosmochimica Acta 69: 5203-5218. DOI 10.1016/j.gca.2005.06.001

Zhu C (2000) Estimate of recharge from radiocarbon dating of groundwater and numerical flow and transport modeling. Water Resources Research 36: 2607-2620

Zijl W (1999) Scale aspects of groundwater flow and transport systems. Hydrogeology Journal 7: 139-150

Zyvoloski G, Kwicklis E, Eddebbarh AA, Arnold B, Faunt C, Robinson BA (2003) The site-scale saturated zone flow model for Yucca Mountain: calibration of different conceptual models and their impact on flow paths. Journal of Contaminant Hydrology 62–63: 731–750

Appendix

Section A5.1: Data on the hydrochemical analysis and isotopic composition of the groundwater samples

Section A8.1: Spatial structure in hydraulic head was generated from the model simulated hydraulic head at the irrigation abstraction depth (at 90 mbgl)

Section A8.2: Vertical structure in hydraulic head was observed in the model simulated head at a central location in the model domain (Kachua)

Section A8.3: Groundwater at variable depths and locations within the model area were tracked backward to the area of recharge

A5.1 Hydrochemical and isotopic data of the groundwater samples

Lab ID	Field ID	Latitude	Longitude	Depth (m)	ORP (mV)	pH	EC (µS/cm)	Temp (^{0}C)	TDS (mg/L)
5	SP0116-16	24.950	91.869	37.0	235.9	5.04	33	24.9	17
6	CU0104-7	23.419	91.136	37.0	227.0	5.88	70	27.9	35
7	SU0116-17	24.920	91.831	145.0	-79.0	6.53	122	25.9	61
8	HG0115-12	24.272	91.390	55.0	-8.4	5.96	138	24.5	69
9	CG0103-5D	23.229	91.307	185.0	61.5	6.28	147	25.2	73
11	SM0116-18	24.903	91.853	34.0	-119.5	7.04	222	27.0	111
12	DT0114-11M	23.597	90.797	87.8	-59.3	6.94	234	26.2	117
13	LC0104-6D	23.174	91.006	195.0	-59.7	6.73	235	27.5	118
15	DT0114-11D	23.597	90.796	295.0	-37.1	6.60	235	26.7	117
16	CG0103-5S	23.229	91.307	85.0	-24.4	6.85	274	25.3	137
17	KHO16S	23.317	90.937	23.3	-91.7	6.86	277	25.9	139
18	DB0103-4D	22.984	91.337	225.0	-92.3	7.07	280	27.8	140
19	BJ0103-3D	22.993	91.091	244.0	-34.7	6.67	339	26.7	169
21	FG0102-1D	23.126	90.756	205.5	-31.7	7.08	365	27.9	182
22	KHO34S	23.336	90.944	24.4	-107.6	7.09	375	26.6	187
23	KHO30S	23.311	90.966	33.0	-115.2	7.15	414	26.2	207
24	KHO62S	23.341	90.843	21.1	-129.0	7.11	472	26.1	236
25	JB0105-10S	23.622	90.860	35.9	-59.0	6.80	506	26.5	253
26	KHO46NS	23.369	90.922	20.0	-141.8	6.87	519	25.9	260
28	RKHO12S	23.341	90.937	29.6	-122.9	7.15	534	26.1	267
29	DS0104-8S	23.606	91.053	38.0	-105.2	7.20	536	25.5	268
31	FG0102-1S	23.126	90.756	11.7	-103.8	7.21	584	25.3	292
33	RLC0104-6S	23.174	91.006	14.3	-136.0	7.44	584	26.1	292
34	NN0105-9D	23.890	90.969	222.0	-37.1	6.29	599	26.5	299
35	KCC-ExS-2	22.796	89.518	120.0	-195.4	7.41	698	26.0	349
36	KHON03S	23.355	90.896	19.8	-107.3	6.59	719	25.9	360
37	KHNP99D	23.389	90.847	229.0	-5.0	6.21	725	26.3	363
38	CL0102-2S	22.768	90.860	7.2	29.0	6.96	751	25.2	375
39	DB0103-4S	22.983	91.337	17.3	-158.9	7.67	769	26.2	384
42	RKCC-0125-19D	22.797	89.554	276.0	-205.6	7.93	786	30.4	393
43	KHON51S	23.319	90.875	17.4	-144.4	7.48	816	26.1	408
44	KHO12D	23.341	90.937	227.0	-78.5	6.90	876	28.0	438
46	KHOP5	23.340	90.923	183.0	-24.2	7.01	877	27.2	438
47	KHO22S	23.308	90.908	29.0	-115.2	7.15	921	26.1	461
48	KHO46ND	23.369	90.922	216.0	-87.0	6.66	946	29.0	473
49	KHNS98D	23.436	90.839	205.0	-44.8	6.35	966	27.4	483
51	KHNS98S	23.436	90.839	23.0	-141.8	7.06	991	25.6	496
52	KCC-0127-24D	22.831	89.552	265.0	-143.4	7.63	1021	30.2	511
53	DS0104-8D	23.606	91.053	135.0	-68.3	6.86	1065	26.4	532
54	KHNP99S	23.389	90.847	17.6	-150.1	7.14	1077	26.0	539
55	KCC-0127-23D	22.844	89.532	288.0	-143.4	7.79	1085	29.5	542
56	CL0102-2D	22.768	90.860	203.0	-95.1	7.07	1177	29.2	588
57	KHO36S	23.360	90.870	18.5	-117.6	7.31	1230	26.0	615
59	RKHOP2	23.340	90.922	336.0	-82.7	6.80	1232	28.5	616
61	KCC-ExB-66	22.790	89.483	143.0	-89.3	6.87	1351	25.9	676
62	KHO61S	23.346	90.855	20.8	-143.8	7.17	1367	25.9	683
63	KHOP4	23.341	90.923	25.0	-116.9	7.10	1460	26.0	730
64	KCC-0128-26D	22.857	89.537	245.0	-106.2	7.51	1515	29.5	757
66	KHO62D	23.341	90.843	225.0	-25.7	6.91	1635	27.0	818
67	KHO34D	23.336	90.945	191.0	-42.5	6.80	1715	27.8	858
68	BJ0103-3S	22.993	91.091	14.3	-130.6	7.73	1889	25.6	956
69	DT0114-11S	23.597	90.797	15.4	-67.0	6.39	1235	25.9	617
71	KHON63D	23.330	90.826	200.0	-33.1	6.53	1904	27.0	952
72	KHON03D	23.355	90.896	125.0	-60.9	6.33	1992	26.9	964
73	KHO61D	23.346	90.855	225.0	-31.8	6.58	2396	26.7	1198
74	KHO56S	23.287	90.939	45.0	-123.3	7.35	2434	26.3	1217
75	KHO36D	23.360	90.870	218.0	-10.0	6.14	2492	26.9	1247
76	KCC-0127-22M	22.764	89.524	119.0	-142.5	7.64	2532	26.7	1266
77	KCC-0125-19S	22.796	89.554	24.0	-123.3	6.94	2577	26.7	1298
79	NN0105-9S	23.890	90.969	62.5	-126.1	7.34	2677	26.0	1314
81	KCC-ExD-2	22.764	89.526	311.0	-101.1	7.60	2902	28.5	1450
82	KHO56D	23.287	90.939	214.0	1.5	6.23	2954	27.1	1477
83	KCC-EsU-2	22.796	89.518	29.0	-74.2	6.23	3208	26.1	1603
84	KCC-0127-25D	22.896	89.506	123.0	-37.1	7.05	3324	27.0	1662
85	KHON51D	23.319	90.875	212.0	-14.0	5.99	3365	27.0	682
86	KHO30D	23.311	90.966	220.0	-1.0	6.14	3390	27.5	1695
87	KHO16D	23.317	90.937	217.0	10.2	6.03	3697	27.5	1848
88	JB0105-10D	23.621	90.860	150.0	1.6	6.29	3812	27.9	1906
89	KHO22D	23.309	90.908	214.0	22.2	6.18	3841	26.9	1920
91	KCC-EdU-6	22.790	89.483	34.0	-107.4	6.58	3842	26.3	1922
92	KCC-0127-25S	22.896	89.506	56.0	18.3	6.76	3937	26.2	1969
93	KCC-0127-24S	22.832	89.552	58.2	-22.8	6.84	4098	27.1	2049
94	KHOP1	23.340	90.923	281.0	-56.1	6.43	4939	28.0	2470
95	KHON63S	23.330	90.826	19.0	-121.8	6.85	5229	26.6	2614
96	KCC-EdU-2	22.764	89.526	30.0	-33.3	6.13	9091	26.5	4544

A5.1: Continued

Lab ID	DO (%)	Ca (mg/L)	K (mg/L)	Mg (mg/L)	Na (mg/L)	Cl (mg/L)	SO_4 (mg/L)	HCO_3 (mg/L)	Fe (mg/L)
5	6	0.80	1.42	2.17	0.60	0.68	1.41	17	0.23
6	59	4.30	0.70	1.19	9.52	2.87	1.11	40	
7	0	0.12	1.43	0.63	26.41	1.14	0.36	63	2.93
8	1	8.50	1.26	3.19	11.49	0.79	1.08	78	7.25
9	28	10.42	2.34	3.87	14.25	0.96	0.83	73	1.14
11	0	22.31	1.60	4.73	18.00	0.79	0.18	115	1.39
12	4	63.75	4.01	27.57	138.90	333.10	0.31	227	29.38
13	3	17.40	2.03	11.46	21.82	3.18	1.69	156	1.74
15	0	21.49	2.19	10.95	20.16	8.36	0.29	146	2.21
16	28	18.17	1.60	11.13	26.91	1.35	0.50	155	2.01
17	0	17.74	7.44	21.94	9.61	5.98	0.67	193	7.26
18	0	12.87	2.74	6.77	40.78	3.02	1.22	363	1.09
19	2	23.03	2.24	12.34	25.18	37.27	0.16	158	3.15
21	14	24.46	4.18	15.13	28.92	1.31	3.05	244	0.96
22	0	22.29	4.67	26.44	12.05	5.36	1.70	212	2.29
23	0	22.95	5.17	30.57	11.72	5.92	2.23	268	2.35
24	0	27.04	8.16	34.20	28.20	18.29	3.80	293	2.87
25	1	11.04	4.19	13.27	86.20	22.57	0.25	263	0.48
26	0	30.38	7.96	25.33	23.67	10.87	2.09	288	8.92
28	0	22.08	6.64	31.94	36.58	4.46	1.38	322	1.69
29	3	25.22	5.36	26.32	63.49	19.96	0.00	412	3.10
31	1	57.61	4.03	26.18	13.33	8.81	4.73	340	3.55
33	1	35.22	7.74	43.71	28.50	58.99	1.18	290	2.42
34	3	33.02	2.46	13.25	61.42	114.21	0.29	158	3.61
35	0	36.45	4.20	19.84	93.97	36.52	1.52	366	0.13
36	0	42.84	5.90	44.06	52.32	12.73	2.06	444	9.31
37	2	29.08	5.86	20.80	83.12	159.75	0.93	151	2.76
38	30	47.28	12.12	42.88	42.41	18.75	4.31	398	0.38
39	3	17.30	9.39	33.96	103.53	58.62	3.14	414	1.53
42	4	14.05	3.91	8.83	150.23	42.58	0.00	390	0.00
43	0	13.76	9.92	16.70	139.40	20.18	0.43	410	1.46
44	0	5.77	9.44	5.35	169.40	145.24	7.43	225	0.36
46	23	3.08	6.03	3.75	183.81	161.27	1.12	249	0.29
47	2	56.08	11.88	63.14	48.17	16.42	0.00	519	4.55
48	0	13.10	3.75	5.14	176.43	211.38	11.51	202	0.64
49	0	63.41	8.23	47.56	57.02	227.58	22.76	190	3.01
51	0	20.50	12.39	25.08	153.94	95.02	5.13	432	1.97
52	10	35.79	5.64	18.35	161.70	154.91	12.14	359	0.07
53	0	6.51	3.38	7.57	233.76	252.36	27.80	195	0.80
54	0	14.47	8.69	16.33	176.66	128.33	4.32	432	1.46
55	23	24.30	4.24	14.02	178.70	116.23	0.64	483	0.07
56	4	33.17	7.32	22.24	206.59	244.33	0.68	305	1.51
57	0	40.29	15.26	40.04	253.42	215.71	0.00	529	3.31
59	1	58.15	10.25	42.24	134.84	336.02	15.96	144	1.91
61	0	114.06	5.93	47.32	100.23	322.90	7.30	293	1.17
62	0	26.96	21.94	59.44	169.20	201.46	2.05	475	3.07
63	18	41.95	16.25	50.43	217.10	223.54	0.72	541	5.27
64	19	53.25	6.21	29.39	234.30	285.23	0.54	434	0.24
66	0	13.50	10.10	7.63	373.33	465.74	21.68	288	0.73
67	0	13.82	15.46	17.63	304.55	409.82	43.39	207	0.96
68	10	12.31	22.19	39.84	352.25	320.80	1.62	693	1.31
69	3	29.64	2.19	7.53	18.24	13.17	1.34	149	1.14
71	0	44.52	4.98	20.86	256.45	475.23	5.17	176	2.24
72	0	51.73	5.91	22.35	294.96	392.04	2.00	361	6.00
73	1	12.98	47.77	35.81	339.09	567.65	7.33	215	1.34
74	0	16.69	18.46	23.61	447.75	427.02	1.38	634	1.95
75	0	132.28	8.55	77.14	308.92	901.49	6.19	151	12.57
76	35	110.30	10.63	70.34	269.53	660.66	0.83	332	0.26
77	44	33.29	9.14	14.84	470.04	335.13	0.77	820	2.03
79	7	22.95	19.31	24.92	424.68	723.45	0.00	175	2.76
81	0	18.88	6.81	18.66	547.42	622.67	7.86	546	0.16
82	3	132.89	13.54	74.73	341.31	881.30	12.02	158	5.29
83	9	163.16	15.81	70.58	418.40	597.05	0.00	800	21.05
84	35	247.21	9.39	95.34	313.36	870.32	0.00	289	3.74
85	1	211.13	5.26	90.76	297.95	957.29	0.00	90	20.15
86	0	128.97	8.01	55.30	481.38	1019.20	30.98	114	13.68
87	0	192.88	7.49	93.14	595.53	1349.31	8.88	166	19.89
88	4	65.91	4.85	41.18	667.68	1106.40	17.30	187	5.66
89	6	84.22	6.74	37.28	609.92	1089.33	91.71	170	9.98
91	0	113.68	13.42	92.63	608.01	793.20	32.66	888	0.96
92	30	192.66	2.51	76.86	573.48	889.49	0.00	693	1.22
93	0	137.57	3.49	77.85	620.58	1098.75	3.65	378	0.86
94	1	108.55	10.76	84.41	805.30	1508.77	144.89	148	6.89
95	0	174.08	19.54	136.46	625.46	1406.03	18.12	480	15.94
96	3	267.26	3.84	106.34	780.85	2691.64	0.00	617	16.01

A5.1: Continued

Lab ID	Mn (mg/L)	P (mg/L)	Si (mg/L)	Al (mg/L)	Sr (mg/L)	Zn (mg/L)	F (mg/L)	As (µg/L)*	NO_3 (mg/L)
5	0.13		2.93	0.11	0.02	0.07	0.12	-7.5	1.12
6		0.09	16.49	0.10	0.07	0.12	0.19	-7.5	13.47
7	0.00	0.46	5.44	0.10	0.00	0.04	0.09	-5.8	3.39
8	0.45	0.01	21.71	0.12	0.09	0.04	0.20	-15.7	3.19
9	0.01	0.00	26.78	0.07	0.15	0.02	0.13	-20.6	3.92
11	0.06	0.07	13.85	0.09	0.20	0.03	0.12	-8.5	4.60
12	4.37	1.65	14.72	0.10	0.55	0.22	0.97	30.5	6.21
13	0.06	0.13	26.09	0.10	0.16	0.02	0.23	-8.3	5.35
15	0.08	0.08	25.91	0.10	0.21	0.10	0.51	-17.1	7.23
16	0.17	0.10	17.17	0.10	0.18	0.04	0.54	-19.5	8.27
17	0.14	1.97	20.43	0.11	0.19	0.03	0.46	128.4	9.05
18	0.09	0.08	19.27	0.09	0.15	0.05	0.34	-4.6	6.42
19	0.08	0.07	23.02	0.10	0.19	0.06	0.80	-13.8	9.32
21	0.05	0.12	19.29	0.08	0.27	0.10	0.17	-15.6	9.50
22	0.11	2.23	18.28	0.12	0.19	0.05	0.29	347.0	10.73
23	0.06	2.00	16.90	0.13	0.24	0.02	0.17	315.0	14.78
24	0.06	2.84	14.40	0.12	0.26	0.05	0.68	499.0	17.99
25	0.04	0.68	17.66	0.12	0.12	0.02	0.89	190.0	9.67
26	0.49	1.45	11.37	0.10	0.29	0.03	0.34	447.7	13.49
28	0.03	2.71	16.23	0.10	0.25	0.02	0.27	350.6	14.69
29	0.04	1.43	14.75	0.12	0.31	0.05	0.53	259.2	10.14
31	1.04	0.72	11.48	0.09	0.29	0.05	0.56	326.8	14.84
33	0.09	1.78	9.64	0.12	0.35	0.02	1.60	753.6	24.21
34	0.12	0.07	24.63	0.12	0.32	0.02	1.32	52.7	8.14
35	0.02	0.06	7.65	0.11	0.43	0.01	1.53	7.0	21.17
36	0.06	2.49	21.75	0.12	0.34	0.08	0.64	113.6	23.18
37	0.19	0.46	22.84	0.09	0.31	0.03	2.12	38.2	11.23
38	0.52	0.10	10.08	0.11	0.36	0.03	0.38	-0.7	12.02
39	0.04	1.77	6.41	0.12	0.24	0.01	1.88	211.2	28.09
42		0.10	8.03	0.13	0.18	0.01	0.60	-4.9	14.70
43	0.02	3.21	9.78	0.12	0.16	0.01	0.37	661.7	11.81
44	0.00	0.21	25.64	0.11	0.07	0.04	1.65	32.0	14.18
46		0.31	24.52	0.12	0.04	0.03	1.89	-13.2	16.32
47	0.04	3.07	15.39	0.13	0.48	0.02	0.63	308.2	13.59
48	0.03	0.21	25.23	0.10	0.12	0.02	1.95	42.5	19.16
49	0.23	0.05	22.89	0.11	0.69	0.02	1.51	-3.6	13.09
51	0.01	4.31	14.62	0.15	0.22	0.01	1.87	247.5	28.22
52		0.08	9.49	0.10	0.34	0.01	3.77	2.0	24.42
53	0.15	0.21	20.37	0.11	0.08	0.08	3.12	6.0	26.38
54	0.00	5.92	13.59	0.10	0.15	0.01	3.42	285.6	30.06
55		0.09	7.93	0.11	0.28	0.01	3.48	-4.7	31.84
56	0.17	0.51	14.27	0.09	0.39	0.03	3.34	2.5	23.46
57	0.10	3.61	12.13	0.11	0.35	0.02	2.64	522.9	28.46
59	0.17	0.21	21.87	0.09	0.56	0.02	3.26	-6.9	15.32
61	0.14	0.11	10.43	0.11	0.71	0.02	3.75	-0.4	24.17
62	0.11	3.90	12.17	0.12	0.37	0.01	3.50	539.3	32.97
63	0.24	3.00	11.33	0.10	0.43	0.03	3.36	220.1	35.97
64	0.06	0.17	8.18	0.09	0.52	0.01	4.02	-7.0	32.38
66	0.07	1.10	16.23	0.11	0.13	0.06	4.49	-5.1	23.85
67	0.08	0.21	22.92	0.11	0.17	0.06	3.38	-6.7	31.53
68	0.06	9.53	11.40	0.09	0.26	0.01	3.61	310.8	42.07
69	0.60	1.27	12.63	0.21	0.13	0.03	1.14	354.9	10.33
71	0.15	0.62	19.33	0.12	0.44	0.03	3.47	-6.6	19.15
72	0.33	0.40	20.28	0.12	0.43	0.03	3.27	2.8	25.87
73	0.51	1.04	15.37	0.13	0.28	0.08	5.28	-0.9	21.18
74	0.06	7.11	14.41	0.11	0.22	0.01	3.43	366.1	41.60
75	0.75	0.56	23.60	0.11	1.22	0.06	4.22	-8.0	16.60
76	0.15	0.15	5.90	0.12	1.21	0.02	3.09	10.7	26.35
77	0.06	2.15	19.86	0.12	0.16	0.02	4.15	5.6	43.90
79	0.14	2.81	7.09	0.07	0.36	0.01	6.40	393.2	0.00
81	0.06	0.31	5.75	0.10	0.29	0.01	3.23	-1.0	34.73
82	0.27	0.35	24.09	0.10	1.02	0.22	3.52	4.0	21.06
83	0.71	4.31	17.53	0.10	0.90	0.02	4.74	137.7	59.13
84	0.78	1.20	5.94	0.10	1.41	0.01	5.20	23.6	37.42
85	1.53	1.75	21.79	0.09	1.59	0.07	6.56	13.5	31.17
86	1.12	0.92	22.62	0.10	0.84	0.12	9.13	0.7	20.35
87	1.08	1.02	27.86	0.13	1.39	0.09	8.94	-16.6	26.42
88	1.24	0.46	22.01	0.09	0.38	0.22	9.80	-2.4	30.51
89	1.14	1.28	22.37	0.11	0.55	0.05	11.55	-1.8	21.69
91	0.47	3.64	15.48	0.12	0.90	0.02	9.00	68.2	70.12
92	1.74	0.82	12.85	0.30	1.07	0.02	7.32	11.7	64.10
93	2.48	1.03	10.36	0.10	0.88	0.03	9.52	-5.2	52.42
94	0.79	0.90	23.50	0.12	0.85	0.03	10.39	-5.1	37.75
95	0.62	3.85	10.97	0.12	1.26	0.02	10.64	651.6	49.67
96	0.62	1.85	9.10	0.12	1.35	0.02	7.45	147.5	0.00

**The minimum detection limit for As is 0.1 µg/L. Negative values are less than the minimum detection limit. These values are censored and kept here for potential statistical use.*

A5.1: Continued

Lab ID	$\delta^{18}O$ ‰	$\delta^{2}H$ ‰	$d^{13}C$ (‰)	CO_2 (cc STP)	Uncorrected $^{14}C/^{12}C$ number (pMC)			Corrected $^{14}C/^{12}C$ (pMC)		
5	-5.07	-36.10	-21.82	5.10	88.62	±	0.59	88.05	±	0.59
6	-5.01	-32.40	-11.42	3.40	124.37	±	0.78	120.98	±	0.76
7	-2.98	-16.50								
8	-4.22	-28.20								
9	-5.37	-33.10	-19.72	5.90	82.69	±	0.61	81.80	±	0.61
11										
12	-5.18	-31.60	-13.76	6.00	27.86	±	0.29	27.23	±	0.28
13	-2.87	-13.50	-6.36	5.00	23.54	±	0.26	22.67	±	0.25
15	-5.46	-31.89	-18.86	5.40	26.75	±	0.27	26.41	±	0.26
16	-5.47	-31.00								
17										
18	-2.74	-16.30	-13.02	2.70	15.75	±	0.20	15.37	±	0.20
19	-3.62	-17.60	-11.66	3.50	24.56	±	0.28	23.90	±	0.27
21	-2.78	-12.30	-7.63	5.40	19.07	±	0.26	18.41	±	0.25
22										
23										
24										
25	-2.58	-18.00								
26										
28										
29	-2.32	-11.60								
31	-3.70	-22.70								
33	0.68	-7.60								
34	-3.46	-18.30	-12.60	4.50	27.29	±	0.27	26.61	±	0.26
35										
36										
37	-3.27	-17.50								
38	-3.48	-21.90								
39	-3.48	-14.80								
42										
43										
44										
46	-3.53	-19.60	-18.09	5.00	25.42	±	0.26	25.06	±	0.26
47	-3.25	-20.40								
48										
49	-3.18	-15.30	-10.44	4.20	22.42	±	0.26	21.76	±	0.25
51	-3.45	-21.90								
52	-3.37	-19.40								
53	-5.05	-32.90	-17.40	3.90	46.04	±	0.37	45.33	±	0.37
54	-2.56	-18.80								
55	-3.39	-15.00								
56	-3.39	-18.90	-11.46	4.80	2.60	±	0.09	2.53	±	0.09
57	-3.92	-21.00								
59	-3.37	-14.60	-13.09	5.20	23.68	±	0.27	23.11	±	0.26
61	-3.98	-28.60								
62										
63	-3.74	-22.60	-6.34	5.90	70.79	±	0.48	68.15	±	0.50
64	-3.80	-20.40	-5.79	6.00	12.04	±	0.17	11.58	±	0.16
66										
67										
68	-2.80	-17.00								
69	-2.75	-18.90	-19.10	5.30	105.98	±	0.66	104.71	±	0.65
71										
72										
73										
74	-4.20	-24.80								
75	-4.63	-31.70								
76	-4.61	-25.20	-6.73	5.90	12.97	±	0.18	12.50	±	0.18
77										
79	-4.99	-26.50								
81	-3.05	-18.40	-4.61	5.20	7.71	±	0.14	7.39	±	0.13
82	-3.95	-23.90								
83										
84	-4.62	-32.60								
85										
86										
87										
88	-4.31	-21.00	-38.57	5.40	6.88	±	0.13	7.07	±	0.14
89	-4.79	-29.40								
91	-5.40	-38.10								
92	-6.73	-43.40								
93	-6.30	-39.80								
94	-4.72	-27.90	-20.99	5.40	35.83	±	0.31	35.53	±	0.31
95										
96	-4.27	-30.40	-9.60	4.80	88.77	±	0.59	86.03	±	0.57

A8.1 Spatial distribution of hydraulic head (m relative to MSL) at 90 mbgl depth simulated by different model representations

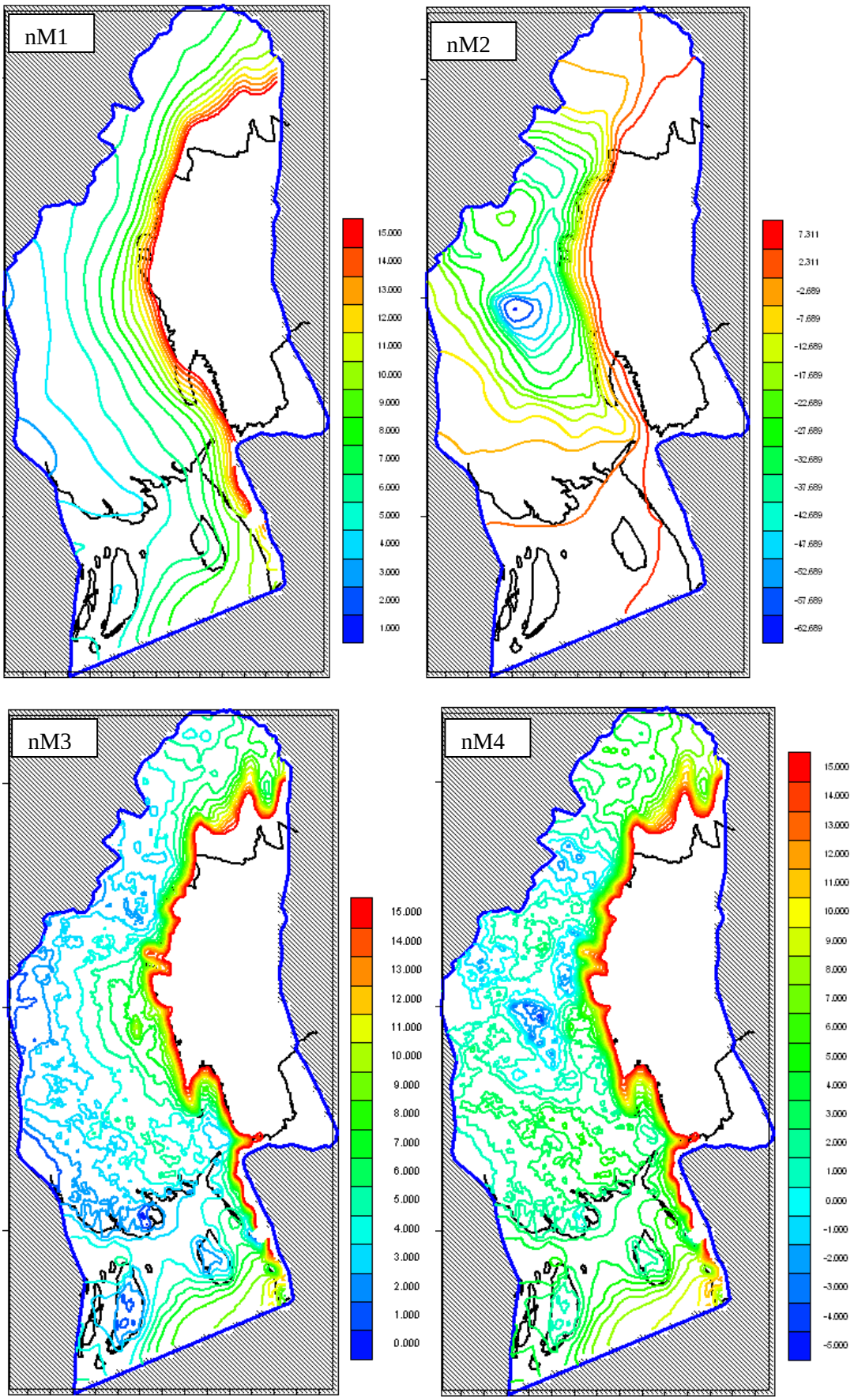

A8.1 Continued

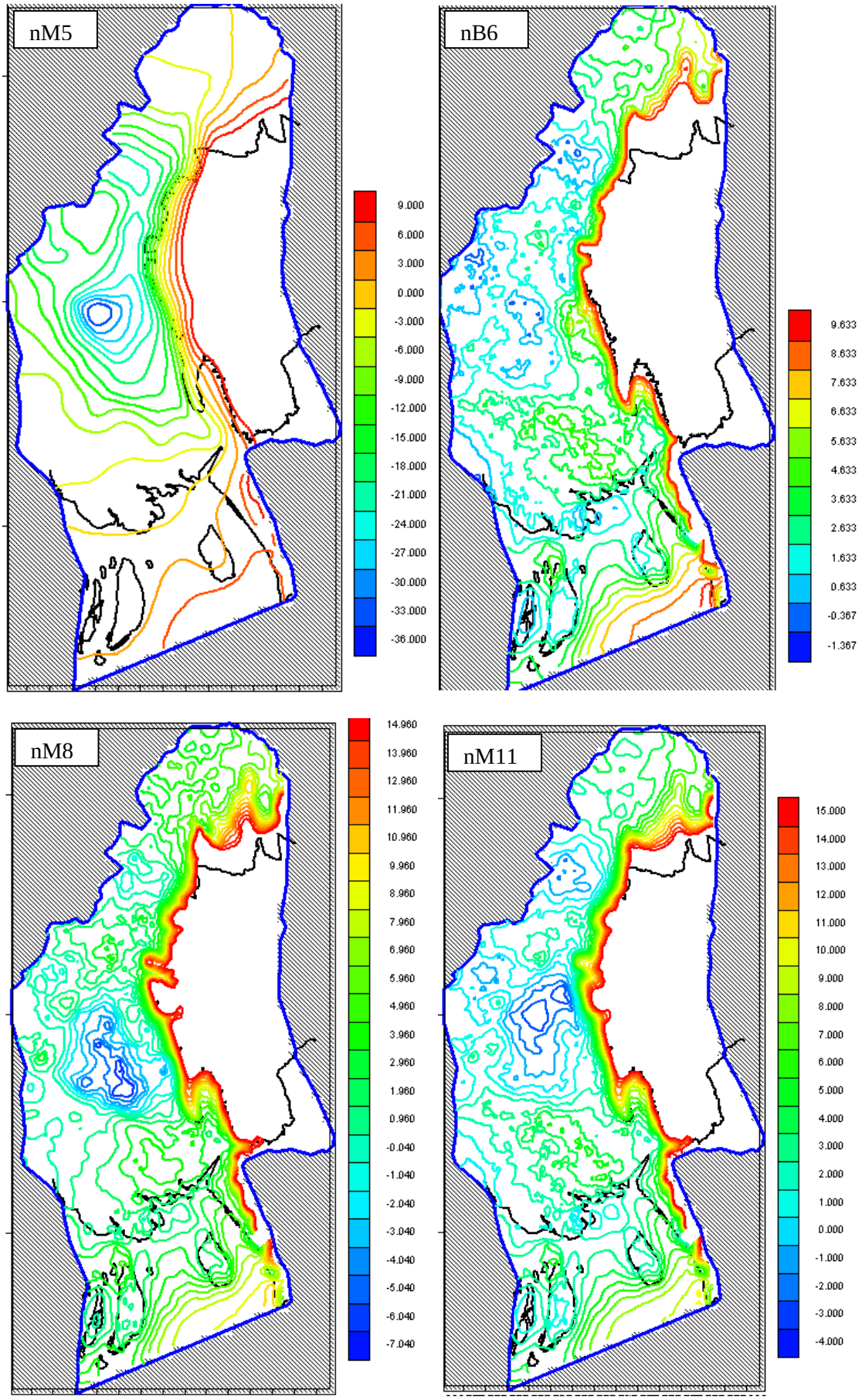

A8.1 Continued

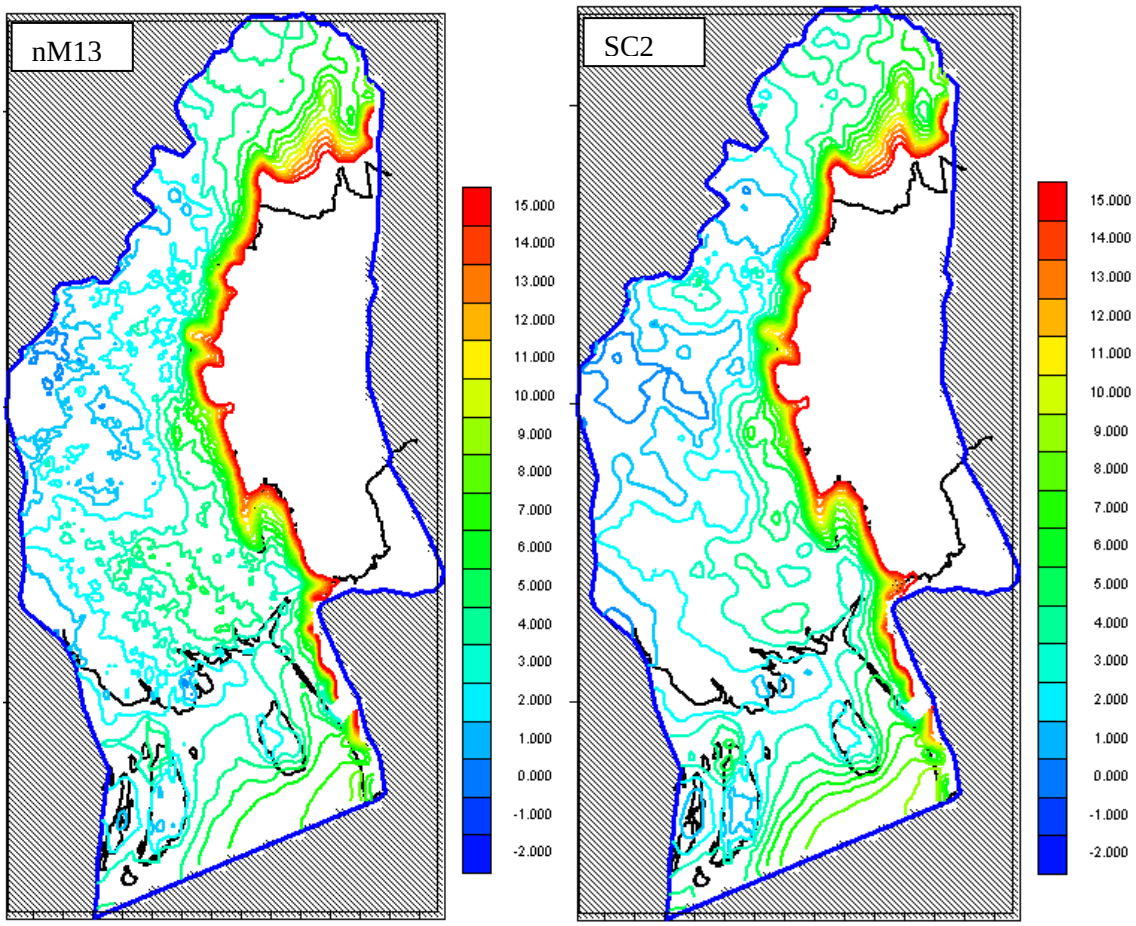

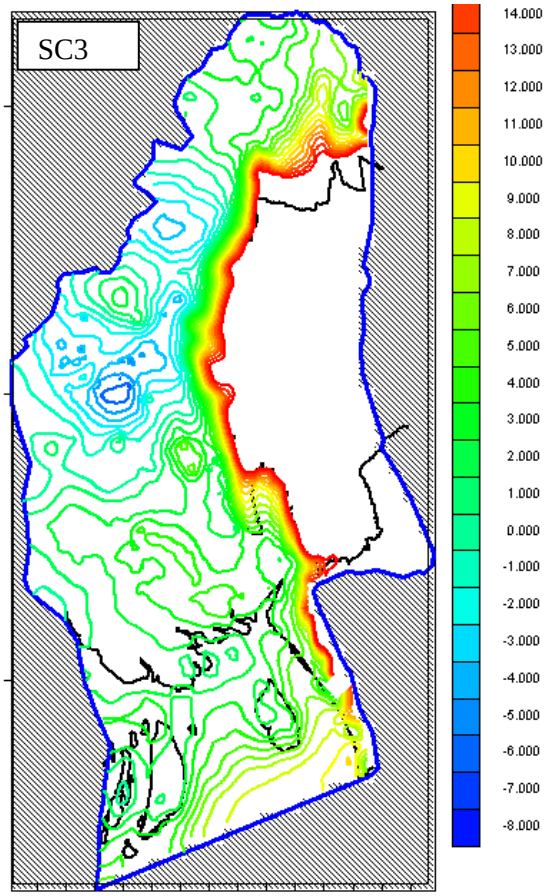

A8.2 Vertical head profile at Kachua (Comparison of observed head and simulated head over time). In the graphs observed head denoted by 'F' and depth of well is 'numeral X10' m; whilst 'M' indicates the model simulated head. Vertical head structure has also shown for four different months.

*Vertical head profile at Kachua for **nM5***

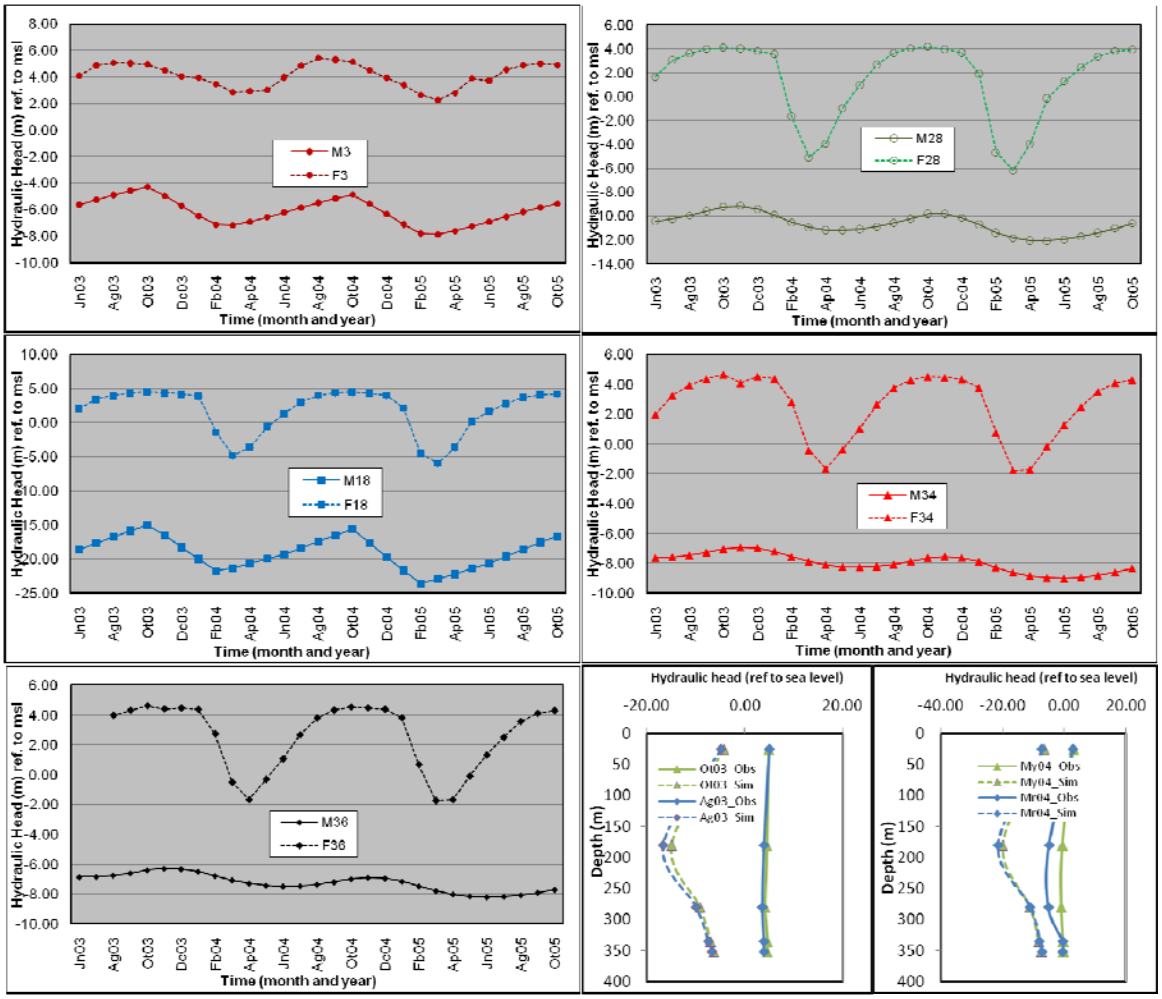

A8.2 Continued

*Vertical head profile at Kachua for **nB6***

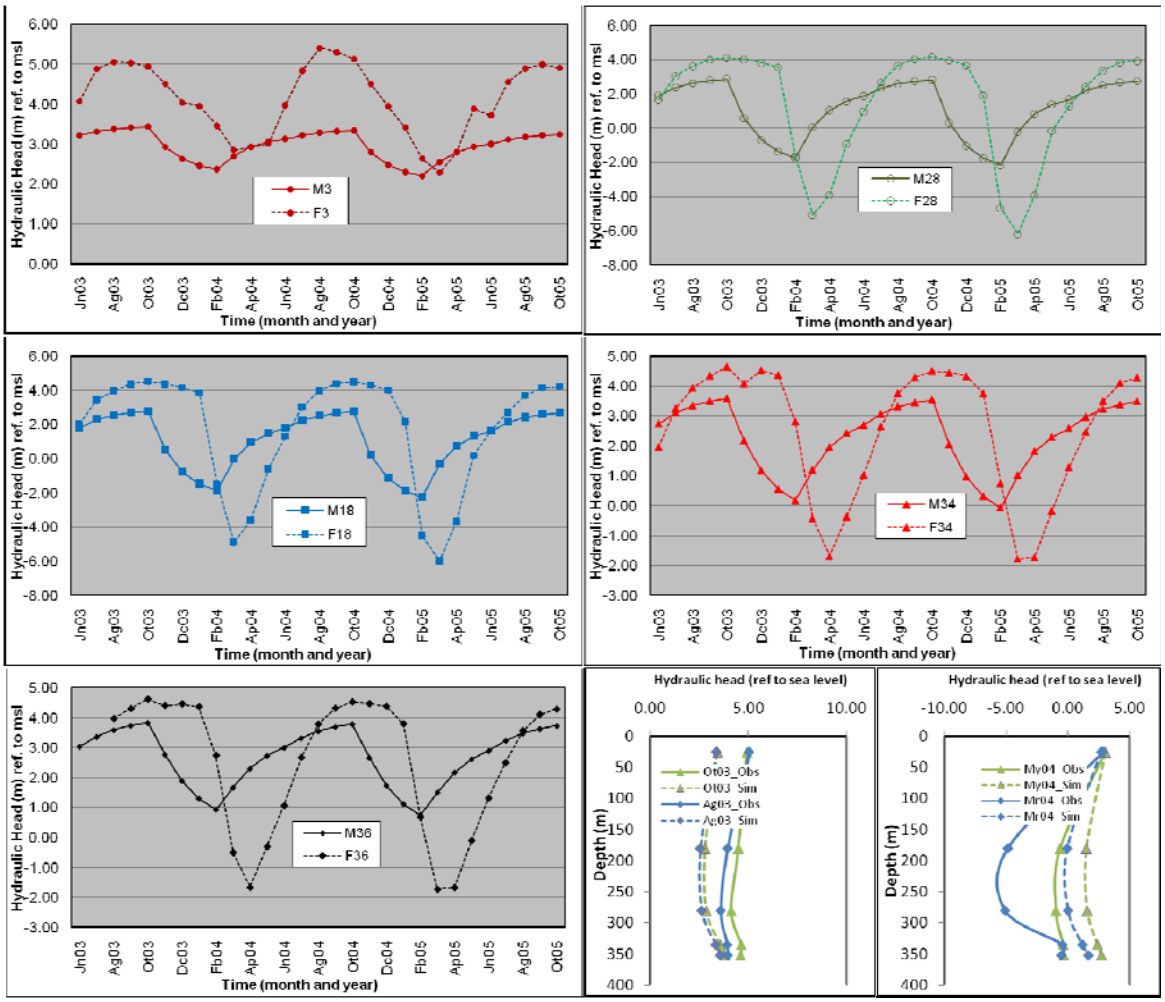

A8.2 Continued

*Vertical head profile at Kachua for **nM8***

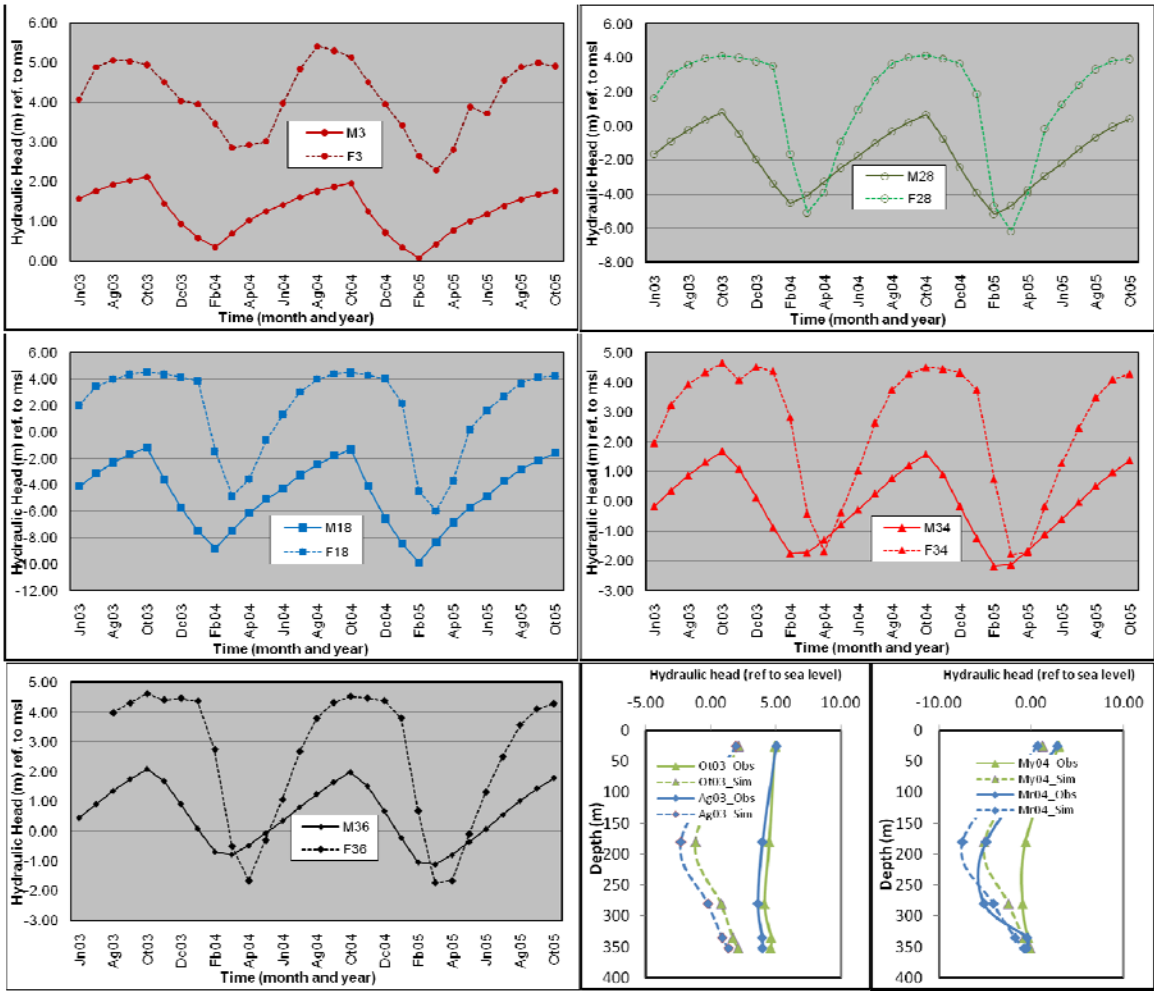

A8.2 Continued

*Vertical head profile at Kachua for **nM13***

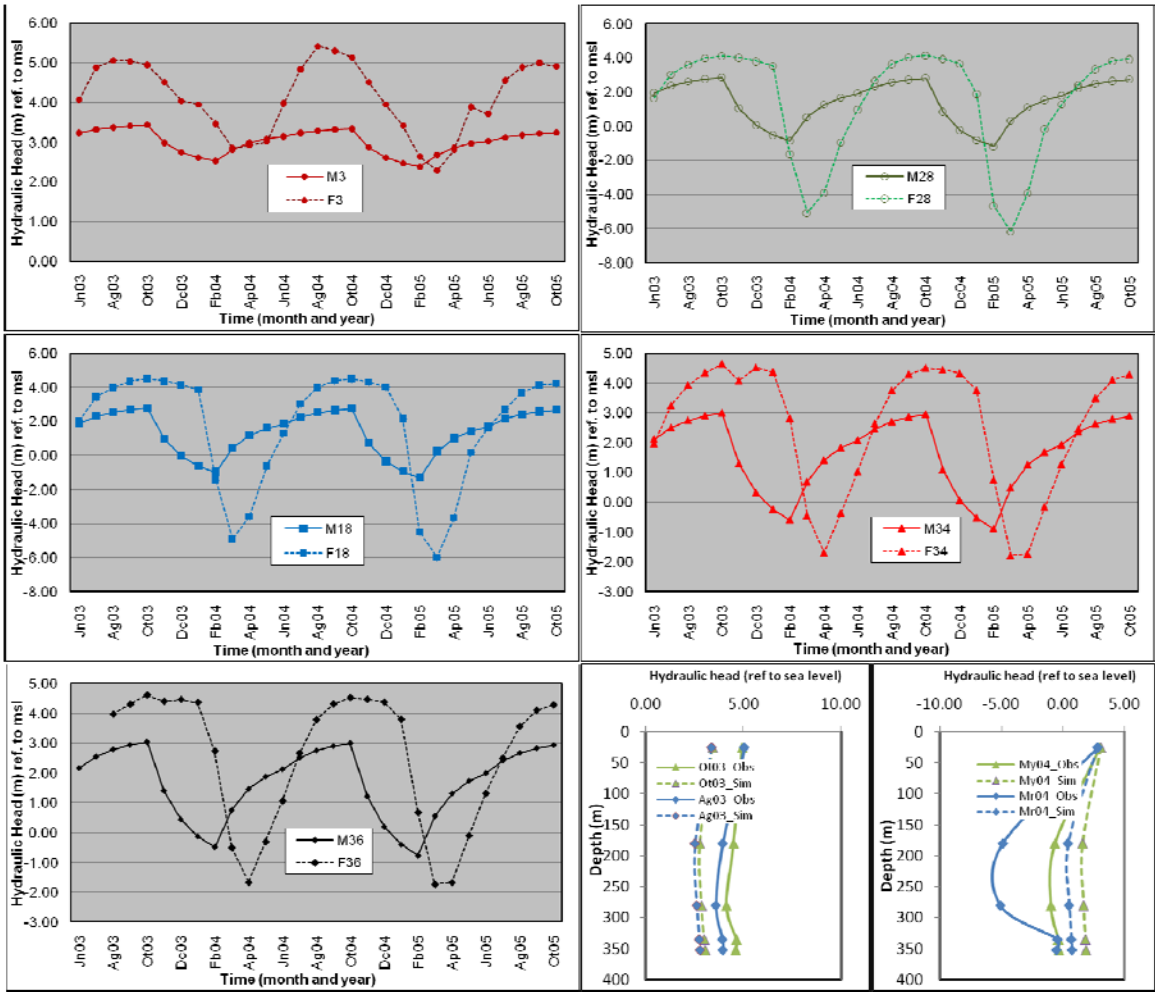

A8.2 Continued

*Vertical head profile at Kachua for **SC2***

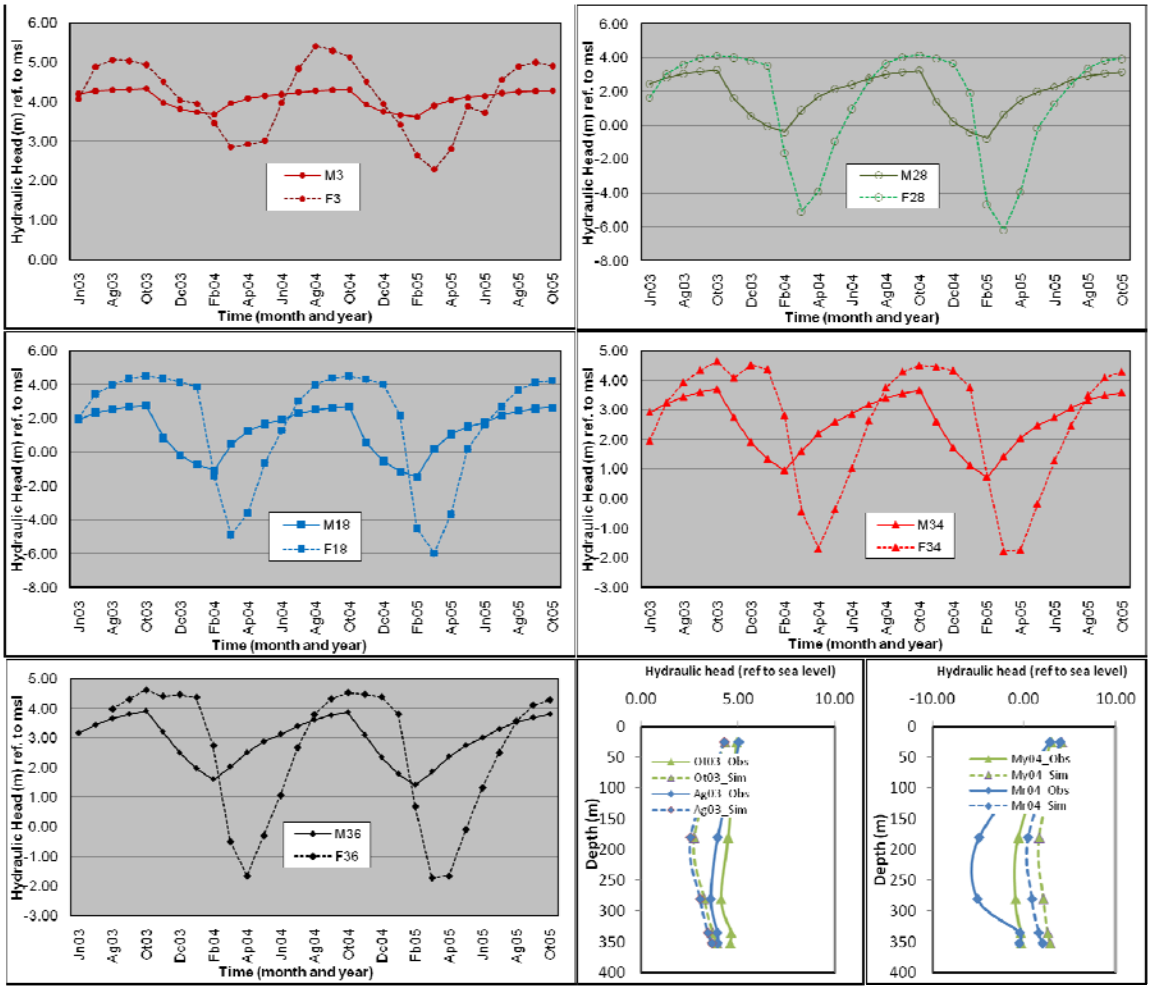

A8.2 Continued

*Vertical head profile at Kachua for **SC3***

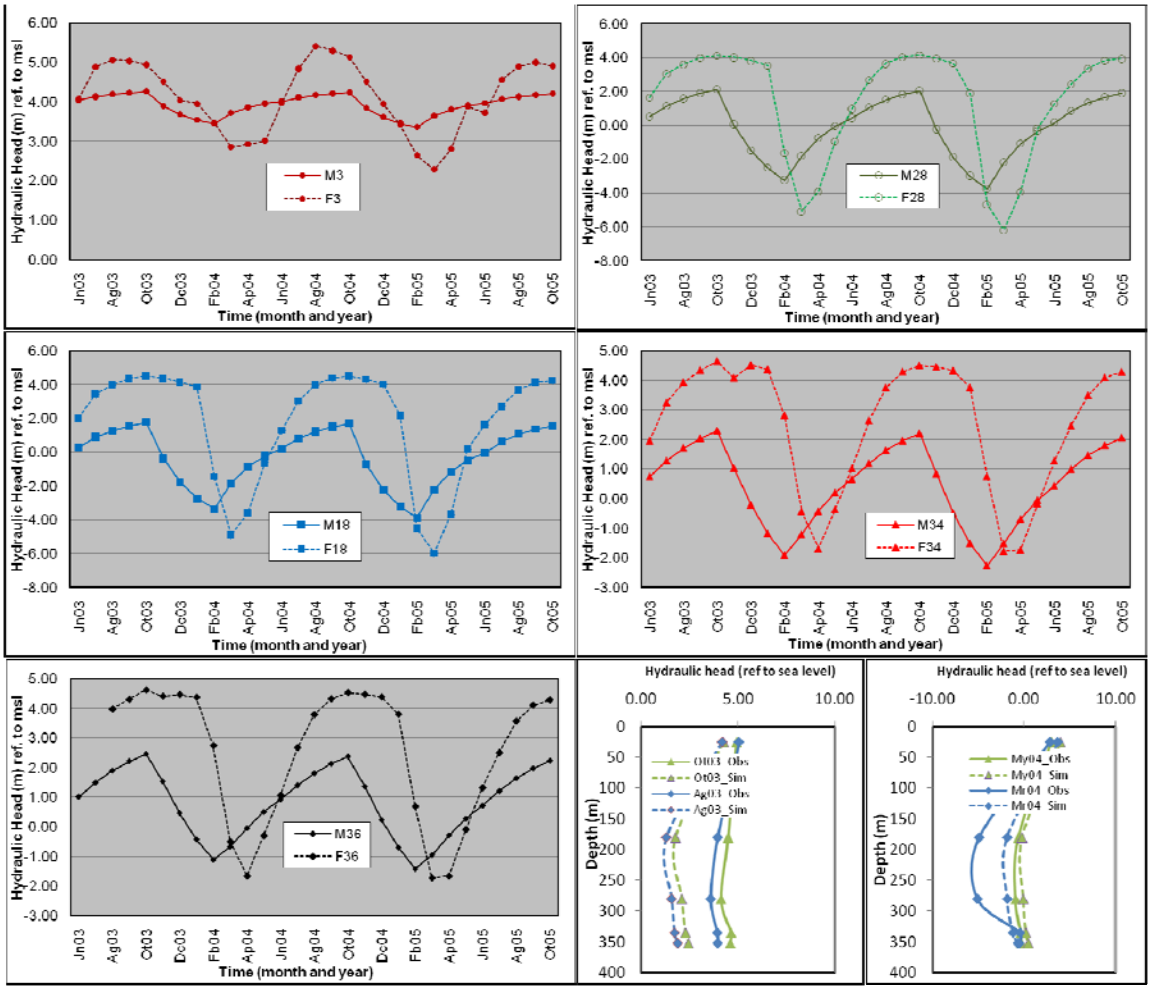

A8.2 Continued

*Vertical head profile at Kachua for **LS1***

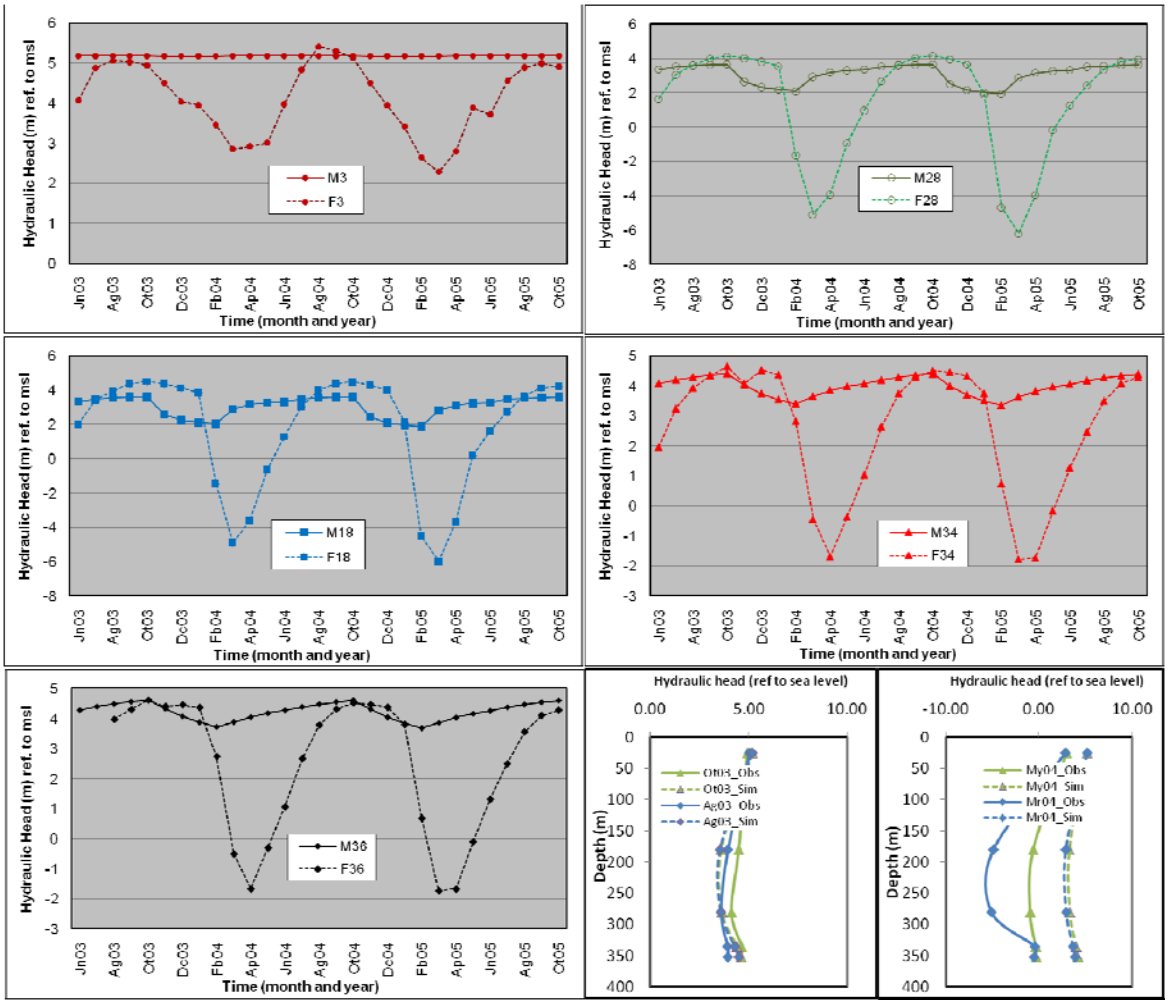

A8.3 Recharge zone delineation (Colour bar indicate travel time in years, and model representation is indicated)

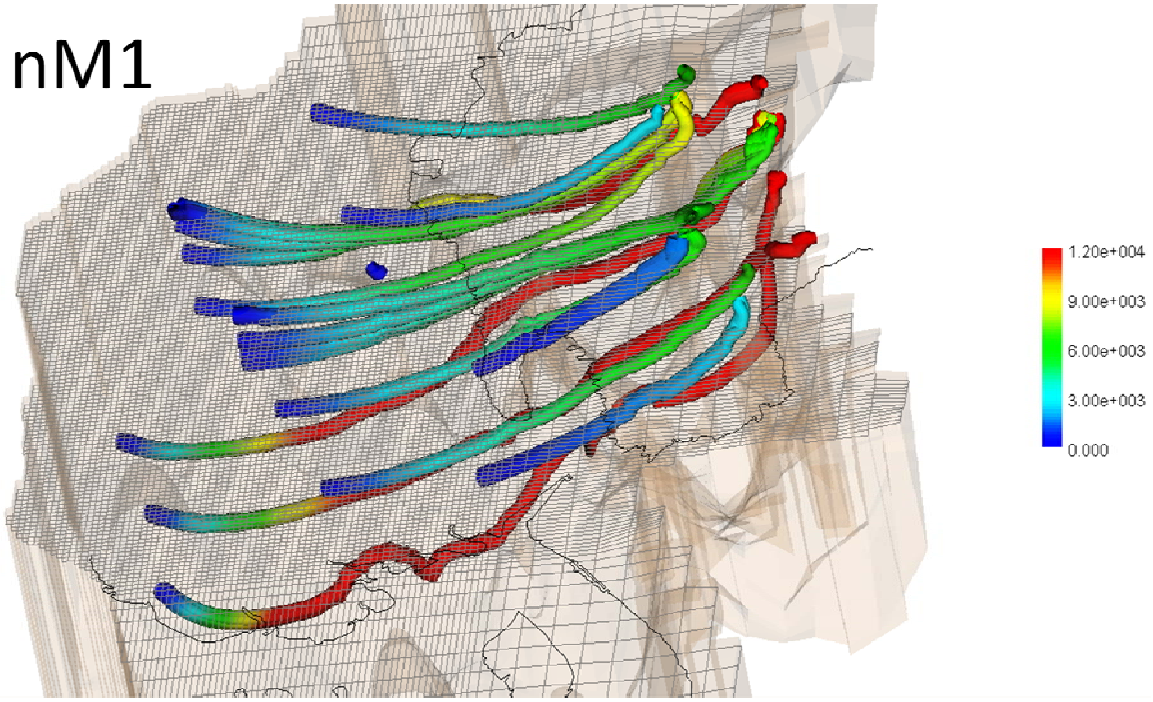

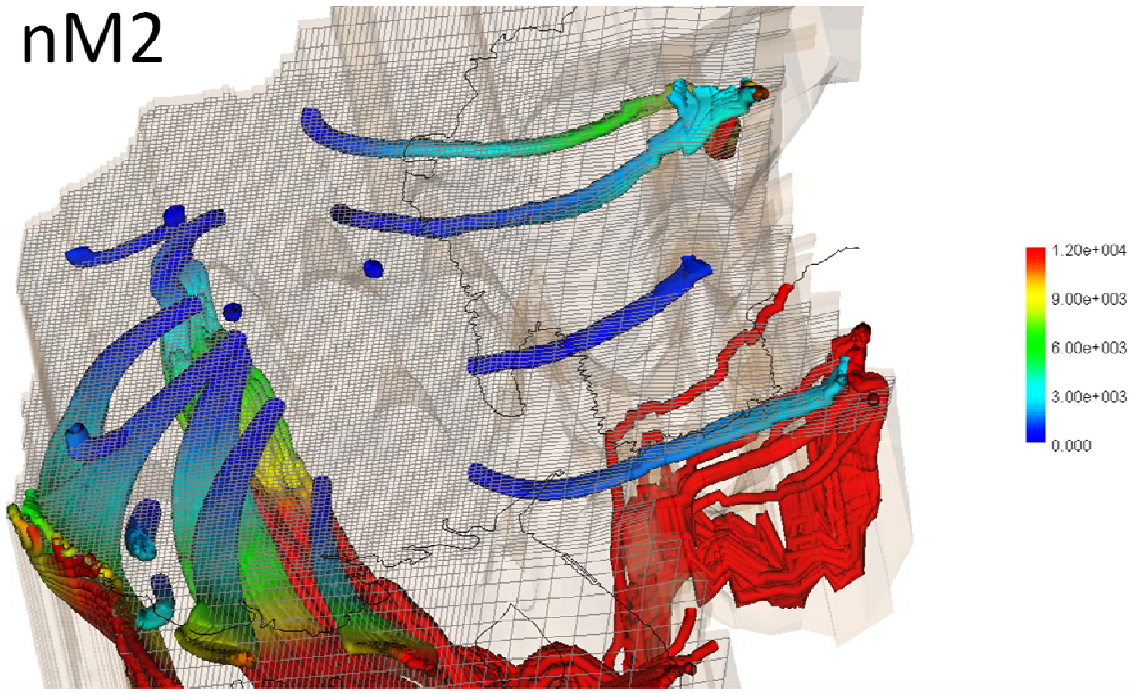

A8.3: Continued

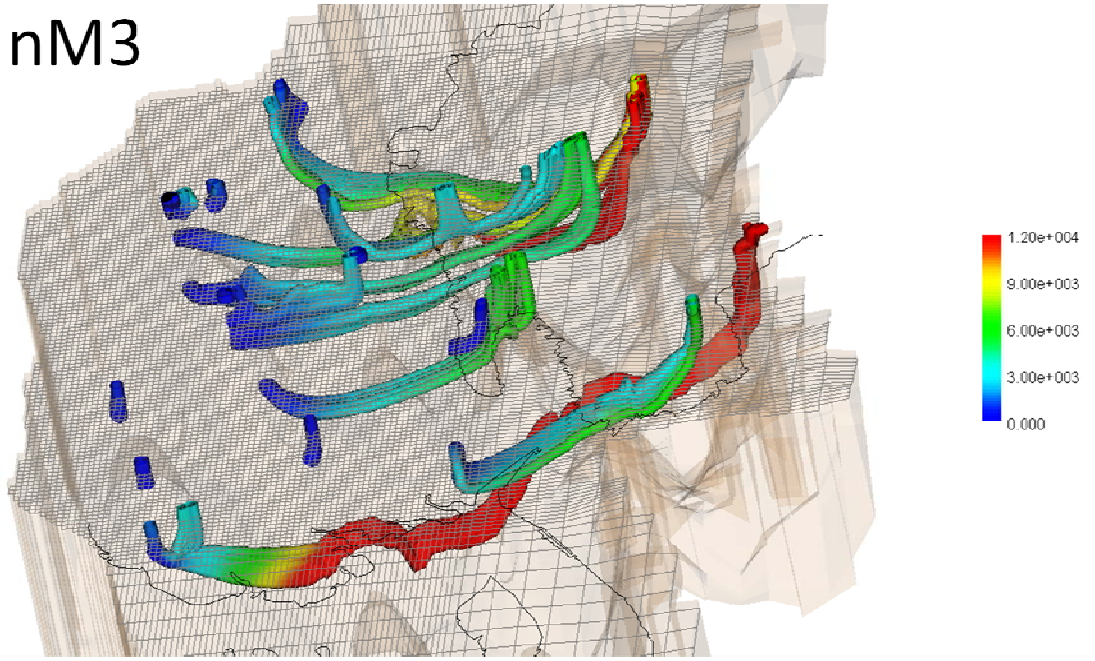

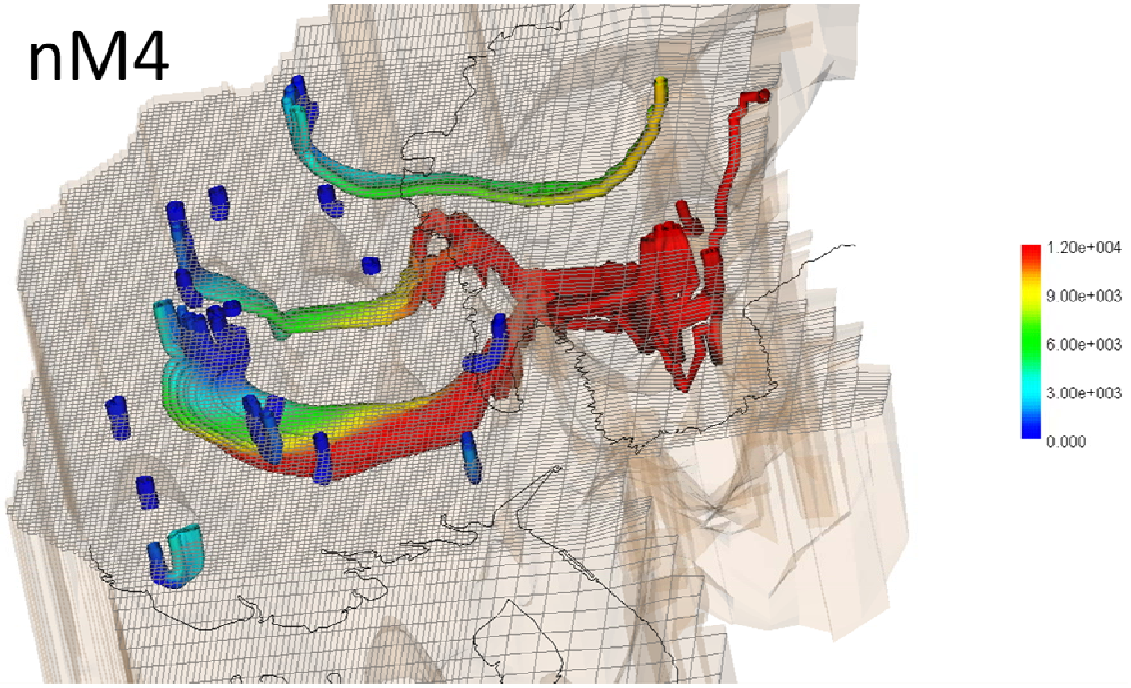

A8.3: Continued

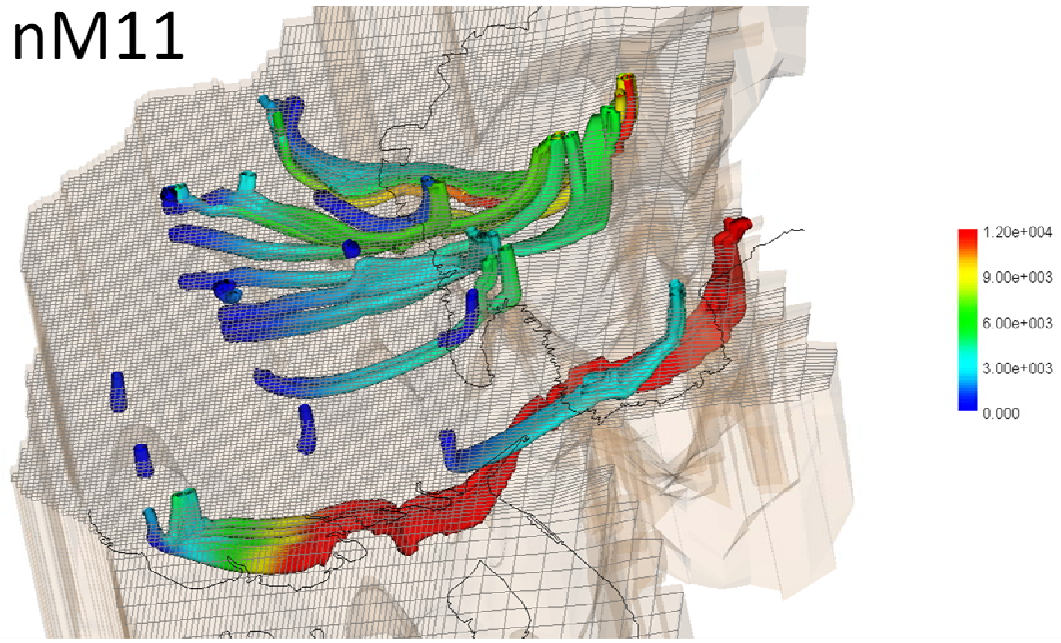

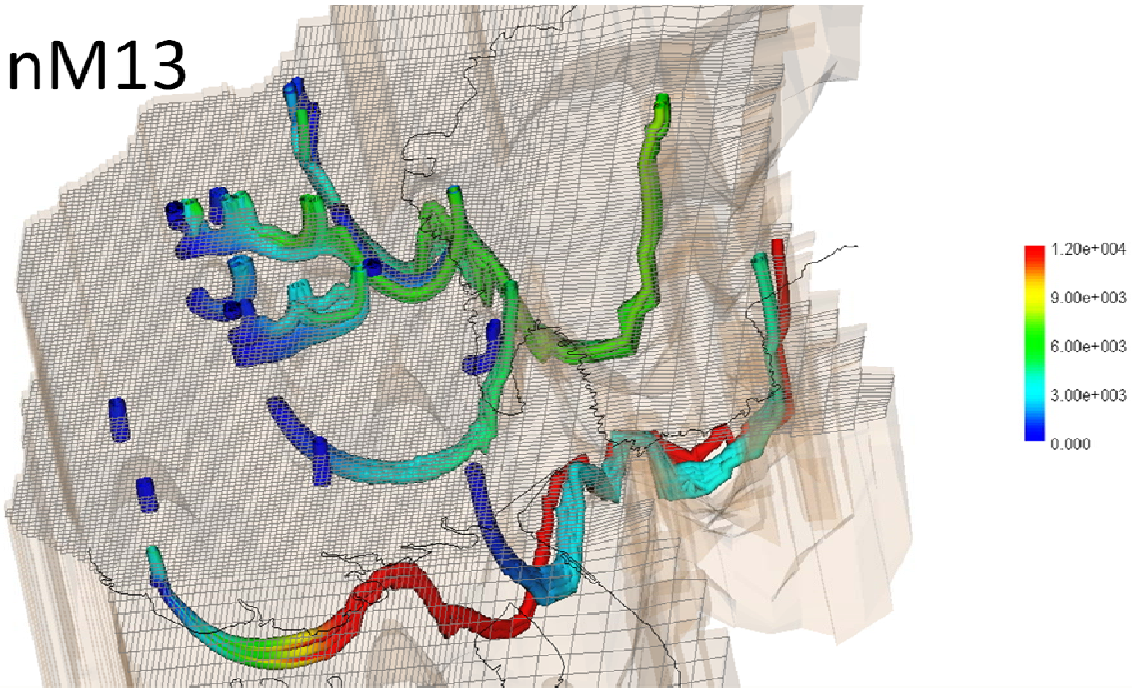

A8.3: Continued

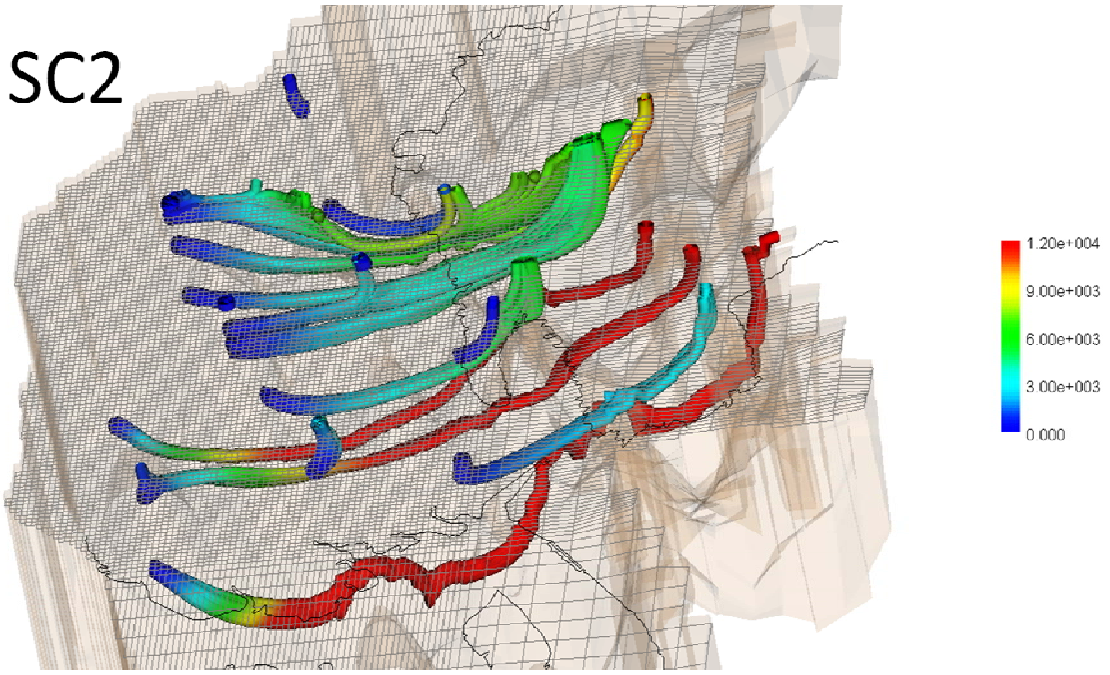

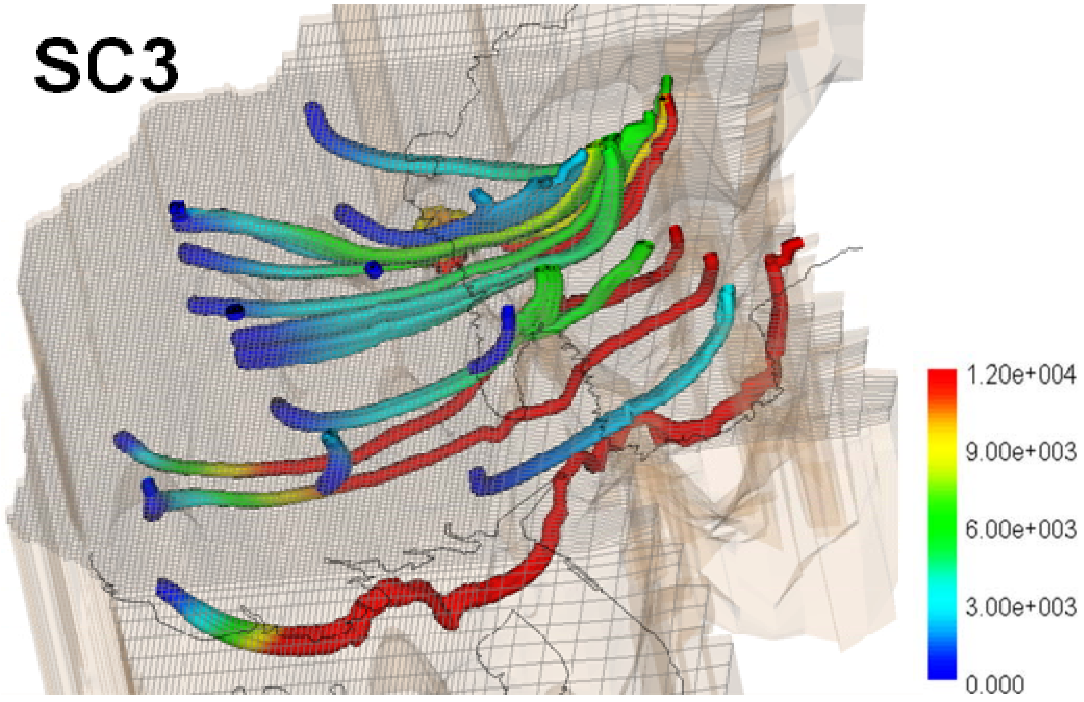

A8.3: Continued